



The Modern Day Heracles
Patient-derived Liver Organoids to Model Rare
Pediatric Liver Diseases

VIVIAN LEHMANN

The Modern Day Heracles

Patient-derived Liver Organoids to
Model Rare Pediatric Liver Diseases

Vivian Lehmann

The Modern Day Heracles - Patient-derived Liver Organoids to Model Rare Pediatric Liver Diseases

Author: Vivian Lehmann

Dissertation Utrecht University, Faculty of Veterinary Medicine

ISBN: 978-94-6483-507-6

Copyright © 2023 Vivian Lehmann

The Netherlands. All rights reserved. No part of this thesis may be reproduced, stored or transmitted in any way or by any means without the prior permission of the author, or when applicable, of the publishers of the scientific papers.

The research described in this dissertation was performed at the department of Clinical Sciences at the Faculty of Veterinary Medicine, Utrecht University and the division Child Health at the Wilhelmina Childrens Hospital, Utrecht within the framework of the Regenerative Medicine track of the Graduate School of Life Sciences at Utrecht University, the Netherlands.

Provided by thesis specialist Ridderprint, ridderprint.nl

Printing: Ridderprint

Layout and design: W. Aalberts, persoonlijkproefschrift.nl

Printing of this thesis was financially supported by the Netherlands Association for the Study of the Liver (NASL) and Axon Medchem.

**The Modern Day Heracles - Patient-derived Liver Organoids
to Model Rare Pediatric Liver Diseases**

De hedendaagse Herakles – patiënt-eigen lever organoïden
voor het modelleren van zeldzame leverziekten bij kinderen
(met een samenvatting in het Nederlands)

Der moderne Herakles – patienteneigene Organoiden zum Modellieren von
seltene Leberkrankheiten bei Kindern
(mit einer Zusammenfassung auf Deutsch)

Proefschrift

ter verkrijging van de graad van doctor aan de
Universiteit Utrecht
op gezag van de
rector magnificus, prof.dr. H.R.B.M. Kummeling,
ingevolge het besluit van het college voor promoties
in het openbaar te verdedigen op
donderdag 30 november 2023 des middags te 2.15 uur

door

Vivian Lehmann
geboren op 26 maart 1994
te Duisburg, Duitsland

Promotoren:

Prof. dr. M.A. Tryfonidou

Dr. B. Spee

Copromotoren:

Dr. S.A. Fuchs

Beoordelingscommissie:

Prof. dr. C.R. Berkers

Prof. dr. A. de Bruin

Prof. dr. J.M. Beekman

Prof. dr. L. van Grunsven

Prof. dr. J.M. Wells

Dit proefschrift werd mogelijk gemaakt met financiële steun van Metakids Research Funding/Vriendenloterij, ZonMW klinische fellows (40-00703-97-13537), ZonMW TAS: Regenerating Intestinal Tissue with Stem cells (40-41400-98-1108) en NWO-domein Toegepaste en Technische Wetenschappen (15498).

CONTENTS

Chapter 1	General Introduction	7
Chapter 2	The potential and limitations of intrahepatic cholangiocyte organoids to study monogenic liver disorders	23
Chapter 3	Human liver organoids to study the pathogenesis of Biliary Atresia	55
Chapter 4	Liver-on-a-tube: Improving hepatic maturation of intrahepatic cholangiocyte organoids with hollow fiber membrane technology to study liver metabolism and disease	119
Chapter 5	Summarizing Discussion	153
Addendum	Nederlandse samenvatting	186
	Deutsche Zusammenfassung	194
	Acknowledgements	204
	Curriculum Vitae	210





1

General Introduction

"Two beautiful eagles swept down from the sky and glided close to Prometheus, blocking the sunlight. Zeus called up to him. 'You will lie chained to this rock forever. (...) Each day these eagles will come to tear out your liver, just as you tore out my heart. They will eat it in front of your eyes. Since you are immortal it will grow back every night. This torture will never end.'"

From Mythos – The Greek Myths Retold, by Stephen Fry¹

Although humans are not immortal Titans, the myth of Prometheus bares some truth: the liver's fascinating regenerative capacity. Since the performance of most organs depends on hepatic functions, liver regeneration is a vital process. Across all vertebrates the liver has evolved to replenish its mass and function after injury.² In healthy humans, 50% of the original liver volume is regenerated within a week of removing 70% of the liver.^{3,4} Within one year organ volume and function approximate pre-operative conditions.

This incredible regenerative capacity is the result of a complex orchestration of signals, including growth factors and altered extracellular matrix (ECM) composition.⁵ These signals promote the self-renewal of each liver cell type after acute injury. However, there are situations, such as viral infections, in which self-renewal of one of the two most abundant liver cell types, hepatocytes and cholangiocytes, is inhibited. To rescue liver function, vertebrates have evolved another mechanism of liver regeneration. Hepatocytes and cholangiocytes can transdifferentiate into the other cell type. In this way, they act as facultative stem cells to replenish the other cell type and secure continued liver function.^{5,6}

Yet, unlike Zeus' claim of infinite liver regrowth in the myth of Prometheus, there are limits to liver regeneration. Chronic liver injury will eventually hamper liver regeneration. The ECM composition changes, an inflammatory environment forms and genetic errors increasingly accumulate as hepatocytes attempt to chronically replenish hepatocyte loss.⁵ As the environmental landscape drastically changes, regeneration signals are lost in translation and liver damage progresses to organ failure. As a result, 17 out of 100,000 adults die in the USA of liver failure annually.⁷ In Europe, deaths due to liver failure amount to a similar number on average but can reach up to 25 out of 100,000 in some countries.⁸

Clearly, solutions for patients with liver disease are urgently needed. A lot of research has been invested in high prevalence disorders such as non-alcoholic fatty liver disease and hepatocellular carcinoma.⁹ Individually rare liver diseases receive less attention even though their cumulative prevalence is significant. About 25% of rare liver diseases affect patients younger than 5 years old, while another

37% affect patient life expectancy significantly.¹⁰ It is challenging to study these diseases because patient numbers are limited, and mature liver functions and functional defects are difficult to model *in vitro*. In this thesis we explore possibilities to investigate these rare pediatric liver diseases and liver functions with the ultimate aim to improve care and treatment options for affected children.

Liver biology

The liver is a vital organ of the body and responsible for a plethora of functions. It acts as a large sieve through which the blood is filtered. Harmful substances are neutralized and replaced with useful molecules including hormones, and proteins.

These processes are facilitated by the architecture of the liver (Figure 1).¹¹⁻¹⁴ Liver tissue is composed of repetitive building blocks, called lobules.¹⁵ Therein hepatocytes, responsible for most of the liver's functions, are arranged in a hexagonal shape around a central vein. Each corner of the hexagon is marked by a portal triad, a grouping of branches of the portal vein, bile duct and hepatic artery. Within a lobule, the hepatocytes are organized into cords. Endothelial cells line the space in between the hepatocyte cords forming sinusoids which radiate toward the central vein.¹⁶ These endothelial cells are fenestrated thus maximizing the contact between hepatocytes and oxygen- and nutrient-rich blood. As the blood progresses through the lobule, its composition changes as cells utilize components and secrete waste products. This creates gradients of oxygen, growth factors and waste products throughout the lobule. Importantly, this varying environment is responsible for variation in hepatocyte function through the liver lobule, also called metabolic zonation.^{17,18} For instance, near the portal triad hepatocytes perform urea synthesis more than toward the central vein, while glycolysis occurs largely in the more central, low-oxygen regions of the lobule.

Hepatocytes make up around 80% of the liver volume.¹⁹ This so-called parenchymal part of the liver is supported by a non-parenchymal cell portion, composed of cholangiocytes, Kupffer cells, hepatic stellate cells, sinusoidal endothelial cells, endothelial cells, and natural killer cells. Each cell type contributes to the functioning of the organ and interacts with hepatocytes to ensure homeostasis. Hepatocytes are responsible for most liver functions. Their polarity facilitates simultaneous interaction with the blood and bile compartments.¹³ The basolateral side of hepatocytes faces the space of Disse, which describes the space between the sinusoidal endothelial cells and hepatocytes.²⁰ Hepatocytes extend villi into the space of Disse to maximize absorption of compounds from the blood. The space of Disse also contains ECM proteins such as fibronectin, laminins, collagens and perlecan, which provide structural support and cell fate cues to hepatocytes.^{21,22} Moreover, Kupffer and hepatic stellate cells reside in this space and are responsible for blood filtration, fat storage and liver regeneration upon

tissue damage.²³⁻²⁵ Where hepatocytes face neighboring hepatocytes the apical cell domain is found.¹³ Here hepatocytes form tight junctions and canaliculi. These canaliculi form an intricate three-dimensional (3D) lattice structure throughout the stacked lobules and feed into the bile ducts.^{26,27} Cholangiocytes, the second most abundant cell type of the liver, line the intra- and extrahepatic bile ducts and facilitate bile flow out of the liver and into the gallbladder and duodenum.^{28,29} Moreover, cholangiocytes control bile composition and homeostasis by secreting or absorbing ions and organic solutes.

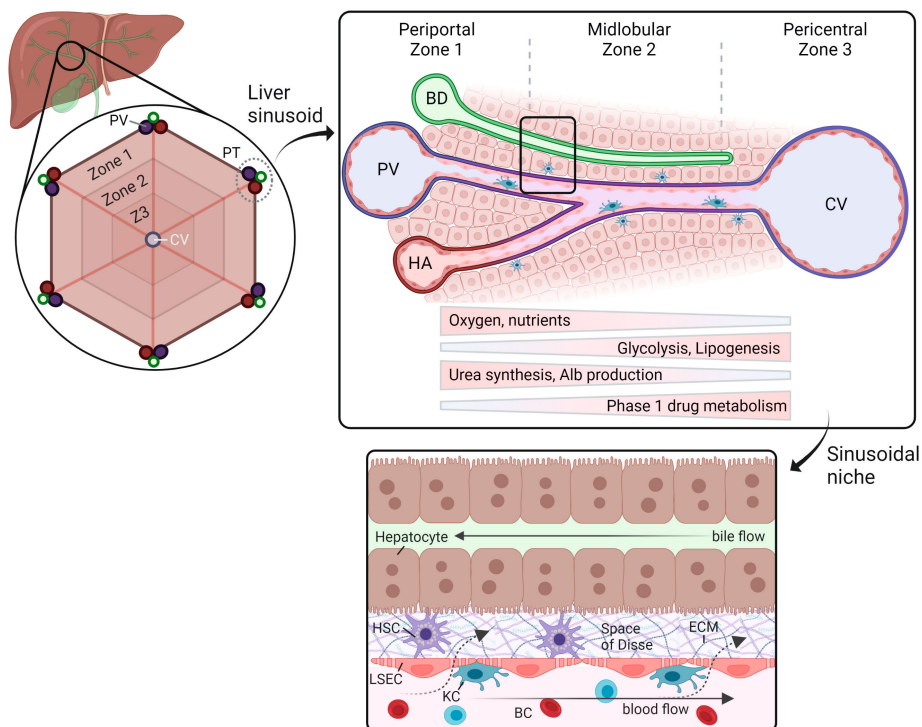


Figure 1. Architecture of the liver lobule and hepatic niche. Alb, albumin; BC, blood cell; BD, bile duct; CV, central vein; ECM, extracellular matrix; HA, hepatic artery; HSC, hepatic stellate cell; KC, Kupffer cell; LSEC, liver sinusoidal endothelial cell; PT, portal triad; PV, portal vein. Adapted and modified from the PhD dissertation of Lianne van Os.

Hepatocytes are responsible for most liver functions. The 3D positioning and polarity of hepatocytes maximizes contact with sinusoids and bile canaliculi to facilitate transport of substrates and waste products across the cell membrane.^{13,14} Incoming nutrients are broken down into building blocks, such as amino acids and energy, which fuel other metabolic reactions.^{13,30} Glucose and insulin homeostasis is achieved through close communication with the pancreas. Depending on whether the body is fasting or feeding hepatocytes can store glucose as glycogen or generate glucose through gluconeogenesis.^{31,32} Similarly, hepatocytes process incoming

lipids for immediate use and can store excess lipids until future use as an energy source.³³ Aside from energy metabolism, hepatocytes are a major factory for blood proteins, such as albumin and clotting factors.^{34,35} Other proteins are degraded by hepatocytes and produce excess toxic nitrogen-rich waste which is converted into urea for safe removal via the kidneys.³⁶ Hepatocytes also produce bile, a soap-like fluid containing bile acids and salts, cholesterol, bilirubin, electrolytes, and other components.³⁷ Bile is secreted into bile canaliculi and transported through the bile ducts to exit the liver. Eventually, bile drains into the gallbladder for storage or delivery to the duodenum to aid in digestion. Bile also acts as a carrier for metabolized xenobiotic waste products. During xenobiotics or drug metabolism, exogenous harmful substances are filtered from the blood and metabolized into harmless waste products.³⁸ Because of this detoxifying function the liver is particularly vulnerable to drug induced liver injury.^{39,40}

Pediatric liver disorders

Malfunction or disruption of the liver's intricate metabolic network can lead to disease. Especially, pediatric liver diseases showcase the vital function of the liver and the problems that arise when a single liver function is deficient. Since the liver is such an important and complex organ, liver transplantation represents the ultimate treatment for many pediatric liver disorders. Listed among the leading causes for pediatric liver transplantations are cholestatic liver diseases, such as biliary atresia, and metabolic disorders.^{41,42} Biliary atresia (BA) is a perinatal disease presenting with obstructed or absent extrahepatic bile ducts and gallbladder thus inhibiting bile drainage from the liver.^{43,44} When left untreated liver damage rapidly progresses to organ failure. The etiology of BA is likely multi-factorial but remains poorly understood. Thus, treatment options for patients are limited to surgical correction and liver transplantation.⁴⁵⁻⁴⁷ Conversely, several other (monogenic) pediatric liver disorders are caused by mutations in a single gene encoding an enzyme or a transporter. This often results in an altered metabolic pathway; key metabolites are missing or accumulate to reach toxic concentrations, as is the case for citrullinemia type I, a urea cycle disorder wherein ammonia is not processed and accumulates in the body.⁴⁸ Primary familial intrahepatic cholestasis represents an example of disorders, where defects in the bile secretion system lead to the accumulation of bile in the liver and consequent hepatocyte damage.⁴⁹ Eventually these functional defects lead to failure of the liver or other organs before patients reach adulthood.⁵⁰ Individual monogenic liver disorders are rare diseases; however, their cumulative occurrence is high, with a frequency of 1 in 2,000 births annually.⁵¹⁻⁵⁴ Yet, heterogeneity, geographic distribution and rarity of each monogenic liver disorder has hampered our understanding of underlying pathophysiology. Tragically, this has also complicated the development of pharmaceutical solutions. Thus, for many

of these pediatric liver disorders medical care is limited to symptomatic treatment, while for others treatment options are entirely non-existent.

Liver models

The development of therapeutic approaches for rare pediatric liver disorders requires robust and personalized *in vitro* models of the liver. Traditional hepatic *in vitro* models comprise two-dimensional cultures of primary human hepatocytes (PHH) and immortalized or cancer-derived cell lines such as HepaRG and HepG2. PHH are considered the gold standard of hepatic *in vitro* models as they are cells with hepatic functions, and they represent the genetic make-up of the donor. However, substantial amounts of liver tissue are required to yield sufficient PHH for research. Thus, personalized research in cells derived from a living donor is not feasible. Cell lines such as HepaRG and HepG2 are widely used, can be upscaled *in vitro* and perform several hepatic functions. Yet, these cell lines do not represent interindividual differences and lack key metabolic enzymes.⁵⁵

Recent developments in stem cell technologies have allowed the generation of hepatocyte-like cells from embryonic stem cells, mesenchymal stem cells (MSCs) or induced pluripotent stem cells (iPSCs).⁵⁶⁻⁶⁰ These stem cells self-renew and can differentiate into various cell types when exposed to appropriate cues. Extensive differentiation protocols have been developed to resemble hepatic organogenesis and produce cells which mimic hepatocyte functions as closely as possible. iPSCs are of particular interest since they can be generated from patients thus opening the doors for studying monogenic liver disorders in a patient-specific setting.⁶¹ Yet, hepatic maturation in these stem cell-based *in vitro* models remains limited compared to *in vivo* hepatocytes or freshly isolated PHH.⁶²⁻⁶⁶

To overcome limitations in hepatic maturity of stem cell-derived hepatocyte-like cells, the microenvironment of these *in vitro* models has been modified to mimic the *in vivo* situation more closely. Strategies include the use of supportive matrices and perfusion with media to mimic blood flow.⁶⁷ Supportive matrices, such as collagen-based gels provide physical support and allow for 3D structures to form. Moreover, the composition of these gels can be fine-tuned to mimic the ECM of the space of Disse and thus provide *in vivo*-like biochemical cues to the cells.⁶⁷ Previous studies have shown improvements in the expression of hepatic markers, such as albumin and drug metabolizing enzyme CYP3A4, upon culturing iPSCs on supportive matrices.^{68,69} Yet, maturation remained incomplete with high expression of fetal hepatocyte markers and significantly lower expression and function of mature hepatocyte markers compared to PHH.

Another aspect of the hepatic niche is the high vascularization and continuous supply of fresh blood to hepatocytes. It is a unique feature of the liver and contributes to the organ's vital functions. Hence, mimicry of blood flow in *in vitro* models represents a logical strategy to improve hepatic maturation.⁶⁷ This is often achieved through continuous perfusion of media through a culture chamber. Continuous perfusion is thought to not only maximize contact with oxygen and nutrients but also to provide control over media composition.⁷⁰ Yet, even with these strategies, hepatic maturation of pluripotent stem cells remains incomplete, thus limiting their application.^{62,71-73}

Apparently, current differentiation conditions of stem cell-derived hepatocyte-like cells are suboptimal, thus hampering full hepatic maturation of employed stem cells.⁶⁷ Most of these model systems make use of pluripotent stem cells which are thought to be capable of differentiating into any cell type. However, it has been shown that tissue origin can affect differentiation potential of pluripotent cells.^{74,75} Therefore, the use of liver-derived cells could be more successful in producing an *in vitro* model expressing mature hepatocyte functions alike PHH.

To that end, liver organoids have been developed from patient-derived liver tissue. Liver organoids are derived from bipotent biliary epithelial cells which self-assemble into hollow spheres in culture.⁷⁶ Organoids can be cultured from digested patient biopsies placed in a laminin-rich hydrogel in 3D culture conditions and specific growth factors. Liver organoids are able to differentiate into both hepatocytes and cholangiocytes, thus opening the avenue to study the whole hepatobiliary system based on a single patient biopsy.⁷⁶⁻⁷⁸ Moreover, it has been reported that liver organoids can be stably cryopreserved and cultured for several months, which is uncommon for primary human cells.⁷⁶ Following the development of organoids from intrahepatic cholangiocytes, organoid cultures from extrahepatic bile ducts and the gallbladder have been generated using similar protocols.^{79,80} Since then, new nomenclature has been developed to distinguish between organoids from different hepatobiliary origin.⁸¹ The liver organoids that were first established by Huch *et al.* in 2015 are now named intrahepatic cholangiocyte organoids (ICOs). Other liver organoids are referred to as hepatocyte organoids, extrahepatic cholangiocyte organoids (ECOs), and gallbladder cholangiocyte organoids (GCOs).

Within the context of rare pediatric liver diseases, the first report on liver organoids presented promising results on pathophysiologic studies using liver organoids from patients suffering from Alagille syndrome and α 1-antitrypsin deficiency.⁷⁶ The prospect of nearly infinitely available patient material with which to study rare diseases was enticing. Consequently, our group at the UMC Utrecht invested in the infrastructure and (inter)national collaborations to generate a Metabolic Biobank involving liver organoids derived from liver tissue of hundreds of healthy and

patient donors. This large biobank of liver organoids from various rare pediatric liver diseases presents a valuable opportunity to unravel the usefulness of liver organoids to aid in mechanistic studies and clinical decision making.

Evaluation and further development of liver organoids as a tool in liver disease research

Upon establishment of liver organoids for our biobank, our knowledge about their applicability in studying disease etiology and pathophysiology was limited. Since the first report on liver organoids, no further information about the range of hepatic functions expressed in liver organoids has been published. Although Huch *et al.*, 2015 demonstrated that multiple hepatocyte functions can be studied in liver organoids, only limited functional comparisons were made with PHH or liver tissue. Meanwhile, gene expression of several hepatic markers, such as albumin, was significantly lower than in liver tissue, indicating that liver organoids might not reflect full hepatocyte maturity. Hence, it remained unclear which hepatic functions and disorders can be studied with liver organoids. In this thesis, we explore the potential of liver organoids to study the pathophysiology of monogenic liver disorders and other rare pediatric liver diseases.

In **Chapter 2**, we explore whether different monogenic liver disorders can be studied in (patient-derived) ICOs. We consider diseases representing various metabolic liver functions, namely amino acid metabolism, copper metabolism, and bile homeostasis and speculate, based on transcriptomic data, which metabolic functions could be studied in ICOs rather than in other cell models, such as fibroblasts. The outcomes shine a light on whether further investments into liver organoid technology as a clinical research tool for liver disorders is warranted by clinicians and research institutes.

The endeavors in uncovering the utility of liver organoids are expanded in **Chapter 3** by exploring whether liver organoids can be used to model pediatric liver diseases with unresolved etiology, like BA. Since BA affects both intra- and extrahepatic bile ducts, we investigate whether organoids from various hepatobiliary regions (ICOs, ECOs and GCOs) of BA patients can be used to study BA etiology. Over the past decades several etiology hypotheses have been proposed, including viral infection, toxin, autoimmune reaction, and genetic predisposition. Of these hypotheses the involvement of viral infections and/or an environmental toxin or toxic metabolite have been the most supported by clinical and experimental evidence.^{43,44,82} To test these hypotheses, we explore whether patient-derived liver organoids intrinsically reflect BA phenotypes compared to healthy donor liver organoids. Moreover, we

explore whether the BA phenotype can be induced in liver organoids upon viral or toxic insults.

Although hepatic functions of liver organoids outperform HepG2 cell lines, hepatic maturity of liver organoids remains lower than what is found *in vivo*.⁷⁶ Therefore, we explore whether hepatic maturation of ICOs can be improved. To this end, we develop and characterize a novel culture method for ICOs in **Chapter 4** by employing several suggested strategies to mimic the hepatic niche. We make use of hollow fiber membranes (HFMs) on the surface of which ICO-derived cells can be cultured. Moreover, we use ECM proteins found in the space of Disse to facilitate cell attachment on HFMs and mimic differentiation cues which cells experience *in vivo*. In addition, HFMs permit internal and external perfusion when connected to a custom bioreactor and perfusion pump thus mimicking blood and bile flow *in vitro*. As an initial proof of concept, we investigate whether patient-derived ICOs can be cultured in the new system. Here the focus is directed towards diseases affecting transmembrane transporters as HFM architecture allows for the separation of apical and basolateral cell compartments putatively facilitating functional studies to study such diseases.

Finally, **Chapter 5** summarizes the findings of the thesis and expands on their implications for the future use of liver organoids. By identifying interfaces among the performed studies and recent literature, future research avenues are proposed to broaden the application range of liver organoids and improve our understanding of disease etiologies. Eventually, we envision that liver organoids will synergize with other hepatocyte models to unravel disease mechanisms and help in identifying safe therapeutic strategies for rare pediatric liver disorders in a personalized manner.

Authorship statement

The idea and set-up of the general introduction were mine; I conducted the literature search and wrote the general introduction. During the whole process I asked for and implemented input and feedback from my supervisory team.

References

1. Fry S. *Mythos*. Penguin Books; 2018. Accessed March 3, 2023. <https://www.penguin.co.uk/books/307476/mythos-by-fry-stephen/9781405934138>
2. Delgado-Coello B. Liver regeneration observed across the different classes of vertebrates from an evolutionary perspective. *Heliyon*. 2021;7(3):e06449. doi:10.1016/J.HELIYON.2021.E06449
3. Haga J, Shimazu M, Wakabayashi G, et al. Liver regeneration in donors and adult recipients after living donor liver transplantation. *Liver Transplantation*. 2008;14(12):1718-1724. doi:10.1002/LT.21622
4. Kim MS, Lee HK, Kim SY, Cho JH. Analysis of the relationship between liver regeneration rate and blood levels. *Pak J Med Sci*. 2015;31(1):31. doi:10.12669/PJMS.311.5864
5. Michalopoulos GK, Bhushan B. Liver regeneration: biological and pathological mechanisms and implications. *Nat Rev Gastroenterol Hepatol*. 2020;18(1):40-55. doi:10.1038/s41575-020-0342-4
6. So J, Kim A, Lee SH, Shin D. Liver progenitor cell-driven liver regeneration. *Exp Mol Med*. 2020;52(8):1230-1238. doi:10.1038/S12276-020-0483-0
7. FastStats - Chronic Liver Disease or Cirrhosis. Accessed March 3, 2023. <https://www.cdc.gov/nchs/fastats/liver-disease.htm>
8. Sheron N, Burra P, Cortez-Pinto H, Lazarus J, Negro F. *HEPAHEALTH Project Report*; 2018. Accessed March 17, 2023. <https://easl.eu/publication/hepahealth-project-report/>
9. Seto WK, Susan Mandell M. Chronic liver disease: Global perspectives and future challenges to delivering quality health care. *PLoS One*. 2021;16(1):e0243607. doi:10.1371/JOURNAL.PONE.0243607
10. Fabris L, Strazzabosco M. Rare and undiagnosed liver diseases: challenges and opportunities. *Transl Gastroenterol Hepatol*. 2021;6:18. doi:10.21037/TGH-2020-05
11. Kalra A, Yetiskul E, Wehrle CJ, Tuma F. Physiology, Liver. In: *StatPearls*. StatPearls Publishing; 2022. Accessed February 27, 2023. <https://www.ncbi.nlm.nih.gov/books/NBK535438/>
12. Vernon H, Wehrle CJ, Alia VSK, Kasi A. Anatomy, Abdomen and Pelvis, Liver. *StatPearls*. Published online November 26, 2022. Accessed February 28, 2023. <https://www.ncbi.nlm.nih.gov/books/NBK500014/>
13. Schulze RJ, Schott MB, Casey CA, Tuma PL, McNiven MA. The cell biology of the hepatocyte: A membrane trafficking machine. *Journal of Cell Biology*. 2019;218(7):2096-2112. doi:10.1083/jcb.201903090
14. Ishibashi H, Nakamura M, Komori A, Migita K, Shimoda S. Liver architecture, cell function, and disease. *Semin Immunopathol*. 2009;31(3):399-409. doi:10.1007/s00281-009-0155-6
15. Rappaport AM, Borowy ZJ, Loughheed WM, Lotto WN. Subdivision of hexagonal liver lobules into a structural and functional unit. Role in hepatic physiology and pathology. *Anat Rec*. 1954;119(1):11-33. doi:10.1002/AR.1091190103
16. Wisse E, Braet F, Luo D, et al. Structure and Function of Sinusoidal Lining Cells in the Liver. *Toxicol Pathol*. 1996;24(1):100-111. doi:10.1177/019262339602400114

17. Hijmans BS, Grefhorst A, Oosterveer MH, Groen AK. Zonation of glucose and fatty acid metabolism in the liver: Mechanism and metabolic consequences. *Biochimie*. 2014;96(1):121-129. doi:10.1016/j.biochi.2013.06.007
18. Katz NR. Metabolic Heterogeneity of Hepatocytes across the Liver Acinus. *J Nutr*. 1992;122(suppl_3):843-849. doi:10.1093/JN/122.SUPPL_3.843
19. Blouin A, Bolender RP, Weibel ER. Distribution of organelles and membranes between hepatocytes and nonhepatocytes in the rat liver parenchyma. A stereological study. *J Cell Biol*. 1977;72(2):441. doi:10.1083/JCB.72.2.441
20. Sanz-García C, Fernández-Iglesias A, Gracia-Sancho J, Arráez-Aybar LA, Nevzorova YA, Cubero FJ. The Space of Disse: The Liver Hub in Health and Disease. *Livers*. 2021;1(1):3-26. doi:10.3390/LIVERS1010002
21. McClelland R, Wauthier E, Uronis J, Reid L. Gradients in the liver's extracellular matrix chemistry from periportal to pericentral zones: Influence on human hepatic progenitors. *Tissue Eng Part A*. 2008;14(1):59-70. doi:10.1089/ten.a.2007.0058
22. Martínez-Hernández A, Amenta PS. The hepatic extracellular matrix. I. Components and distribution in normal liver. *Virchows Archiv A Pathol Anat*. 1993;423:1-11. doi:10.1007/BF01606425
23. Hendriks HFJ, Verhoofstad WAMM, Brouwer A, De Leeuw AM, Knook DL. Perisinusoidal fat-storing cells are the main vitamin A storage sites in rat liver. *Exp Cell Res*. 1985;160(1):138-149. doi:10.1016/0014-4827(85)90243-5
24. Senoo H. Structure and function of hepatic stellate cells. *Medical Electron Microscopy*. 2004;37(1):3-15. doi:10.1007/S00795-003-0230-3
25. Nguyen-Lefebvre AT, Horuzsko A. Kupffer Cell Metabolism and Function. *J Enzymol Metab*. 2015;1(1):101. Accessed May 23, 2023. <https://www.ncbi.nlm.nih.gov/pmc/articles/PMC4771376/>
26. Gallin WJ. Development and maintenance of bile canaliculi in vitro and in vivo. *Microsc Res Tech*. 1997;39(5):406-412. doi:10.1002/(SICI)1097-0029(19971201)39:5<406::AID-JEMT3>3.0.CO;2-E
27. Tsukada N, Ackerley CA, Phillips MJ. The structure and organization of the bile canalicular cytoskeleton with special reference to actin and actin-binding proteins. *Hepatology*. 1995;21(4):1106-1113. doi:10.1002/HEP.1840210433
28. Banales JM, Huebert RC, Karlsen T, Strazzabosco M, LaRusso NF, Gores GJ. Cholangiocyte pathobiology. *Nat Rev Gastroenterol Hepatol*. 2019;16(5):269. doi:10.1038/S41575-019-0125-Y
29. Tabibian JH, Masyuk AI, Masyuk T V., O'Hara SP, LaRusso NF. Physiology of Cholangiocytes. *Compr Physiol*. 2013;3(1):541-565. doi:10.1002/CPHY.C120019
30. Dutta S, Mishra SP, Sahu AK, et al. Hepatocytes and Their Role in Metabolism. In: *Drug Metabolism*. IntechOpen; 2021. doi:10.5772/INTECHOPEN.99083
31. Radziuk J, Pye S. Hepatic glucose uptake, gluconeogenesis and the regulation of glycogen synthesis. *Diabetes Metab Res Rev*. 2001;17(4):250-272. doi:10.1002/DMRR.217
32. Trefts E, Williams AS, Wasserman DH. Exercise and the Regulation of Hepatic Metabolism. *Prog Mol Biol Transl Sci*. 2015;135:203-225. doi:10.1016/BS.PMBTS.2015.07.010
33. Scorletti E, Byrne CD. Omega-3 Fatty Acids, Hepatic Lipid Metabolism, and Nonalcoholic Fatty Liver Disease. *Annu Rev Nutr*. 2013;33:231-248. doi:10.1146/annurev-nutr-071812-161230
34. Peters T Jr. *All About Albumin*. Elsevier; 1995. doi:10.1016/B978-0-12-552110-9.X5000-4

35. Levitt DG, Levitt MD. Human serum albumin homeostasis: A new look at the roles of synthesis, catabolism, renal and gastrointestinal excretion, and the clinical value of serum albumin measurements. *Int J Gen Med*. 2016;9:229-255. doi:10.2147/IJGM.S102819
36. Adeva MM, Souto G, Blanco N, Donapetry C. Ammonium metabolism in humans. *Metabolism*. 2012;61(11):1495-1511. doi:10.1016/J.METABOL.2012.07.007
37. Boyer JL, Soroka CJ. Bile formation and secretion: An update. *J Hepatol*. 2021;75(1):190-201. doi:10.1016/J.JHEP.2021.02.011
38. Zanger UM, Schwab M. Cytochrome P450 enzymes in drug metabolism: Regulation of gene expression, enzyme activities, and impact of genetic variation. *Pharmacol Ther*. 2013;138(1):103-141. doi:10.1016/J.PHARMTHERA.2012.12.007
39. Andrade RJ, Chalasani N, Björnsson ES, et al. Drug-induced liver injury. *Nat Rev Dis Primers*. 2019;5(1):58. doi:10.1038/s41572-019-0105-0
40. Jaeschke H, Gores GJ, Cederbaum AI, Hinson JA, Pessayre D, Lemasters JJ. Mechanisms of Hepatotoxicity. *Toxicological Sciences*. 2002;65(2):166-176. doi:10.1093/TOXSCI/65.2.166
41. Smith SK, Miloh T. Pediatric Liver Transplantation. *Clin Liver Dis*. 2022;26(3):521-535. doi:10.1016/j.cld.2022.03.010
42. Mullapudi B, Hendrickson R. Pediatric liver transplantation. *Semin Pediatr Surg*. 2022;31(3):151191. doi:10.1016/j.sempedsurg.2022.151191
43. Asai A, Miethke A, Bezerra JA. Pathogenesis of biliary atresia: Defining biology to understand clinical phenotypes. *Nat Rev Gastroenterol Hepatol*. 2015;12(6):342-352. doi:10.1038/nrgastro.2015.74
44. Hartley JL, Davenport M, Kelly DA. Biliary atresia. *The Lancet*. 2009;374(9702):1704-1713. doi:10.1016/S0140-6736(09)60946-6
45. Ishitani MB. Biliary atresia and the Kasai portoenterostomy: Never say never? *Liver Transplantation*. 2001;7(9):831-832. doi:10.1053/JLTS.2001.0070831
46. Bijl EJ, Bharwani KD, Houwen RHJ, de Man RD. The long-term outcome of the Kasai operation in patients with biliary atresia: a systematic review. *Neth J Med*. 2013;71(4):170-173. Accessed March 22, 2023. <https://pubmed.ncbi.nlm.nih.gov/23723110/>
47. Shneider BL, Brown MB, Haber B, et al. A multicenter study of the outcome of biliary atresia in the United States, 1997 to 2000. *J Pediatr*. 2006;148(4):467-474.e1. doi:10.1016/J.JPEDI.2005.12.054
48. Engel K, Höhne W, Häberle J. Mutations and polymorphisms in the human argininosuccinate synthetase (ASS1) gene. *Hum Mutat*. 2009;30(3):300-307. doi:10.1002/humu.20847
49. Davit-Spraul A, Gonzales E, Baussan C, Jacquemin E. Progressive familial intrahepatic cholestasis. *Orphanet J Rare Dis*. 2009;4(1):1. doi:10.1186/1750-1172-4-1
50. Fagioli S, Daina E, D'Antiga L, Colledan M, Remuzzi G. Monogenic diseases that can be cured by liver transplantation. *J Hepatol*. 2013;59(3):595-612. doi:10.1016/J.JHEP.2013.04.004
51. Ferreira CR, van Karnebeek CDM, Vockley J, Blau N. A proposed nosology of inborn errors of metabolism. *Genetics in Medicine*. 2019;21(1):102-106. doi:10.1038/s41436-018-0022-8
52. Waters D, Adeloye D, Woolham D, Wastnedge E, Patel S, Rudan I. Global birth prevalence and mortality from inborn errors of metabolism: A systematic analysis of the evidence. *J Glob Health*. 2018;8(2):021102. doi:10.7189/jogh.08.021102
53. Stalke A, Skawran B, Auber B, et al. Diagnosis of monogenic liver diseases in childhood by next-generation sequencing. *Clin Genet*. 2018;93(3):665-670. doi:10.1111/CGE.13120

54. Vaisitti T, Peritore D, Magistroni P, et al. The frequency of rare and monogenic diseases in pediatric organ transplant recipients in Italy. *Orphanet J Rare Dis*. 2021;16(1):1-17. doi:10.1186/s13023-021-02013-x
55. Stanley LA, Wolf CR. Through a glass, darkly? HepaRG and HepG2 cells as models of human phase I drug metabolism. *Drug Metab Rev*. 2022;54(1):46-62. doi:10.1080/03602532.2022.2039688
56. Fu Y, Deng J, Jiang Q, et al. Rapid generation of functional hepatocyte-like cells from human adipose-derived stem cells. *Stem Cell Res Ther*. 2016;7(1). doi:10.1186/S13287-016-0364-6
57. Huang J, Guo X, Li W, Zhang H. Activation of Wnt/ β -catenin signalling via GSK3 inhibitors direct differentiation of human adipose stem cells into functional hepatocytes. *Scientific Reports 2017 7:1*. 2017;7(1):1-12. doi:10.1038/srep40716
58. Okura H, Komoda H, Saga A, et al. Properties of hepatocyte-like cell clusters from human adipose tissue-derived mesenchymal stem cells. *Tissue Eng Part C Methods*. 2010;16(4):761-770. doi:10.1089/ten.TEC.2009.0208
59. Hannan NRF, Segeritz CP, Touboul T, Vallier L. Production of hepatocyte-like cells from human pluripotent stem cells. *Nat Protoc*. 2013;8(2):430-437. doi:10.1038/nprot.2012.153
60. Duan Y, Ma X, Zou WEI, et al. Differentiation and Characterization of Metabolically Functioning Hepatocytes from Human Embryonic Stem Cells. *Stem Cells*. 2010;28(4):674-686. doi:10.1002/STEM.315
61. Liu J, Cui Y, Shi L, Luan J, Zhou X, Han JA. A cellular model for Wilson's disease using patient-derived induced pluripotent stem cells revealed aberrant b-catenin pathway during osteogenesis. *Biochem Biophys Res Commun*. 2019;513(2):386-391. doi:10.1016/j.bbrc.2019.04.013
62. Bell CC, Lauschke VM, Vorrink SU, et al. Transcriptional, Functional, and Mechanistic Comparisons of Stem Cell-Derived Hepatocytes, HepaRG Cells, and Three-Dimensional Human Hepatocyte Spheroids as Predictive In Vitro Systems for Drug-Induced Liver Injury. *Drug Metabolism and Disposition*. 2017;45(4):419-429. doi:10.1124/DMD.116.074369
63. Ulvestad M, Nordell P, Asplund A, et al. Drug metabolizing enzyme and transporter protein profiles of hepatocytes derived from human embryonic and induced pluripotent stem cells. *Biochem Pharmacol*. 2013;86(5):691-702. doi:10.1016/J.BCP.2013.06.029
64. Kvist AJ, Kanebratt KP, Walentinsson A, et al. Critical differences in drug metabolic properties of human hepatic cellular models, including primary human hepatocytes, stem cell derived hepatocytes, and hepatoma cell lines. *Biochem Pharmacol*. 2018;155:124-140. doi:10.1016/J.BCP.2018.06.026
65. Yu Y, Liu H, Ikeda Y, et al. Hepatocyte-like cells differentiated from human induced pluripotent stem cells: Relevance to cellular therapies. *Stem Cell Res*. 2012;9(3):196-207. doi:10.1016/J.SCR.2012.06.004
66. Yu Y, Wang X, Nyberg SL. Potential and Challenges of Induced Pluripotent Stem Cells in Liver Diseases Treatment. *J Clin Med*. 2014;3(3):997. doi:10.3390/JCM3030997
67. Chen C, Soto-Gutierrez A, Baptista PM, Spee B. Biotechnology Challenges to In Vitro Maturation of Hepatic Stem Cells. *Gastroenterology*. 2018;154(5):1258-1272. doi:10.1053/j.gastro.2018.01.066
68. Kanninen LK, Porola P, Niklander J, et al. Hepatic differentiation of human pluripotent stem cells on human liver progenitor HepaRG-derived acellular matrix. *Exp Cell Res*. 2016;341(2):207-217. doi:10.1016/j.yexcr.2016.02.006

69. Kanninen LK, Harjumäki R, Peltoniemi P, et al. Laminin-511 and laminin-521-based matrices for efficient hepatic specification of human pluripotent stem cells. *Biomaterials*. 2016;103:86-100. doi:10.1016/j.BIOMATERIALS.2016.06.054
70. Bale SS, Borenstein JT. Microfluidic Cell Culture Platforms to Capture Hepatic Physiology and Complex Cellular Interactions. *Drug Metabolism and Disposition*. 2018;46(11):1638-1646. doi:10.1124/DMD.118.083055
71. Luo Y, Lou C, Zhang S, et al. Three-dimensional hydrogel culture conditions promote the differentiation of human induced pluripotent stem cells into hepatocytes. *Cytotherapy*. 2018;20(1):95-107. doi:10.1016/j.jcyt.2017.08.008
72. Pettinato G, Ramanathan R, Fisher RA, Mangino MJ, Zhang N, Wen X. Scalable Differentiation of Human iPSCs in a Multicellular Spheroid-based 3D Culture into Hepatocyte-like Cells through Direct Wnt/ β -catenin Pathway Inhibition. *Sci Rep*. 2016;6:32888. doi:10.1038/SREP32888
73. Gieseck RL, Hannan NRF, Bort R, et al. Maturation of Induced Pluripotent Stem Cell Derived Hepatocytes by 3D-Culture. *PLoS One*. 2014;9(1):e86372. doi:10.1371/JOURNAL.PONE.0086372
74. Lee JH, Lee JB, Shapovalova Z, et al. Somatic transcriptome priming gates lineage-specific differentiation potential of human-induced pluripotent stem cell states. *Nat Commun*. 2014;5(1):1-13. doi:10.1038/NCOMMS6605
75. Hu S, Zhao MT, Jahanbani F, et al. Effects of cellular origin on differentiation of human induced pluripotent stem cell-derived endothelial cells. *JCI Insight*. 2016;1(8):85558. doi:10.1172/JCI.INSIGHT.85558
76. Huch M, Gehart H, Van Boxtel R, et al. Long-term culture of genome-stable bipotent stem cells from adult human liver. *Cell*. 2015;160(1-2):299-312. doi:10.1016/j.cell.2014.11.050
77. Wang Z, Faria J, Penning LC, Masereeuw R, Spee B. Tissue-Engineered Bile Ducts for Disease Modeling and Therapy. *Tissue Eng Part C Methods*. 2021;27(2):59-76. doi:10.1089/ten.TEC.2020.0283
79. Roos FJM, Verstegen MMA, Muñoz Albarinos L, et al. Human Bile Contains Cholangiocyte Organoid-Initiating Cells Which Expand as Functional Cholangiocytes in Non-canonical Wnt Stimulating Conditions. *Front Cell Dev Biol*. 2021;8:630492. doi:10.3389/fcell.2020.630492
80. Rimland CA, Tilson SG, Morell CM, et al. Regional Differences in Human Biliary Tissues and Corresponding In Vitro-Derived Organoids. *Hepatology*. 2021;73(1):247-267. doi:10.1002/HEP.31252
81. Marsee A, Roos FJ, Verstegen MM, et al. Building consensus on definition and nomenclature of hepatic, pancreatic, and biliary organoids. *Cell Stem Cell*. 2021;28(5):816-832. doi:10.1016/j.stem.2021.04.005
82. Bezerra JA. Biliary Atresia-Translational Research on Key Molecular Processes Regulating Biliary Injury and Obstruction. *Chang Gung Med J*. 2006;29(3):222-230. Accessed January 11, 2021. <https://pubmed.ncbi.nlm.nih.gov/16924882/>



2

The potential and limitations of intrahepatic cholangiocyte organoids to study monogenic liver disorders

Vivian Lehmann, Imre F. Schene, A. Ibrahim Ardisasmita, Nalan Liv, Tineke Veenendaal, Judith Klumperman, Hubert P.J. van der Doef, Henkjan J. Verkade, Monique Versteegen, Luc J.W. van der Laan, Judith Jans, Nanda Verhoeven-Duif, Peter van Hasselt, Edward Nieuwenhuis, Bart Spee*, Sabine A. Fuchs*#

*Both authors contributed equally

#on behalf of United for Metabolic Diseases (UMD)

*Adapted from the original manuscript: The potential and limitations of intrahepatic cholangiocyte organoids to study inborn errors of metabolism. Published in: **Journal of Inherited Metabolic Disease** (2022) Oct;45(2):353-365. doi: 10.1002/JIMD.12450*

Abstract

Monogenic (metabolic) liver disorders comprise a diverse group of individually rare disorders that affect metabolic pathways and healthy cellular functioning. Mutations lead to enzymatic deficiency or dysfunction, which results in intermediate metabolite accumulation or deficit leading to disease phenotypes. Currently, treatment options for many monogenic liver disorders are insufficient. Rarity of individual monogenic liver disorders hampers therapy development and phenotypic and genetic heterogeneity suggest beneficial effects of personalized approaches. Recently, cultures of patient-own intrahepatic cholangiocyte organoids (ICOs) have been established. Since most metabolic genes are expressed in the liver, patient-derived ICOs represent exciting possibilities for *in vitro* modeling and personalized drug testing for monogenic liver disorders. However, the exact application range of ICOs remains unclear. To address this, we examined which metabolic pathways can be studied with ICOs and what the potential and limitations of patient-derived ICOs to model metabolic functions are. We present functional assays in patient ICOs with defects in branched-chain amino acid metabolism (methylmalonic acidemia), copper metabolism (Wilson disease) and transporter defects (cystic fibrosis). We discuss the broad range of functional assays that can be applied to ICOs, but also address the limitations of this patient-specific cell model. In doing so, we aim to guide the selection of the appropriate cell model for studies of a specific disease or metabolic process.

Introduction

Monogenic (metabolic) liver disorders comprise a broad category of disorders affecting metabolic pathways and healthy cellular functioning, with a cumulative prevalence of approximately 1 in 2,000 live births annually.¹⁻⁴ While current technological progress has increasingly improved early diagnosis of monogenic liver disorders, full mechanistic understanding and treatments beyond symptomatic approaches remain limited.⁵ To study monogenic liver disorders and address the urgent need for novel treatments,⁶ human *in vitro* models which recapitulate the patient's genetic make-up and tissue function are needed.

In recent years, organoids have been increasingly employed to model various organs.⁷⁻⁹ Organoids are three-dimensional (3D) cell cultures that can be established from liver progenitors, induced pluripotent stem cells or embryonic stem cells. Upon differentiation organoids recapitulate cellular and functional aspects of the organ of origin and have been proposed for use as preclinical tools for personalized medicine.¹⁰⁻¹⁴

In 2015, liver organoids were generated from patient-derived LGR5-positive bipotent cholangiocyte progenitors.⁵ To differentiate these organoids from other liver-derived organoids, they have been named intrahepatic cholangiocyte organoids (ICOs).^{8,15} ICOs recapitulate patients' individual genetic make-up, retain tissue specific functions without the need for genetic reprogramming, and can be differentiated toward hepatocyte-like cells. Moreover, ICOs are suitable for long-term culture, while remaining genetically stable.⁸

Patient derived ICOs have been used to phenotype human disease, including cancer, Alagille syndrome and alpha-1 antitrypsin deficiency.^{8,16-18} However, it has also become clear that not all liver functions are well reflected in ICOs.¹⁹ Thus, the question remains which metabolic categories and monogenic liver disorders can be studied with ICOs and whether ICOs represent advantages over other patient-derived cell models such as fibroblasts.

To address this, we investigated the potential and limitations of patient-derived ICOs to model metabolic functions. We describe the ease of establishing and expanding ICOs from small biopsies and present a range of functional assays that can be applied to ICOs. By also addressing current limitations in *in vitro* modeling, we hope to guide the selection process of the appropriate model to study monogenic liver disorders.

Materials & Methods

Organoid generation and culture

Liver tissue was obtained from explant tissue (0.5-1 cm³) or needle biopsies (~5 mm³) after patient informed consent. Use of patient tissue for our studies was ethically approved by the different collaborating University Centers (MEC-2014-060; STEM 1-402/K). Liver cells were isolated as described previously.⁸ Briefly, liver cells were isolated by mechanical fragmentation, followed by washing with cold AddMEM/F12 (Gibco) containing 1% (v/v) penicillin-streptomycin (Gibco), 1% (v/v) GlutaMax (Gibco), 10 mM HEPES (Gibco). Subsequently, the tissue was enzymatically digested in Hank's Balanced Salt Solution (Gibco) containing 0.25 mg/mL collagenase D, 0.1 mg/mL DNase I for 20 minutes at 37°C, centrifuged at 250 g at 4°C and supernatant removed. Throughout this process the digest was not filtered but plated for culture immediately. The pelleted digest was plated in 10 µl droplets of 70% (v/v) Matrigel™ (Corning) and cultured in seeding medium (SM) containing AddMEM/F12, 1% (v/v) penicillin-streptomycin, 1% (v/v) GlutaMax, 10 mM HEPES, 2% B27 without vitamin A (Gibco), 1.25 mM N-Acetylcysteine (Sigma), 10 mM nicotinamide (Sigma), 10 nM gastrin (Sigma), 10% RSPO1 (v/v) conditioned media (homemade), 50 ng/mL EGF (Peprotech), 100 ng/mL FGF10 (Peprotech), 25 ng/mL HGF (Peprotech), 5 mM A83-01 (Tocris), 10 mM forskolin (Tocris), 25 ng/mL Noggin (Peprotech), 30% (v/v) Wnt conditioned media (CM, homemade), 10 µM Y27632 (Sigma Aldrich) and 2 µM human embryonic stem cell cloning recovery solution (hES, Stemgent). All cultures were kept in a humidified atmosphere of 95% air and 5% CO₂ at 37°C and media were refreshed every other day. Once ICOs formed, Noggin, Wnt CM, Y27632 and hES were removed from the SM, now termed expansion medium (EM). ICO cultures were passaged 1:4 to 1:10 every 7-10 days by mechanical dissociation. For differentiation ICOs were pre-treated with 25 ng/mL BMP7 (Peprotech) for 3 days, whereafter media were changed to differentiation media (DM) containing AddMEM/F12 medium supplemented with, 1% B27, EGF (50 ng/mL), 1.25 mM N-Acetylcysteine, gastrin (10 nM), HGF (25 ng/mL), FGF19 (100 ng/mL, Peprotech), A8301 (500 nM), DAPT (10 µM, Selleckchem), BMP7 (25 ng/mL), and dexamethasone (30 µM, Sigma-Aldrich). After 8 days of differentiation ICOs were used for functional or gene expression analyses.

Immunohistochemistry

Wholemout immunohistochemistry on ICOs was performed as described,²⁰ using primary and secondary antibodies (Table S1-2). Briefly, prior to harvesting ICOs, cultures were incubated with Cell Recovery Solution (Corning) at 4°C for 30 minutes. Thereafter, ICOs were collected, briefly washed and the pellet was resuspended in 4% buffered formaldehyde (Klinipath) and incubated at room temperature (RT) for 45 minutes. Fixed ICOs were stored in 70% ethanol at 4°C until further use. Nuclei were stained with 0.5 µg/mL DAPI (Sigma-Aldrich). Imaging was performed on a Leica TCS SP8 confocal microscope.

LC-MS/MS

ICOs and culture media of one MMA patient and one healthy control were harvested and stored at -80°C until further use. Methanol was added to the culture medium to extract the acylcarnitines and free carnitine. For intracellular analyses ICOs were bullet blended in ice cold methanol. Stable isotope internal standards (D3-carnitine, D3-C4-carnitine, D3-C8-carnitine, D3-C16 carnitine) and acetonitrile were added, and samples were vortexed and centrifuged (5 minutes, 16000 g). The methanol eluate was evaporated under heated (40°C) nitrogen to dryness and butylated for 15 minutes at 60°C . Excess reagent was evaporated to dryness and residue was reconstituted in 100 μL acetonitrile. Concentrations of free carnitine and acylcarnitines were analyzed by flow injection using liquid chromatography (Alliance 2790, Waters) coupled to a Micromass QuattroUltima mass spectrometer (HPLC/MS/MS).²¹

Copper toxicity assay

ICOs of one healthy control and one Wilson disease patient were incubated with EM containing copper(II)chloride (CuCl_2) for 72 h. Cell viability was assessed by quantifying necrosis marker propidium iodide (0.1 mg/mL, Thermo- Fisher) and DNA marker Hoechst (5 $\mu\text{g}/\text{mL}$, Sigma-Aldrich) signals after 15 minutes of incubation at 37°C . For this, whole Matrigel™ droplets were imaged with an inverted Olympus IX53 epifluorescence microscope at 2x magnification and quantified in ImageJ software (Win64 version: <https://imagej.net/Fiji/Downloads>).

Forskolin-induced swelling assay

ICOs of one CFTR patient and three healthy controls were treated as described previously.¹⁸ Briefly, 1000 cells were seeded in 5 μL Matrigel™ droplets per well of a 96 wells plate and cultured for 3 days in EM with 10 μM Y27632. Thereafter, Y27632 and FSK were removed, and culture proceeded for 3 days. Next, ICOs were treated with calcein-AM (10 μM , Invitrogen) for 30 minutes at 37°C , 0-10 μM FSK was added and ICOs were analyzed by confocal live-cell microscopy (LSM710, Zeiss, 5x objective). For drug screening, patient ICOs were preincubated for 72 h with 15 μM of VX-809 (Selleck Chemicals LLC), while 15 μM of VX-770 (Selleck Chemicals LLC) was added just before analysis. For CFTR inhibition a combination of 50 μM CFTR_{inh}-172 (Sigma) and 50 μM GlyH-101 (Calbiochem) was added to respective conditions 3 hours before analysis. Forskolin-induced swelling (FIS) of ICOs was automatically determined by quantifying total ICO area relative to $t = 0$ with Volocity imaging software (Improvision). After correcting for the average area of 0 μM FSK, each condition was analyzed in triplicate to determine the average area under the curve (AUC) using Graphpad Prism.

RNA sequencing and analysis

Total RNA was isolated from two healthy control ICO cultures using Trizol LS reagent (Invitrogen) and stored at -80°C until further processing. ICO mRNA was isolated using Poly(A) Beads (NEXTflex). Sequencing libraries were prepared using the Rapid Directional RNA-Seq Kit (NEXTflex) and sequenced on a NextSeq500 (Illumina) to produce 75 base long reads (Utrecht DNA Sequencing Facility). Raw sequencing data of primary healthy fibroblasts (GSM1306659, GSM3146360, GSM3067785, GSM3067799) and healthy liver tissue (SAMN07109073, GSM3442821, GSM3442822) were obtained from the European Nucleotide Archive (ENA). Read mapping of all data sets was performed on the Galaxy web platform (usegalaxy.eu)²² using Gencode human reference genome sequence release 33 (GRCh38.p13), Gencode comprehensive gene annotation v33, and RNA STAR tool (Galaxy Version 2.7.2b). Read counts were obtained using the “--quantMode GeneCounts” option in STAR. Count normalization and variance-stabilizing transformation were performed using DESeq2 package (v. 1.30.1), followed by vst transformation and quantile normalization. PCA and pearson correlation analysis showed no observable study-specific batch effects (data not shown). Heatmaps were generated using pheatmap package (v. 1.0.12) in R (v3.6.3). The log₂ fold change relative to the mean expression of the genes across all fibroblast and ICO DM samples was determined. Finally, genes were sorted for best expression in DM ICOs and into metabolic categories based on categorizations of Vademecum Metabolicum, KEGG, Human Protein Atlas and Metabolic Atlas.²³⁻²⁵

Resin Electron microscopy (EPON)

Healthy control ICOs were fixed in half strength Karnovsky fixative (2.5% Glutaraldehyde (EMS), 2% Formaldehyde (Sigma), pH 7.4) at RT for 2 h. ICOs were rinsed and stored in 1M Phosphate Buffer (pH 7.4) at 4°C until further processing. Post-fixation was performed with 1% OsO₄, 1.5% K₃Fe(III)(CN)₆ in 1M Phosphate Buffer (pH 7.4) for 2 h. ICOs were then dehydrated in a series of acetone, and embedded in Epon (SERVA). Ultrathin sections were cut (Leica Ultracut UCT), collected on formvar and carbon coated transmission electron microscopy (TEM) grids, and stained with uranyl acetate and lead citrate (Leica AC20). Micrographs were collected on a JEM1010 (JEOL) equipped with a Veleta 2k×2k CCD camera (EMSIS, Munster, Germany) or on a Tecnai12 (FEI Thermo Fisher) equipped with a Veleta 2k×2k CCD camera (EMSIS, Munster, Germany) and operating SerialEM software.

Immuno-Electron microscopy

Healthy control ICOs of one donor were fixed by adding freshly-prepared 4% formaldehyde (Sigma-Aldrich) in 0.1 M phosphate buffer (pH 7.4) in the presence or absence of 0.2% glutaraldehyde (Polysciences Inc.) to an equal volume of culture medium. After 10 minutes fixative was refreshed to continue fixation for 2 h. Cells were stored in 1% formaldehyde at 4°C until further processing. Embedding,

ultrathin cryosectioning and immunogold labelling were performed as described.²⁶ In brief, fixed ICOs were washed with 0.05 M glycine in PBS, embedded in 12% gelatin in PBS, 37°C, solidified on ice and cut into small blocks. Cryoprotection was performed by infiltrating blocks overnight in 2.3 M sucrose at 4°C. Blocks were mounted on aluminum pins and frozen in liquid nitrogen. Ultrathin cryosections (60 nm) were cut (Leica EM UC7), transferred on TEM grids with a 1:1 mixture of 2.3 M sucrose and 1.8% methylcellulose, and immunolabelled using primary antibodies (Table S3). Primary antibodies were detected by Protein A conjugated to 10 nm or 15 nm gold particles (Cell Microscopy Core, Utrecht, The Netherlands). Pictures were collected on aJEM1010 (JEOL) equipped with a Veleta 2k×2k CCD camera (EMSIS) or on a Tecnai12 (FEI Thermo Fisher) running SerialEM software.²⁷ Quantifications of catalase labelled organelles of 2 cryosections per condition were performed in ImageJ (Win64 version: <https://imagej.net/Fiji/Downloads>).

Results

Organoid generation and culture

ICO generation is simple and can be achieved within 3-7 days (Figure 1A) from a biopsy of approximately 5 mm³. This small amount of tissue is often available from clinical procedures, without additional surgical intervention. Tissue can be dissociated and seeded for culture directly or be stored at 4°C up to 1 week or at -80°C in Recovery™ Cell Culture Freezing Medium (Gibco) for long-term storage prior to ICO generation (personal experience). Thereby exchange of tissue between different hospitals and research centers is facilitated. Tissue digests are cultured in Matrigel™ droplets, wherein progenitor cells self-organize into polarized ICOs within 3-7 days (Figure 1). Apical markers such as MDR1 localize to the inner membrane of the cystic ICO, while basolateral markers such as MRP3 localize to the basolateral domain. On average, ICO formation efficiency is 80-90% for both healthy and patient donors (Figure S1A). The majority reaches 90% confluency 7 days post isolation, with a variance of up to 2 weeks since a minority of donor ICOs performs poorly (Figure S1A). Once confluent, ICOs are removed from Matrigel™ and passaged at an average split ratio of 1:5, resulting in a full well plate three weeks post isolation (Figure 1A, Figure S1B). This quantity suffices for initial gene expression, histology and functional analyses, while remaining ICOs can be expanded further for biobanking, functional studies, genetic engineering and/or differentiation (Figure 1A).^{8,28} Throughout differentiation ICOs condense, displaying a thicker cell layer than in expansion medium (EM, Figure 1B), and hepatic characteristics such as albumin production, urea elimination and phase I enzyme activity increase.⁸

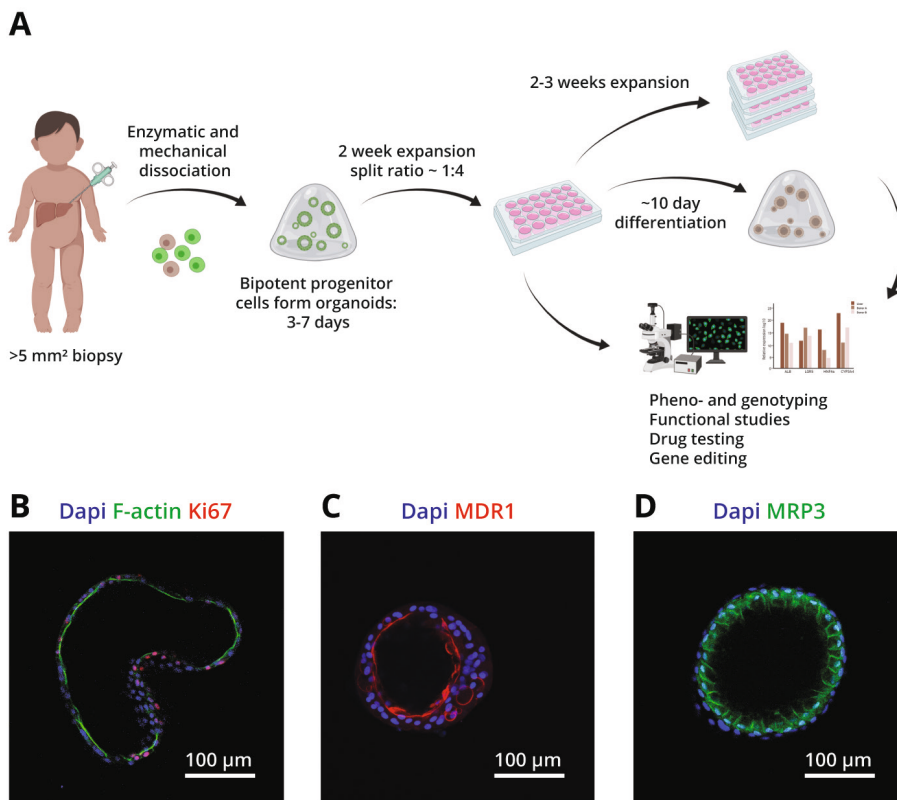


Figure 1. Overview of organoid generation, use and characteristics. **A)** Organoid generation from biopsy to *in vitro* culture can be achieved within 3 weeks, whereafter geno- and phenotyping, functional assays, drug testing, gene editing and/or differentiation can take place. **B)** Organoids express proliferation marker Ki67 and apical marker F-actin in expansion conditions (EM). After differentiation (DM), organoids condense and display more mature liver functions and stronger polarization, as exemplified by the apical transporter MDR1 and the basolateral transporter MRP3. Nuclear staining is shown with Dapi.

Metabolic processes and diseases to study in patient ICOs

ICOs have been shown to retain aspects of liver function *in vitro* such as glycogen storage and albumin secretion.⁸ We further investigated which general and liver metabolic functions can be studied with ICOs.

Basic metabolism

Basic metabolic processes such as amino acid and energy metabolism occur in various tissues throughout the body. One example is branched chain amino acid (BCAA) metabolism which is affected in patients suffering from organic acidemia, such as methylmalonic acidemia (MMA). Monogenic defects in the genes methylmalonyl-CoA mutase (*MMUT*, 609058), metabolism of cobalamin associated

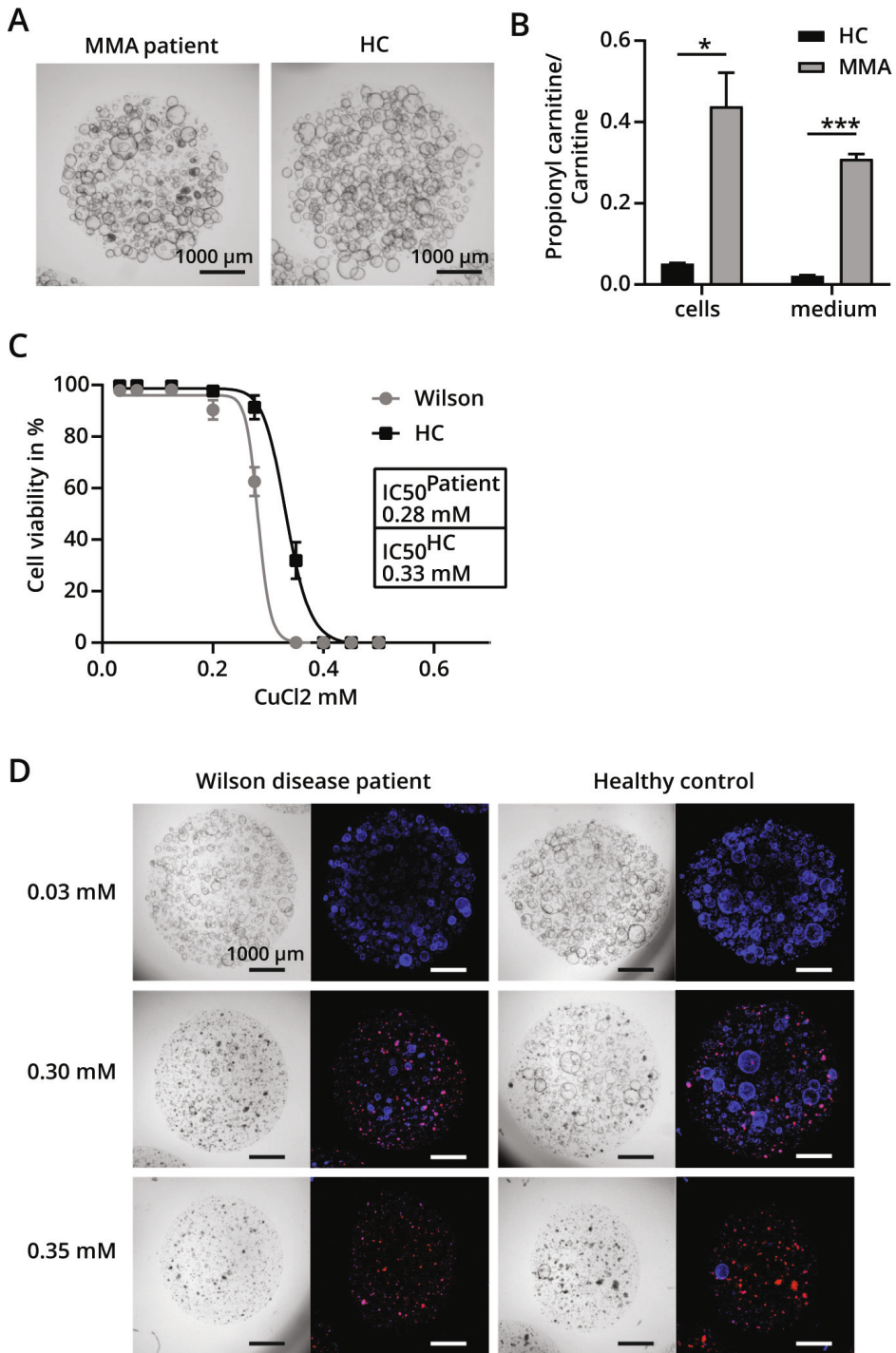
A (*MMAA*, 607481), B (*MMAB*, 607568), D (*MMADHC*, 611935), and methylmalonyl-CoA epimerase (*MCEE*, 608419) lead to disruption of the enzymatic chain that constitutes BCAA metabolism. Consequently, methylmalonic acid, propionic acid and respective carnitines accumulate in patient organs causing metabolic crisis, neurological symptoms, kidney failure and blindness.

As a proof of principle that basic metabolic processes can be studied in ICOs, we established ICOs from an MMA patient with homozygous *mut^o* mutations (c.1280G>T, p.Gly427Val). MMA patient and healthy control ICOs displayed similar growth rates and culture longevity (Figure 2A). LC-MS/MS acylcarnitine analysis of expanded ICOs cells and culture media revealed significantly increased propionylcarnitine concentrations in patient ICOs and media compared to controls (Figure 2B, Figure S1C, D). However, methylmalonylcarnitine was not detectable in patient and control ICOs (Figure S1C, D), which may reflect insufficient sensitivity of our assay because methylmalonylcarnitine concentrations in plasma from MMA patients can be 50-fold lower than propionylcarnitine concentrations (personal experience). Propionylcarnitine is an intermediate product in the BCAA metabolism upstream from methylmalonyl-coenzyme A mutase and is used as a clinical biomarker.^{29,30} Our results suggest that ICOs could serve to study basic metabolic functions such as BCAA metabolism using routine LC-MS/MS analyses.

Liver specific metabolism

Other metabolic processes, such as metal- and drug-metabolism, are liver specific. Wilson disease (277900) represents a genetic defect in copper metabolism. Mutations in the gene ATPase copper transporting beta (*ATP7B*, 606882) lead to accumulation of toxic amounts of copper in the liver. Patients currently rely on life-long symptomatic treatment. Therapy development would benefit from organ and patient specific models that can model the more than 500 different known mutations in *ATP7B*.³¹

Therefore, we investigated copper metabolism in patient ICOs (c.[1288dup(;);1288dup] p.[(Ser430Lysfs*5)(;)(Ser430Lysfs*5)]). Under normal culture conditions no morphological, growth rate, nor longevity differences were observed between healthy control and Wilson disease patient ICOs (Figure 2D, 0.03 mM CuCl₂). However, patient ICOs showed increased sensitivity to copper treatment, with an IC₅₀ of 0.28 mM CuCl₂ compared to 0.33 mM in healthy control ICOs (Figure 2C-D). Putatively, similar storage diseases may be phenotyped with ICOs through provision of relevant substrates.



← **Figure 2. Functional assays revealing disease phenotypes in patient ICOs.** **A)** Representative cultures of MMA patient and HC ICOs under EM. **B)** Branched-chain amino acid metabolism defect exemplified by significantly increased propionylcarnitine to carnitine ratio in ICOs of an MMA patient (n = 2; *, p-value = 0.0221 in cells; ***, p-value = 0.0009 in medium). **C)** Copper metabolism defect exemplified by increased sensitivity to copper (CuCl₂) toxicity in ICOs of a Wilson disease patient compared to a HC after 72 hours of exposure (n = 12). **D)** Brightfield and IF images of the viability assay in **C** showing key concentrations of CuCl₂. Red signal corresponds to necrosis marker propidium iodide; blue signal indicates DNA. EM, expansion condition; HC, healthy control; ICO, intrahepatic cholangiocyte organoid; MMA, methylmalonic acidemia

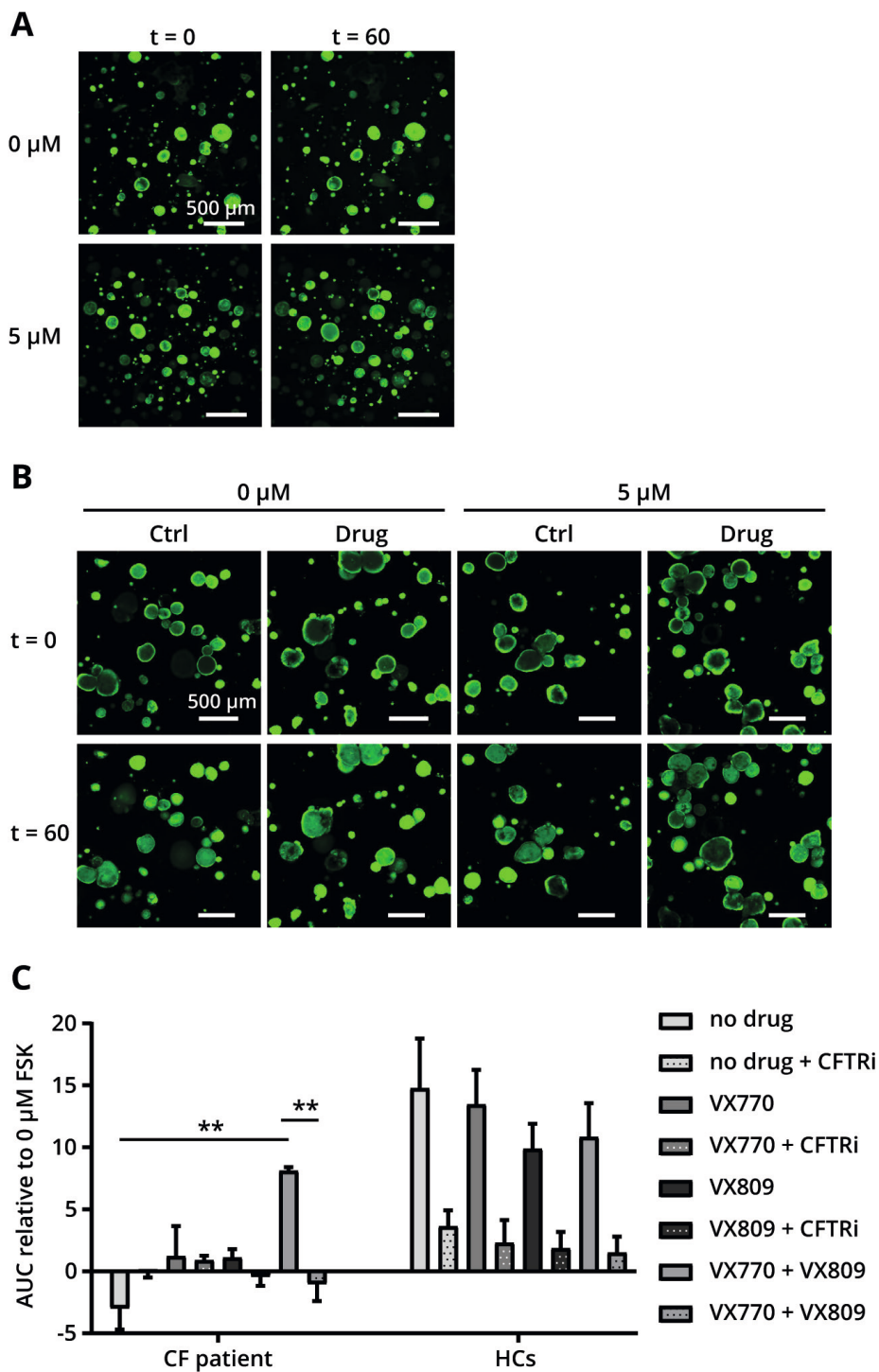
Functions dependent on 3D structure

Substrate and waste product transport across cells is crucial for many physiologic processes, including bile and mucus metabolism. This process is affected in cystic fibrosis (CF, 219700), a disease caused by mutations in the gene encoding for the cystic fibrosis transmembrane conductance regulator (CFTR).³² This transmembrane protein transports chloride ions to aid in mucus and bile homeostasis. Mutations of the *CFTR* gene (602421) are highly heterogeneous across the population and so are responses to different treatment strategies. Organoids are highly suitable for studying effects of individual *CFTR* mutations due to their patient-specific origin, unique 3D constellation and polarity. Substrate and waste product transport across the cell can easily be studied in organoids due to the separated inner apical and outer basolateral domain (Figure 1B). Intestinal organoids are already used to predict medication response for patients using the forskolin-induced swelling (FIS) assay.¹⁸ Bile excretion from hepatocytes into bile canaliculi reflects a similar process, which is affected in some CF patients and many patients with intrahepatic cholestasis.

We investigated apical transport and medication response in ICOs from a CF patient compound heterozygous for F508del (c.1521_1523delCTT, p.Phe508del) and R1162X (c.3484C>T, p.Arg1162X)(Figure 3). CF patient ICOs showed impaired swelling in response to forskolin exposure, which corresponds to increased bile viscosity as observed in CF patients. This phenotype was rescued by addition of the corrector and potentiator combination VX809-770. Using similar approaches, other apical or basolateral functions may also be tested in ICOs.

Metabolic functions not detected in ICO cultures

For some cellular and metabolic functions ICOs appear less suitable. We experienced this for cytosolic aminoacyl-tRNA synthetase (ARS) deficiencies, an increasingly recognized group of diseases with varying clinical phenotypes. To investigate disease mechanism and improve treatment strategies we established ICOs from a patient with isoleucyl-tRNA synthetase (*IARS*, 600709, c.1305G>C (p.Trp435Cys), c.3377dup (p.Asn1126fs)) deficiency. The most prominent clinical phenotype of patients, namely dysmaturity and severe failure to thrive,³³ was closely recapitulated by these ICOs. Concurrently, not enough ICOs could be generated to perform functional assays



← **Figure 3. Functional assays revealing CF phenotypes in patient ICOs.** Impaired apical transport can be studied in ICOs as exemplified by defect and rescued CFTR function in ICOs of a Cystic fibrosis patient. Green color = intracellular calcein. **A-B)** Representative images of CF patient (**B**) and HC (**A**) ICO swelling. **C)** AUC of CF patient (n = 3) and HC (n = 6) ICO swelling with or without the drugs VX809 and VX-770 (**, p-value < 0.0031) and with or without CFTR inhibitor (**, p-value < 0.0028). AUC, area under the curve; CF, cystic fibrosis; CFTR, cystic fibrosis transmembrane conductance regulator; ctrl, control; EM, expansion condition; FSK, forskolin; HC, healthy control; ICO, intrahepatic cholangiocyte organoid; t, time

(Figure S1B, E, F). Thus, faithful disease modeling hampered the use of IARS deficient ICOs for unravelling the disease mechanism. Conversely, patient fibroblast growth was sufficient to devise a treatment strategy which was successfully translated to the clinics.³⁴ This indicates that, for some monogenic liver disorders, alternative patient-derived cell models should be explored if patient ICOs do not meet the practical requirements, such as expression of genes of interest and cell growth, to unravel disease mechanisms.

Moreover, we anticipate that hyperoxaluria type 1 (PH1, 259900), caused by mutations in the gene alanine-glyoxylate aminotransferase (*AGXT*, 604285), cannot be studied in ICOs, since *AGXT* is not expressed in healthy ICOs under current culturing conditions (Figure S2D).

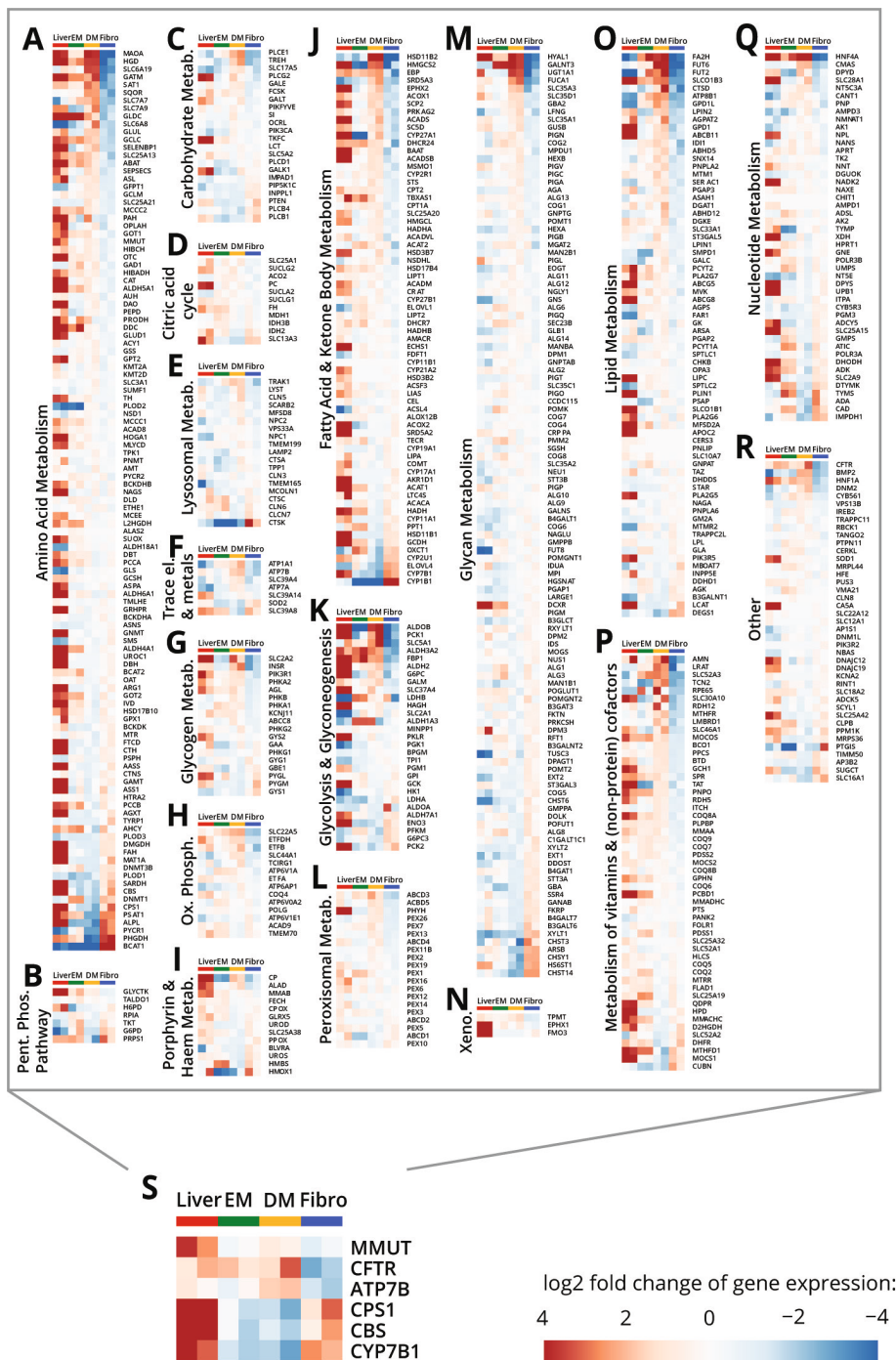
To gain broader insight in the metabolic functions that can be studied in ICOs, we investigated the geno- and phenotype of ICOs in more detail.

Expression of genes involved in monogenic liver disorders

Bulk RNA sequencing (RNAseq) was analyzed for expression of genes involved in monogenic liver disorders using the Radboudumc Exome panel for metabolic disorders.³⁵ Healthy ICO data were compared to whole liver and fibroblasts, the latter of which is the most commonly used *in vitro* model for monogenic liver disorders.^{1,36-39}

We found a great variety in ICO gene expression, confirming our previous notion that ICOs are a suitable *in vitro* model for a specific selection of metabolic categories (Figure 4, Figure S2A-D). Interestingly, this variation was also observed within each metabolic category of ICOs and fibroblasts. Neither model expressed more than 60% of the panel genes of any metabolic category well (Figure S2A). Good gene expression in ICOs was frequently paired with poor expression in fibroblasts and vice versa (Figure 4, Figure S2B). This insight could facilitate decision making for future studies.

Nonetheless, expression of 30% of all panel genes was higher in ICOs than fibroblasts (Figure S2A). These genes constitute a variety of metabolic categories, including



← **Figure 4. Visualizations of log₂ fold changes in gene expression of genes affected in monogenic liver disorders** in expanded (EM, n = 2) and differentiated (DM, n = 2) ICOs, fibroblasts (Fibro, n = 2) and whole liver tissue (n = 2). log₂ fold changes are relative to the mean expression of the genes across all fibroblast and ICO DM samples. Exome panel genes are divided into metabolic categories Amino Acid Metabolism (**A**), Pentose Phosphate Pathway (**B**), Carbohydrate Metabolism (other) (**C**), Citric acid cycle (**D**), Lysosomal Metabolism (**E**), Trace element and Metal Metabolism (**F**), Glycogen Metabolism (**G**), Oxidative Phosphorylation (**H**), Porphyrin and Haem Metabolism (**I**), Fatty Acid and Ketone Body Metabolism (**J**), Glycolysis and Glyconeogenesis (**K**), Peroxisomal Metabolism (**L**), Glycan Metabolism (**M**), Xenobiotics Metabolism (**N**), Lipid Metabolism (**O**), Metabolism of vitamins and (non-protein) cofactors (**P**), Nucleotide Metabolism (**Q**), Other (**R**). **S**) Example genes better expressed in ICOs or fibroblasts. ICO, intrahepatic cholangiocyte organoid

oxidative phosphorylation, metal, and amino acid metabolism (Figure 4, Figure S2B). For example, expression of *MMUT*, *CFTR*, and *ATP7B* in ICOs was comparable to that in the liver, whereas fibroblasts displayed lower expression (Figure 4A, F, R, S). This suggests that ICOs are suitable to study diseases related to these genes, as confirmed by our functional assays (Figure 2-3).

In fibroblasts 22% of all panel genes were better expressed than in ICOs (Figure S2A). Examples include *CPS1*, *CBS* and *CYP7B1* (Figure 4A, J, S). Poor expression of *CPS1* and *CBS* in ICOs highlights that ICOs fail to represent certain liver-specific functions despite being derived from this organ. This led us to investigate the cell characteristics of ICOs using electron microscopy.

ICO cell morphology and organelles

Several metabolic functions depend on specific cell organelles (Figure 5A). Hence, ICOs should exhibit all organelles necessary for the function to be studied.

Transmission electron microscopy (TEM) analysis showed that healthy ICO cells in EM and differentiation media (DM) have a nucleus, mitochondria, golgi, lysosomes, rough endoplasmic reticulum, and villi (Figure 5B, C). Catalase-stained peroxisomes were identified in both conditions (Figure 5D). However, catalase signals in DM were mostly found in golgi-budding vesicles which could not be found in EM or control HepG2 cells, thus suggesting immature peroxisomes in DM. Peroxisomes in EM and DM ICOs were significantly smaller than in HepG2 cells, a cell model widely viewed to have high morphological similarity to primary human hepatocytes (Figure S3A, B).

Notably, EM ICO cells displayed some liver functionality as they contained glycogen rosettes. Moreover, desmosomes and interdigitations between cells and more compact villi facing ICO lumen indicate apical domains needed for bile salt secretion (Figure S3C). In contrast, the basolateral domain appeared smooth and without villi, concurring with immunofluorescence analyses (Figure 1B).

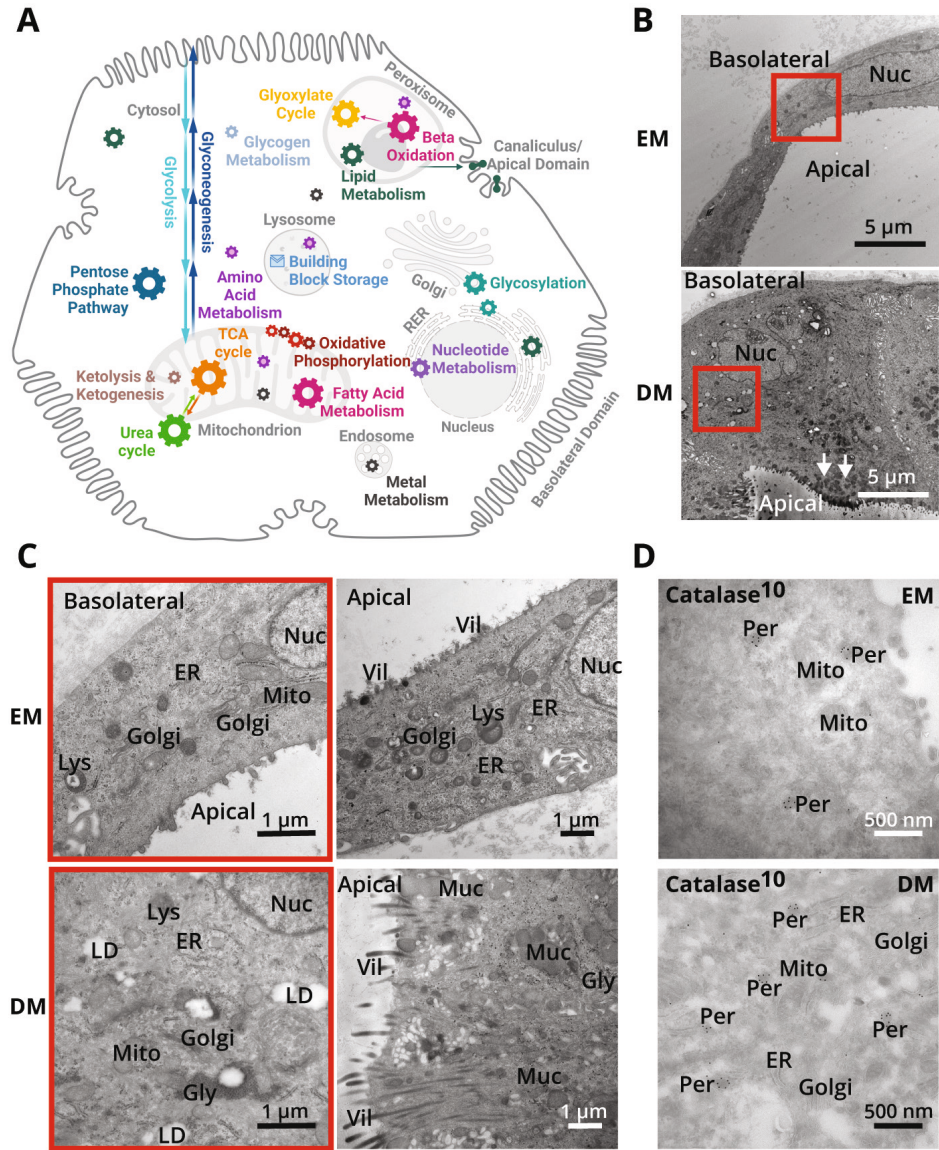


Figure 5. **A)** schematic representation of a hepatocyte showing metabolic functions and approximate organelle locations. Organelle sizes not to scale. **B)** TEM images of HC ICO cells in EM and DM displaying differences in ICO wall thickness. Arrows indicate mucus fields. Red squares indicate magnification regions shown in **C**. **C)** TEM images of HC ICO cells in EM and DM displaying the major organelles visible in these cells (left), mucus and villi presence (middle). **D)** Immunoelectron microscopy images of catalase-stained peroxisomes of HC ICO cells in EM and DM. TEM, transmission electron microscopy; DM, differentiation condition; EM, expansion condition; Gol, golgi; Gly, glycogen rosettes; Lys, lysosomes; Mit, mitochondria; Nuc, nucleus; Per, peroxisomes; ER, endoplasmic reticulum; Vil, villi.

Interestingly, differentiation induced formation of large mucus fields, located towards the apical domain (Figure 5B). Apical villi in DM ICOs appeared slightly longer and were organized in bundles, putatively to make way for mucus secretion, as would be compatible with biliary rather than hepatic differentiation (Figure 5C, middle). Moreover, DM cells showed more lipid droplets compared to EM (Figure 5C, Figure S3C). Occasionally, we found DM cells with less mucus and shorter, more compact villi. Together with the variable transcriptome profile, ICOs appear to undergo heterogenic maturation with current DM, showing cholangiocyte and hepatic characteristics.

Discussion

Mechanistic studies and treatment development for rare diseases are limited by the small number and geographic distribution of patients. Recently developed organoid models promise exciting possibilities for patient-specific preclinical studies. However, it is currently unknown for which specific metabolic functions and diseases ICOs can be effectively used. To address this, we present our experience with ICOs and evaluate the potential and limitations of patient-derived ICOs to study metabolic functions.

We show that ICOs can be used to study basic metabolism, more specific hepatic functions, and transport functions, exemplified, respectively, by pathways of BCAA metabolism, copper metabolism and chloride transport. We noticed that gene expression in ICOs and fibroblasts varied within each metabolic category. Cell model choice should be done case by case with focus on the gene/pathway of interest. ICO transcriptome variance was supported by TEM analysis which revealed that ICOs are composed of intermediate cell types with progenitor cell, hepatic and biliary characteristics. Likely, the cells' ductal origin as well as the environmental stimuli offered to ICOs promote this intermediary cell type. Indeed, it is well known that environmental stimuli affect cell fate.⁴⁰⁻⁴⁴ Adjustments in differentiation media and hydrogel composition could favor expression of some as of yet absent metabolic functions. We and other research groups are currently exploring different approaches to achieve improved separate hepatic or cholangiocyte differentiation of ICOs.⁴¹ We anticipate new insights to arise and be adopted widely in the coming decade. Until then, this paper addresses the recurring queries on ICO use for current clinical and research questions.

Several cell models are available for research of monogenic liver disorders, including ICOs, fibroblasts, cell lines, primary hepatocytes and induced pluripotent stem cells (Table 1). Most of these cell models are suitable for personalized medicine approaches and biobanking. Cell model choice will depend on the specific study

goal, availability of patient cells through skin and/or liver biopsy, representation of metabolic function, costs and expertise. Although ICOs require some expertise and investment, they score high for other categories. ICOs not only express a variety of genes affected in monogenic liver disorders, but time to first assay and ease of handling are additional advantages. Moreover, ICO culture is versatile; both long-term three-dimensional and two-dimensional transwell cultures are possible, as previously reported for gut organoids.⁴⁵

Moreover, ICO generation and differentiation does not require genetic reprogramming or immortalization.^{46,47} Previous *in vitro* copper metabolism studies were performed in genetically induced fibroblasts or embryonic stem cells.⁴⁸⁻⁵⁰ We show this can also be done in ICOs which retain the original patient genome.^{8,47,51} Further studies are needed to determine applicability of Wilson disease ICOs for personalized drug testing.^{52,53}

To study basic metabolism, a hepatic phenotype is not required. Although transcriptome analysis favors ICOs to study methylmalonic acidemia (MMA; Figure 3, Figure S2B, C), several studies have reported successful phenotyping of MMA in patient fibroblasts and immortalized kidney tubule cells, derived from patient urine.⁵⁴⁻⁵⁶ This illustrates that lower expression of genes does not necessarily result in absence of a disease phenotype. In ICOs derived from MMA patients, we discerned significantly increased concentrations of the clinical biomarker propionylcarnitine, which represents a first step toward studying MMA treatment response in a personalized setting in ICOs.

Table 1. Comparison of various cell models for *in vitro* modelling of monogenic liver disorders

	ICOs	Fibroblasts	Liver cell lines	PHH	iPSCs
2D culture	+	+	+	+	+
3D culture	+	-	-	-	+/-
Personalized medicine	+	+	-	+/-	+
Long-term cultures	+	+	+	-	+
Biobanking potential	+	+	+	+/-	+
Ease of handling / assays	+	+	+	-	-
Time to first assays	3 weeks	6 weeks	immediate	<1 week	6 weeks
Culturing costs/expertise	high	low	low	intermediate	high
Hepatocyte functions	+/-	-	+	++	+/-
Cholangiocyte functions	+/-	-	-	-	+/-
Functions affected by disease	+/-	+/- -	++/-	++/-	+/-

Abbreviations: iPSCs, induced pluripotent stem cells; PHH, primary human hepatocytes; +, applicable; ++, very applicable; -, not applicable; (+)+/(-), applicable with limitations, while ++ and - - indicate better or worse; 2D, two-dimensional; 3D, three-dimensional.

Importantly, ICO differentiation capacity varies between donors. It is currently unclear whether this relates to a specific biopsy, isolation or a donor's genetic background or age. It has been shown that extrahepatic cholangiocyte progenitors cannot differentiate to hepatocytes, indicating that the location of cholangiocyte progenitors is crucial for their differentiation potential.^{57,58} Yet, this interdonor variability does not hamper studying intradonor differences after treatment.

When patient material is scarce, patient mutations may be introduced in cells.⁴⁸ Current CRISPR-based technologies are also applicable to ICOs.^{28,59,60} Moreover, mechanistic insight can be achieved by editing different genes in a pathway. Evidently, artificial ICO models of monogenic liver disorders may be helpful in investigating the gene in isolation, but not for personalized strategies.

Complete absence of a key pathway gene is likely to hamper studies thereof. For example, we expect oxalate metabolism studies in ICOs to be impeded by absence of expression of the peroxisomal *AGXT* gene. Peroxisomal assembly genes such as the *PEX*, *PPAR* and *ABCD* families were well expressed, suggesting availability of peroxisome machinery in ICOs. In contrast, electron microscopy analysis revealed a reduced peroxisome size. Peroxisome biogenesis is highly plastic and dependent on nutrient availability and culture confluency.⁶¹⁻⁶⁵ This has been shown for HepG2 peroxisomes which transiently become tubular rather than spherical during periods of rapid growth.⁶⁴ The smaller peroxisomes in ICOs might represent this transient morphology in peroxisome biogenesis. Provision of relevant substrates in culture media as well as improved differentiation conditions might promote peroxisome maturation and expression of as of yet absent genes.

Initially ICOs were described as a liver model to study specific hepatic functions. Concurrently, ICOs were shown to eliminate urea, metabolize drugs and secrete albumin.^{8,16,17} ICOs are derived from bi-potent cholangiocyte progenitors, but current methods do not suffice to generate a pure population of mature hepatocytes. With current methods, ICOs are suitable for studying a selection of basic, hepatic and cholangiocyte metabolic functions. Prior to using ICOs for a specific research question, expression of the corresponding pathway and/or function should be considered. If the full spectrum of mature hepatic functions is required, a different cell model is more suitable.

Recently, hepatocyte organoids were established from fetal hepatocytes.⁶⁶ These showed an improved hepatic phenotype compared to ICOs. We anticipate that generation of hepatocyte organoids from pediatric and adult tissue will provide an improved hepatic patient-specific *in vitro* model and will fill some gaps in patient-related research on monogenic liver disorders.

To conclude, we provide an overview of metabolic functions and monogenic liver disorders which can be studied with ICOs. The presence of mitochondria, lysosomes and the ER combined with good gene expression in energy, amino acid and lipid metabolism suggest that ICOs are suitable to study related functions and diseases. Furthermore, the three-dimensional nature of ICOs renders the model highly suitable for transepithelial transport studies. We present several functional assays with which to study drug responses preclinically. This is especially relevant for monogenic liver disorders where global patient numbers and geographic distribution do not allow for standard clinical drug testing. Our transcriptome data may be of help to decide whether ICOs are a suitable model for a specific research question. For diseases that can currently not be studied with ICOs, we anticipate that improved culturing conditions and/or adult hepatocyte organoids will be available in the near future.

Authorship statement

I collated information on existing patient ICOs and preliminary transcriptomic and functional studies performed by colleagues. I extended this work by designing additional studies, generated new data, performed data management, and conducted the data analysis and interpretation for most parts. LC-MS/MS and TEM were performed by TV and NL, while AIA (PhD candidate) performed the bioinformatics analyses. I wrote the first draft of the manuscript and implemented the contributions of the co-authors and external reviewers up to the final publication. During the whole process I asked for and implemented input and feedback from the other contributors to this study.

References

1. Ferreira CR, van Karnebeek CDM, Vockley J, Blau N. A proposed nosology of inborn errors of metabolism. *Genetics in Medicine*. 2019;21(1):102-106. doi:10.1038/s41436-018-0022-8
2. Waters D, Adeyoye D, Woolham D, Wastnedge E, Patel S, Rudan I. Global birth prevalence and mortality from inborn errors of metabolism: A systematic analysis of the evidence. *J Glob Health*. 2018;8(2):021102. doi:10.7189/jogh.08.021102
3. Stalke A, Skawran B, Auber B, et al. Diagnosis of monogenic liver diseases in childhood by next-generation sequencing. *Clin Genet*. 2018;93(3):665-670. doi:10.1111/CGE.13120
4. Vaisitti T, Peritore D, Magistroni P, et al. The frequency of rare and monogenic diseases in pediatric organ transplant recipients in Italy. *Orphanet J Rare Dis*. 2021;16(1):1-17. doi:10.1186/s13023-021-02013-x
5. Stenton SL, Prokisch H. Genetics of mitochondrial diseases: Identifying mutations to help diagnosis. *EBioMedicine*. 2020;56:102784. doi:10.1016/j.ebiom.2020.102784
6. Tarasenko TN, Mcguire PJ. The liver is a metabolic and immunologic organ: A reconsideration of metabolic decompensation due to infection in inborn errors of metabolism (IEM). *Mol Genet Metab*. 2017;121:283-288. doi:10.1016/j.ymgme.2017.06.010
7. Sato T, Vries RG, Snippert HJ, et al. Single Lgr5 stem cells build crypt-villus structures in vitro without a mesenchymal niche. *Nature*. 2009;459(7244):262-265. doi:10.1038/NATURE07935
8. Huch M, Gehart H, Van Boxtel R, et al. Long-term culture of genome-stable bipotent stem cells from adult human liver. *Cell*. 2015;160(1-2):299-312. doi:10.1016/j.cell.2014.11.050
9. Lancaster MA, Renner M, Martin CA, et al. Cerebral organoids model human brain development and microcephaly. *Nature*. 2013;501(7467):373-379. doi:10.1038/NATURE12517
10. Huch M, Koo BK. Modeling mouse and human development using organoid cultures. *Development*. 2015;142(18):3113-3125. doi:10.1242/DEV.118570
11. Fatehullah A, Tan SH, Barker N. Organoids as an in vitro model of human development and disease. *Nature Cell Biology* 2016 18:3. 2016;18(3):246-254. doi:10.1038/NCB3312
12. Nagle PW, Coppes RP. Current and Future Perspectives of the Use of Organoids in Radiobiology. *Cells*. 2020;9(12):2649. doi:10.3390/cells9122649

13. Kim J, Koo BK, Knoblich JA. Human organoids: model systems for human biology and medicine. *Nat Rev Mol Cell Biol.* 2020;21(10):571-584. doi:10.1038/s41580-020-0259-3
14. Clevers H. Modeling Development and Disease with Organoids. *Cell.* 2016;165(7):1586-1597. doi:10.1016/j.cell.2016.05.082
15. Marsee A, Roos FJ, Versteegen MM, et al. Building consensus on definition and nomenclature of hepatic, pancreatic, and biliary organoids. *Cell Stem Cell.* 2021;28(5):816-832. doi:10.1016/j.stem.2021.04.005
16. Gómez-Mariano G, Matamala N, Martínez S, et al. Liver organoids reproduce alpha-1 antitrypsin deficiency-related liver disease. *Hepatol Int.* 2020;14(1):127-137. doi:10.1007/s12072-019-10007-y
17. Nuciforo S, Heim MH. Organoids to model liver disease. *JHEP Reports.* 2020;3(1):100198. doi:10.1016/j.jhepr.2020.100198
18. Dekkers JF, Wiegerinck CL, De Jonge HR, et al. A functional CFTR assay using primary cystic fibrosis intestinal organoids. *Nat Med.* 2013;19(7):939-945. doi:10.1038/nm.3201
19. Ardisasmita AI, Schene IF, Joore IP, et al. A comprehensive transcriptomic comparison of hepatocyte model systems improves selection of models for experimental use. *Commun Biol.* 2022;5(1):1094. doi:10.1038/s42003-022-04046-9
20. Dekkers JF, Alieva M, Wellens LM, et al. High-resolution 3D imaging of fixed and cleared organoids. *Nat Protoc.* 2019;14(6):1756-1771. doi:10.1038/s41596-019-0160-8
21. De Sain-Van Der Velden MGM, Diekman EF, Jans JJ, et al. Differences between acylcarnitine profiles in plasma and bloodspots. *Mol Genet Metab.* 2013;110(1-2):116-121. doi:10.1016/j.ymgme.2013.04.008
22. Afgan E, Baker D, Batut B, et al. The Galaxy platform for accessible, reproducible and collaborative biomedical analyses: 2018 update. *Nucleic Acids Res.* 2018;46(W1):W537-W544. doi:10.1093/nar/gky379
23. The Human Protein Atlas. Accessed May 26, 2021. <https://www.proteinatlas.org/>
24. Zschocke J, Hoffmann GF. *Vademecum Metabolicum*. 3rd ed. (Karnebeek C van, Lee J, Houben R, eds.). Milupa Metabolics GmbH; 2011.
25. Metabolic Atlas. Accessed May 26, 2021. <https://metabolicatlas.org/>
26. Slot JW, Geuze HJ. Cryosectioning and immunolabeling. *Nat Protoc.* 2007;2(10):2480-2491. doi:10.1038/nprot.2007.365
27. Mastrorarde DN. Automated electron microscope tomography using robust prediction of specimen movements. *J Struct Biol.* 2005;152(1):36-51. doi:10.1016/j.jsb.2005.07.007
28. Schene IF, Joore IP, Oka R, et al. Prime editing for functional repair in patient-derived disease models. *Nat Commun.* 2020;11(1):1-8. doi:10.1038/s41467-020-19136-7
29. Haijes HA, Willemsen M, van der Ham M, et al. Direct infusion based metabolomics identifies metabolic disease in patients' dried blood spots and plasma. *Metabolites.* 2019;9(1):12. doi:10.3390/metabo9010012
30. Haijes HA, Jans JJM, Van Der Ham M, Van Hasselt PM, Verhoeven-Duif NM. Understanding acute metabolic decompensation in propionic and methylmalonic acidemias: A deep metabolic phenotyping approach. *Orphanet J Rare Dis.* 2020;15(1):68. doi:10.1186/s13023-020-1347-3
31. Kenney SM, Cox DW. Sequence Variation Database for the Wilson Disease Copper Transporter, ATP7B. *Hum Mutat.* 2007;28(12):1171-1177. doi:10.1002/humu.20586

32. Rafeeq MM, Murad HAS. Cystic fibrosis: Current therapeutic targets and future approaches. *J Transl Med*. 2017;15(1):84. doi:10.1186/s12967-017-1193-9
33. Fuchs SA, Schene IF, Kok G, et al. Aminoacyl-tRNA synthetase deficiencies in search of common themes. *Genetics in Medicine*. 2019;21(2):319-330. doi:10.1038/s41436-018-0048-y
34. Kok G, Tseng L, Schene IF, et al. Treatment of ARS-deficiencies with specific amino acids. *Genetics in Medicine*. 2021;23(11):2202-2207. doi:10.1038/s41436-021-01249-z
35. Exome sequencing diagnostics - Radboudumc. Accessed May 29, 2023. <https://www.radboudumc.nl/en/patient-care/patient-examinations/exome-sequencing-diagnostics/exomepanelspreviousversions/exomepanelspreviousversions/metabolic-disorders>
36. Cameron JM, Levandovskiy V, Mackay N, Robinson BH. Respiratory chain analysis of skin fibroblasts in mitochondrial disease. *Mitochondrion*. 2004;4:387-394. doi:10.1016/j.mito.2004.07.039
37. Ferreira CR, Gahl WA. Lysosomal storage diseases. *Transl Sci Rare Dis*. 2017;2:1-71. doi:10.3233/TRD-160005
38. Soiferman D, Saada A. The Use of Fibroblasts from Patients with Inherited Mitochondrial Disorders for Pathomechanistic Studies and Evaluation of Therapies. In: V.K. Gribkoff, E.A. Jonas, J.M. Hardwick, eds. *The Functions, Disease-Related Dysfunctions, and Therapeutic Targeting of Neuronal Mitochondria*. John Wiley; 2015:378-398. doi:10.1002/9781119017127.ch18
39. Diekman EF, Ferdinandusse S, Van Der Pol L, et al. Fatty acid oxidation flux predicts the clinical severity of VLCAD deficiency. *Genetics in Medicine*. 2015;17(12):989-994. doi:10.1038/gim.2015.22
40. Jaramillo M, Yeh H, Yarmush ML, Uygun BE. Decellularized human liver extracellular matrix (hDLM)-mediated hepatic differentiation of human induced pluripotent stem cells (hiPSCs). *J Tissue Eng Regen Med*. 2018;12(4):e1962-e1973. doi:10.1002/term.2627
41. Chen C, Soto-Gutierrez A, Baptista PM, Spee B. Biotechnology Challenges to In Vitro Maturation of Hepatic Stem Cells. *Gastroenterology*. 2018;154(5):1258-1272. doi:10.1053/j.gastro.2018.01.066
42. McClelland R, Wauthier E, Uronis J, Reid L. Gradients in the liver's extracellular matrix chemistry from periportal to pericentral zones: Influence on human hepatic progenitors. *Tissue Eng Part A*. 2008;14(1):59-70. doi:10.1089/ten.a.2007.0058
43. Wouters OY, Ploeger DTA, van Putten SM, Bank RA. 3,4-Dihydroxy-L-Phenylalanine as a Novel Covalent Linker of Extracellular Matrix Proteins to Polyacrylamide Hydrogels with a Tunable Stiffness. *Tissue Eng Part C Methods*. 2016;22(2):91-101. doi:10.1089/ten.tec.2015.0312
44. Brill S, Zvibel I, Halpern Z, Oren R. The role of fetal and adult hepatocyte extracellular matrix in the regulation of tissue-specific gene expression in fetal and adult hepatocytes. *Eur J Cell Biol*. 2002;81(1):43-50. doi:10.1078/0171-9335-00200
45. Sasaki N, Miyamoto K, Maslowski KM, Ohno H, Kanai T, Sato T. Development of a Scalable Coculture System for Gut Anaerobes and Human Colon Epithelium. *Gastroenterology*. 2020;159:388-390.e5. doi:10.1053/j.gastro.2020.03.021
46. Attwood S, Edel M. iPS-Cell Technology and the Problem of Genetic Instability—Can It Ever Be Safe for Clinical Use? *J Clin Med*. 2019;8(3):288. doi:10.3390/jcm8030288
47. Prior N, Inacio P, Huch M. Liver organoids: From basic research to therapeutic applications. *Gut*. 2019;68(12):2228-2237. doi:10.1136/gutjnl-2019-319256

48. Kim D, Kim SB, Ryu JL, et al. Human Embryonic Stem Cell-Derived Wilson's Disease Model for Screening Drug Efficacy. *Cells*. 2020;9(4):872. doi:10.3390/cells9040872
49. Liu J, Cui Y, Shi L, Luan J, Zhou X, Han JA. A cellular model for Wilson's disease using patient-derived induced pluripotent stem cells revealed aberrant b-catenin pathway during osteogenesis. *Biochem Biophys Res Commun*. 2019;513(2):386-391. doi:10.1016/j.bbrc.2019.04.013
50. Tsvikovskii R, Efremov RG, Lutsenko S. The role of the invariant His-1069 in folding and function of the Wilson's disease protein, the human copper-transporting ATPase ATP7B. *Journal of Biological Chemistry*. 2003;278(15):13302-13308. doi:10.1074/jbc.M300034200
51. Kraiczky J, Nayak KM, Howell KJ, et al. Intestinal inflammation DNA methylation defines regional identity of human intestinal epithelial organoids and undergoes dynamic changes during development. *Gut*. 2019;68:49-61. doi:10.1136/gutjnl-2017-314817
52. Vivet therapeutics. VTX-801 - Wilson disease therapeutics. Accessed May 29, 2023. <https://www.vivet-therapeutics.com/pipeline/wilsons-disease-at-a-glance/>
53. Schilsky M, Patel A, Liapakis A, To U. Efficacy and Safety of WTX101 Administered for 48 Weeks Versus Standard of Care in Wilson Disease Subjects. Yale Center for Clinical Investigation. Published 2019. Accessed March 18, 2021. <https://medicine.yale.edu/ycci/trial/4007/?tab=healthPro>
54. Luciani A, Schumann A, Berquez M, et al. Impaired mitophagy links mitochondrial disease to epithelial stress in methylmalonyl-CoA mutase deficiency. *Nat Commun*. 2020;11(1):1-21. doi:10.1038/s41467-020-14729-8
55. Anzmann AF, Pinto S, Busa V, et al. Multi-omics studies in cellular models of methylmalonic acidemia and propionic acidemia reveal dysregulation of serine metabolism. *Biochim Biophys Acta Mol Basis Dis*. 2019;1865(12):165538. doi:10.1016/j.bbadis.2019.165538
56. Rincón A, Aguado C, Desviat LR, Sánchez-Alcudia R, Ugarte M, Pérez B. Propionic and methylmalonic acidemia: Antisense therapeutics for intronic variations causing aberrantly spliced messenger RNA. *Am J Hum Genet*. 2007;81(6):1262-1270. doi:10.1086/522376
57. Verstegen MMA, Roos FJM, Burka K, et al. Human extrahepatic and intrahepatic cholangiocyte organoids show region-specific differentiation potential and model cystic fibrosis-related bile duct disease. *Sci Rep*. 2020;10(1):21900. doi:10.1038/s41598-020-79082-8
58. Rimland CA, Tilson SG, Morell CM, et al. Regional Differences in Human Biliary Tissues and Corresponding In Vitro-Derived Organoids. *Hepatology*. 2021;73(1):247-267. doi:10.1002/HEP.31252
59. Artegiani B, Hendriks D, Beumer J, et al. Fast and efficient generation of knock-in human organoids using homology-independent CRISPR-Cas9 precision genome editing. *Nat Cell Biol*. 2020;22(3):321-331. doi:10.1038/s41556-020-0472-5
60. Artegiani B, van Voorthuijsen L, Lindeboom RGH, et al. Probing the Tumor Suppressor Function of BAP1 in CRISPR-Engineered Human Liver Organoids. *Cell Stem Cell*. 2019;24(6):927-943.e6. doi:10.1016/j.stem.2019.04.017
61. Yan M, Rayapuram N, Subramani S. The control of peroxisome number and size during division and proliferation. *Curr Opin Cell Biol*. 2005;17(4):376-383. doi:10.1016/j.ceb.2005.06.003
62. Hashimoto T. Peroxisomal B-Oxidation Enzymes. *Cell Biochem Biophys*. 2000;32(Spring):63-72. doi:10.1385/cbb:32:1-3:63

63. Smith JJ, Brown TW, Eitzen GA, Rachubinski RA. Regulation of peroxisome size and number by fatty acid β -oxidation in the yeast *Yarrowia lipolytica*. *Journal of Biological Chemistry*. 2000;275(26):20168-20178. doi:10.1074/jbc.M909285199
64. Grabenbauer M, Sätzler K, Baumgart E, Dariush Fahimi H. Three-Dimensional Ultrastructural Analysis of Peroxisomes in HepG2 Cells. *Cell Biochem Biophys*. 2000;32(Spring):37-49. doi:10.1385/cbb:32:1-3:37
65. Miyazawa S, Furuta S, Osumi T, Hashimoto T. Turnover of enzymes of peroxisomal beta-oxidation in rat liver. *Biochim Biophys Acta*. 1980;630(3):367-374. doi:10.1016/0304-4165(80)90285-8
66. Hu H, Gehart H, Artegiani B, et al. Long-Term Expansion of Functional Mouse and Human Hepatocytes as 3D Organoids. *Cell*. 2018;175(6):1591-1606.e19. doi:10.1016/j.cell.2018.11.013

Supplemental Data

Supplemental Materials and Methods

HepG2 cells for Immuno-Electron microscopy

HepG2 cells (ATCC, clone HB-8065) were grown on 100 mm petri dishes in MEM Hanks supplemented with 10% fetal bovine serum (Sigma), 2 mM L-glutamine (Invitrogen) and 100 units per 100 $\mu\text{g ml}^{-1}$ penicillin/streptomycin (Invitrogen) at 37°C/5% CO₂. Cells were fixed by adding freshly prepared 4% w/v PFA (Polysciences) in 0.1 M phosphate buffer (pH 7.4) to an equal volume of culture medium for 5 minutes, followed by post-fixation in 4% w/v PFA at 4°C overnight. Ultrathin cryosectioning and immunogold labelling were performed as previously described.²⁶

Supplemental Tables

Table S1. Primary antibodies for immunofluorescence

Antigen	Supplier	Cat. number	Raised in	Dilution	Incubation
F-actin	Life Technologies	A12379	-	1:400	o/n 4°C
Ki67	Abcam	ab16667	rabbit	1:100	o/n 4°C
MDR1	Novus bio	NBP1-90291	rabbit	1:500	o/n 4°C
MRP3	Abcam	ab3375	mouse	1:100	o/n 4°C

Table S2. Secondary antibodies for immunofluorescence

Antigen	Supplier	Cat. number	Raised in	Dilution	Incubation
Anti-mouse Alexa 488	Life technologies	A11029	goat	1:100	o/n 4°C
Anti-rabbit Alexa 568	Life technologies	A11036	goat	1:100	o/n 4°C

Table S3. Primary antibodies for immuno-electron microscopy

Antigen	Supplier	Cat. number	Raised in	Dilution	Incubation
α -Catalase	Rockland	200-4151	rabbit	1:1500	1h RT
α -Lysozyme	Dako	A0099	rabbit	1:1000	1h RT

Table S4. Validated primers for quantification of AGXT gene expression

Primer name	sequence (5'-3')	Tm	use
AGXT-F1	CATCTCCTTCAGTGACAAGG	59	RT-qPCR
AGXT-R1	ACTTGATGTCCAGGTAGAAGG	59	RT-qPCR

Supplemental Figures

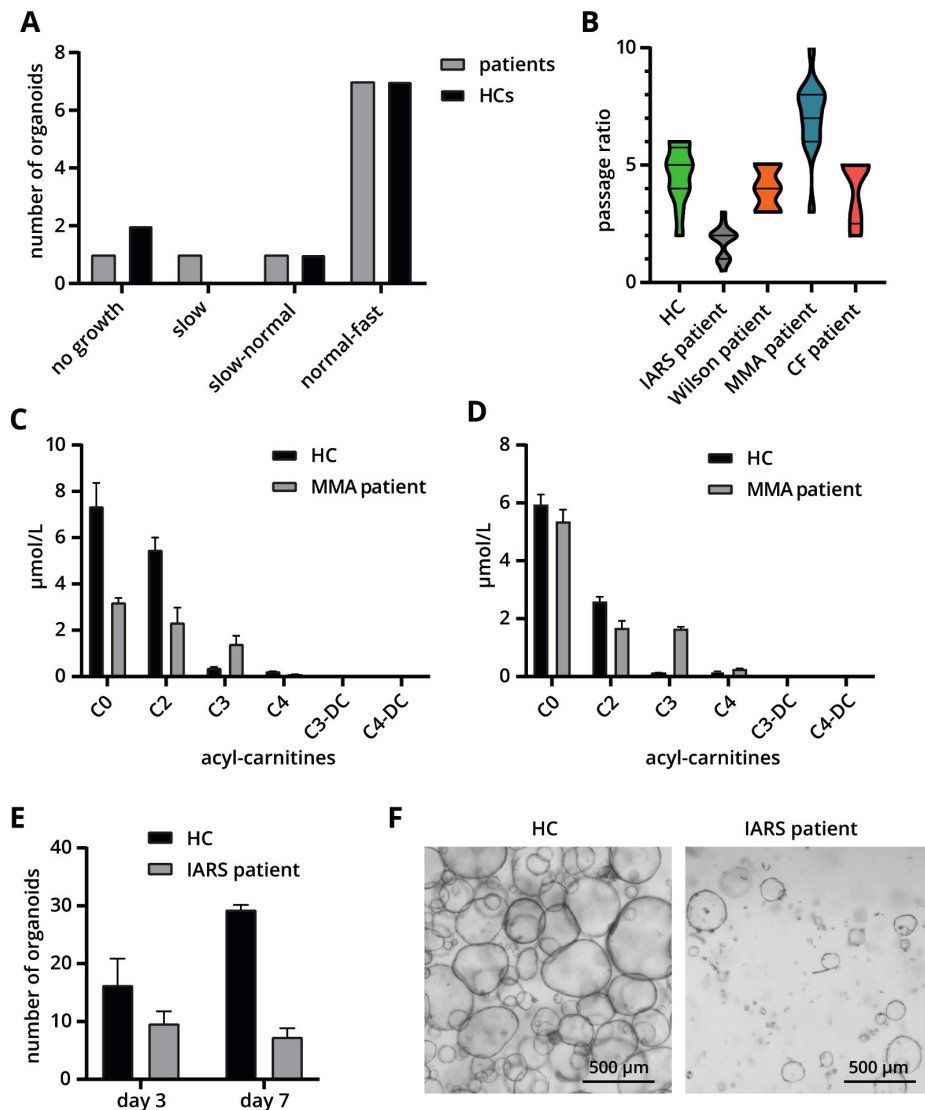


Figure S1. Healthy and patient ICO behavior. **A)** Growth rates of various HC and patient ICOs. **B)** ICO passage ratios observed during maintenance culture of one IARS, one MMA, one Wilson disease and one CF patient and 12 HCs. **C-D)** Acylcarnitines detected during LC-MS/MS analysis of ICO cells (**C**) and culture media (**D**) of one MMA patient and one HC (n=2). (Acyl)carnitines were identified as follows: C0, free carnitine; C2, acetylcarnitine; C3, propionylcarnitine; C4, butyrylcarnitine; C3-DC, malonylcarnitine; C4-DC, succinyl/methylmalonylcarnitine. **E-F)** Poor growth of ICOs of an IARS patient compared to a HC. CF, cystic fibrosis; HC, healthy control; IARS, isoleucyl-tRNA synthetase; ICO, intrahepatic cholangiocyte organoid; MMA, methylmalonic acidemia; methylmalonic acidemia

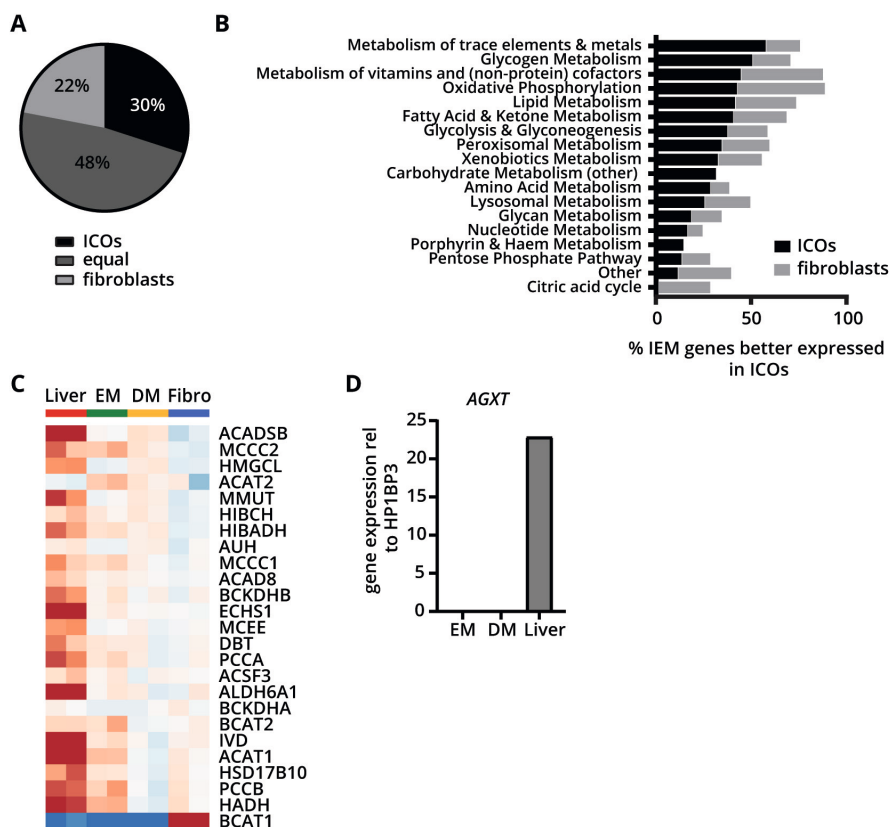


Figure S2. Quantification of the expression of metabolic categories in HC ICOs (n=2) and healthy fibroblasts (n=2). **A**) Percentages of total exome panel genes which are better expressed in HC ICOs, fibroblasts or equally in both cell models. **B**) Percentages of exome panel genes better expressed in HC ICOs (black) and fibroblasts (grey) displayed for each metabolic category. **C**) Visualizations of log₂ fold change expression genes involved in branched chain amino acid metabolism in expanded (EM) and differentiated (DM) HC ICOs, fibroblasts, and whole liver. **D**) Expression of the gene *AGXT* is absent in HC ICOs. HC, healthy control; ICO, intrahepatic cholangiocyte organoid

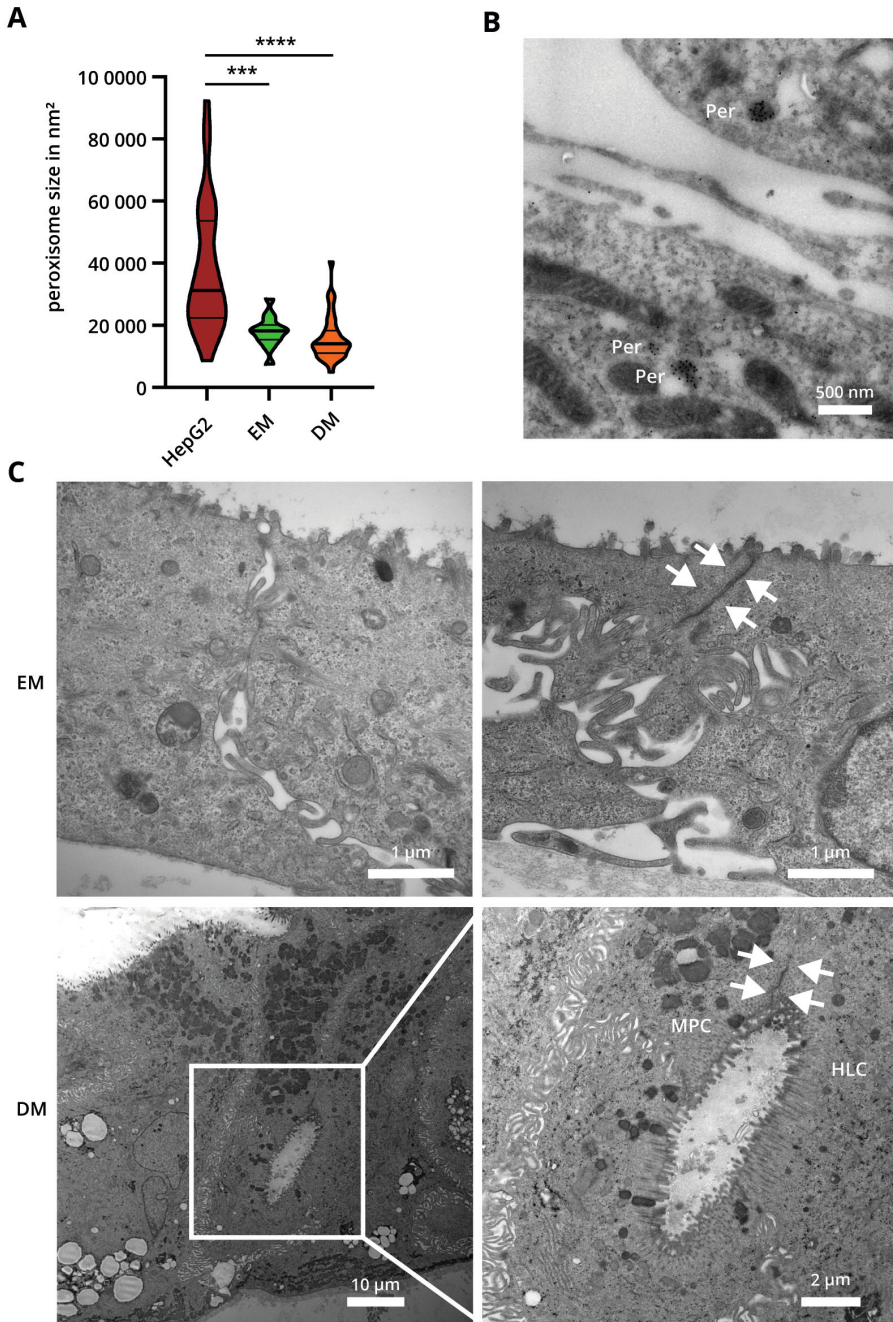


Figure S3. TEM images of ICO and HepG2 cells. A) Peroxisome size in ICOs is significantly smaller than in HepG2 (***, p-value = 0.007; ****, p-value <0.001). **B)** Catalase-stained peroxisomes in HepG2. **C)** Macroviews of EM and DM ICO cells reveals desmosomes (arrows) and interdigitations between cells. DM ICOs contain cells resembling hepatocyte-like cells (HLC) and mucus producing cells (MPC). DM, differentiation condition; EM, expansion condition



3

Human liver organoids to study the pathogenesis of Biliary Atresia

Vivian Lehmann, Imre F. Schene, A. Ibrahim
Ardisasmita, L. Agnes Grutters, Karlijn van Adrichem,
Anne van der Mareel, Marianna A. Tryfonidou, Bart
Spee, Jan B.F. Hulscher, Sabine A. Fuchs

Manuscript in preparation

Abstract

Biliary atresia (BA) is a rare disease of infancy affecting the biliary tree. Extrahepatic bile duct obstruction, rapidly progressive fibrosis and obliteration of the intrahepatic bile ducts are hallmarks of BA pathology. Despite decades of research, BA pathophysiology is poorly defined. The most common hypothesis suggests that environmental insults and a putative genetic predisposition could collectively lead to BA. There are no preventive or curative options, in part due to the unresolved disease mechanism. Treatment generally consists of surgical restoration of bile flow; yet, BA remains the leading cause for pediatric liver transplantations. In recent years, the use of animal models has been helpful in uncovering BA pathogenesis. However, species differences limit full recapitulation of human BA and animal models are limited in unraveling cell-specific mechanisms. This underlines the need for a human *in vitro* model of BA. To this end, we investigated whether human liver organoids are useful in studying BA pathogenesis *in vitro*. We characterized growth and morphology of intrahepatic (ICO), extrahepatic (ECO) and gallbladder cholangiocyte organoids (GCOs) of BA patients and compared these with healthy control patients and non-BA disease control patients. While BA ICOs displayed decreased growth rates compared to control ICOs, cells could be expanded sufficiently for functional assays and cryopreservation. As an exploratory study we have analyzed transcriptional differences between BA and control liver organoids. While we observed no clear morphological differences, BA liver organoids displayed abnormal expression of genes involved in cell-ECM interaction. As a first translational step to identify whether liver organoids are suitable to study the effects of potential environmental causes of BA, we treated BA and control liver organoids with the toxin biliatresone and the viral analog poly I:C. Biliatresone elicited increased expression of genes involved in glutathione metabolism regardless of the disease background. While poly I:C evoked inflammatory responses in all liver organoids, BA liver organoids displayed unique aberrancies in expression of genes associated with ECM-remodeling and HLA class II histocompatibility antigens not found in control liver organoids. Taken together, our results indicate that human liver organoids are a promising patient-specific *in vitro* model of BA pathogenesis.

Introduction

Biliary atresia (BA) is a rare disease of infancy and the leading cause for pediatric liver transplantations.^{1,2} In a majority of cases, infants present with jaundice, obstructed extrahepatic bile ducts, and a contracted or absent gallbladder.^{3,4} Moreover, the intrahepatic bile ducts are sporadically inflamed and fibrotic which commonly progresses to whole liver fibrosis and bile duct obstruction.^{3,4} If left untreated patients die of liver failure by the age of two years.⁵ The only available treatment to date consists of surgical correction of the extrahepatic atresia. During this so-called Kasai hepato-portoenterostomy extrahepatic bile ducts and the gallbladder are removed, and the liver is directly connected to the small intestine to facilitate bile efflux. Despite this surgical intervention, obstruction of intrahepatic bile ducts and liver fibrosis continues, eventually causing liver failure. As a result, 45-70% of patients with BA still require liver transplantation.⁶⁻¹⁰

The limitations of treatment options are in part related to the poorly defined pathogenesis of BA. Various factors have been suggested to be involved in BA pathogenesis including genetic susceptibility factors, viral infection, autoimmunity, and environmental toxins.^{3,11} Familial cases are rare and evidence for genetic factors is limited.^{12,13} Spatiotemporal patterns of BA pathology suggest that environmental events primarily contribute to BA.^{11,14} Alternatively, a genetic predisposition in combination with an environmental insult could collectively lead to BA.^{4,15}

One of the most supported pathogenesis hypotheses proposes that a perinatal viral infection alone or in combination with a dysregulated immune response causes BA. This is supported by the fact that viruses and immune cell accumulations are often found in bile ducts of BA patients at the moment of diagnosis. To test this hypothesis, a murine model of BA was generated by infecting newborn mice with strains of the *Rhesus* rotavirus.¹⁶⁻²⁰ This murine model displays several similarities with human BA, such as obstruction and inflammation of the extrahepatic bile duct. Attempts to map out the underlying mechanism have suggested infiltrating macrophages, T cells and natural killer cells, and high levels of proinflammatory agents IFN- γ and IL-33 as key players.^{3,21} Moreover, murine cholangiocyte cells exposed to the rotavirus have been shown to play a role as immune modulators through cytokine secretion.^{22,23} Within this context, cholangiocytes are the first line of defense and known for their active participation in the immune response through the production of various cytokines and antigen presentation.²⁴⁻³⁰ Aberrancies in cholangiocyte immune modulation might therefore play a role in the regional specificity of BA. Hence, models of human cholangiocytes could aid in understanding BA pathogenesis.

An alternative hypothesis proposes an environmental toxin to induce cholangiocyte injury and bile duct obstruction. Outbreaks of BA-like phenotypes in Australian

livestock led to the discovery of biliatresone, a plant isoflavonoid.^{31,32} This toxin was shown to induce malformation of bile ducts in larval zebrafish and mice.³¹⁻³⁴ *In vitro*, biliatresone caused loss of cellular polarity and obstruction of the lumen of murine cholangiocyte spheroids akin to bile duct atresia *in vivo*.^{31,34} Moreover, these studies suggested that biliatresone acts via upregulating glutathione metabolism genes, thus reducing available glutathione, as well as destabilizing microtubules and downregulating *Sox17*, an important transcription factor involved in endodermal differentiation during embryogenesis and biliary tree maintenance.^{35,36} Although it is unlikely that pregnant women or their newborns are exposed to biliatresone, these findings suggest that any toxin or genetic predisposition that affects glutathione metabolism, microtubules or endodermal differentiation could potentially lead to BA. Hence, biliatresone is a valuable tool to define the molecular mechanism and potential toxic causative factors of human BA.

Although experimental animal models have been helpful in studying BA pathogenesis, they are limited in unraveling cell-specific mechanisms. The regional specificity of BA suggests that cholangiocytes are the key affected cell type of the disease.^{21,37} In addition, delayed appearance of intrahepatic bile duct obstruction suggests that within the cholangiocyte population further location-specific sensitivity to underlying disease mechanisms exists. Therefore, studying cholangiocyte subpopulations of the different affected regions is of great importance to unravel pathophysiology. Moreover, while disease onset is exclusive to the perinatal period, the exact timing and putative role of cholangiocyte maturation in the disease mechanism remains elusive. Thus, it would be highly valuable to be able to study varying degrees of cholangiocyte maturity in a human *in vitro* model representing the different regions of the biliary tree.

In recent years, a human *in vitro* system was developed which promises long-term patient-specific research on intra- and extrahepatic cholangiocyte biology and disease; liver organoids.³⁸ Liver organoids are self-assembled hollow spheres cultured in a three-dimensional (3D) laminin-rich matrix. These organoids can be generated from bipotent cholangiocyte progenitor cells, derived from the human intra- and extrahepatic bile ducts as well as the gallbladder.³⁸⁻⁴¹ Small biopsies suffice to generate large amounts of patient cells which can be expanded long-term and cryopreserved, while retaining their genetic integrity.³⁸⁻⁴¹ We have demonstrated that progenitor and differentiated intrahepatic cholangiocyte organoids (ICOs) do not fully resemble mature hepatocytes, but rather retain cholangiocyte characteristics.⁴² Previous work has shown that extrahepatic and gallbladder cholangiocyte organoids cultured in the original expansion and differentiation media for ICOs resemble cholangiocytes of different maturation states closely.^{38,43,44} Collectively, these characteristics make liver organoids an exciting model to study BA pathophysiology and putative underlying spatiotemporal factors.

In this study, we established and characterized intrahepatic (ICOs), extrahepatic (ECOs) and gallbladder cholangiocyte organoids (GCOs) derived from BA patients, patients suffering from other diseases and healthy controls (Figure 1). We analyzed organoid growth behavior, morphology, and transcriptome differences between control and BA patient liver organoids at different developmental stages, with or without exposure to environmental insults (biliatresone and the viral analog poly I:C). In doing so, we have taken the first step toward developing a human patient-specific *in vitro* model of BA pathogenesis.

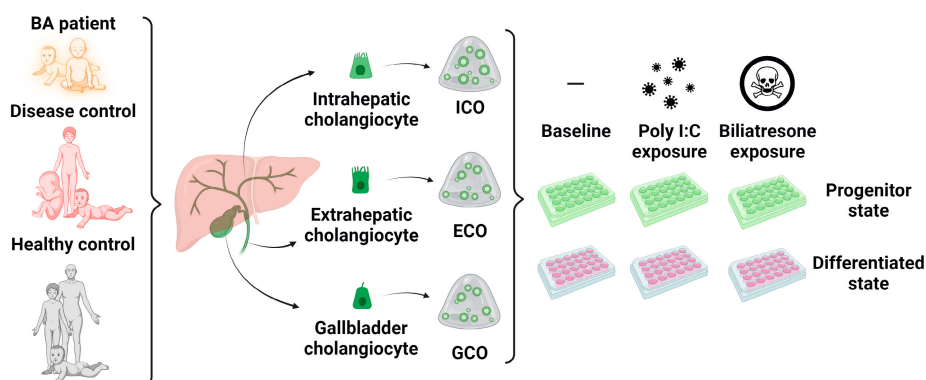


Figure 1. Experimental approach. Intrahepatic, extrahepatic and gallbladder cholangiocytes were sampled from biliary atresia (BA) patients, healthy control patients and non-BA disease control patients to generate organoids for each patient *in vitro*. Liver organoids were characterized at baseline and after exposure to environmental insults poly I:C or biliatresone at different cholangiocyte maturation states (progenitor or differentiated). ECO, extrahepatic cholangiocyte organoid; GCO, gallbladder cholangiocyte organoid; ICO, intrahepatic cholangiocyte organoid.

Materials & Methods

Organoid culture

BA (n=30) and healthy (n=11) and non-BA disease (n=17) control ICOs, ECOs and GCOs were established from explant tissue collected during liver transplantation, liver needle biopsies or Kasai portoenterostomy after patient informed consent (Table S1). We received ethical approval for the use of patient material from different collaborating University Centers (MEC-2014-060; STEM 1-402/K; Metabolic Biobank: 19-489). All organoid types were established as described previously.⁴² Briefly, processed tissue was cultured in droplets of 70% (v/v) Matrigel™ (Corning) and seeding medium containing AddMEM/F12 (Gibco), 1% (v/v) penicillin-streptomycin (Gibco), 1% (v/v) GlutaMax (Gibco), 10 mM HEPES (Gibco), 2% (v/v) B27 without

vitamin A (Gibco), 1.25 mM N-Acetylcysteine (Sigma), 10 mM nicotinamide (Sigma), 10 nM gastrin (Sigma), 10% RSPO1 (v/v) conditioned media (homemade), 50 ng/mL EGF (PeproTech), 100 ng/mL FGF10 (PeproTech), 25 ng/mL HGF (PeproTech), 5 μ M A83-01 (Tocris Bioscience), 10 μ M forskolin (Tocris Bioscience), 25 ng/mL Noggin (PeproTech), 30% (v/v) Wnt conditioned media (CM, homemade), 10 μ M Y27632 (Sigma Aldrich) in 24-well plate formats. Once organoids had formed, media were switched to expansion medium by removing Noggin, Wnt CM and Y27632 from the seeding medium. Every 7 to 10 days, the cultures were passaged by mechanical fragmentation at split ratios 1:1 to 1:5. Once a minimum of ~15% of a confluent organoid culture plate free of debris was obtained, organoids were mechanically fragmented and cryopreserved in Recovery™ Cell Culture Freezing Medium (Gibco) according to the manufacturer's protocol and stored at -196°C for biobanking. Statistical differences in growth performance were determined using unpaired t-test assuming Gaussian distribution. For hepatobiliary differentiation, organoids were pre-treated with 25 ng/mL BMP7 (PeproTech) for 3 days. Thereafter media were changed to differentiation media composed of AdDMEM/F12 medium supplemented with, 1% (v/v) penicillin-streptomycin, 1% (v/v) GlutaMax, 10 mM HEPES, 1% (v/v) B27, EGF (50 ng/mL), 1.25 mM N-Acetylcysteine, gastrin (10 nM), HGF (25 ng/mL), FGF19 (100 ng/mL, PeproTech), A83-01 (500 nM), DAPT (10 μ M, Selleck Chemicals), BMP7 (25 ng/mL), and dexamethasone (30 μ M, Sigma). All cultures were kept in a humidified atmosphere of 20% O₂ and 5% CO₂ at 37°C and media were refreshed every other day.

Optimizing exposure conditions for environmental factors biliatresone and poly I:C

To determine working concentrations of biliatresone (Axon Medchem) and poly I:C (InvivoGen), single cell or confluent BA and control organoid cultures were exposed to 0-8 μ g/mL biliatresone, 0-200 μ g/mL poly I:C or DMSO control matching biliatresone volumes in expansion medium without the antioxidant N-Acetylcysteine for 24 hours. N-Acetylcysteine was omitted since it was previously reported to interfere with effects of environmental stressors such as biliatresone.^{33,34} To obtain single cells, BA and control organoids were harvested with AdDMEM/F12 medium supplemented with, 1% (v/v) penicillin-streptomycin, 1% (v/v) GlutaMax, 10 mM and HEPES and briefly centrifuged at 190 g for 5 minutes at 4°C. Next, cell pellets were digested in TriPLE™ Select (Gibco) until single cells by repeated cycles of mechanical fragmentation and 3-minute incubations in a 37°C waterbath. Single cells were then diluted in expansion medium without N-Acetylcysteine containing 10 μ M Y27632 (Sigma), counted manually and diluted in 70% (v/v) Matrigel™ to reach 125,000 cells/mL. Single cells were treated with varying concentrations of biliatresone for 9 days in expansion medium without N-Acetylcysteine. To determine the working concentration for poly I:C, BA and control organoids were seeded at 2×10^6 single cells/mL and expanded for 4 days and immediately challenged with

poly I:C or differentiated for 4 days without N-Acetylcysteine. For the poly I:C challenge, organoids were incubated with 0-200 µg/mL poly I:C for 24 hours in expansion or differentiation medium without N-Acetylcysteine. For biliatresone and poly I:C cell viability was assessed using the CellTiter-Glo® Luminescent Cell Viability Assay (Promega) according to the manufacturer's protocol or by quantifying necrosis marker propidium iodide (0.1 mg/mL, Thermo- Fisher) and calcein-AM (0.5 µM, Santa Cruz Biotechnology) signals after 15 minutes of incubation at 37°C. For the latter, whole Matrigel™ droplets were imaged with an inverted Olympus IX53 epifluorescence microscope at 2x magnification and quantified in ImageJ software (Win64 version: <https://imagej.net/Fiji/Downloads>). For downstream quantitative RT-qPCR, organoids were grown to confluency after mechanical fragmentation and exposed to 0.5 or 2 µg/mL biliatresone or 20 or 80 µg/mL poly I:C for 24 hours without N-Acetylcysteine. After incubation, organoids were harvested with cold AdDMEM/F12, the cell pellets were washed three times, and then stored at -80°C until further processing for gene expression analysis.

To determine exposure timing for biliatresone on established organoids, differentiation medium of BA and control organoids was supplemented with or without 2 µg/mL biliatresone without N-Acetylcysteine at different days of differentiation and incubated for indicated times (day 4, 0 and 24 hours; day 7, 96 hours; day 8, 96 hours). To determine exposure timing for poly I:C, BA and control organoids were exposed to 80 µg/mL poly I:C on differentiation day 1, 2, 3, 4 and 6 for 24 hours without N-Acetylcysteine. After incubation, organoids were harvested with cold AdDMEM/F12, the cell pellets were washed three times, and then stored at -80°C until further processing for gene expression analysis.

Exposure with environmental factors for polarity analysis and RNA sequencing

After passaging organoids into 96- or 24-well plates by mechanical fragmentation, organoids were either cultured in expansion or differentiation medium without N-Acetylcysteine. At differentiation day 4, differentiated and matching expanded organoids were exposed to 2 µg/mL biliatresone, 80 µg/mL poly I:C or DMSO control matching biliatresone volumes in media without N-Acetylcysteine. Poly I:C conditions were harvested for RNA isolation after 6 hours or fixated for immunofluorescence after 2 hours, while biliatresone and DMSO conditions were harvested or fixated after 24 hours.

RNA isolation and quantitative RT-qPCR

RNA was isolated from organoid cultures using the RNeasy Mini Kit (Qiagen) or Total RNA Purification Kit (Norgen Biotek) according to the manufacturers' protocols including the use of β-mercaptoethanol (Merck). RNA used for sequencing was stored at -80°C until further processing. RNA used for real-time quantitative PCR

(RT-qPCR) was quantified using a D-1000 spectrophotometer (NanoDrop, Thermo Fisher Scientific) and cDNA was synthesized using the iScript cDNA synthesis kit (Bio-Rad) according to the manufacturer's protocol. Relative mRNA of genes of interest was quantified by RT-qPCR using the SYBR Green method (Bio-Rad) and validated primers (Table S1). Normalization was performed using the stably expressed reference gene *HP1BP3*.

RNA sequencing

RNA quality was tested with a Bioanalyzer 2100 expert using the Eukaryote Total RNA Nano assay according to the manufacturer's protocol. Samples with a RIN above 7.5 and a minimum of 4 nM were sent for library preparation using Truseq RNA stranded polyA and sequencing using Illumina NextSeq2000 by Utrecht Sequencing Facility, with a run type of 1x50 bp. Donors were randomly split over two separate runs with 35 and 43 samples each. Different conditions of each donor were analyzed in the same run. Quality control on raw FASTQ files was done with FastQC (v0.11.8). Low quality reads and adapter were trimmed using TrimGalore (v0.6.5). SortMeRNA (v4.3.3) was used to filter out rRNA reads. Afterwards, reads were aligned to the reference genome Human-GRCh37 using STAR (v2.7.3a) aligner. Read counts were then generated using the Subread FeatureCounts module (v2.0.0). Differential gene expression analysis was performed using DESeq2 (v1.30.1).⁴⁵ Differentially expressed genes were identified using the following parameters: lfcThreshold of 0 and adjusted p-value <0.05 using the Benjamini and Hochberg method. Normalized counts were generated by applying DESeq2 variance-stabilizing transformation. Principal component analysis plots and heatmaps were created using normalized counts and plotted using ggplot2 (v.3.3.3) and pheatmap (v1.0.12), respectively. Enrichment analysis of differentially expressed genes was done using Enrichr web application using KEGG pathway annotations (<https://maayanlab.cloud/Enrichr/>).⁴⁶⁻⁴⁸ Manual crosschecks were done by consulting Uniprot and the Human Protein Atlas. Protein network analysis was done using the web application STRING (<https://string-db.org/>).⁴⁹⁻⁵³

Wholemout Immunofluorescence

For wholemount immunofluorescence organoid cultures were fixated in 96-well plates in 4% buffered formaldehyde (v/v) (Klinipath) for 1 hour at room temperature (RT). After washing three times with PBS for 5 minutes at RT samples were stored in PBS at 4°C until further use. To initiate immunofluorescence staining, samples were treated with permeabilization buffer composed of PBS and 0.3% Triton X-100 (v/v) for 30 minutes at 4°C. Next, samples were treated with blocking buffer composed of permeabilization buffer and 5% BSA (w/v) (Sigma Aldrich) for 1 hour at RT. Organoids were then incubated with Alexa Fluor™ 488 Phalloidin (Invitrogen) overnight at 4°C. Thereafter, samples were washed three times for 20 minutes at RT using permeabilization buffer. Next, nuclei were stained with 0.5 µg/mL DAPI (Sigma-

Aldrich) for 15 minutes at RT and washed again. Samples were kept in FluorSafe (Merck) and imaged within one week using a Leica TCS SP8confocal microscope. Culture wells contained between 20 and 80 organoids for all experiments, and a minimum of three photographs were taken per well. Only spheroids that were fully visible along the Z-axis were scored for polarity. Photographs were taken at the midsection of each organoid, where the luminal diameter was greatest.

Results

BA liver organoids display differences in growth performance

After processed biopsies were placed in culture, cultures were inspected for formation of budding organoid structures every few days. Outgrowth success, defined as outgrowth of cystic organoids, was very similar between BA (82%), healthy (91%) and disease control ICOs (87%; Figure 2A, G). Moreover, organoids emerged within similar timeframes, when comparing BA ICOs (7 ± 2.7 days), healthy (8.8 ± 1.8 days) and disease control ICOs (6.6 ± 4.4 days; Figure 2B). Notably, BA and other disease ICOs displayed much larger variation in outgrowth rate, suggesting that disease (severity) might affect cholangiocyte progenitor outgrowth. In comparison, outgrowth was slightly less successful for BA ECOs (73%; Figure 2A). However, the small sample size of the healthy and disease control ECO groups hampers interpretation of reduced outgrowth of ECOs and putative BA specificity. Larger sample sizes and evaluation of donor-matched ICO, ECO and GCOs are needed to draw firm conclusions.

Once organoid lines were established, the cultures were passaged regularly as the organoids expanded. Interestingly, growth rates of established BA ECO lines did not differ from healthy or disease control ECOs (Figure 2C). In contrast, BA ICOs displayed significantly lower growth rates compared to healthy control ICOs, as evidenced by significantly lower split ratios ($p = 0.0003$; Figure 2C). This growth behavior was BA specific as disease control ICO growth rates did not significantly differ from healthy control ICOs.

Some BA organoid lines collapsed during culture (37%; Figure 2D-F). Disease control organoids collapsed too, albeit with lower frequency (17%; Figure 2D). More BA organoid lines collapsed before rather than after cryopreservation (Figure 2E). Most BA organoid lines that collapsed before cryopreservation did so at low passage numbers, however this was not statistically significant ($p > 0.05$; Figure 2F). Other disease derived organoids also occasionally collapsed after storage at higher passage numbers than BA organoids, albeit without statistical significance ($p > 0.05$; Figure 2E-F).

Optimization of exposure conditions

Among the different factors putatively involved in BA pathogenesis a viral or toxic insult are the most supported by clinical and experimental evidence.^{3,4,11} To test whether and under which conditions mimics of such environmental factors could elicit a BA-like phenotype in liver organoids, we conducted pilot studies using the toxin biliatresone and the viral analog poly I:C.

Biliatresone affects single cell viability and glutathione metabolism in liver organoids

Previously, the toxin biliatresone was shown to induce a BA-like phenotype in livestock, zebrafish, and rodents *in vivo* and *in vitro*.^{31,33,34,54} We performed preliminary tests to determine whether biliatresone exposure conditions reported for murine *in vitro* models would elicit similar phenotypes in human liver organoids. Single cells showed increasing sensitivity to increasing concentrations of biliatresone regardless of disease or organoid type, as indicated by increased cell death and failure to form organoids (Figure 3A-B). Biliatresone did not affect morphology of established organoids (Figure 3B). Due to the stark differences in single cell viability after exposure to 0.5 and 2 $\mu\text{g}/\text{mL}$ biliatresone, we investigated effects of both concentrations on a transcriptomic level in established organoids (Figure 3C), with a focus on key glutathione metabolism genes *GCLC*, *GCLM* and *GSTO-1* and generic cell stress marker *HSP90*.^{33,34} As described in other models, biliatresone increased expression of these cell stress genes in a dose dependent manner in our organoids. Moreover, expression of glutathione metabolism genes *GCLC*, *GCLM* and *GSTO-1* was highest after exposure at day four of differentiation (Figure 3D). Based on these findings, we decided to expose organoids in the progenitor state and after 4 days of differentiation to 2 $\mu\text{g}/\text{mL}$ biliatresone for 24 hours for further transcriptomic and polarity analyses.

Poly I:C elicits immune responses in liver organoids

We investigated whether, and under which conditions, a viral insult, such as the immunostimulant poly I:C, would elicit a BA-like phenotype in liver organoids. This synthetic double stranded RNA mimics molecular patterns of viral infection and is widely used to study anti-viral responses *in vitro*. When testing various poly I:C concentrations on BA and control ICOs and ECOs, most organoid lines showed no change in cell viability when exposed to concentrations up to 80 $\mu\text{g}/\text{mL}$ poly I:C for 24 hours (Figure 3E). At 200 $\mu\text{g}/\text{mL}$ poly I:C cell viability declined clearly in all organoid lines. Notably, one disease control ICO line showed increased sensitivity to poly I:C from 25 $\mu\text{g}/\text{mL}$ onwards. Upon exposure to 20 and 80 $\mu\text{g}/\text{mL}$ poly I:C, expression of inflammatory markers *NKB* and *CXCL-8* increased in a dose dependent manner (Figure 3F); distinct cellular responses were elicited by the higher poly I:C concentration. Next, we tested whether liver organoids of different maturation states display varying degrees of sensitivity to 80 $\mu\text{g}/\text{mL}$ poly I:C. Expression of

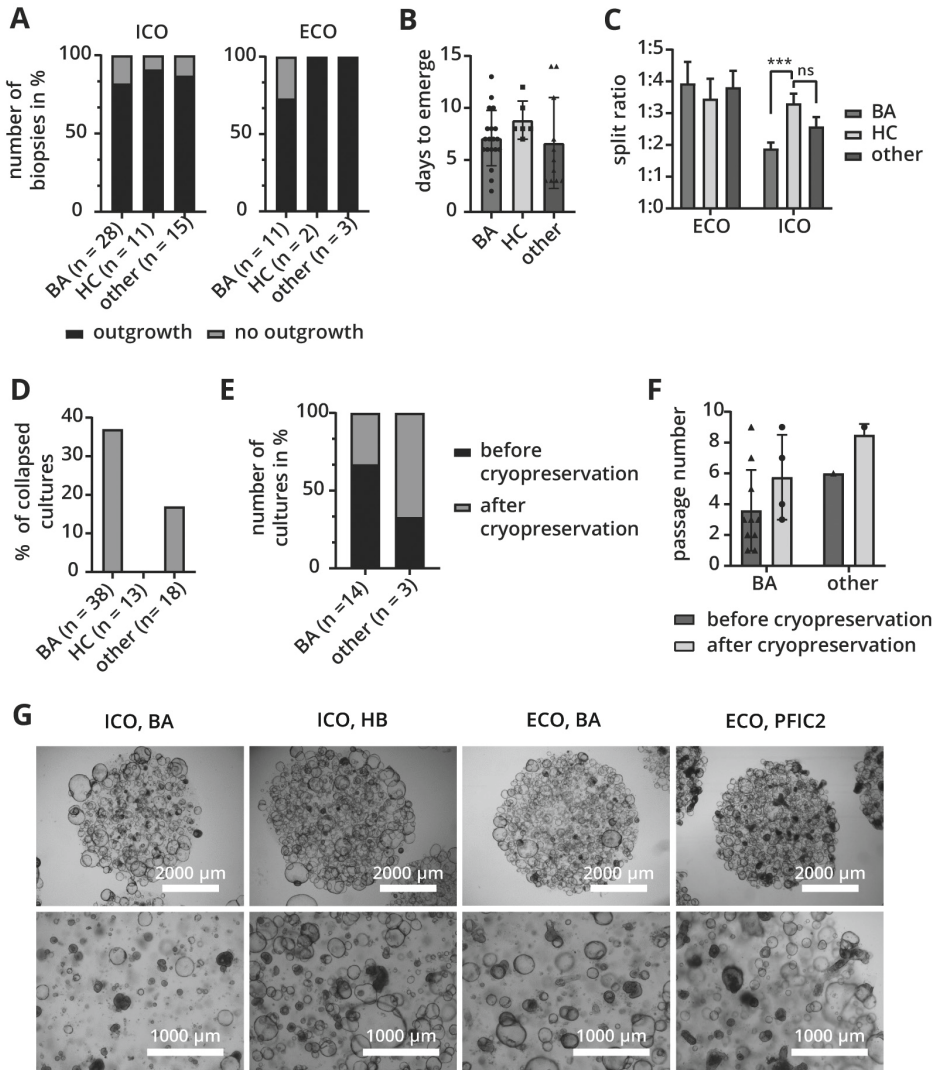
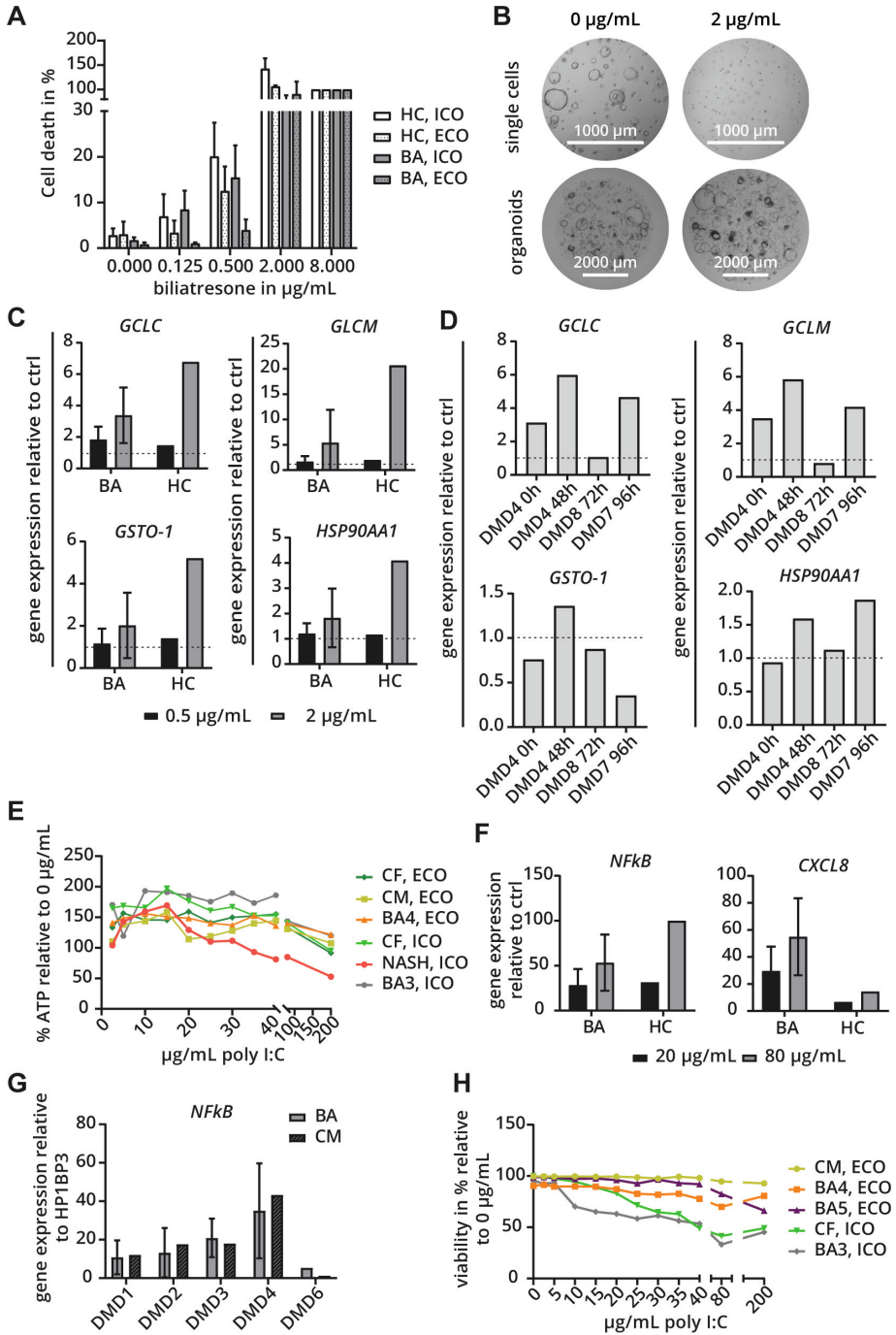


Figure 2. Liver organoid growth. **A**) Organoid outgrowth from intrahepatic (ICOs) and extrahepatic bile duct (ECOs). **B**) Time until organoids emerged from processed biopsies in days. **C**) Growth rates of liver organoids depicted as weekly split ratios of BA ECOs (n = 8), healthy control (HC) ECOs (n = 3), disease control (other) ECOs (n = 2), BA ICOs (n = 24), HC ICOs (n = 10) and other ICOs (n = 13). Statistical analysis was performed using unpaired t-test assuming Gaussian distribution; ***p = 0.003, ns = p > 0.05. **D**) Percentage of collapsed organoid cultures. **E**) Percentage of BA and disease control liver organoids collapsed before or after cryopreservation. **F**) Passage numbers at which cultures collapsed before or after cryopreservation. No statistical significance was found among the groups (p > 0.05) using unpaired t-test assuming Gaussian distribution. **G**) Representative brightfield images of BA and control (HB, PFIC2) ICO and ECO cultures. BA, biliary atresia; HB, hepatoblastoma; PFIC2, progressive familial intrahepatic cholestasis type 2



← **Figure 3. Biliatresone and poly I:C toxicity and timing.** **A)** Cell death of BA and control (HC) ICOs and ECOs after exposure to varying biliatresone concentrations for 9 days post single cell seeding. Each condition was measured in triplicate. **B)** Representative brightfield images of one BA ICO line exposed to biliatresone or DMSO control as single cells (top) or established organoids (bottom). **C)** Gene expression of cell stress markers in established BA (n = 5) and control (HC; n = 1) ICOs exposed to 0.5 and 2 µg/mL biliatresone shown relative to DMSO control (dotted line). **D)** Gene expression of cell stress markers of one differentiated BA organoid line after exposure to 2 µg/mL biliatresone relative to DMSO control (dotted line). Exposure was started at the indicated day of differentiation (DMDx) and samples were harvested and analyzed after the indicated hours of incubation (h). **E)** Cell viability of progenitor BA and control (CF, CM, NASH) ICOs and ECOs exposed to varying concentrations of poly I:C depicted as percentage (%) of cellular ATP relative to non-exposed conditions of each organoid line. **F)** Gene expression of inflammatory markers in progenitor BA (n = 5) and control (HC; n = 1) liver organoids after 24 hours exposure to different poly I:C concentrations relative to non-exposed control (ctrl) conditions. **G)** Gene expression of *NFKB* in BA (n = 2) and control (CM; n = 1) ECOs exposed to 80 µg/mL poly I:C for 24 hours at different days of differentiation relative to reference gene *HP1BP3*. **H)** Cell viability of BA and control (CF, CM) ICOs and ECOs differentiated for 4 days and exposed to varying concentrations of poly I:C for 24 hours relative to non-exposed conditions of each organoid line. Donor IDs are defined in more detail in Table S1. BA, biliary atresia; CF, cystic fibrosis; CM, choledocal malformation; ECO, extrahepatic cholangiocyte organoid; HC, healthy control; ICO, intrahepatic cholangiocyte organoid; NASH, nonalcoholic steatohepatitis

NFKB increased dramatically over the first few days of differentiation of both BA and healthy control liver organoids, peaking at day four (Figure 3G). Meanwhile, exposure at day six of differentiation elicited no to little additional change in gene expression.

Interestingly, ECOs and ICOs differentiated for four days displayed different sensitivities to poly I:C (Figure 3H). Differentiated ECOs displayed very limited decline in viability at any poly I:C concentration, while the viability of differentiated ICOs dropped to 50% around 30 µg/mL poly I:C. This could suggest that poly I:C toxicity is dependent on the donor, the maturation status, and the anatomical origin of the organoids. To gain insight into the underlying differences we proceeded with transcriptome analyses of various BA, healthy and disease control liver organoids of progenitor and differentiation states. To retain sufficient cell numbers for transcriptome analyses, liver organoids were exposed to 80 µg/mL poly I:C for 6 hours which had previously been shown to induce immune responses in intestinal organoids.⁵⁵

Underlying disease or exposure to environmental insults does not affect liver organoid morphology

Morphologically, no differences were observed between the groups. All organoid lines, irrespective of organoid type, maturation state, disease history or exposure to environmental insults (biliatresone or poly I:C), showed predominantly cystic organoids with occasional small dense organoids (Figure 2G, Figures S1-2). During

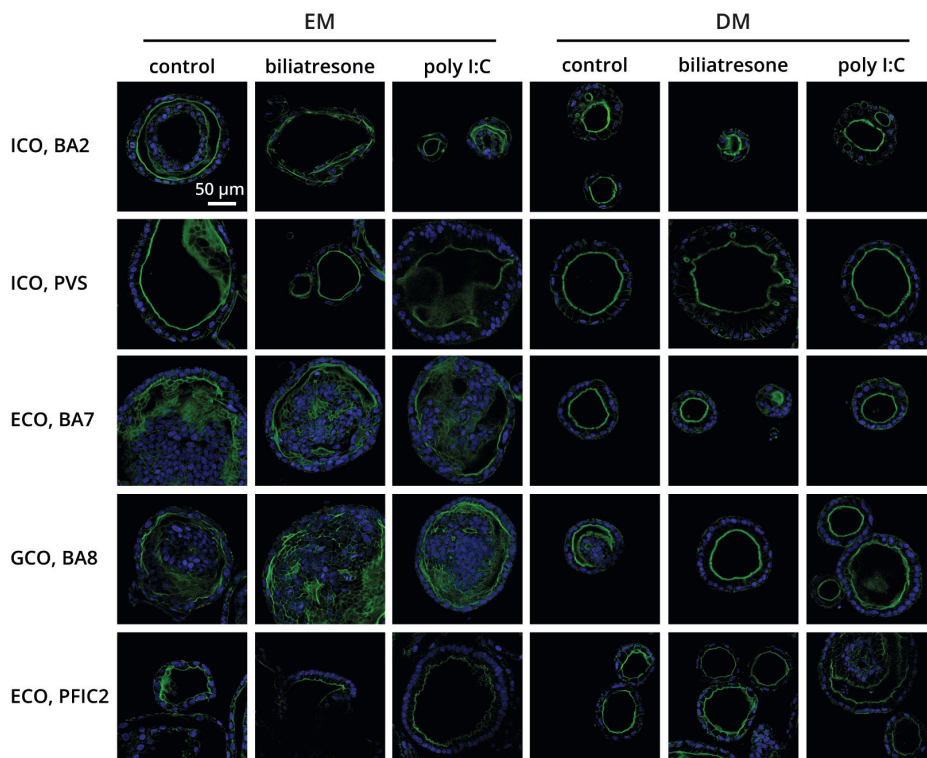


Figure 4. Polarity of progenitor and differentiated liver organoids after exposure to environmental insults biliatresone and poly I:C. Immunofluorescence images of F-actin (green) and Dapi (blue) of progenitor (EM) and differentiated (DM) BA and control (PVS, PFIC2) ICOs, ECOs and GCOs exposed to 2 $\mu\text{g}/\text{mL}$ biliatresone or DMSO control for 24 hours and 80 $\mu\text{g}/\text{mL}$ poly I:C for 2 hours. Donor IDs are defined in more detail in Table S1. BA, biliary atresia; ECO, extrahepatic cholangiocyte organoid; GCO, gallbladder cholangiocyte organoid; ICO, intrahepatic cholangiocyte organoid; PFIC2, progressive familial intrahepatic cholestasis type 2; PVS, pulmonic valve stenosis

differentiation organoid morphologies changed as expected; organoids condensed slightly, and cell layers became thicker and darker. The most predominant morphologic characteristic of the BA phenotype, namely loss of bile duct polarity and obstruction of the ducts, was not observed in our organoids. All BA and control organoids showed normal polarity in EM and DM with the apical domain facing the lumen as shown by F-actin stainings (Figure 4).

Transcriptome analysis

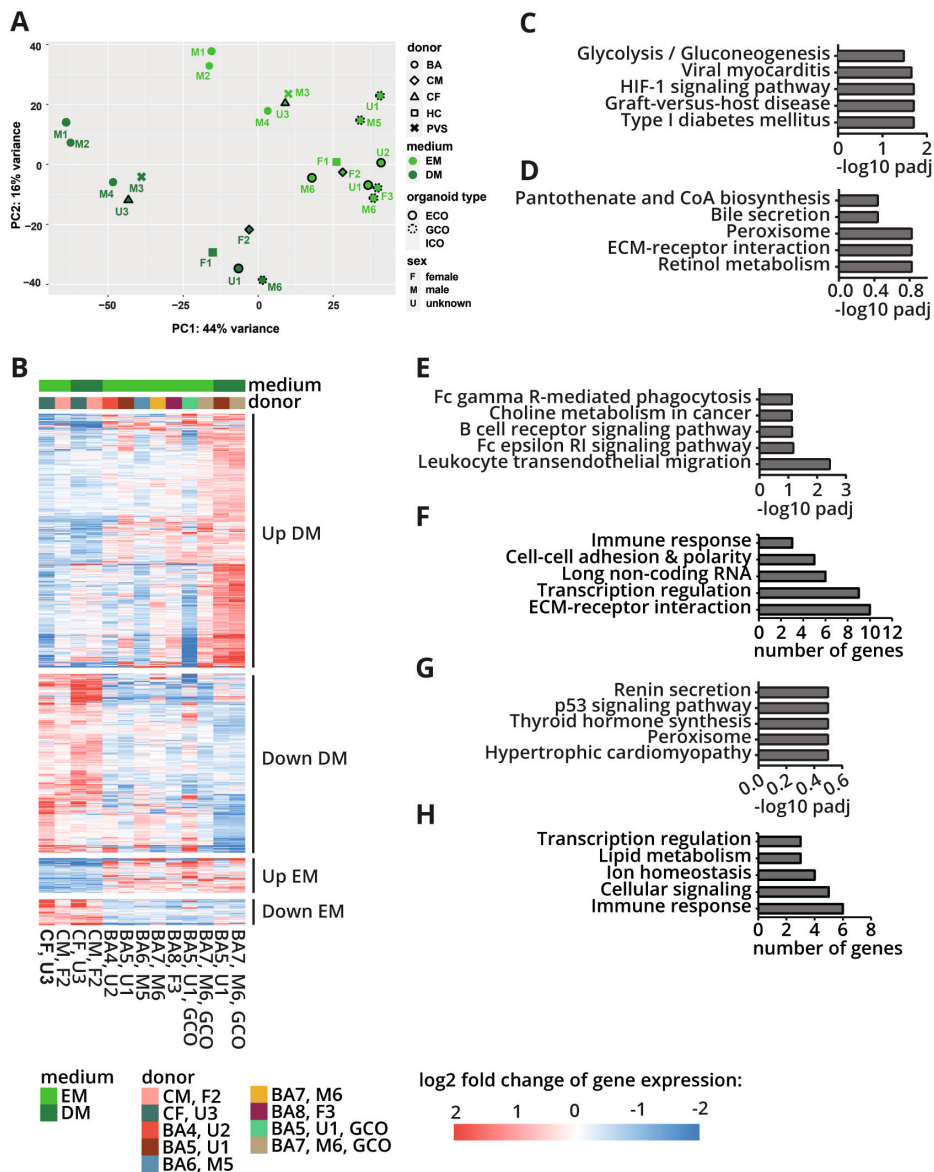
Baseline

While BA and control liver organoids did not differ morphologically, we investigated whether there were transcriptomic differences that may provide avenues to further explore at the functional level in a targeted manner. Principal component analysis revealed that BA and control organoids clustered together both in progenitor and differentiated state (Figure 5A). However, progenitor and differentiated organoids clustered separately, suggesting that the biggest differences between samples were caused by the differentiation status rather than disease type. GCOs clustered with ECOs, while ICOs separated from the extrahepatic organoid types, thus supporting previous reports of regional specificity of intra- and extrahepatic organoid types.⁴³ From here on ECOs and GCOs were grouped for further analyses and will be collectively referred to as ECOs.

We observed differences, but not a clear separation between BA and control organoids (Figure 5A), with 1 of 2 controls clustering with the BA group of the same organoid type. Closer analysis of differentially expressed genes (DEGs) revealed differences of the transcriptome between BA and healthy controls: most DEGs were found in differentiated ECOs with 582 upregulated and 374 downregulated DEGs (Figure S3B). Progenitor ICOs showed 200 upregulated and 66 downregulated DEGs (Figure S3C). Differentiated ICOs showed 159 upregulated and 148 downregulated DEGs (Figure S3D), while progenitor ECOs showed 68 upregulated and 52 downregulated DEGs (Figure S3E). Closer inspection of individual gene expression patterns showed clear differences between BA and healthy control organoids for most identified DEGs (Figure 5B, Figure 6A), but not for all. Potentially, the small number of healthy and disease controls caused these genes to not be identified as significantly differentially expressed in healthy and disease controls.

To gain insight into the biological functions associated with the identified DEGs, pathway enrichment analyses were done using EnrichR and the top five pathways for each condition were identified (Figure 5C-H, Figure 6B-E). Upregulated DEGs of differentiated BA ECOs compared to control ECOs were associated with the hypoxia inducible factor 1 (HIF-1) signaling pathway and glycolysis/gluconeogenesis (*EGLN3*, *PFKL*, *NOS3*, *PGK1*, *SLC2A1*, *ALDOC*, *TIMP1*, *ENO2*, *ALDOA*, *HK2*, *PDK1*, *VEGFA*, *ACSS2*, *PCK1*), as well as several (auto)immune reactions (i.e. graft-versus-host, type I diabetes mellitus disease, viral myocarditis) (*IL1B*, *HLA-B*, *HLA-C*, *HLA-A*, *HLA-F*, *HLA-G*, *HLA-E*, *RAC2*, *CD55*) (Figure 5C).

Differentiated BA ECOs displayed downregulation of hepatic functions and ECM-receptor interactions (Figure 5D). Despite low to moderate confidence of accuracy in these pathway enrichments ($-\log_{10}$ adjusted p-value = 0.4-0.8 and 1.5-2), manual



← **Figure 5. Transcriptome analysis of BA liver organoids at baseline.** **A)** Two-way principal component (PC) analysis of BA (ECOs, n = 3; GCOs, n = 4; ICOs, n = 3) and control (CF, CM, HC, PVS; ECOs, n = 2; ICOs, n = 2) liver organoids. **B)** Visualizations of log₂ fold changes in gene expression of up- (Up) and downregulated (Down) DEGs in differentiated (DM) and progenitor (EM) BA and control (CM, CF) ECOs. log₂ fold changes are relative to the mean expression of the genes across all samples. **C-D)** EnrichR pathway enrichment analysis of DEGs upregulated (**C**) and downregulated (**D**) in differentiated BA ECOs with confidence of accuracy indicated as the adjusted p-value (padj). **E-H)** EnrichR (**E, G**) and manual (**F, H**) pathway enrichment analysis of DEGs upregulated (**E-F**) and downregulated (**G-H**) in progenitor BA ECOs with indicated confidence of accuracy (padj) or number of genes. The adjusted p-value was determined by EnrichR using the Benjamini-Hochberg method with a cutoff of 0.05. Donor IDs are defined in more detail in Table S1. BA, biliary atresia; CF, cystic fibrosis; CM, choledocal malformation; DEG, differentially expressed gene; ECO, extrahepatic cholangiocyte organoid; GCO, gallbladder cholangiocyte organoid; HC, healthy control; ICO, intrahepatic cholangiocyte organoid; PVS, pulmonic valve stenosis

inspection of the genes associated with the mentioned pathways confirmed correct categorization by the software. Specifically, downregulated DEGs were associated with peroxisome metabolism (*PECR, GNPAT, AGPS, ACSL5, BAAT, XDH, DDO*), ECM-receptor interaction (*ITGB1, VTN, RELN, ITGB5, LAMB1, CD36, CD44*), vitamin and CoA metabolism (*ALDH1A3, ALDH1A2, CYP1A1, UGT2A3, LRAT, ADH6, ALDH1B1, VNN2, AASDHPPT*), and bile secretion (*ABCC4, SLC10A2, UGT2A3, SLC5A1, BAAT, PRKACB*). Notably, identified pathways for differentiated BA ECOs were based on 7 and 4% of the downregulated and upregulated DEGs, respectively. Hence, these results should be interpreted with care.

Upregulated DEGs of progenitor BA ECOs compared to progenitor control ECOs were associated with immune response pathways (*CDH5, RAC2, CLDN18, CTNNA3, VAV1, INPP5D*) and choline metabolism in cancer (*SLC44A5, DGKB, RAC2*) (Figure 5E). However, manual crosschecks revealed incorrect pathway prediction, despite moderate prediction confidence of the generated pathway enrichment (-log₁₀ adjusted p-value = 1-3). This was likely due to the low number of DEGs in this condition (n = 68). Instead, the top five associated pathways included ECM-receptor interaction, transcription regulation, long non-coding RNAs, cell-cell adhesion and polarity, and immune response (Figure 5F, Table S3).

Downregulated DEGs of progenitor BA ECOs compared to progenitor control ECOs were associated with hypertrophic cardiomyopathy (*TNNC1, AGT*), peroxisome metabolism (*PECR, GNPAT*), thyroid hormone synthesis (*IYD, GPX3*), p53 signaling (*CCND2, SESN3*) and renin secretion (*AGT, AQP1*) (Figure 5G). These pathway enrichments were generated with low confidence of accuracy (-log₁₀ adjusted p-value = ~0.5), again likely due to the low number of DEGs (n = 52). Manual inspection indeed revealed that most downregulated DEGs in progenitor BA ECOs

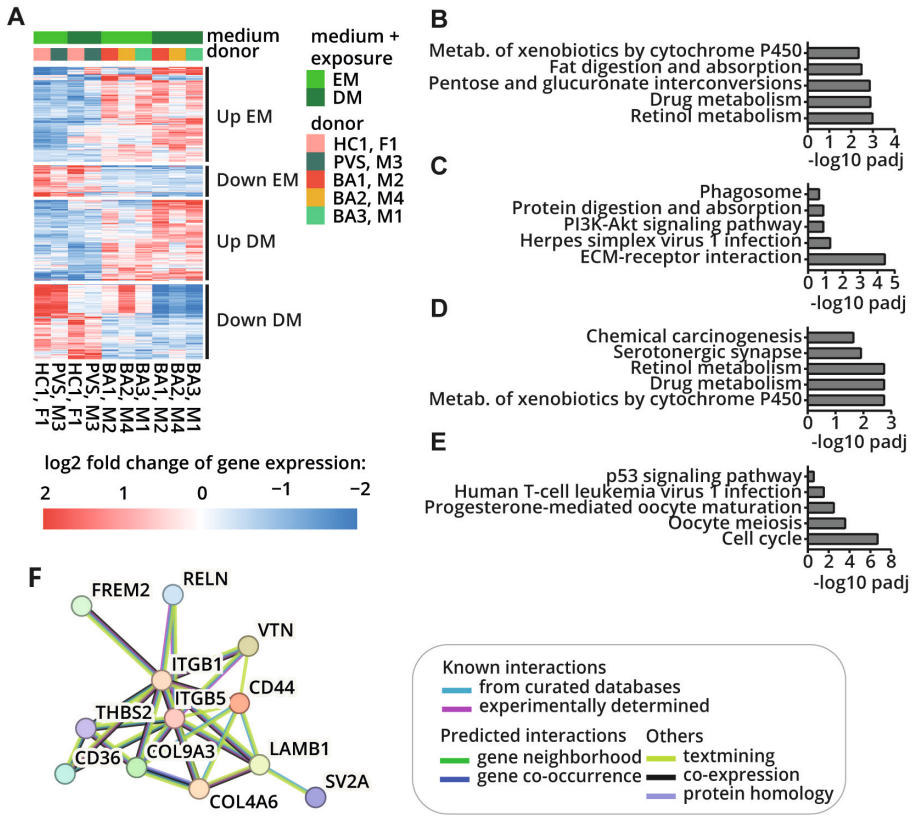


Figure 6. Gene expression patterns and pathway enrichment of DEGs of BA ICOs at baseline. **A**) Visualizations of log₂ fold changes in gene expression relative to the mean expression of the genes across all samples of up- (Up) and downregulated (Down) DEGs in progenitor (EM) and differentiated (DM) BA and control (HC, PVS) ICOs. **B-E**) EnrichR pathway enrichment analysis of DEGs upregulated (**B**) and downregulated (**C**) in progenitor ICOs and DEGs upregulated (**D**) and downregulated (**E**) in differentiated BA ICOs with confidence of accuracy indicated as the adjusted p-value (padj). The adjusted p-value was determined by EnrichR using the Benjamini-Hochberg method with a cutoff of 0.05. **F**) STRING network analysis of DEGs identified to be downregulated in progenitor and differentiated BA ICOs and ICOs. Donor IDs are defined in more detail in Table S1. BA, biliary atresia; DEG, differentially expressed gene; HC, healthy control; ICO, intrahepatic cholangiocyte organoid; PVS, pulmonic valve stenosis

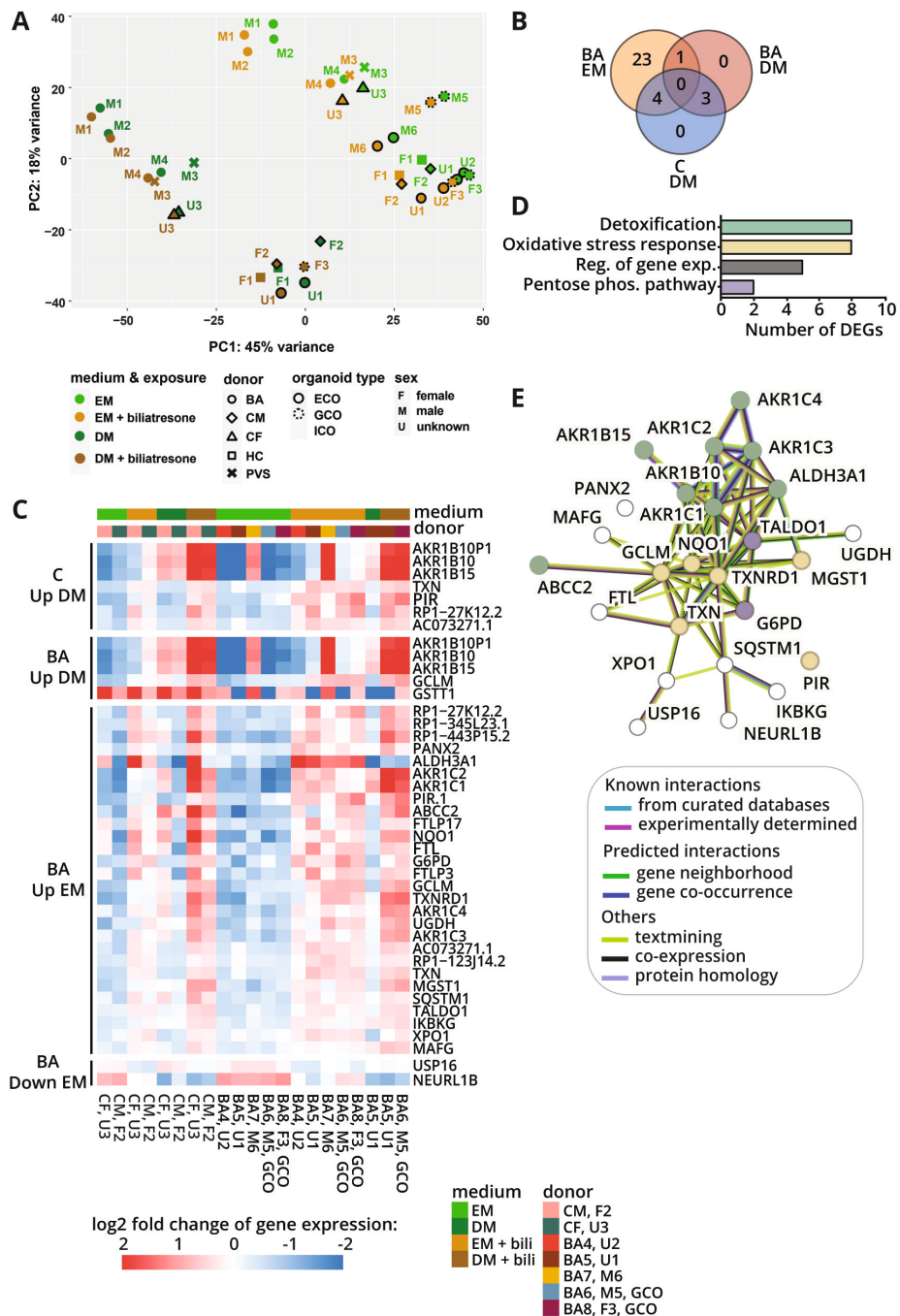
are rather involved in immune response, cellular signaling, ion homeostasis, lipid metabolism and transcription regulation (Figure 5H, Table S4).

Pathway analyses suggested that progenitor BA ICOs were more differentiated toward the hepatic fate compared to control ICOs, as they displayed higher expression of genes associated with mature hepatocytes such as metabolism of retinol, xenobiotics, carbohydrates, and fat (*CYP2C9*, *UGT1A1*, *DHRS9*, *UGT1A4*, *CYP3A4*, *CYP2C18*, *UGT1A6*, *GSTA2*, *CYP2C19*, *XDH*, *AKR1B10SORD*, *ABCA1*, *DGAT2*, *APOA1*, *APOA4*, *APOB*) (Figure 6B). Pathways downregulated in progenitor BA ICOs included viral infection (*ZNF793*, *ZNF737*, *ZNF85*, *ZNF439*, *HLA-DPB1*, *ZNF43*, *ZNF563*) and phagocytosis (*HLA-DPB1*, *THBS2*, *CORO1A*) (Figure 6C).

Of note, most of the genes associated with viral infection and phagocytosis in these analyses are better known to be involved in transcription regulation. Other downregulated functions in progenitor BA ICOs included ECM-receptor interaction (*SV2A*, *COL4A6*, *COL9A3*, *THBS2*, *CD44*, *FREM2*), PI3K-Akt signaling (*NR4A1*, *COL4A6*, *COL9A3*, *THBS2*, *FGFR1*) and protein processing (*COL13A1*, *COL4A6*, *COL9A3*), which were associated with reduced cell proliferation, as may be expected with increased differentiation toward the hepatic fate.⁵⁶⁻⁵⁸

DEGs of differentiated BA ICOs were associated with similar pathways as progenitor BA ICOs, namely increased hepatocyte maturation and decreased proliferation (Figure 6D-E). The pathways associated with hepatic maturation included xenobiotics and retinol metabolism (*CYP2C9*, *CYP2C8*, *UGT1A1*, *ADH1B*, *CYP2C18*, *UGT1A6*, *CYP2C19*, *XDH*, *AKR1C1*, *EPHX1*). Functions of serotonergic synapse and chemical carcinogenesis were also found in differentiated BA ICOs, however, closer inspection revealed that most of these genes were identical to DEGs identified for xenobiotics and retinol metabolism, except for *ITPR1* and *HTR1B* which were associated with synaptic cell signaling. DEGs downregulated in differentiated BA ICOs were associated with cell cycle and concur with decreased proliferation (*CDC20*, *CCNA2*, *CCNB2*, *CCNB1*, *PTTG1*, *ESPL1*, *PLK1*, *BUB1B*, *TTK*, *CDC25C*, *MAD2L1*). DEGs of the pathways of oocyte meiosis and maturation, viral infection, and p53 signaling were identical to those mentioned for cell cycle pathway, except for *GTSE1* which is thought to inhibit mitosis progression.⁵⁹

In summary, BA liver organoids displayed specific transcriptomic differences compared to control organoids. Progenitor BA ECOs showed increased cell-ECM interaction and decreased immune response which was reversed for differentiated BA ECOs. Meanwhile, progenitor and differentiated BA ICOs showed increased hepatic differentiation, while cell cycle regulation and cell-ECM interaction were decreased.



← **Figure 7. Transcriptome analysis of BA liver organoids exposed to biliatresone. A)** Two-way principal component (PC) analysis of BA (ECOs, n = 3; GCOs, n = 2; ICOs, n = 3) and control (CF, CM, HC, PVS; ECOs, n = 2; ICOs, n = 2) liver organoids. **B)** Venn diagram of DEGs identified for progenitor (EM) and differentiated (DM) BA and control (C) ECOs exposed to 2 µg/mL biliatresone compared to those exposed with DMSO. **C)** Visualizations of log₂ fold changes in gene expression of identified up- and downregulated DEGs in progenitor (EM) or differentiated (DM) control (C: CF, CM) and BA ECOs. log₂ fold changes are relative to the mean expression of the genes across all samples. **D)** Manually collated biological functions of DEGs shown in **C**. **E)** STRING network analysis of DEGs shown in **C**. Node colors correspond to the biological functions: green, detoxification; yellow, oxidative stress response; purple, pentose phosphate pathway; white, other. Donor IDs are defined in more detail in Table S1. BA, biliary atresia; CF, cystic fibrosis; CM, choledocal malformation; DEG, differentially expressed gene; ECO, extrahepatic cholangiocyte organoid; GCO, gallbladder cholangiocyte organoid; HC, healthy control; ICO, intrahepatic cholangiocyte organoid; PVS, pulmonic valve stenosis

Biliatresone

Biliatresone treatment had limited effects on human liver organoids (Figure 7, Figure S4). According to principal component analysis BA and control organoids clustered together in both maturation states (Figure 7A). Meanwhile, separate clustering of progenitor and differentiated organoids suggested that the biggest difference between samples was caused by the differentiation status rather than disease type. Moreover, no clear separation between BA and control organoids nor between ICOs and ECOs was identified. One of each of the respective control organoid donors clustered with the opposite organoid type.

Nonetheless, biliatresone induced some transcriptomic changes. 31 DEGs were found in BA ECOs exposed to biliatresone compared to BA ECOs not exposed to the toxin, of which 23 were significantly upregulated in progenitor BA ECOs (Figure 7B). Despite not having been identified as significantly dysregulated in control ECOs, expression patterns of the 31 DEGs identified showed similar expression patterns in control ECOs (Figure 7C). For instance, the gene *ABCC2* was upregulated in progenitor and differentiated ECOs of both BA patients and controls (Figure 7C). This may well relate to the relatively low number of control ECOs studied. Overall, these observations suggest that healthy and BA ECOs are equally susceptible to biliatresone. Importantly, interdonor differences were observed potentially indicating that some donors are more or less susceptible to biliatresone, regardless of donor disease history. Similar to baseline differences, expression of upregulated genes was generally highest in differentiated ECOs. However, progenitor ECOs exposed to biliatresone showed upregulation of the same genes, albeit overall lower. To identify overarching pathways stimulated by biliatresone, pathway enrichment analyses were carried out using EnrichR. However, outcomes were only available for 30% of submitted genes, likely due to the small number of DEGs. Hence, biological functions for DEGs of biliatresone exposed samples were manually identified by

← **Figure 8. Transcriptome analysis of BA liver organoids exposed to poly I:C.** **A)** Two-way principal component (PC) analysis of BA (ECOs, n = 3; GCOs, n = 2; ICOs, n = 3) and control (CF, CM, HC, PVS; ECOs, n = 2; ICOs, n = 2) liver organoids. **B-I)** Venn diagrams of DEGs identified when comparing BA with control (C) liver organoids exposed to poly I:C and when comparing BA liver organoids treated with (poly I:C) or without (ctrl) poly I:C to identify a subset of DEGs specific for BA liver organoids: **B)** DEGs upregulated in progenitor ICOs. **C)** DEGs downregulated in progenitor ICOs. **D)** DEGs upregulated in differentiated ICOs. **E)** DEGs downregulated in differentiated ICOs. **F)** DEGs downregulated in differentiated ECOs. **G)** DEGs upregulated in differentiated ECOs. **H)** DEGs downregulated in progenitor ECOs. **I)** DEGs upregulated in progenitor ECOs. **J-K)** Visualizations of log₂ fold changes in gene expression of up- and downregulated DEGs of progenitor (EM) or differentiated (DM) BA and control (CF, CM, HC, PVS) ICOs (**J**) and ECOs (**K**). log₂ fold changes are relative to the mean expression of the genes across all samples. Donor IDs are defined in more detail in Table S1. BA, biliary atresia; CF, cystic fibrosis; CM, choledocal malformation; DEG, differentially expressed gene; ECO, extrahepatic cholangiocyte organoid; GCO, gallbladder cholangiocyte organoid; HC, healthy control; ICO, intrahepatic cholangiocyte organoid; PVS, pulmonic valve stenosis

consulting Uniprot and the Human Protein Atlas, or literature when databases were not informative.

Among the upregulated DEGs in biliary atresia treated organoids of BA and control ECOs two major groups were identified (Figure 7D). These were associated with detoxification of xenobiotics (*AKR1B10*, *AKR1B15*, *AKR1C1*, *AKR1C2*, *AKR1C3*, *AKR1C4*, *ALDH3A1*, *ABCC2*) and the oxidative stress response including several glutathione metabolism genes (*PIR*, *TXN*, *GCLM*, *GSTT1*, *MGST1*, *NQO1*, *TXNRD1*, *ABCC2*). The third largest group of upregulated DEGs comprised many long non-coding RNAs (*RP1-27K12.2*, *RP11-123J14.2*, *RP11-345L23.1*, *RP11-443P15.2*), which are generally thought to be involved in the regulation of gene expression and associated with various pathologies such as cancer.⁶⁰⁻⁶² Other functions associated with upregulated DEGs included pentose phosphate pathway (*G6PD*, *TALDO*), transcription factor (*MAFG*), iron storage (*FTL*), NFκB activation (*IKBKKG*), paracrine signaling associated with pathology (*PANX2*^{63,64}), autophagy (*SQSTM1*), biosynthesis of ECMs (*UGDH*), nuclear export (*XPO1*), and a few pseudogenes (*AKR1B10P1*, *FTLP3*, *FTLP17*). Two downregulated DEGs were identified and were associated with mitosis regulation (*USP16*) and positive regulation of Notch (*NEURL1B*). Network analyses were carried out using STRING to predict putative interactions of proteins encoded by the identified DEGs (Figure 7E). This revealed that most genes involved in xenobiotics, glutathione metabolism and the pentose phosphate pathway are closely interconnected, suggesting functional significance of the identified DEGs after challenging organoids with biliary atresia.

Poly I:C

Exposure of liver organoids to the viral analog poly I:C caused a large transcriptomic shift (Figure 8, Figure S5). Principal component analysis revealed that BA, healthy and disease control organoids in progenitor and differentiation state all shift away from baseline (Figure 8A). As was observed for biliary atresia and baseline analyses, ECOs and GCOs separated from ICOs, except for one healthy and one disease control donor which clustered with the opposite organoid type group.

Analysis of the DEGs revealed upregulation of inflammatory pathways in BA, healthy and disease control organoids, indicating that the cells responded to poly I:C (Figure S6). Closer inspection revealed BA patient-specific changes with the majority being upregulated in BA progenitor ECOs (3,049 upregulated DEGs; Figure S5-6). Comparison of individual donor expression patterns revealed that expression patterns in healthy and disease control organoids followed similar patterns to those derived from BA patients but did not reach statistical significance likely due to the small sample size (data not shown). Hence, to identify DEGs exclusive to BA organoids, we generated an artificial filter by generating a subset of DEGs that differed statistically significantly between BA and control organoids exposed to poly I:C as well as between BA organoids treated with or without poly I:C (Figure 8B-I). Side by side comparison of the donors revealed that this subset of DEGs was indeed exclusive for BA ECOs exposed to poly I:C (Figure 8J-K).

To identify biological functions likely affected by the identified subset of DEGs, we performed pathway enrichment using EnrichR. As experienced previously, small numbers of DEGs resulted in pathway enrichments with low confidence of accuracy (Figure S7). Hence, further data interpretation was conducted by consulting Uniprot and the Human Protein Atlas.

Upregulated DEGs of progenitor BA compared to control ICOs were associated with cell morphology and matrix interaction, immune response, long non-coding RNAs, signal transduction, and lipid metabolism (Figure 9A, Table S5). Meanwhile, half of the downregulated DEGs of progenitor BA compared to control ICOs were associated with mitosis regulation, while the remaining DEGs were associated with cell morphology and matrix interaction, transcription regulation, histone modification, and immune response (Figure 9B, Table S6). Upregulated DEGs in differentiated BA compared to control ICOs were associated with similar functions, namely apoptosis regulation, cell morphology and matrix interaction, immune response, signal transduction, and cell stress response (Figure 9C, Table S7). Downregulated DEGs in differentiated BA compared to control ICOs were similarly associated with mitosis regulation, transcription regulation, DNA metabolism, long non-coding RNAs, and signal transduction (Figure 9D, Table S8).

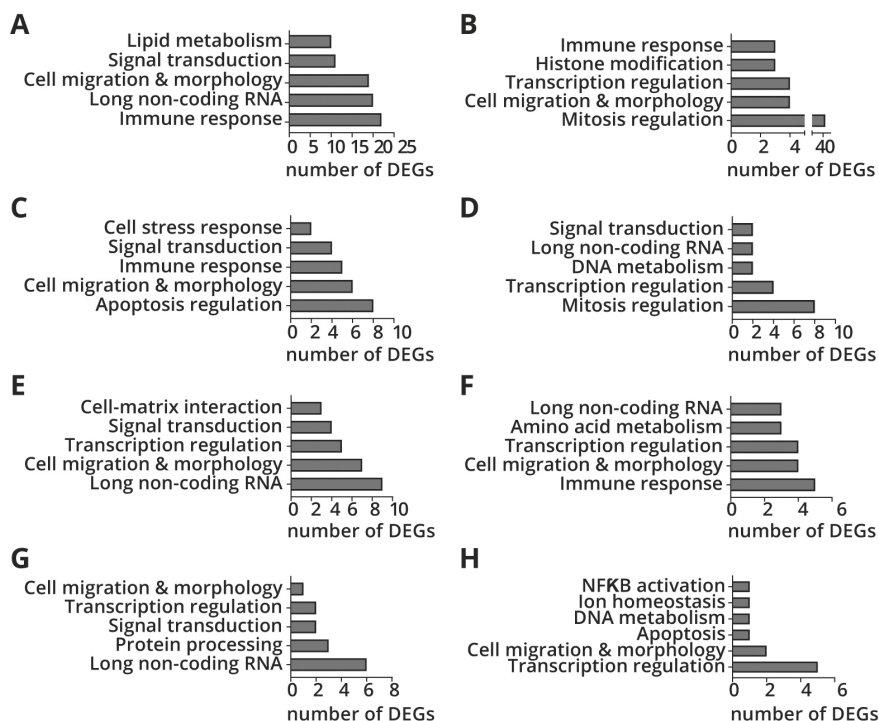


Figure 9. Manually collated biological functions of DEGs specific for BA ICOs and ECOs exposed to poly I:C. A-H) Biological functions of DEGs upregulated in progenitor ICOs (A), downregulated in progenitor ICOs (B), upregulated in differentiated ICOs (C), downregulated in differentiated ICOs (D), downregulated in differentiated ECOs (E), upregulated in differentiated ECOs (F), downregulated in progenitor ECOs (G), upregulated in progenitor ECOs (H). BA, biliary atresia; DEG, differentially expressed gene; ECO, extrahepatic cholangiocyte organoid; ICO, intrahepatic cholangiocyte organoid

DEGs downregulated in differentiated BA compared to control ECOs were associated with long non-coding RNAs, cell morphology and matrix interaction, transcription regulation, signal transduction, and cell and tissue development (Figure 9E, Table S9). Upregulated DEGs of differentiated BA compared to control ECOs were associated with immune response, cell morphology and matrix interaction, transcription regulation, amino acid metabolism, and long non-coding RNAs (Figure 9F, Table S10). Meanwhile, downregulated DEGs in progenitor BA compared to control ECOs were associated with long non-coding RNAs, protein processing, signal transduction, transcription regulation, and cell morphology and matrix interaction (Figure 9G, Table S11). Upregulated DEGs of progenitor BA compared to control ECOs were associated with transcription regulation, cell morphology and matrix interaction, apoptosis, DNA metabolism, ion homeostasis, and NFKB activation (Figure 9H, Table S12).

In summary, poly I:C elicits specific effects in BA patient liver organoids. In progenitor BA ICOs we observed decreased cell cycle regulation, and dysregulation of cell-ECM interaction and immune response. Similarly, differentiated BA ICOs displayed reduced cell cycle regulation, while expression of cell-ECM interaction and apoptosis regulation was reduced. Meanwhile, progenitor BA ECOs displayed downregulation of protein processing and upregulation of cell-ECM interaction and transcription regulation. In differentiated BA patient ECOs we observed upregulation of immune response and dysregulation of cell-ECM interaction and transcription regulation.

Discussion

Despite decades of research, the pathophysiology of biliary atresia (BA) remains elusive. In the present study, we investigated BA patient-derived cholangiocyte organoids as a human *in vitro* model for BA. To our knowledge, this study is the first to characterize organoids derived from various regions of the biliary tree of BA patients in a progenitor state and a more mature, differentiated state, with and without exposure to toxins and viral insults. In doing so we have generated a human *in vitro* model comprising spatiotemporal and endo- and exogenic factors potentially influencing BA pathogenesis.

Baseline

Since the start of our study, other groups have established ICOs from BA patients.^{65,66} Similar to our experience, the group of prof. dr. Jorge Bezerra reported cystic organoid formation from liver tissue of 20 BA patients in 2022.⁶⁵ In contrast, in 2020 prof. dr. Paul Kwong Hang Tam's group generated ICOs from 14 BA patients and reported mostly dense structures with slow proliferation.⁶⁶ While the group of prof. dr. Jorge Bezerra used the same protocol as we used, prof. dr. Paul Kwong Hang Tam's protocol involved MACS single cell sorting. This relatively harsher protocol may well exert stress on the cells, negating outgrowth of the cells and reducing organoid formation success. Biopsy timing is unlikely to have caused the differences in organoid formation success since biopsies were obtained shortly preceding or during the Kasai procedure in all studies. Alternatively, differences between the Asian, European and American BA patient populations might be reflected by these variations. Previous epidemiological studies revealed that BA prevalence is highest in Taiwan and Japan with 1 in 5,000 births, while it is much lower in the USA with 1 in 15,000 births and Europe, where it ranges from 1 in 17,000-19,000 births annually.⁶⁷⁻⁷² It may be interesting to study putative genetic factors, such as single nucleotide polymorphisms, underlying this variation in global prevalence.^{15,73-75} To that end, an overarching global study using harmonized methodology could be orchestrated to characterize BA in patients and matching patient organoids.

While organoid macrostructures, organoid formation success and cryopreservation were comparable between our findings and those of the group of prof. dr. Jorge Bezerra, they and prof. dr. Paul Kwong Hang Tam's group both reported aberrant polarities in BA ICOs.^{65,66} Apical and basolateral markers such as F-actin and β -catenin were reported to be homogeneously distributed across cell membranes, thus increasing epithelial permeability. Conversely, we observed no differences in polarity, nor morphology. The most striking difference between our culturing protocols was the use of 100% (v/v) Cultrex™ BME in the other two studies versus 70% (v/v) Matrigel™ culture ECM in our study. Cultrex™ BME and Matrigel™ production and thus composition is very similar and these products are assumed to be interchangeable.⁷⁶⁻⁷⁸ However, it is well known that ECM stiffness can affect cell phenotypes significantly.⁷⁹⁻⁸³ The use of 70% versus 100% (v/v) Matrigel™ doubles the stiffness from 50 to 100 Pa.⁸⁴ Stiffer ECMs are known to induce endothelial to mesenchymal transition *in vitro*.⁷⁹ Hence, aberrant polarity reported by other groups might indicate endothelial to mesenchymal transition, which has also previously been associated with BA.^{79,80,85} Likely, the use of softer ECM prevents endothelial to mesenchymal transition in our organoids and thus prevents BA phenotype from materializing in our cultures. Moreover, the stiffer ECM might mimic the *in vivo* fibrotic environment more closely, and thus provide more physiological cues to generate BA phenotypes in ICOs.⁷⁹ Interestingly, a recent study evaluating a synthetic polyethylene glycol (PEG)-based hydrogel found that hydrogel stiffness nearing that of *in vivo* fibrotic tissue hampered organoid formation and elicited increased expression of cell stress genes.⁸⁶ Future evaluation of the effect of softer and stiffer ECM for each liver organoid type of different BA patient populations would be very valuable to confirm whether a BA phenotype can be manipulated through biomaterial stiffness in human liver organoids. Such a study would require a harmonized methodology, such as the use of the same ECM, rheology tests, and the investigation of relevant cellular characteristics, such as cell-ECM interaction, cell stress, cell mobility, cell proliferation, and the degree of endothelial to mesenchymal transition.

Within this context, it is interesting to stress that modulated ECM composition, ECM remodeling molecules, and aberrant ECM receptor expression have all been previously associated with BA.³ In line with this, we observed downregulated expression of genes involved in ECM-receptor interactions in progenitor and differentiated BA ICOs and differentiated BA ECOs involving encoded proteins that are also functionally closely interconnected (Figure 6F). A previous study identified similar proteins to be involved in BA, with several microRNAs differentially expressed in BA bile and liver tissue.⁸⁷ Network analyses showed that these microRNAs were closely associated with genes involved in ECM-receptor interactions, such as *CD44*, *ITGB1* (encoding integrin subunit beta 1), other integrins, laminins, and collagens. *CD44* encodes for a cell surface glycoprotein which interacts with the ECM and other

cells and is thus involved in cell-cell interactions, cell migration, and differentiation. Moreover, *CD44* is a common marker of cholangiocytes in injured livers.⁸⁸⁻⁹⁰ Previously, *CD44* was associated with BA through a comprehensive analysis of SNPs and transcriptomics of BA patients.⁹¹ Another study reported significant reduction in *LAMB1* (encoding laminin subunit beta 1) and *ITGB1* expression in livers of another BA patient population.⁹² Laminins are key components of the ECM and contribute to cell attachment and differentiation. Meanwhile, integrin beta-1 is responsible for epithelial polarization and can facilitate viral entry into cholangiocytes.⁹³⁻⁹⁷ Reduction in ECM components as well as ECM-receptors can thus lead to aberrant morphologies and functions as observed in BA. The lack of morphological abnormalities in liver organoids in our study suggests that the culture conditions, most likely related to the relatively soft ECM employed, prevented morphological presentation of the observed transcriptomic differences between BA and control organoids. Adjustments to ECM and medium compositions to mimic the *in vivo* microenvironment more closely might provoke manifestation of the morphological consequences of the transcriptomic differences. Despite absence of BA-like morphologies, significantly reduced proliferation, downregulation in cell-ECM interaction, and upregulation of hepatic differentiation indicate that our BA organoids reflect a BA-specific phenotype.

Biliatresone

Exposure to biliatresone did not elicit a BA patient-specific response in liver organoids. Morphology and transcriptome of BA, healthy and disease control liver organoids were similar. These findings suggest that biliatresone acts independently of underlying genetic predispositions, which may mean that anyone could acquire BA if exposed to toxins akin to biliatresone.

We are the first to show upregulation of glutathione metabolism genes in human ECOs in response to biliatresone. Glutathione metabolism may be upregulated to counteract the toxic effect of biliatresone which is in line with previous findings in murine cholangiocyte spheroids.^{34,54} In these studies, biliatresone caused rapid consumption of glutathione which in turn lead to altered expression of Wnt and Notch targets and eventually caused *SOX17* expression to decline. The latter is responsible for cholangiocyte polarity, thus explaining how transcriptional changes would lead to polarity defects in BA. We did not detect differential expression of *SOX17* in response to biliatresone, which might explain why we did not observe any morphological changes. Potentially, exposure conditions for biliatresone such as concentration or timing were insufficient to elicit differential expression of *SOX17*. Since species differences in xenobiotics metabolism are well known, human cells may require different exposure regimes to the toxin biliatresone than those used in rodents and fish.⁹⁸

While clear transcriptomic changes in BA ECOs were observed, biliatresone had no effect on BA ICOs. This finding might reflect spatial differences of BA pathology *in vivo* where extrahepatic bile ducts are initially and more severely affected. Studies in mice and zebrafish models reported higher sensitivity of extrahepatic cholangiocytes to biliatresone due to their net lower redox reserve.^{31,33,34,99} This might explain why we did not observe effects in ICOs. Interestingly, the only other study using human organoids demonstrated that ICOs developed BA morphology when exposed to biliatresone.¹⁰⁰ Key differences between the latter and our study are differential matrix stiffness and exposure time. Matrix stiffness has previously been shown to alter glutathione metabolism.^{101,102} Cells cultured using softer matrices were shown to be more resistant to oxidative stress by replenishing the redox balance rapidly. Meanwhile, cells cultured using stiffer matrices were less responsive to oxidative stress. It is likely that a stiffer matrix better mimics *in vivo* ECM stiffness surrounding bile ducts. Yet, little is known about *in vivo* ECM stiffness surrounding bile ducts, since suitable techniques are only just being developed.¹⁰³ Altogether, we argue that ECM stiffness of *in vitro* models of BA may be a crucial aspect that dictates morphology and polarity of organoids and requires consideration in the future.

Sensitivity differences between intra- and extrahepatic cholangiocytes might also reflect the spatiotemporal differences of intra- and extrahepatic bile duct obstruction of *in vivo* BA. If intrahepatic cholangiocytes are more resistant to oxidative stress, prolonged exposure to stress through biliatresone treatment might be needed to induce morphological and functional changes. A recent study using human ICOs showed that a 5-day incubation with 2 µg/ml biliatresone elicited aberrant polarity and increased permeability compared to controls.¹⁰⁰ This suggests that longer incubation times may be needed to study biliatresone effects in human ICOs. Moreover, this may imply species differences in biliatresone effects, since mouse cholangiocyte spheroids were previously reported to react with abnormal polarity within 6-24 hours of treatment with biliatresone.^{31,34,54} Notably, differences in ECM composition used in murine studies may be another factor.³¹

Poly I:C

We found that ECM remodeling and pro-fibrotic signals, hallmarks of the BA phenotype, were reflected in the transcriptomes of BA liver organoids treated with poly I:C. Cell morphology and ECM remodeling were among the most dysregulated biological functions associated with DEGs in BA ICOs and ECOs after poly I:C treatment. Among these gene sets, upregulation of *SLIT2* and *SLIT3* in differentiated ICOs and ECOs are of particular interest. These genes encode proteins which are not only involved in cell morphology and migration, but are also capable of recruiting immune cells such as macrophages.^{104,105} Through interaction with proteins of the Roundabout (ROBO) family, SLIT proteins have been shown to activate hepatic stellate cells in the liver, eventually leading to fibrosis.^{106,107} Importantly, *SLIT2* was

shown to be upregulated in livers from patients suffering from primary biliary cirrhosis and more recently in BA patients.^{108,109} Expression of the SLIT signaling partner *ROBO1* was also recently found to be upregulated in livers of BA patients.¹¹⁰ We observed that *SLIT2* upregulation was also accompanied by *ROBO1* upregulation in differentiated ICOs, thus supporting the notion that pro-fibrotic signals in these cultures are upregulated upon poly I:C stimulation.

Up- or downregulation of various ECM interaction genes after poly I:C treatment could suggest that BA organoids are remodeling their environment in an attempt to counteract the viral insult. Poly I:C treatment also induced upregulation of *CD44* in differentiated ECOs. Aside from its role in ECM-interaction, CD44 is also thought to be involved in reactions to viral infections, with some findings suggesting a role in viral replication and distribution, while others reported anti-viral functions of CD44.¹¹¹⁻¹¹³ Meanwhile, *NPNT* was downregulated in differentiated ECOs exposed to poly I:C. *NPNT* encodes the ECM protein nephronectin; the functional ligand of integrin beta-1. Already low expression of *ITGB1* in differentiated BA ECOs compared to disease controls might mean that a viral insult reduces cell-matrix interaction even further by simultaneously reducing expression of ECM component NPNT. Altogether, these findings suggest that BA cells are attempting to remodel their environment upon viral infection. Indeed, ECM remodeling is well known to play an active part in immune response and modulation thereof.^{114,115} ECM composition is crucial to maintain controlled immune responses as deficiency of several ECM proteins has been shown to tip the balance of immune cell populations, thus leading to skewed and uncontrolled immune responses and eventual pathology.¹¹⁴⁻¹¹⁷ To unravel the functional consequences of the altered ECM remodeling process in ICOs and ECOs, co-cultures with immune cells, such as T cells or Kupffer cells, could be informative future approaches.

Besides remodeling the surrounding ECM and recruiting immune cells through soluble factors, cholangiocytes have also been proposed to act as antigen presenting cells.²⁴⁻²⁶ We observed upregulation of various HLA class II histocompatibility antigens in BA ECOs at baseline and ICOs after poly I:C exposure, indicating that antigen presenting properties of cholangiocytes are retained *in vitro*. Importantly, various proteins involved in antigen presentation have previously been reported to be enriched in liver tissue of BA patients.^{3,118,119} This suggests that organoids offer a possibility to study BA patient-specific HLA reactions and polymorphisms *in vitro*. To investigate this notion, it would be interesting to evaluate protein expression in livers and matched organoids from a larger cohort of BA patients. Moreover, functional evaluation of immune modulation could be studied through stimulating immune cells with organoid media or through co-culture.

While we observed clear changes in organoid transcriptomes after poly I:C treatment, we could not observe lumen obstruction or polarity changes typical for BA *in vivo* and previously reported in poly I:C treated healthy control ICOs by prof. dr. Paul Kwong Hang Tam's group.¹²⁰ Importantly, in this study, the same stiffer ECM was used as in their previous studies, when compared to our softer ECM. Moreover, poly I:C exposure with 40 µg/ml was started three days after seeding single cells. While it is not fully clear from the report whether poly I:C exposure was continuous, the group observed morphological changes after 14 days. Since the different findings may relate to differences in protocols, it is important to carefully consider exposure protocol design in addition to ECM stiffness in future studies.

Limitations & future perspectives

Regional heterogeneity of BA pathology may be connected to functional and morphological cholangiocyte heterogeneity throughout the biliary tree.^{30,121} Liver organoids derived from the different regions may therefore be useful in studying BA.⁴³ While we did not perform direct transcriptomic comparisons of liver organoid types, we observed grouping of BA ICOs from ECOs and GCOs in principal component analyses. Moreover, the observed differences in organoid culture stability and growth rate, as well as differential up- and down regulated pathways between ICOs and ECOs suggest that regional differences are retained in this model. The use of donor-matched organoids of each region for follow-up bioinformatics and functional analyses comparing the organoid types directly will be useful to address regional differences.

Similarly, we could not clearly define the maturity and temporal factors that contribute to BA pathology. While this may relate to the relatively low numbers of control samples, the differentiation medium should also be considered. This differentiation medium was originally designed to promote hepatocyte maturation.³⁸ Although previous work has demonstrated that all three types of liver organoids generally retain important cholangiocyte characteristics in this medium, exact parallels to the *in vivo* developing biliary tree remain elusive.^{42,43} It would be worthwhile to explore alternative cholangiocyte specific differentiation media.^{65,122-124} Moreover, cross-matching transcriptomes to the healthy developing human biliary tree could help to parallel liver organoid maturation stadia *in vitro* to *in vivo* biliary tree development stadia.

Nonetheless, we observed clear differences between BA and healthy and disease control organoids. Interestingly, treatment with poly I:C seemed to elicit BA specific responses, while biliatresone elicited transcriptomic changes regardless of disease history. This could suggest that the viral hypothesis of BA pathology is linked to underlying genetic factors, while toxins or metabolites akin to biliatresone act independently of underlying genetic factors.¹²⁴ Importantly, increased response to poly I:C by BA organoids might be the result of a previous *in vivo* infection having

created an epigenetic memory. Repeated exposure of healthy control organoids with poly I:C or a rotavirus might aid in clarifying this matter in the future.

Importantly, interdonor variations were observed with some BA organoids displaying transcriptomes more similar to healthy or disease control organoids and vice versa. Future comparison with clinical presentations of BA patients and control donors might reveal whether these transcriptomic differences in patient organoids reflect disease severity *in vivo*. Moreover, since BA pathogenesis is thought to be a multifactorial process, it may well be that differences in genetic predispositions and/or previous *in vivo* exposure to environmental stimuli caused sensitivity differences in BA liver organoids *in vitro*.

Conclusion

The present exploratory study suggests that differences between healthy control and BA liver organoids can be observed *in vitro* even in the absence of distinct morphological differences (Figure 10). Thus, human liver organoids represent an interesting human patient-specific *in vitro* model of BA pathogenesis, capable of showcasing effects of environmental causes of BA using biliatresone and the viral analog poly I:C. Dysregulated ECM-cell interaction and enhanced expression of certain antigen presenting genes specifically expressed in BA patients at baseline and after a viral insult, suggest that cholangiocytes may play a role in modulating the immune system and thereby contribute to BA pathology. It remains to be determined if abnormal immune modulation may also be the consequence rather than the cause of BA. We believe that modeling BA with human liver organoids has the potential to further unravel detailed BA mechanisms.

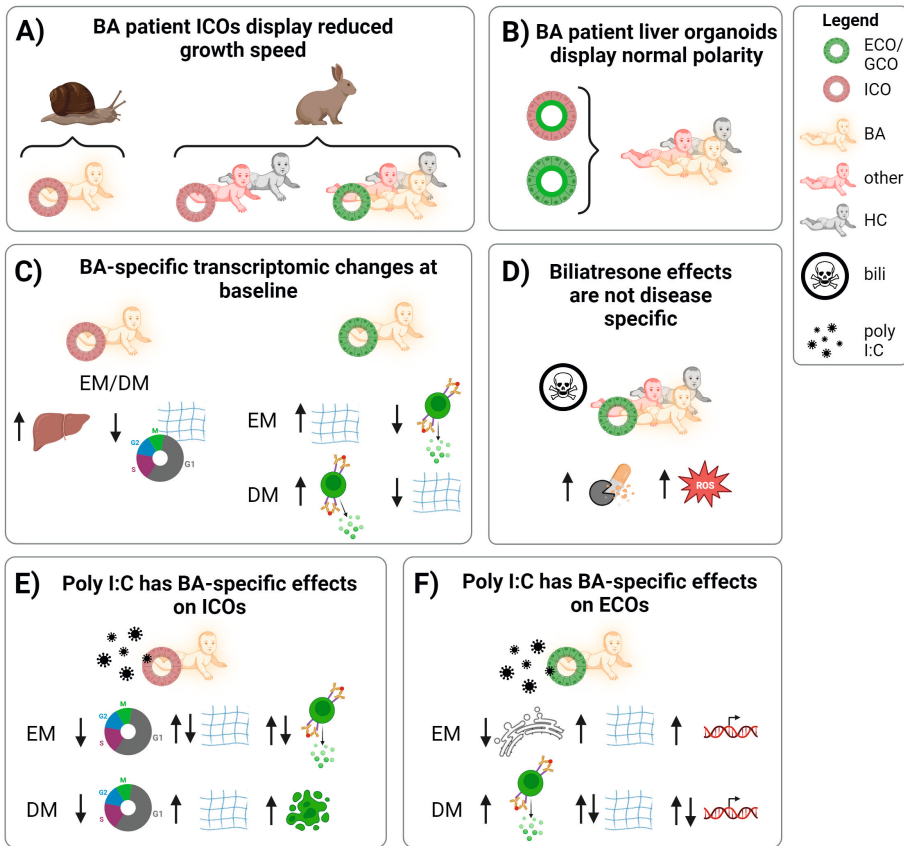


Figure 10. Summary of the main findings of this study. **A)** BA patient ICOs display lower growth rates compared to other BA patient and control liver organoids. **B)** BA patient liver organoids display a normal polarity with the apical domain facing the lumen. **C)** BA liver organoids display specific transcriptomic differences compared to control organoids. Progenitor and differentiated BA patient ICOs show increased hepatic differentiation and decreased cell cycle regulation and cell-ECM interaction. Progenitor BA patient ECOs show increased cell-ECM interaction and decreased immune response and vice versa for BA patient ECOs. **D)** The toxin biliary atresone elicits increases in detoxification and oxidative stress response in all organoid types regardless of disease history. **E)** Poly I:C elicits BA-specific effects in BA patient ICOs. In progenitor BA patient ICOs poly I:C elicits downregulation of cell cycle regulation, and dysregulation of cell-ECM interaction and immune response. In differentiated BA patient ICOs poly I:C elicits downregulation of cell cycle regulation and upregulation of cell-ECM interaction and apoptosis regulation. **F)** Poly I:C elicits BA-specific effects in BA patient ECOs. In progenitor BA patient ECOs poly I:C elicits downregulation of protein processing and upregulation of cell-ECM interaction and transcription regulation. In differentiated BA patient ECOs poly I:C elicits upregulation of immune response and dysregulation of cell-ECM interaction and transcription regulation. BA, biliary atresia; bili, biliary atresone; DM, differentiated cell state; ECO, extrahepatic cholangiocyte organoid; EM, progenitor cell state; GCO, gallbladder cholangiocyte organoid; HC, healthy control; ICO, intrahepatic cholangiocyte organoid; other, non-BA disease control

Authorship statement

SAF and JBFH conceptualized the idea of modeling biliary atresia using patient-derived liver organoids. IFS (PhD candidate) and I designed and proposed the methodology and the experimental design. Preliminary work was performed together with LAG, KvA and AvdM (MSc students), while I designed and performed experiments leading up to the bioinformatics analyses. I performed data management and conducted a majority of the data analysis. Meanwhile AIA (PhD candidate) performed the bioinformatics analyses and I interpreted the biological relevance of the results. I wrote the first draft of the manuscript and implemented the contributions of the co-authors and external reviewers up to the current manuscript. During the whole process I asked for and implemented input and feedback from the other contributors to this study.

References

1. Mullanpudi B, Hendrickson R. Pediatric liver transplantation. *Semin Pediatr Surg.* 2022;31(3). doi:10.1016/j.sempedsurg.2022.151191
2. Smith SK, Miloh T. Pediatric Liver Transplantation. *Clin Liver Dis.* 2022;26(3):521-535. doi:10.1016/j.cld.2022.03.010
3. Asai A, Miethke A, Bezerra JA. Pathogenesis of biliary atresia: Defining biology to understand clinical phenotypes. *Nat Rev Gastroenterol Hepatol.* 2015;12(6):342-352. doi:10.1038/nrgastro.2015.74
4. Hartley JL, Davenport M, Kelly DA. Biliary atresia. *The Lancet.* 2009;374(9702):1704-1713. doi:10.1016/S0140-6736(09)60946-6
5. Pinto RB, Schneider ACR, da Silveira TR. Cirrhosis in children and adolescents: An overview. *World J Hepatol.* 2015;7(3):392. doi:10.4254/WJH.V7.I3.392
6. Ishitani MB. Biliary atresia and the Kasai portoenterostomy: Never say never? *Liver Transplantation.* 2001;7(9):831-832. doi:10.1053/JLTS.2001.0070831
7. Bijl EJ, Bharwani KD, Houwen RHJ, de Man RD. The long-term outcome of the Kasai operation in patients with biliary atresia: a systematic review. *Neth J Med.* 2013;71(4):170-173. Accessed March 22, 2023. <https://pubmed.ncbi.nlm.nih.gov/23723110/>
8. Shneider BL, Brown MB, Haber B, et al. A multicenter study of the outcome of biliary atresia in the United States, 1997 to 2000. *J Pediatr.* 2006;148(4):467-474.e1. doi:10.1016/j.jpeds.2005.12.054
9. Nio M, Ohi R, Miyano T, Saeki M, Shiraki K, Tanaka K. Five- and 10-year survival rates after surgery for biliary atresia: a report from the Japanese biliary atresia registry. *J Pediatr Surg.* 2003;38(7):997-1000. doi:10.1016/S0022-3468(03)00178-7
10. Chung PHY, Chan EKW, Yeung F, et al. Life long follow up and management strategies of patients living with native livers after Kasai portoenterostomy. *Scientific Reports 2021 11:1.* 2021;11(1):1-9. doi:10.1038/S41598-021-90860-W
11. Bezerra JA. Biliary Atresia-Translational Research on Key Molecular Processes Regulating Biliary Injury and Obstruction. *Chang Gung Med J.* 2006;29(3):222-230. Accessed January 11, 2021. <https://pubmed.ncbi.nlm.nih.gov/16924882/>
12. Lachaux A, Descos B, Plauchu H, et al. Familial extrahepatic biliary atresia. *J Pediatr Gastroenterol Nutr.* 1988;7(2):280-283. doi:10.1097/00005176-198803000-00020
13. Fallon SC, Chang S, Finegold MJ, Karpen SJ, Brandt ML. Discordant presentation of biliary atresia in premature monozygotic twins. *J Pediatr Gastroenterol Nutr.* 2013;57(4):e22-e23. doi:10.1097/MPG.0b013e31826a1044
14. Tiao MM, Tsai SS, Kuo HW, Chen CL, Yang CY. Epidemiological features of biliary atresia in Taiwan, a national study 1996–2003. *J Gastroenterol Hepatol.* 2008;23(1):62-66. doi:10.1111/J.1440-1746.2007.05114.X
15. Bessho K, Satomura Y. Genetics and Epigenetics in the Pathogenesis of Biliary Atresia. In: *Introduction to Biliary Atresia.* Springer, Singapore; 2021:41-46. doi:10.1007/978-981-16-2160-4_7
16. Petersen C, Biermanns D, Kuske M, Schäkel K, Meyer-Junghänel L, Mildemberger H. New aspects in a murine model for extrahepatic biliary atresia. *J Pediatr Surg.* 1997;32(8):1190-1195. doi:10.1016/S0022-3468(97)90680-1

17. Riepenhoff-talty M, Schaeckel K, Clark HF, et al. Group A Rotaviruses Produce Extrahepatic Biliary Obstruction in Orally Inoculated Newborn Mice. *Pediatric Research* 1993 33:4. 1993;33(4):394-399. doi:10.1203/00006450-199304000-00016
18. Szavay PO, Leonhardt J, Czech-Schmidt G, Petersen C. The role of reovirus type 3 infection in an established murine model for biliary atresia. *European Journal of Pediatric Surgery*. 2002;12(4):248-250. doi:10.1055/s-2002-34477
19. Bangaru B, Morecki R, Glaser JH, Gartner LM, Horwitz MS. Comparative studies of biliary atresia in the human newborn and reovirus-induced cholangitis in weanling mice - PubMed. *Lab Invest*. 1980;43(5):456-462. Accessed March 23, 2023. <https://pubmed.ncbi.nlm.nih.gov/7421127/>
20. Mohanty SK, Donnelly B, Bondoc A, et al. Rotavirus Replication in the Cholangiocyte Mediates the Temporal Dependence of Murine Biliary Atresia. *PLoS One*. 2013;8(7):e69069. doi:10.1371/JOURNAL.PONE.0069069
21. Hertel PM, Estes MK. Rotavirus and biliary atresia: Can causation be proven? *Curr Opin Gastroenterol*. 2012;28(1):10-17. doi:10.1097/MOG.0b013e32834c7ae4
22. Barnes BH, Tucker RM, Wehrmann F, Mack DG, Ueno Y, Mack CL. Cholangiocytes as immune modulators in rotavirus-induced murine biliary atresia. *Liver International*. 2009;29(8):1253-1261. doi:10.1111/J.1478-3231.2008.01921.X
23. Jafri M, Donnelly B, Bondoc A, Allen S, Tiao G. Cholangiocyte secretion of chemokines in experimental biliary atresia. *J Pediatr Surg*. 2009;44(3):500-507. doi:10.1016/j.jpedsurg.2008.07.007
24. Horst AK, Kumashie KG, Neumann K, Diehl L, Tiegs G. Antigen presentation, autoantibody production, and therapeutic targets in autoimmune liver disease. *Cell Mol Immunol*. 2021;18(1):92-111. doi:10.1038/S41423-020-00568-6
25. Mehrfeld C, Zenner S, Kornek M, Lukacs-Kornek V. The contribution of non-professional antigen-presenting cells to immunity and tolerance in the liver. *Front Immunol*. 2018;9:635. doi:10.3389/FIMMU.2018.00635/BIBTEX
26. Schruppf E, Tan C, Karlsen TH, et al. The biliary epithelium presents antigens to and activates natural killer T cells. *Hepatology*. 2015;62(4):1249. doi:10.1002/HEP.27840
27. Chen XM, O'Hara SP, LaRusso NF. The immunobiology of cholangiocytes. *Immunol Cell Biol*. 2008;86(6):497-505. doi:10.1038/ICB.2008.37
28. Pinto C, Giordano DM, Maroni L, Marzioni M. Role of inflammation and proinflammatory cytokines in cholangiocyte pathophysiology. *Biochimica et Biophysica Acta (BBA) - Molecular Basis of Disease*. 2018;1864(4):1270-1278. doi:10.1016/J.BBADIS.2017.07.024
29. Björkström NK. Immunobiology of the biliary tract system. *J Hepatol*. 2022;77(6):1657-1669. doi:10.1016/J.JHEP.2022.08.018
30. Banales JM, Huebert RC, Karlsen T, Strazzabosco M, LaRusso NF, Gores GJ. Cholangiocyte pathobiology. *Nat Rev Gastroenterol Hepatol*. 2019;16(5):269. doi:10.1038/S41575-019-0125-Y
31. Lorent K, Gong W, Koo KA, et al. Identification of a plant isoflavonoid that causes biliary atresia. *Sci Transl Med*. 2015;7(286). doi:10.1126/SCITRANSLMED.AAA1652
32. Estrada MA, Zhao X, Lorent K, et al. Synthesis and Structure-Activity Relationship Study of Biliatresone, a Plant Isoflavonoid That Causes Biliary Atresia. *ACS Med Chem Lett*. 2018;9(1):61-64. doi:10.1021/acsmedchemlett.7b00479

33. Zhao X, Lorent K, Wilkins BJ, et al. Glutathione antioxidant pathway activity and reserve determine toxicity and specificity of the biliary toxin biliaryresone in zebrafish. *Hepatology*. 2016;64(3):894-907. doi:10.1002/hep.28603
34. Waisbourd-Zinman O, Koh H, Tsai S, et al. The toxin biliaryresone causes mouse extrahepatic cholangiocyte damage and fibrosis through decreased glutathione and SOX17. *Hepatology*. 2016;64(3):880-893. doi:10.1002/hep.28599
35. Yin C. Molecular mechanisms of Sox transcription factors during the development of liver, bile duct, and pancreas. *Semin Cell Dev Biol*. 2017;63:68. doi:10.1016/j.semcdb.2016.08.015
36. Spence JR, Lange AW, Lin SCJ, et al. Sox17 regulates organ lineage segregation of ventral foregut progenitor cells. *Dev Cell*. 2009;17(1):62. doi:10.1016/j.devcel.2009.05.012
37. Mack CL, Sokol RJ. Unraveling the Pathogenesis and Etiology of Biliary Atresia. *Pediatric Research* 2005 57:7. 2005;57(7):87-94. doi:10.1203/01.pdr.0000159569.57354.47
38. Huch M, Gehart H, Van Boxtel R, et al. Long-term culture of genome-stable bipotent stem cells from adult human liver. *Cell*. 2015;160(1-2):299-312. doi:10.1016/j.cell.2014.11.050
39. Sampaziotis F, Justin AW, Tysoe OC, et al. Reconstruction of the mouse extrahepatic biliary tree using primary human extrahepatic cholangiocyte organoids. *Nat Med*. 2017;23(8):954-963. doi:10.1038/nm.4360
40. Lugli N, Kamileri I, Keogh A, et al. R-spondin 1 and noggin facilitate expansion of resident stem cells from non-damaged gallbladders. *EMBO Rep*. Published online 2016. doi:10.15252/embr.201642169
41. Roos FJM, Versteegen MMA, Muñoz Albarinos L, et al. Human Bile Contains Cholangiocyte Organoid-Initiating Cells Which Expand as Functional Cholangiocytes in Non-canonical Wnt Stimulating Conditions. *Front Cell Dev Biol*. 2021;8:1924. doi:10.3389/fcell.2020.630492/BIBTEX
42. Lehmann V, Schene IF, Ardisasmita AI, et al. The potential and limitations of intrahepatic cholangiocyte organoids to study inborn errors of metabolism. *J Inherit Metab Dis*. 2022;45(2):353-365. doi:10.1002/jimd.12450
43. Rimland CA, Tilson SG, Morell CM, et al. Regional Differences in Human Biliary Tissues and Corresponding In Vitro-Derived Organoids. *Hepatology*. 2021;73(1):247-267. doi:10.1002/HEP.31252
44. Versteegen MMA, Roos FJM, Burka K, et al. Human extrahepatic and intrahepatic cholangiocyte organoids show region-specific differentiation potential and model cystic fibrosis-related bile duct disease. *Sci Rep*. 2020;10(1):21900. doi:10.1038/s41598-020-79082-8
45. Love MI, Huber W, Anders S. Moderated estimation of fold change and dispersion for RNA-seq data with DESeq2. *Genome Biol*. 2014;15(12):1-21. doi:10.1186/S13059-014-0550-8/FIGURES/9
46. Xie Z, Bailey A, Kuleshov M V., et al. Gene Set Knowledge Discovery with Enrichr. *Curr Protoc*. 2021;1(3):e90. doi:10.1002/CPZ1.90
47. Kuleshov M V., Jones MR, Rouillard AD, et al. Enrichr: a comprehensive gene set enrichment analysis web server 2016 update. *Nucleic Acids Res*. 2016;44(W1):W90-W97. doi:10.1093/NAR/GKW377
48. Chen EY, Tan CM, Kou Y, et al. Enrichr: interactive and collaborative HTML5 gene list enrichment analysis tool. *BMC Bioinformatics*. 2013;14. doi:10.1186/1471-2105-14-128

49. Snel B, Lehmann G, Bork P, Huynen MA. STRING: a web-server to retrieve and display the repeatedly occurring neighbourhood of a gene. *Nucleic Acids Res.* 2000;28(18):3442-3444. doi:10.1093/NAR/28.18.3442
50. Jensen LJ, Kuhn M, Stark M, et al. STRING 8--a global view on proteins and their functional interactions in 630 organisms. *Nucleic Acids Res.* 2009;37(Database issue). doi:10.1093/NAR/GKN760
51. von Mering C, Jensen LJ, Kuhn M, et al. STRING 7--recent developments in the integration and prediction of protein interactions. *Nucleic Acids Res.* 2007;35(suppl_1):D358-D362. doi:10.1093/NAR/GKL825
52. Franceschini A, Lin J, Von Mering C, Jensen LJ. SVD-phy: improved prediction of protein functional associations through singular value decomposition of phylogenetic profiles. *Bioinformatics.* 2016;32(7):1085-1087. doi:10.1093/BIOINFORMATICS/BTV696
53. Szklarczyk D, Kirsch R, Koutrouli M, et al. The STRING database in 2023: protein-protein association networks and functional enrichment analyses for any sequenced genome of interest. *Nucleic Acids Res.* 2023;51(D1):D638-D646. doi:10.1093/NAR/GKAC1000
54. Fried S, Gilboa D, Har-Zahav A, et al. Extrahepatic cholangiocyte obstruction is mediated by decreased glutathione, Wnt and Notch signaling pathways in a toxic model of biliary atresia. *Sci Rep.* 2020;10:1-10. doi:10.1038/s41598-020-64503-5
55. Stanifer ML, Mukenhirn M, Muenchau S, et al. Asymmetric distribution of TLR3 leads to a polarized immune response in human intestinal epithelial cells. *Nat Microbiol.* 2020;5(1):181-191. doi:10.1038/S41564-019-0594-3
56. Bao Y, Wang L, Shi L, et al. Transcriptome profiling revealed multiple genes and ECM-receptor interaction pathways that may be associated with breast cancer. *Cell Mol Biol Lett.* 2019;24(1):1-20. doi:10.1186/S11658-019-0162-0/FIGURES/7
57. Schlie-Wolter S, Ngezahayo A, Chichkov BN. The selective role of ECM components on cell adhesion, morphology, proliferation and communication in vitro. *Exp Cell Res.* 2013;319(10):1553-1561. doi:10.1016/J.YEXCR.2013.03.016
58. Yeh MH, Tzeng YJ, Fu TY, et al. Extracellular Matrix-receptor Interaction Signaling Genes Associated with Inferior Breast Cancer Survival. *Anticancer Res.* 2018;38(8):4593-4605. doi:10.21873/ANTICANRES.12764
59. Monte M, Collavin L, Lazarevic D, Utrera R, Dragani TA, Schneider C. Cloning, chromosome mapping and functional characterization of a human homologue of murine gtse-1 (B99) gene. *Gene.* 2000;254(1-2):229-236. doi:10.1016/S0378-1119(00)00260-2
60. Fu J, Qin W, Tong Q, et al. A novel DNA methylation-driver gene signature for long-term survival prediction of hepatitis-positive hepatocellular carcinoma patients. *Cancer Med.* 2022;11(23):4721-4735. doi:10.1002/CAM4.4838
61. Ashouri A, Sayin VI, Van den Eynden J, Singh SX, Papagiannakopoulos T, Larsson E. Pan-cancer transcriptomic analysis associates long non-coding RNAs with key mutational driver events. *Nat Commun.* 2016;0:13197. doi:10.1038/NCOMMS13197
62. Pan Z, Mao W, Bao Y, Zhang M, Su X, Xu X. The long noncoding RNA CASC9 regulates migration and invasion in esophageal cancer. *Cancer Med.* 2016;5(9):2442. doi:10.1002/CAM4.770
63. Maes M, Crespo Yanguas S, Willebrords J, Cogliati B, Vinken M. Connexin and pannexin signaling in gastrointestinal and liver disease. *Transl Res.* 2015;166(4):332. doi:10.1016/J.TRSL.2015.05.005

64. Maes M, Decroock E, Cogliati B, et al. Connexin and pannexin (hemi)channels in the liver. *Front Physiol.* 2013;4. doi:10.3389/FPHYS.2013.00405
65. Amarachintha SP, Mourya R, Ayabe H, et al. Biliary organoids uncover delayed epithelial development and barrier function in biliary atresia. *Hepatology.* 2022;75(1):89-103. doi:10.1002/HEP.32107
66. Babu RO, Lui VCH, Chen Y, et al. Beta-amyloid deposition around hepatic bile ducts is a novel pathobiological and diagnostic feature of biliary atresia. *J Hepatol.* 2020;73(6):1391-1403. doi:10.1016/j.jhep.2020.06.012
67. Chardot C, Carton M, Spire-Bendelac N, Pommelet C Le, Golmard JL, Auvert B. Epidemiology of biliary atresia in France: A national study 1986-96. *J Hepatol.* 1999;31(6):1006-1013. doi:10.1016/S0168-8278(99)80312-2
68. Chung PHY, Zheng S, Tam PKH. Biliary atresia: East versus west. *Semin Pediatr Surg.* 2020;29(4):150950. doi:10.1016/j.SEMPEDSURG.2020.150950
69. Jimenez-Rivera C, Jolin-Dahel KS, Fortinsky KJ, Gozdyra P, Benchimol EI. International incidence and outcomes of biliary atresia. *J Pediatr Gastroenterol Nutr.* 2013;56(4):344-354. doi:10.1097/MPG.0B013E318282A913
70. McKiernan PJ, Baker AJ, Kelly DA. The frequency and outcome of biliary atresia in the UK and Ireland. *Lancet.* 2000;355(9197):25-29. doi:10.1016/S0140-6736(99)03492-3
71. Davenport M, De Ville De Goyet J, Stringer MD, et al. Seamless management of biliary atresia in England and Wales (1999–2002). *The Lancet.* 2004;363(9418):1354-1357. doi:10.1016/S0140-6736(04)16045-5
72. Hsiao CH, Chang MH, Chen HL, et al. Universal screening for biliary atresia using an infant stool color card in Taiwan. *Hepatology.* 2008;47(4):1233-1240. doi:10.1002/HEP.22182
73. Scheemaeker S, Inglebert M, Daminet S, et al. Organoids of patient-derived medullary thyroid carcinoma: The first milestone towards a new in vitro model in dogs. *Vet Comp Oncol.* 2023;21(1):111-122. doi:10.1111/VCO.12872
74. Chen X, Qian W, Song Z, Li QX, Guo S. Authentication, characterization and contamination detection of cell lines, xenografts and organoids by barcode deep NGS sequencing. *NAR Genom Bioinform.* 2020;2(3). doi:10.1093/NARGAB/LQAA060
75. Hendriks D, Brouwers JF, Hamer K, et al. Engineered human hepatocyte organoids enable CRISPR-based target discovery and drug screening for steatosis. *Nature Biotechnology* 2023. Published online February 23, 2023:1-15. doi:10.1038/s41587-023-01680-4
76. Fridman R, Benton G, Aranoutova I, Kleinman HK, Bonfil RD. Increased initiation and growth of tumor cell lines, cancer stem cells and biopsy material in mice using basement membrane matrix protein (Cultrex or Matrigel) co-injection. *Nature Protocols* 2012 7:6. 2012;7(6):1138-1144. doi:10.1038/NPROT.2012.053
77. Arnaoutova I, George J, Kleinman HK, Benton G. The endothelial cell tube formation assay on basement membrane turns 20: State of the science and the art. *Angiogenesis.* 2009;12(3):267-274. doi:10.1007/s10456-009-9146-4
78. Lee GY, Kenny PA, Lee EH, Bissell MJ. Three-dimensional culture models of normal and malignant breast epithelial cells. *Nature Methods* 2007 4:4. 2007;4(4):359-365. doi:10.1038/NMETH1015
79. Ruitter FAA, Morgan FLC, Roumans N, et al. Soft, Dynamic Hydrogel Confinement Improves Kidney Organoid Lumen Morphology and Reduces Epithelial–Mesenchymal Transition in Culture. *Advanced Science.* 2022;9(20):2200543. doi:10.1002/ADVS.202200543

80. Gilchrist CL, Darling EM, Chen J, Setton LA. Extracellular Matrix Ligand and Stiffness Modulate Immature Nucleus Pulposus Cell-Cell Interactions. *PLoS One*. 2011;6(11):e27170. doi:10.1371/JOURNAL.PONE.0027170
81. Mittal N, Tasnim F, Yue C, et al. Substrate Stiffness Modulates the Maturation of Human Pluripotent Stem-Cell-Derived Hepatocytes. *ACS Biomater Sci Eng*. 2016;2(9):1649-1657. doi:10.1021/acsbiomaterials.6b00475
82. Li W, Li P, Li N, et al. Matrix stiffness and shear stresses modulate hepatocyte functions in a fibrotic liver sinusoidal model. *Am J Physiol Gastrointest Liver Physiol*. 2021;320(3):G272-G282. doi:10.1152/ajpgi.00379.2019
83. Kourouklis AP, Kaylan KB, Underhill GH. Substrate stiffness and matrix composition coordinately control the differentiation of liver progenitor cells. *Biomaterials*. 2016;99:82-94. doi:10.1016/j.biomaterials.2016.05.016
84. Slater K, Partridge J, Nandivada H. *Tuning the Elastic Moduli of Corning® Matrigel® and Collagen I 3D Matrices by Varying the Protein Concentration.*; 2017.
85. Malik A, Thanekar U, Mourya R, Shivakumar P. Recent developments in etiology and disease modeling of biliary atresia: a narrative review. *Dig Med Res*. 2020;3(0):59-59. doi:10.21037/DMR-20-97
86. Sorrentino G, Rezakhani S, Yildiz E, et al. Mechano-modulatory synthetic niches for liver organoid derivation. *Nat Commun*. 2020;11(1):1-10. doi:10.1038/s41467-020-17161-0
87. Smith M, Zuckerman M, Kandaneeratchi A, Thompson R, Davenport M. Using next-generation sequencing of microRNAs to identify host and/or pathogen nucleic acid signatures in samples from children with biliary atresia – a pilot study. *Access Microbiol*. 2020;2(7). doi:10.1099/ACMI.0.000127
88. Xu B, Broome U, Ericzon BG, Sumitran-Holgersson S. High frequency of autoantibodies in patients with primary sclerosing cholangitis that bind biliary epithelial cells and induce expression of CD44 and production of interleukin 6. *Gut*. 2002;51(1):120-127. doi:10.1136/GUT.51.1.120
89. Mikami T, Saegusa M, Mitomi H, Yanagisawa N, Ichinoe M, Okayasu I. Significant correlations of E-cadherin, catenin, and CD44 variant form expression with carcinoma cell differentiation and prognosis of extrahepatic bile duct carcinomas. *Am J Clin Pathol*. 2001;116(3):369-376. doi:10.1309/VV6D-3GAH-VEJM-DUJT
90. Cruickshank SM, Southgate J, Wyatt JI, Selby PJ, Trejdosiewicz LK. Expression of CD44 on bile ducts in primary sclerosing cholangitis and primary biliary cirrhosis. *J Clin Pathol*. 1999;52(10):730-734. doi:10.1136/JCP.52.10.730
91. Min J, Ningappa M, So J, Shin D, Sindhi R, Subramaniam S. Systems Analysis of Biliary Atresia Through Integration of High-Throughput Biological Data. *Front Physiol*. 2020;11. doi:10.3389/fphys.2020.00966
92. Whitby T, Schroeder D, Kim HS, et al. Modifications in Integrin Expression and Extracellular Matrix Composition in Children with Biliary Atresia. *Klin Padiatr*. 2015;227(1):15-22. doi:10.1055/s-0034-1389906
93. Co JY, Margalef-Català M, Li X, et al. Controlling Epithelial Polarity: A Human Enteroid Model for Host-Pathogen Interactions. *Cell Rep*. 2019;26(9):2509-2520. doi:10.1016/j.celrep.2019.01.108
94. Lee JL, Streuli CH. Integrins and epithelial cell polarity. *J Cell Sci*. 2014;127(Pt 15):3217-3225. doi:10.1242/JCS.146142

95. Myllymäki SM, Teräväinen TP, Manninen A. Two distinct integrin-mediated mechanisms contribute to apical lumen formation in epithelial cells. *PLoS One*. 2011;6(5). doi:10.1371/JOURNAL.PONE.0019453
96. Jafri M, Donnelly B, Allen S, et al. Cholangiocyte expression of $\alpha 2\beta 1$ -integrin confers susceptibility to rotavirus-induced experimental biliary atresia. *Am J Physiol Gastrointest Liver Physiol*. 2008;295(1):G16-G26. doi:10.1152/ajpgi.00442.2007
97. Fleming FE, Graham KL, Takada Y, Coulson BS. Determinants of the Specificity of Rotavirus Interactions with the $\alpha 2\beta 1$ Integrin. *Journal of Biological Chemistry*. 2011;286(8):6165-6174. doi:10.1074/JBC.M110.142992
98. Toutain PL, Ferran A, Bousquet-Mélou A. Species differences in pharmacokinetics and pharmacodynamics. *Handb Exp Pharmacol*. 2010;199:19-48. doi:10.1007/978-3-642-10324-7_2
99. Zhao X, Lorent K, Escobar-Zarate D, et al. Impaired Redox and Protein Homeostasis as Risk Factors and Therapeutic Targets in Toxin-Induced Biliary Atresia. *Gastroenterology*. 2020;159(3):1068-1084.e2. doi:10.1053/j.gastro.2020.05.080
100. Yue H, Sivasankaran Menon S, Ottakandathil Babu R, et al. Environmental toxin biliatresone can induce biliary atresia: evidence from human liver organoids. Published online November 3, 2022. doi:10.21203/RS.3.RS-2185022/V1
101. Romani P, Nirchio N, Arboit M, et al. Mitochondrial fission links ECM mechanotransduction to metabolic redox homeostasis and metastatic chemotherapy resistance. *Nat Cell Biol*. 2022;24(2):168-180. doi:10.1038/s41556-022-00843-w
102. Li Y, Lang J, Ye Z, et al. Effect of Substrate Stiffness on Redox State of Single Cardiomyocyte: A Scanning Electrochemical Microscopy Study. *Anal Chem*. 2020;92(7):4771-4779. doi:10.1021/acs.analchem.9b03178
103. Girard E, Chagnon G, Gremen E, et al. Biomechanical behaviour of human bile duct wall and impact of cadaveric preservation processes. *J Mech Behav Biomed Mater*. 2019;98:291-300. doi:10.1016/j.jmbbm.2019.07.001
104. Wang L, Zheng J, Pathak JL, et al. SLIT2 Overexpression in Periodontitis Intensifies Inflammation and Alveolar Bone Loss, Possibly via the Activation of MAPK Pathway. *Front Cell Dev Biol*. 2020;8:593. doi:10.3389/FCELL.2020.00593/BIBTEX
105. Geraldo LH, Xu Y, Jacob L, et al. SLIT2/ROBO signaling in tumor-associated microglia and macrophages drives glioblastoma immunosuppression and vascular dysmorphia. *J Clin Invest*. 2021;131(16). doi:10.1172/JCI141083
106. Chang J, Lan T, Li C, et al. Activation of Slit2-Robo1 signaling promotes liver fibrosis. *J Hepatol*. 2015;63(6):1413-1420. doi:10.1016/j.jhep.2015.07.033
107. Zeng Z, Wu Y, Cao Y, et al. Slit2-Robo2 signaling modulates the fibrogenic activity and migration of hepatic stellate cells. *Life Sci*. 2018;203:39-47. doi:10.1016/j.lfs.2018.04.017
108. Zhang J, Luo Y, Feng M, Xia Q. Identification of Liver Immune Microenvironment-Related Hub Genes in Liver of Biliary Atresia. *Front Pediatr*. 2022;9:1492. doi:10.3389/FPED.2021.786422/BIBTEX
109. Li C, Yang G, Lin L, et al. Slit2 signaling contributes to cholestatic fibrosis in mice by activation of hepatic stellate cells. *Exp Cell Res*. 2019;385(1):111626. doi:10.1016/j.yexcr.2019.111626
110. Pang X, Cao J, Chen S, et al. Unsupervised Clustering Reveals Distinct Subtypes of Biliary Atresia Based on Immune Cell Types and Gene Expression. *Front Immunol*. 2021;12. doi:10.3389/fimmu.2021.720841

111. Iqbal J, Sarkar-Dutta M, McRae S, Ramachandran A, Kumar B, Waris G. Osteopontin Regulates Hepatitis C Virus (HCV) Replication and Assembly by Interacting with HCV Proteins and Lipid Droplets and by Binding to Receptors α V β 3 and CD44. *J Virol.* 2018;92(13):e02116-17. doi:10.1128/JVI.02116-17
112. Murakami T, Kim J, Li Y, Green GE, Shikanov A, Ono A. Secondary lymphoid organ fibroblastic reticular cells mediate trans-infection of HIV-1 via CD44-hyaluronan interactions. *Nature Communications* 2018 9:1. 2018;9(1):1-14. doi:10.1038/S41467-018-04846-W
113. Li Y, Li J, Wang X, Wu Q, Yang Q. Role of intestinal extracellular matrix-related signaling in porcine epidemic diarrhea virus infection. *Virulence.* 2021;12(1):2352. doi:10.1080/21505594.2021.1972202
114. Sutherland TE, Dyer DP, Allen JE. The extracellular matrix and the immune system: A mutually dependent relationship. *Science.* 2023;379(6633):eabp8964. doi:10.1126/science.abp8964
115. Tomlin H, Piccinini AM. A complex interplay between the extracellular matrix and the innate immune response to microbial pathogens. *Immunology.* 2018;155(2):186-201. doi:10.1111/imm.12972
116. Kanayama M, Xu S, Danzaki K, et al. Skewing of the population balance of lymphoid and myeloid cells by secreted and intracellular osteopontin. *Nat Immunol.* 2017;18(9):973-984. doi:10.1038/NI.3791
117. Breuilh L, Vanhoutte F, Fontaine J, et al. Galectin-3 Modulates Immune and Inflammatory Responses during Helminthic Infection: Impact of Galectin-3 Deficiency on the Functions of Dendritic Cells. *Infect Immun.* 2007;75(11):5148. doi:10.1128/IAI.02006-06
118. Davenport M, Gonde C, Redkar R, et al. Immunohistochemistry of the liver and biliary tree in extrahepatic biliary atresia. *J Pediatr Surg.* 2001;36(7):1017-1025. doi:10.1053/JPSU.2001.24730
119. Dillon PW, Belchis D, Minnick K, Tracy T. Differential Expression of the Major Histocompatibility Antigens and ICAM-1 on Bile Duct Epithelial Cells in Biliary Atresia. *Tohoku J Exp Med.* 1997;181(1):33-40. doi:10.1620/TJEM.181.33
120. Chung PHY, Babu RO, Wu Z, Wong KKY, Tam PKH, Lui VCH. Developing Biliary Atresia-like Model by Treating Human Liver Organoids with Polyinosinic:Polycytidylic Acid (Poly (I:C)). *Curr Issues Mol Biol.* 2022;44(2):644-653. doi:10.3390/CIMB44020045
121. Han Y, Glaser S, Meng F, et al. Recent advances in the morphological and functional heterogeneity of the biliary epithelium. *Exp Biol Med (Maywood).* 2013;238(5):549-565. doi:10.1177/1535370213489926
122. Sampaziotis F, De Brito MC, Geti I, Bertero A, Hannan NRF, Vallier L. Directed differentiation of human induced pluripotent stem cells into functional cholangiocyte-like cells. *Nat Protoc.* 2017;12(4):814-827. doi:10.1038/nprot.2017.011
123. Sampaziotis F, De Brito MC, Madrigal P, et al. Cholangiocytes derived from human induced pluripotent stem cells for disease modeling and drug validation. *Nat Biotechnol.* 2015;33(8):845-852. doi:10.1038/NBT.3275
124. Wang Z, Faria J, van der Laan LJW, Penning LC, Masereeuw R, Spee B. Human Cholangiocytes Form a Polarized and Functional Bile Duct on Hollow Fiber Membranes. *Front Bioeng Biotechnol.* 2022;10:868857. doi:10.3389/fbioe.2022.868857

Supplemental Data

Supplemental Figures

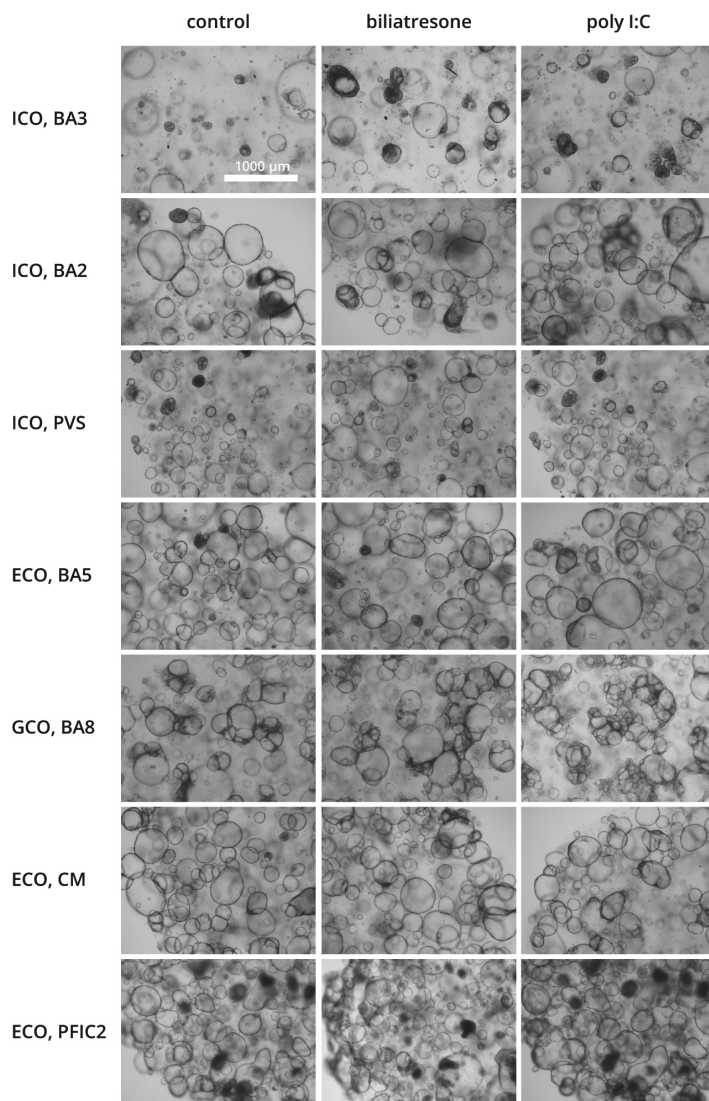


Figure S1. Morphology of progenitor liver organoids after exposure to environmental insults biliatresone and poly I:C. Representative brightfield images of progenitor BA and control (PVS, PFIC2) ICOs, ECOs and GCOs exposed to 2 $\mu\text{g}/\text{mL}$ biliatresone or DMSO control for 24 hours and 80 $\mu\text{g}/\text{mL}$ poly I:C for 6 hours. Donor IDs are defined in more detail in Table S1. BA, biliary atresia; CM, choledocal malformation; ECO, extrahepatic cholangiocyte organoid; GCO, gallbladder cholangiocyte organoid; HC, healthy control; ICO, intrahepatic cholangiocyte organoid; PFIC2, progressive familial intrahepatic cholestasis type 2; PVS, pulmonic valve stenosis

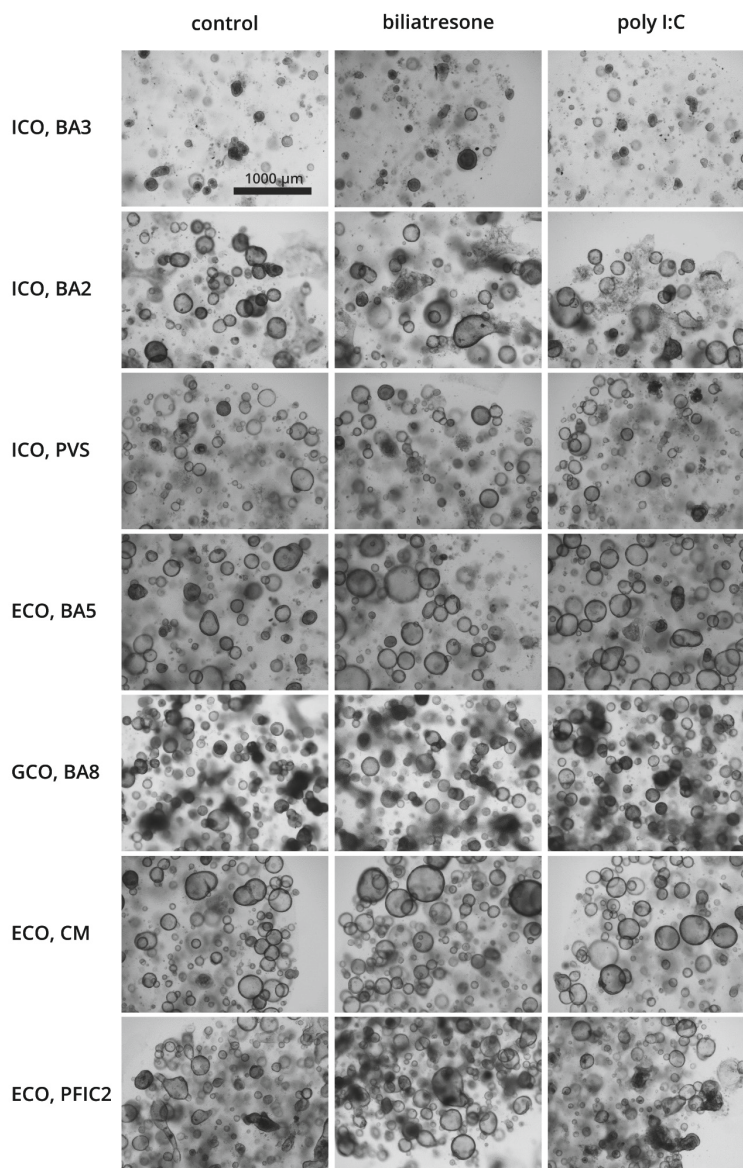


Figure S2. Morphology of differentiated liver organoids after exposure to environmental insults biliatresone and poly I:C. Representative brightfield images of differentiated BA and control (CM, PVS, PFIC2) ICOs, ECOs and GCOs exposed to 2 $\mu\text{g}/\text{mL}$ biliatresone or DMSO control for 24 hours and 80 $\mu\text{g}/\text{mL}$ poly I:C for 6 hours. Donor IDs are defined in more detail in Table S1. BA, biliary atresia; CM, choledocal malformation; ECO, extrahepatic cholangiocyte organoid; GCO, gallbladder cholangiocyte organoid; HC, healthy control; ICO, intrahepatic cholangiocyte organoid; PFIC2, progressive familial intrahepatic cholestasis type 2; PVS, pulmonic valve stenosis

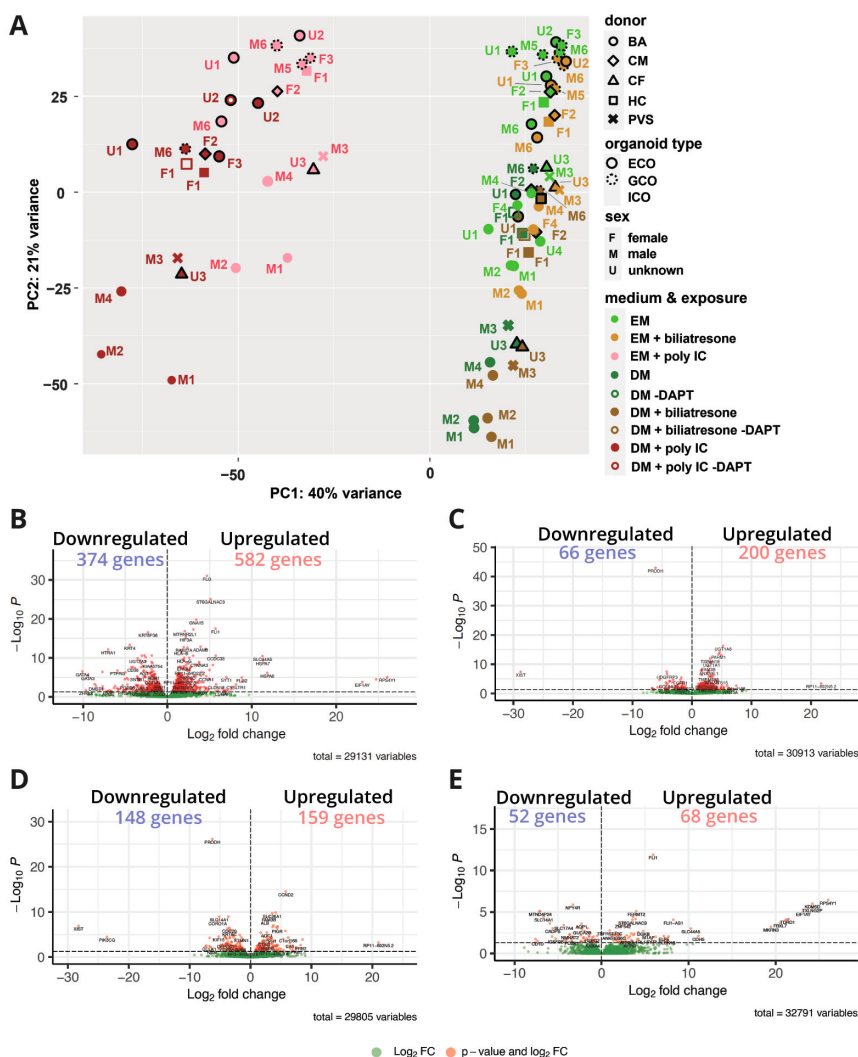


Figure S3. Transcriptome analysis of BA liver organoids at baseline and exposed to biliatresone or poly I:C. **A**) Two-way principal component (PC) analysis of progenitor (EM) and differentiated (DM) BA (ECOs, n = 3; GCOs, n = 4; ICOs, n = 6) and control (CF, CM, HC, PVS; ECOs, n = 2; ICOs, n = 2) liver organoids exposed to DMSO control, biliatresone or poly I:C with or without the addition of DAPT to the differentiation medium. **B-E**) Volcano plots of DEGs identified for BA liver organoids when compared to control organoids at baseline: **B**) differentiated ECOs, **C**) progenitor ICOs, **D**) differentiated ICOs, **E**) progenitor ECOs. Donor IDs are defined in more detail in Table S1. BA, biliary atresia; CF, cystic fibrosis; CM, choledocal malformation; DEG, differentially expressed gene; ECO, extrahepatic cholangiocyte organoid; GCO, gallbladder cholangiocyte organoid; HC, healthy control; ICO, intrahepatic cholangiocyte organoid; PVS, pulmonic valve stenosis

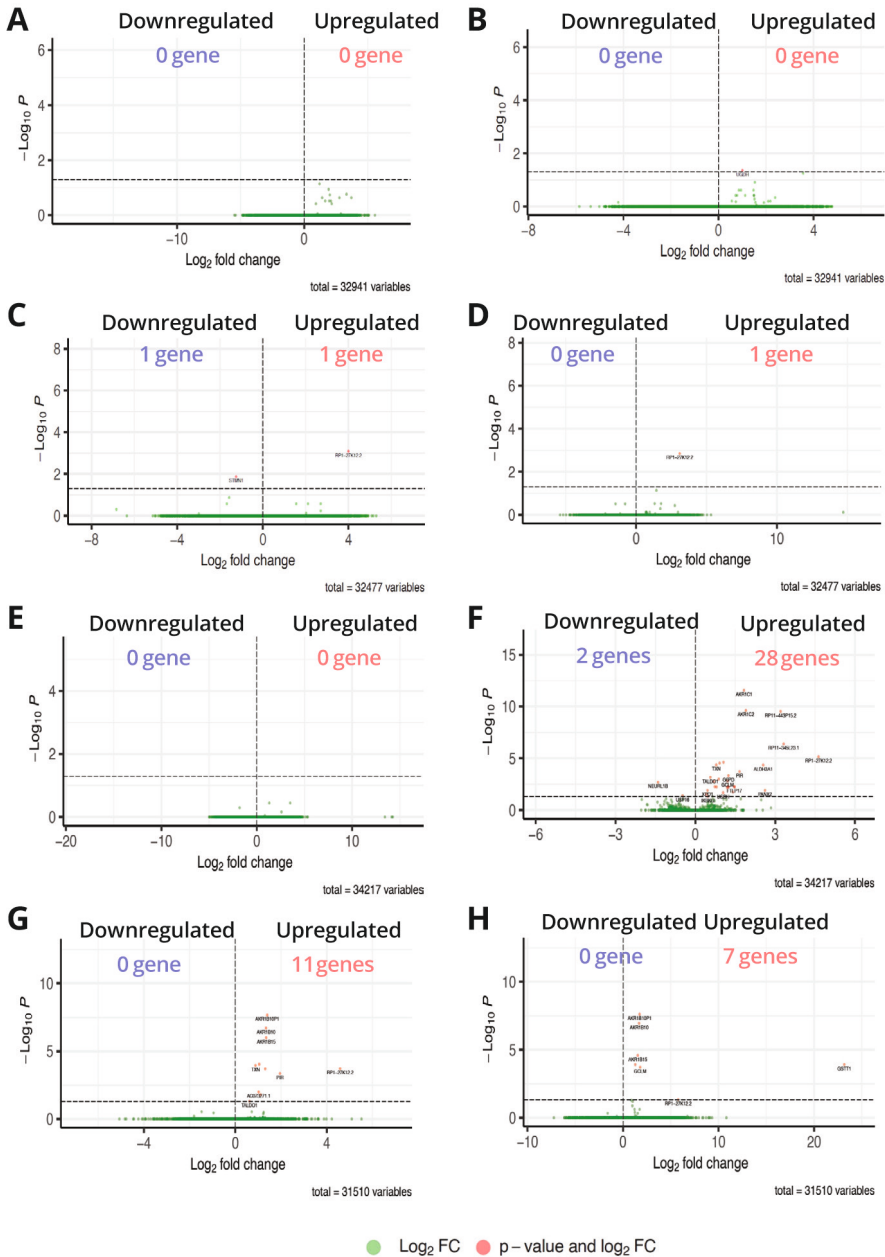


Figure S4. DEGs identified for BA liver organoids exposed to biliary atresia. Volcano plots of DEGs identified for BA and control liver organoids when compared to DMSO conditions: **A**) progenitor control ICOs, **B**) progenitor BA ICOs, **C**) differentiated control ICOs, **D**) differentiated BA ICOs, **E**) progenitor control ECOs, **F**) progenitor BA ECOs, **G**) differentiated control ECOs, **H**) differentiated BA ECOs. BA, biliary atresia; DEG, differentially expressed gene; ECO, extrahepatic cholangiocyte organoid; ICO, intrahepatic cholangiocyte organoid

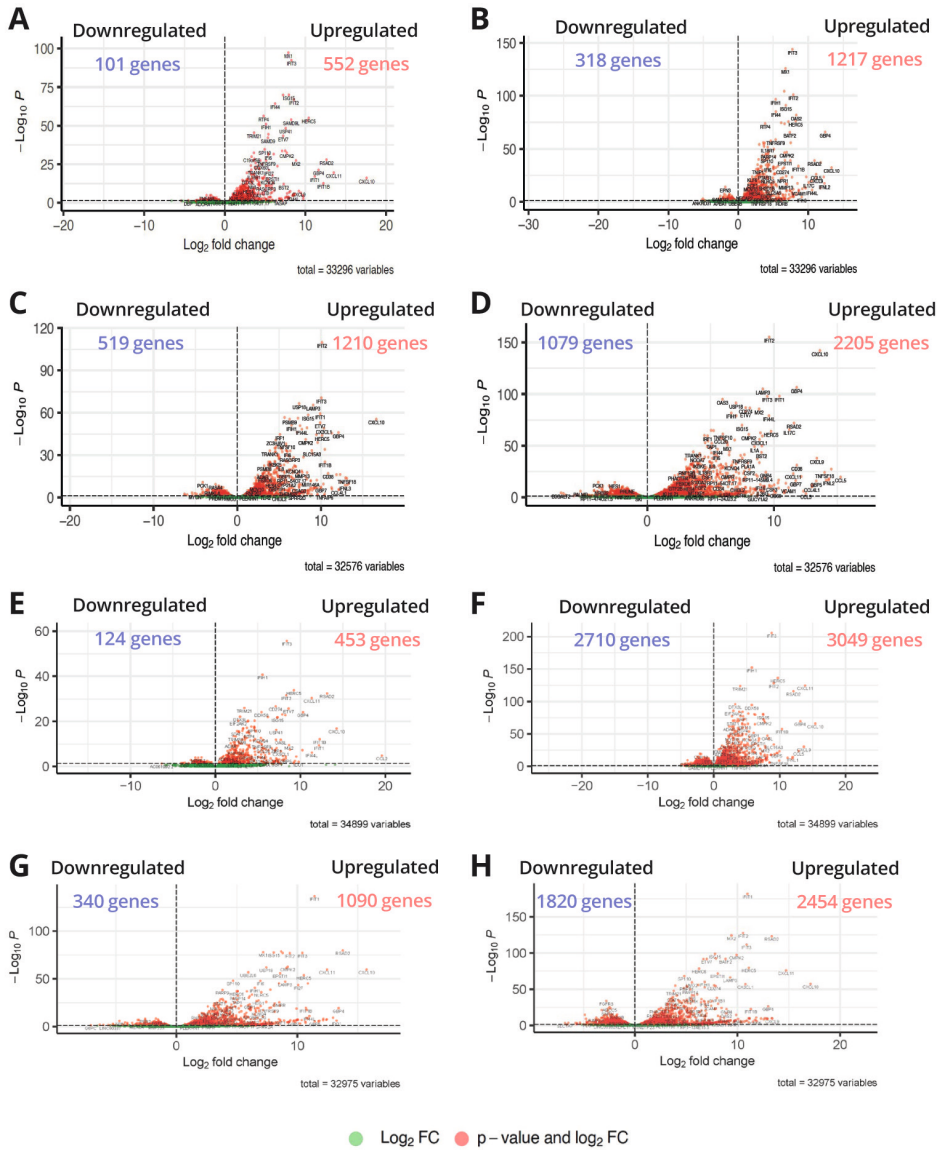
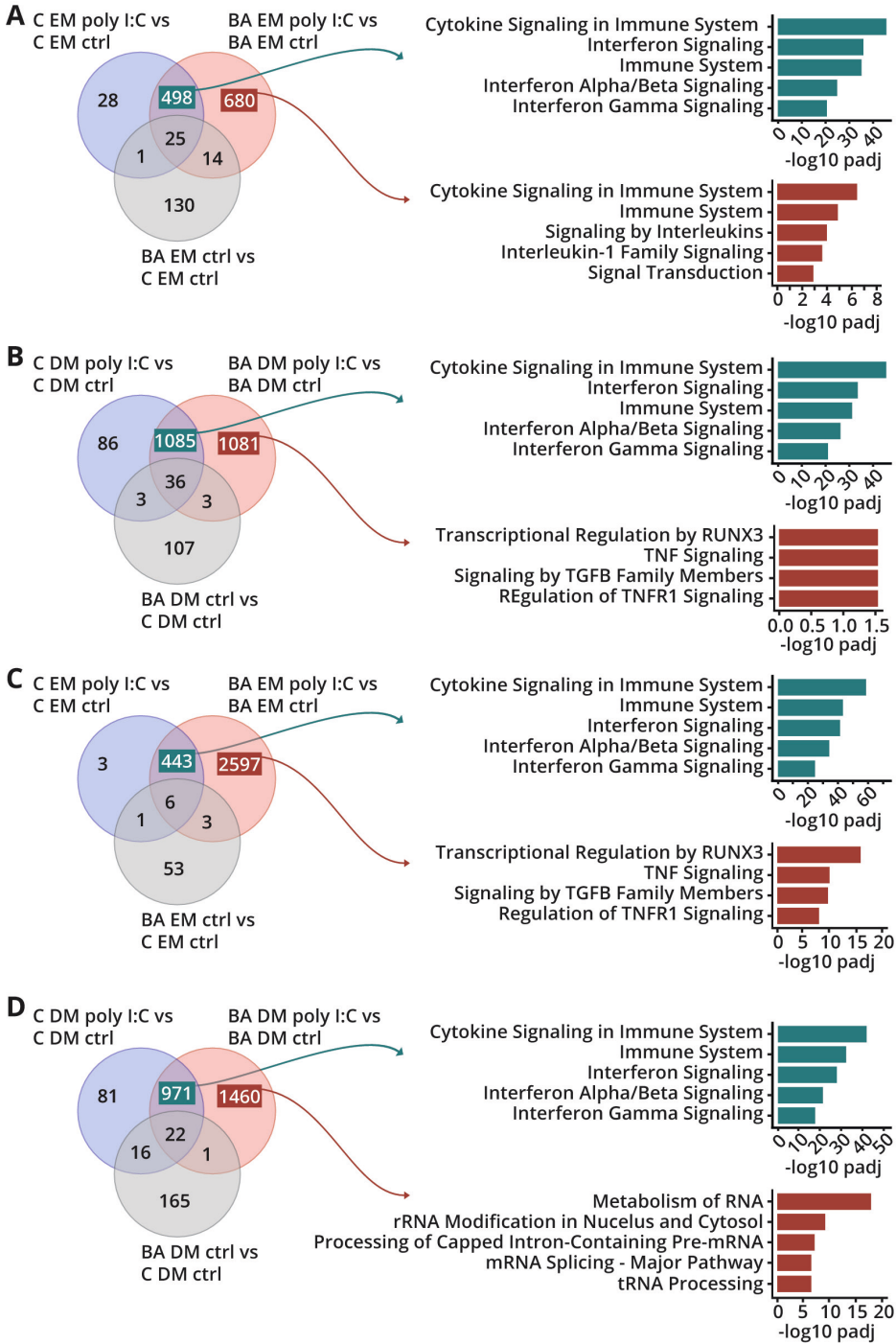


Figure S5. DEGs identified for BA liver organoids exposed to poly I:C. Volcano plots of DEGs identified for BA and control liver organoids when compared to DMSO conditions: **A**) progenitor control ICOs, **B**) progenitor BA ICOs, **C**) differentiated control ICOs, **D**) differentiated BA ICOs, **E**) progenitor control ECOs, **F**) progenitor BA ECOs, **G**) differentiated control ECOs, **H**) differentiated BA ECOs. BA, biliary atresia; ECO, extrahepatic cholangiocyte organoid; ICO, intrahepatic cholangiocyte organoid

3



← **Figure S6. DEGs and pathway enrichment for BA and control liver organoids exposed to poly I:C prior to artificial filter.** Venn diagrams and an EnrichR pathway enrichment of DEGs identified for progenitor (EM) and differentiated (DM) BA and control (C) liver organoids exposed to 80 µg/mL poly I:C compared to those exposed to DMSO. Confidence of accuracy is indicated as adjusted p-value (padj) which was determined by EnrichR using the Benjamini-Hochberg method with a cutoff of 0.05. **A)** Progenitor ICOs. **B)** Differentiated ICOs. **C)** Progenitor ECOs. **D)** Differentiated ECOs. BA, biliary atresia; DEG, differentially expressed gene; ECO, extrahepatic cholangiocyte organoid; ICO, intrahepatic cholangiocyte organoid

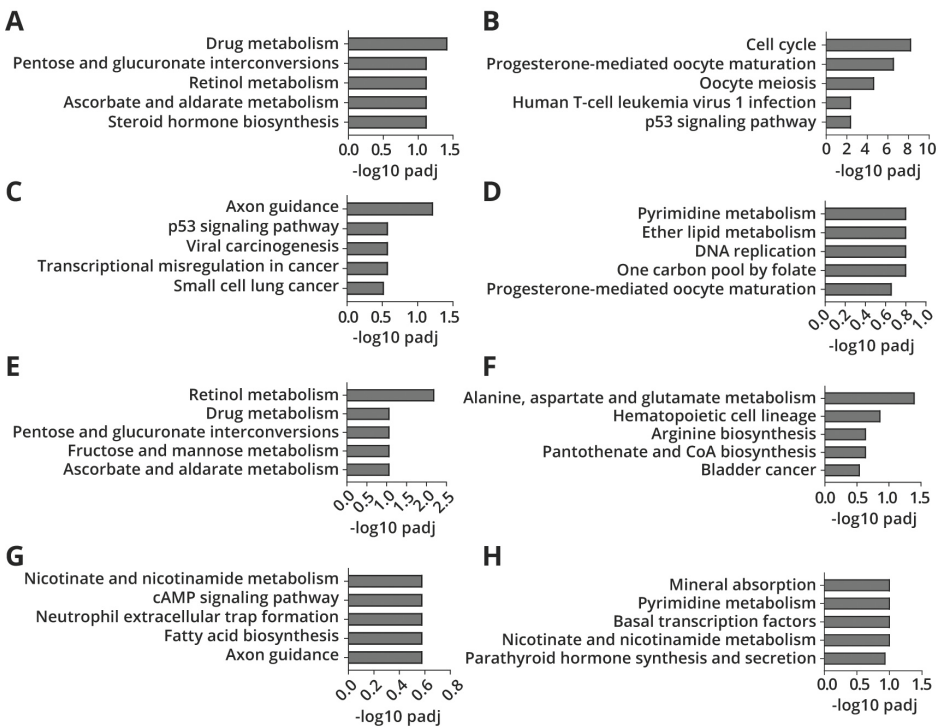


Figure S7. EnrichR pathway enrichment of DEGs specific for BA ICOs and ECOs exposed to poly I:C. Biological functions of DEGs upregulated in progenitor ICOs (**A**), downregulated in progenitor ICOs (**B**), upregulated in differentiated ICOs (**C**), downregulated in differentiated ICOs (**D**), downregulated in differentiated ECOs (**E**), upregulated in differentiated ECOs (**F**), downregulated in progenitor ECOs (**G**), upregulated in progenitor ECOs (**H**). Confidence of accuracy is indicated as adjusted p-value (padj) which was determined by EnrichR using the Benjamini-Hochberg method with a cutoff of 0.05. BA, biliary atresia; DEG, differentially expressed gene; ECO, extrahepatic cholangiocyte organoid; ICO, intrahepatic cholangiocyte organoid

3

Supplemental Tables

Table S1. Patient details on disease type, additional reasons for sampling a biopsy, type of organ of origin, age, sex and whether patient organoids were used for transcriptomics analyses.

Donor ID	Disease	Biopsy reason	Organ type	Age	Sex	RNA sequencing
A1AT	Alpha-1 antitrypsin deficiency	Liver transplantation	Liver	Neonate	M	
BA01	Biliary atresia	N/A	Liver	Neonate	M	Y
BA02	Biliary atresia	N/A	Liver	1 year	M	Y
BA03	Biliary atresia	Diagnostic biopsy	Liver	1 month	M	Y
BA04	Biliary atresia	Diagnostic biopsy	Bile Duct	Neonate	N/A	Y
BA04	Biliary atresia	Diagnostic biopsy	Liver	Neonate	N/A	
BA05	Biliary atresia	Diagnostic biopsy	Bile Bladder	Neonate	N/A	Y
BA05	Biliary atresia	Diagnostic biopsy	Bile Duct	Neonate	N/A	Y
BA05	Biliary atresia	Diagnostic biopsy	Liver	Neonate	N/A	Y
BA06	Biliary atresia	Diagnostic biopsy	Bile Bladder	Neonate	M	Y
BA06	Biliary atresia	Diagnostic biopsy	Liver	Neonate	M	
BA07	Biliary atresia	Kasai	Bile Bladder	Neonate	M	Y
BA07	Biliary atresia	Kasai	Bile Duct	Neonate	M	Y
BA07	Biliary atresia	Kasai	Liver	Neonate	M	
BA08	Biliary atresia	Diagnostic biopsy	Bile Bladder	Neonate	F	Y
BA08	Biliary atresia	Diagnostic biopsy	Liver	Neonate	F	
BA09	Biliary atresia	N/A	Liver	Neonate	F	Y
BA10	Biliary atresia	Diagnostic biopsy	Liver	Neonate	F	Y
BA11	Biliary atresia	N/A	Liver	N/A	N/A	
BA12	Biliary atresia	N/A	Liver	Neonate	F	
BA13	Biliary atresia	N/A	Liver	Neonate	F	
BA14	Biliary atresia	N/A	Liver	Neonate	F	
BA15	Biliary atresia	N/A	Liver	Neonate	F	

Table S1. Patient details on disease type, additional reasons for sampling a biopsy, type of organ of origin, age, sex and whether patient organoids were used for transcriptomics analyses.

Donor ID	Disease	Biopsy reason	Organ type	Age	Sex	RNA sequencing
BA16	Biliary atresia	N/A	Bile Duct	N/A	N/A	
BA16	Biliary atresia	N/A	Liver	N/A	N/A	
BA17	Biliary atresia	N/A	Liver	N/A	N/A	
BA18	Biliary atresia	N/A	Liver	N/A	N/A	
BA21	Biliary atresia	Diagnostic biopsy	Bile Duct	Neonate	N/A	
BA21	Biliary atresia	Diagnostic biopsy	Liver	Neonate	N/A	
BA22	Biliary atresia	Kasai	Bile Duct	Neonate	M	
BA22	Biliary atresia	Kasai	Liver	Neonate	M	
BA23	Biliary atresia	Diagnostic biopsy	Liver	Neonate	F	
BA24	Biliary atresia	Diagnostic biopsy	Liver	Neonate	F	
BA25	Biliary atresia	Diagnostic biopsy	Liver	Neonate	N/A	
BA26	Biliary atresia	Diagnostic biopsy	Liver	1 year	N/A	
BA27	Biliary atresia	Diagnostic biopsy	Liver	1 year	F	
BA28	Biliary atresia	Diagnostic biopsy	Liver	1 year	F	
BA29	Biliary atresia	N/A	Liver	2 months	F	
BA30	Biliary atresia	N/A	Bile Bladder	Neonate	M	
BA30	Biliary atresia	N/A	Liver	Neonate	M	
C	Cardiomyopathy	N/A	Liver	Foetus 23 weeks + 6 days	N/A	
CD	Congenital diarrhea	Diagnostic biopsy	Liver	10 years	F	
CF	Cystic fibrosis	Liver transplantation	Bile Duct	Adult	N/A	Y
CF	Cystic fibrosis	Liver transplantation	Liver	Adult	N/A	
CM	Choledocal malformation	N/A	Bile Duct	5 years	F	Y

Table S1. Patient details on disease type, additional reasons for sampling a biopsy, type of organ of origin, age, sex and whether patient organoids were used for transcriptomics analyses.

Donor ID	Disease	Biopsy reason	Organ type	Age	Sex	RNA sequencing
CTX	Cerebrotendinous xanthomatosis	Diagnostic biopsy	Liver	Neonate	M	
FL	Fatty liver	Diagnostic biopsy	Liver	15 years	M	
GD	Gaucher's disease	Diagnostic biopsy	Liver	4 years	M	
HB	Hepatoblastoma	Resection of healthy tissue from transplantation receiver liver	Liver	5 years	M	
HC01	Healthy	Perinatal asphyxia	Liver	3 days	F	Y
HC02	Healthy	Perinatal asphyxia	Liver	8 days	F	
HC03	Healthy	Perinatal asphyxia	Liver	5 days	M	
HC04	Healthy	Volvulus	Liver	Neonate	N/A	
HC05	Healthy	Premature rupture of membranes	Liver	Foetus 23 weeks	M	
HC06	Healthy	Premature rupture of membranes	Liver	Foetus 22 weeks	N/A	
HC07	Healthy	Premature rupture of membranes	Liver	Foetus 23 weeks	N/A	
HC08	Healthy	Liver transplantation donor	Liver	30 years	F	
HC09	Healthy	Liver transplantation donor	Liver	Adult	N/A	
HC10	Healthy	N/A	Bile Duct	Adult	N/A	
HC10	Healthy	N/A	Liver	Adult	N/A	
HC11	Healthy	N/A	Bile Duct	Adult	N/A	
HC11	Healthy	N/A	Liver	Adult	N/A	

Table S1. Patient details on disease type, additional reasons for sampling a biopsy, type of organ of origin, age, sex and whether patient organoids were used for transcriptomics analyses.

Donor ID	Disease	Biopsy reason	Organ type	Age	Sex	RNA sequencing
HC12	Healthy	Liver transplantation donor	Liver	N/A	M	
IBD/PSC	Inflammatory bowel disease + primary sclerosing cholangitis	N/A	Liver	12 years	F	
LALD	Lysosomal acid lipase deficiency	Diagnostic biopsy	Liver	4 years	M	
NASH	Nonalcoholic steatohepatitis	Diagnostic biopsy	Liver	N/A	N/A	
NPC1	Niemann-Pick disease, type C1	N/A	Liver	Neonate	M	
NTD	Neural tube defect	N/A	Liver	Foetus 22 weeks	M	
PFIC2	Progressive familial intrahepatic cholestasis type 2	Bile stoma	Bile Duct	7 years	F	
PVS	Pulmonic valve stenosis	N/A	Liver	2 days	M	Y
S	Sarcoidosis	Diagnostic biopsy	Liver	13 years	F	

Abbreviations: F, female; Kasai, Kasai hepato-portoenterostomy; M, male; N/A, information not available; Y, yes.

Table S2. Validated primers for RT-qPCR

Primer name	sequence (5'-3')	T _m in °C
<i>GCLC_Fw</i>	ATGGAGGTGCAATTAACAGAC	62
<i>GCLC_Rv</i>	ACTGCATTGCCACCTTTGCA	62
<i>GCLM_Fw</i>	CATTTACAGCCTTACTGGGAGG	62
<i>GCLM_Rv</i>	ATGCAGTCAAATCTGGTGGCA	62
<i>GSTO-1_Fw</i>	GAACGGCTGGAAGCAATGAAG	62
<i>GSTO-1_Rv</i>	TGCCATCCACAGTTTCAGTTT	62
<i>HSP90AA1_Fw</i>	GGCAGAGGCTGATAAGAACG	62
<i>HSP90AA1_Rv</i>	CCCAGACCAAGTTTGATCATCC	62
<i>NFKB_Fw</i>	TGTGCTTCGAGTGACTGACC	62
<i>NFKB_Rv</i>	TCACCCACATCACTGAACG	62
<i>CXCL8_Fw</i>	GGCACAAACTTTCAGAGACAG	62
<i>CXCL8_Rv</i>	ACACAGAGCTGCAGAAATCAGG	62
<i>HP1BP3_Fw</i>	CCCACGTCCCAAGATGGAT	62
<i>HP1BP3_Rv</i>	CTGATGCACCACTTCTTGAA	62

Abbreviations: Fw, forward; T_m, melting temperature; Rv, reverse

Table S3. Manually determined functions of upregulated DEGs of BA progenitor ECOs at baseline

Function	Number of DEGs	DEGs
ECM-receptor interaction	10	<i>MFAP5, ST6GALNAC3, FSTL1, COL5A1, EGFL7, ST3GAL6, NID2, FERMT2, COL6A1, GALNT6</i>
Transcription regulation	9	<i>EIF1AY, FLI1, ZNF486, ZNF682, RIPPLY3, ZNF154, ELF5, ZNF542, ETV7</i>
Long non-coding RNA	6	<i>SBF2-AS1, RP11-345J4.6, TTTY15, RP3-391O22.3, LINC00342, LINC00365</i>
Pseudogene	6	<i>TXLNG2P, FLI1-AS1, CYP4F35P, CYP4F29P, ANKRD20A11P, HLA-J</i>
unknown	5	<i>FSD1L, LRRN3, TMEM71, SLC44A5, ANKRD36C</i>
Cell-cell adhesion & polarity	5	<i>CLDN18, CDH5, CTNNA3, RAC2, VAV1</i>
Immune response	2	<i>INPP5D, VAV1, IL1RL1</i>
Lipid metabolism	3	<i>APOL4, DGKB, PLTP</i>
Cellular signaling	2	<i>SYT1, CYSLTR1</i>
Cytoskeletal organization	2	<i>STMN2, CORO1A</i>
Meiosis regulation	2	<i>TDRD1, M1AP</i>
Mitosis regulation	2	<i>FBXL7, CCNA1</i>
Amino acid metabolism	1	<i>RIMKLB</i>
Apoptosis	1	<i>RAC2</i>
Apoptosis prevention	1	<i>TNFRSF10C</i>
Autoimmunity	1	<i>CD274</i>
Cellular stress response	1	<i>ATF3</i>
Dioxin mediated cell death	1	<i>AHRR</i>
Histone modification	1	<i>KDM5D</i>
Mesenchymal to epithelial transition	1	<i>TCF15</i>
Monocarboxylic acid transport	1	<i>SLC16A14</i>
Neuronal development	1	<i>KCTD15</i>
Ribosomal RNA metabolism	1	<i>RPS4Y1</i>
TGF- β signaling	1	<i>GDF15</i>
Ubiquitination	1	<i>MKRN3</i>
Wnt signaling	1	<i>DAAM2</i>
Xenobiotics metabolism	1	<i>CBR3</i>

Abbreviations: BA, biliary atresia; DEG, differentially expressed gene; ECO, extrahepatic cholangiocyte organoid

Table S4. Manually determined functions of downregulated DEGs of BA progenitor ECOs at baseline

Function	Number of DEGs	DEGs
Immune response	6	<i>CCL28, CD1D, SIRPB1, HNMT, C2CD4B, VNN1</i>
Pseudogene	6	<i>MTND4P24, TEKT4P2, KRT18P19, KRT18P64, KRT8P25, PDZK1P1</i>
Cellular signalling	5	<i>PTPRG, PKIA, NPY4R, REEP6, FGFR3</i>
Ion homeostasis	4	<i>AQP1, GUCA2B, ANO10, SLC17A4</i>
Lipid metabolism	3	<i>SPTLC2, GNPAT, PECR</i>
Transcription regulation	3	<i>SALL1, ZFHX4, OTX1</i>
Cell-cell adhesion	2	<i>PCDHA12, IGSF9B</i>
Cytoskeletal organization	2	<i>TANC2, TNNC1</i>
Exocytosis	2	<i>CPLX2, ANXA4</i>
Long non-coding RNA	2	<i>RP11-783K16.5, RP5-1185I7.1</i>
Mitosis regulation	2	<i>CCND2, HECW2</i>
Oxidative stress response	2	<i>SESN3, GPX3</i>
Apoptosis inhibition	1	<i>APIP</i>
Blood pressure regulation	1	<i>AGT</i>
Degradation of cellular structures	1	<i>KLK7</i>
ECM-receptor interaction	1	<i>HSPG2</i>
Erythrocyte maturation	1	<i>C1orf186</i>
Histone binding	1	<i>APCS</i>
Hormone metabolism	1	<i>IYD</i>
Negative regulator of TGF-beta signalling	1	<i>PMEPA1</i>
Protein processing	1	<i>CADPS</i>
Pyridine nucleotide biosynthesis	1	<i>NMNAT2</i>
Transmembrane protein sorting	1	<i>PDZK1</i>
unknown	1	<i>AC069213.1</i>
Urea transport	1	<i>SLC14A1</i>

Abbreviations: BA, biliary atresia; DEG, differentially expressed gene; ECO, extrahepatic cholangiocyte organoid

Table S5. Manually determined functions of upregulated DEGs of progenitor BA patient ICOs exposed to poly I:C

Function	Number of DEGs	DEGs
Cell morphology & matrix interaction	24	<i>ADAMTS15, HYAL4, LAD1, MMP12, SPOCK1, S100A4, BRSK2, CDHR2, DENND2D, EPHB6, KAL1, KIAA1462, MAST3, MDGA1, MYO10, NPHS1, NRXN3, NXPE2, PSTPIP2, RND1, ROBO1, SDK2, TPPP, PPAP2B</i>
Immune response	22	<i>S100A4, BATF, C1orf168, CALCA, CD40, CLEC2D, EBF4, EDN2, HLA-DRA, LIF, LRMP, PIP, PTX3, RIPK2, SARM1, SCAMP5, SERPINB4, SLPI, TRBV30, SERPINB3, PPAPDC2, PPAP2B</i>
Long non-coding RNA	20	<i>AC009014.3, AC009133.14, AC019117.2, AFAP1-AS1, BX255923.3, LINC00886, LINC00982, NEAT1, NOP14-AS1, RP11-266K4.9, RP11-275F13.1, RP11-294O2.2, RP11-356J5.12, RP11-363E7.4, RP11-403I13.7, RP11-140K8.5, RP11-551L14.1, RP11-552J9.9, RP11-561O23.5, RP11-95M15.1</i>
unknown	16	<i>BCAS1, CRCT1, FAM83F, FSTL4, MS4A8, MSMB, MYEQV, OAF, SELM, TMEM51, TTC39A, XAGE1A, XAGE1B, XAGE1C, XAGE1D, XAGE1E</i>
Signal transduction	11	<i>MFAP3L, PMEPA1, LYNX1, PCSK1N, PPP4R4, PTGFR, RHBDL2, SPRR3, ST5, STK40, SULF2</i>
Lipid metabolism	10	<i>CYP2C18, CYP2C19, PPAPDC2, PPAP2B, ABCG1, ABHD2, APOB, DGAT2, HSD17B2, TM6SF2</i>
Apoptosis regulation	9	<i>FAM3B, ITPR1, LITAF, RASSF4, RHOB, RNF144B, S100A4, SERPINB3, TRAF1</i>
Detoxification	6	<i>CES2, UGT1A1, UGT1A4, UGT1A6, CYP2C18, CYP2C19</i>
Cell stress response	5	<i>DUSP1, FICD, HERPUD1, IGF1R, SAA2</i>
Transcription regulation	5	<i>ARNT2, BCL9L, GATA5, TP53INP2, ZNF703</i>
Cell & tissue development	4	<i>GTSF1, MAF, OLFM2, RCAN1</i>
Ion homeostasis	4	<i>FXYD3, HCN4, SLC26A1, TSPAN18</i>
Protein processing	4	<i>PCSK6, GRIP1, RAB3C, RAB6B</i>
Mitosis regulation	3	<i>TPPP, CCND2, NCCRP1</i>
Oxidative stress response	3	<i>GPX3, GSTA4, PYROXD1</i>
Amino acid metabolism	2	<i>ACMSD, AOC1</i>
Bile acid metabolism	2	<i>HSD3B7, ACOX2</i>
Defensive mucus	2	<i>MUC12, PGC</i>
Histone modification	2	<i>HDAC9, HIST1H2BC</i>
Hormone regulation	2	<i>C12orf39, RAMP1</i>
Wnt regulation	2	<i>MCC, WNT4</i>

Table S5. Manually determined functions of upregulated DEGs of progenitor BA patient ICOs exposed to poly I:C

Function	Number of DEGs	DEGs
Pseudogene	2	<i>AKR1B10P1, UGT1A2P</i>
Vitamin metabolism	2	<i>SLC23A2, VDR</i>
Autophagy	1	<i>WDR45</i>
Calcium-mediated intracellular processes	1	<i>CPNE7</i>
Glycoprotein metabolism	1	<i>CHSY3</i>
Golgi apparatus	1	<i>FAM174B</i>
Insulin metabolism & signaling	1	<i>INSL4</i>
Pyroptosis	1	<i>DFNA5</i>

Abbreviations: BA, biliary atresia; DEG, differentially expressed gene; ICO, intrahepatic cholangiocyte organoid

Table S6. Manually determined functions of downregulated DEGs of progenitor BA patient ICOs exposed to poly I:C

Function	Number of DEGs	DEGs
Mitosis regulation	43	<i>RNF157, DLGAP5, ASPM, AURKA, BUB1B, CCNA2, CCNB1, CCNB2, CCNF, CDC25C, CDCA2, CDCA5, CDCA8, CDK1, CDK4, CDKN2C, CENPA, CENPE, CENPF, CENPJ, CEP128, CEP55, FAM72A, FAM83D, KIF11, KIF20A, KIF23, KIF2C, MAD2L1, NDC80, NEK2, NUF2, PLK1, PRC1, PSRC1, RACGAP1, SAPCD2, SPAG5, TACC3, TPX2, UBE2C, PBK, DEPDC1</i>
Pseudogene	6	<i>HMG2N2P21, HMG2N2P28, HMG2N2P36, HMG2N2P5, HMG2N2P6, PTTG3P</i>
Cell morphology & matrix interaction	5	<i>DIAPH3, EPN3, GAS2L3, HMMR, TIAM1</i>
Transcription regulation	4	<i>CDCA7L, SPDEF, TOP2A, HMGB2</i>
unknown	4	<i>CCDC18, FAM72B, FAM72C, FAM72D</i>
Histone modification	3	<i>HMG2N2, PHF19, TEX15</i>
Immune response	3	<i>MATR3, PBK, HMGB2</i>
Long non-coding RNA	3	<i>RP11-363E7.4, RP11-417L14.1, RP11-701I24.1</i>
DNA metabolism	2	<i>PARBPB, UBE2T</i>
Protein processing	2	<i>APBA1, RHOBTB3</i>
Signal transduction	2	<i>STMN1, TMEM181</i>
Amino acid metabolism	1	<i>SHMT1</i>
Apoptosis regulation	1	<i>RNF157</i>
Bile acid metabolism	1	<i>ACOX2</i>
Insulin signaling	1	<i>GRB14</i>
Lipid metabolism	1	<i>OXCT1</i>
Meiosis regulation	1	<i>SGOL2</i>
NFkB activation	1	<i>DEPDC1</i>
Negative regulation of immune response	1	<i>TRIM59</i>
Positive regulation of Wnt	1	<i>FRAT2</i>

Abbreviations: BA, biliary atresia; DEG, differentially expressed gene; ICO, intrahepatic cholangiocyte organoid

Table S7. Manually determined functions of upregulated DEGs of differentiated BA patient ICOs exposed to poly I:C

Function	Number of DEGs	DEGs
Apoptosis regulation	8	<i>CASP3, LITAF, NTN1, RHOB, RNF144B, TP53BP2, MDM2, TRAF1</i>
Cell morphology & matrix interaction	6	<i>DOCK4, GAS7, MAST4, NXPE2, ROBO1, SLIT2</i>
Immune response	5	<i>FCGR2A, MIR155HG, PGLYRP4, PTX3, RFTN1</i>
Signal transduction	4	<i>HCAR1, PTGFR, RASGEF1B, TBC1D2B</i>
unknown	4	<i>FAM124A, GRAMD3, OGFRL1, YPEL2</i>
Cell stress response	2	<i>CREBRF, DNAJB6</i>
Glycoprotein metabolism	2	<i>B4GALT6, CSGALNACT1</i>
Mitosis regulation	2	<i>BUB1, UHMK1</i>
Protein processing	2	<i>TVP23B, TVP23C</i>
Amino acid metabolism	1	<i>PIPOX</i>
Cell & tissue development	1	<i>BMPR1B</i>
Detoxification	1	<i>SNN</i>
Hormone regulation	1	<i>C12orf39</i>
Host-virus interaction	1	<i>TMPRSS2</i>
Ion homeostasis	1	<i>SLC8A3</i>
Pseudogene	1	<i>MTND5P14</i>
Transcription regulation	1	<i>ZNF267</i>

Abbreviations: BA, biliary atresia; DEG, differentially expressed gene; ICO, intrahepatic cholangiocyte organoid

Table S8. Manually determined functions of downregulated DEGs of differentiated BA patient ICOs exposed to poly I:C

Function	Number of DEGs	DEGs
Mitosis regulation	8	<i>ARHGEF39, AURKA, CCNF, CDCA8, GPSM2, RACGAP1, SAPCD2, TACC3</i>
Transcription regulation	4	<i>CDCA7L, ONECUT3, OSR1, SOX21</i>
DNA metabolism	2	<i>DNA2, TYMS</i>
Long non-coding RNA	2	<i>DYNLL1-AS1, RP11-469H8.6</i>
Signal transduction	2	<i>ADRA2A, GNB1L</i>
Lipid metabolism	1	<i>GDPD3</i>
unknown	1	<i>AIM1L</i>
Histone modification	1	<i>WHSC1</i>
Ion homeostasis	1	<i>SLC26A1</i>

Abbreviations: BA, biliary atresia; DEG, differentially expressed gene; ICO, intrahepatic cholangiocyte organoid

Table S9. Manually determined functions of downregulated DEGs of differentiated BA patient ECOs exposed to poly I:C

Function	Number of DEGs	DEGs
Pseudogene	10	<i>ADH5P2, KRT18P18, KRT18P23, KRT18P55, KRT18P65, KRT8P10, KRT8P14, KRT8P35, KRT8P45, KRT8P50</i>
Long non-coding RNA	9	<i>FAM85A, LINC00589, NPSR1-AS1, RP11-618I10.1, RP11-626H12.1, RP11-790I12.1, RP11-790I12.2, RP11-813N20.1, RP6-74O6.2</i>
Cell morphology & matrix interaction	9	<i>DEF6, EPHB6, HMHA1, KIF3C, SIGLEC15, ADAM8, HABP2, NPNT</i>
Transcription regulation	5	<i>CHD5, HDAC5, PBX4, RBM46, SEPSECS</i>
Signal transduction	5	<i>ARHGEF10L, GAREML, LYPD6B, PDE7B, RAB27A</i>
unknown	4	<i>ANKRD37, CCDC33, SH3D21, SLC22A18AS</i>
Cell & tissue development	3	<i>CTXN1, FGFR2, OTX1</i>
Detoxification	3	<i>UGT2B11, UGT2B28, AOX1</i>
Immune response	3	<i>SIRPB1, SPON2, SIRPA</i>
Ion homeostasis	3	<i>CASR, SYT17, ANO10</i>
Protein processing	3	<i>MLPH, REEP6, UNC13C</i>
Mitosis regulation	2	<i>TMEM98, TRNP1</i>
Glycoprotein metabolism	2	<i>PMM1, ST3GAL6</i>
Lipid metabolism	2	<i>INSIG2, PLD1</i>
Vitamin metabolism	2	<i>AMN, LRAT</i>
Angiogenesis	1	<i>VEGFB</i>
Glycolysis	1	<i>ALDOC</i>
Hormone metabolism	1	<i>IYD</i>
Mitophagy	1	<i>NIPSNAP1</i>
NFKB activation	1	<i>PELI2</i>
Oxidative stress response	1	<i>CERKL</i>
Apoptosis	1	<i>ADAMTSL4</i>

Abbreviations: BA, biliary atresia; DEG, differentially expressed gene; ECO, extrahepatic cholangiocyte organoid

Table S10. Manually determined functions of upregulated DEGs of differentiated BA patient ECOs exposed to poly I:C

Function	Number of DEGs	DEGs
Immune response	5	<i>CXCL17, UBASH3B, VNN2, ZDHHC11, CD55</i>
Cell morphology & matrix interaction	5	<i>DNAH17, PALLD, SLIT3, CD44, MMP1</i>
Transcription regulation	4	<i>MT-TM, NUCB2, TFAP2C, ZNF37A</i>
Amino acid metabolism	3	<i>DDO, GPT2, SLC7A2</i>
Long non-coding RNA	3	<i>RNF144A-AS1, RP11-1246C19.1, RP11-253E3.3</i>
Protein processing	3	<i>ERO1LB, FBXO39, CADPS2</i>
unknown	2	<i>AC017076.5, AC116366.6</i>
Mitosis regulation	1	<i>STAG1</i>
DNA damage response	1	<i>RNF144A</i>
Ion homeostasis	1	<i>SCN3A</i>
Necrosis	1	<i>GSDMC</i>
Pseudogene	1	<i>CSAG4</i>

Abbreviations: BA, biliary atresia; DEG, differentially expressed gene; ECO, extrahepatic cholangiocyte organoid

Table S11. Manually determined functions of downregulated DEGs of progenitor BA patient ECOs exposed to poly I:C

Function	Number of DEGs	DEGs
Long non-coding RNA	6	<i>AL162759.1, PCAT6, RP11-475I24.3, RP11-480I12.7, RP4-800M22.1, SBF2-AS1</i>
unknown	4	<i>AC006273.5, C14orf105, MROH6, NIPAL3</i>
Protein processing	3	<i>ARL17A, ARL17B, REEP6</i>
Signal transduction	2	<i>DIRAS2, RAC2</i>
Transcription regulation	2	<i>HDAC5, ZNF675</i>
Calcium-mediated intracellular processes	1	<i>CPNE2</i>
Cell & tissue development	1	<i>PTCH1</i>
Cell morphology & matrix interaction	1	<i>PARD3B</i>
Co-factor metabolism	1	<i>NMNAT3</i>
Lipid metabolism	1	<i>CBR4</i>
Mitophagy	1	<i>NIPSNAP1</i>
Pseudogene	1	<i>CALM2P3</i>

Abbreviations: BA, biliary atresia; DEG, differentially expressed gene; ECO, extrahepatic cholangiocyte organoid

Table S12. Manually determined functions of upregulated DEGs of progenitor BA patient ECOs exposed to poly I:C

Function	Number of DEGs	DEGs
Transcription regulation	5	<i>ATAD2B, CSRP1, NGDN, SALL1, TBP</i>
Cell morphology & matrix interaction	2	<i>LYPD3, PDZD2</i>
Apoptosis	1	<i>ITPRIP</i>
DNA metabolism	1	<i>PNP</i>
Ion homeostasis	1	<i>SLC34A2</i>
NFKB activation	1	<i>FKBP5</i>

Abbreviations: BA, biliary atresia; DEG, differentially expressed gene; ECO, extrahepatic cholangiocyte organoid



4

Liver-on-a-tube: Improving hepatic maturation of intrahepatic cholangiocyte organoids with hollow fiber membrane technology to study liver metabolism and disease

Vivian Lehmann, Adam Myszczyzyn, Manon C. Bouwmeester, A. Ibrahim Ardismita, Theo Sinnige, Marianna A. Tryfonidou, Rosalinde Masereeuw, Sabine A. Fuchs, Bart Spee

Manuscript in preparation

Abstract

Current preclinical models often fail to adequately predict drug-induced liver toxicity, which has led to cases of post-marketing withdrawal. As a result, research has turned toward improving human liver *in vitro* models through closer mimicry of the hepatic microenvironment. Patient-derived intrahepatic cholangiocyte organoids (ICOs) have previously been praised for their potential application in preclinical studies. Yet, hepatic maturation of ICOs remains limited. Here, we aimed to improve the hepatic identity of ICOs and facilitate transepithelial transport of drugs by culturing ICO-derived cells on hollow fiber membranes (HFMs) coated with ECM proteins of the hepatic niche. We show that HFM architecture improves hepatic maturation compared to conventional ICO culture in Matrigel™ droplets. Moreover, human recombinant laminins are suitable candidates to replace Matrigel™ on HFMs. Key hepatic markers such as albumin, cytochromes P450 3A4, 2C9, 2B6, and UGT are well expressed in HFM cultures and display similar functionality compared to gold standards, such as PHH and HepaRG. Furthermore, HFM cultures allow for transepithelial transport studies as shown by ATP-binding cassette (ABC) transporter expression and activity. Moreover, we show that patient-derived ICO cells cultured on HFMs can model progressive familial intrahepatic cholestasis (PFIC) type 3 and reflect the patient's impaired MDR3 activity. We envision that this system will be interfaced with a perfusion bioreactor and used to test therapeutics for PFIC3 and other ABC transporter disorders. Moreover, a modular hepatocyte like-HFM bioreactor system allows for connection with HFM systems of other organs, thus allowing for high content pharmacology studies in a patient-specific manner.

Introduction

The liver is the primary organ for drug metabolism, thereby making it prone to drug induced injury. Pre-clinical testing repeatedly fails to predict drug induced liver injury (DILI) and has led to post-marketing withdrawal of drugs.¹⁻⁴ Liver failure is also seen in rare monogenic disorders affecting liver metabolism.^{5,6} Progressive familial intrahepatic cholestasis (PFIC) represents a group of monogenic disorders resulting in deficient bile trafficking machinery. Based on the affected gene, PFIC is subtyped in PFIC1, affecting the lipid flippase required for adequate apical membrane structure, PFIC2, affecting the bile salt export pump (BSEP), and PFIC3 affecting the multidrug resistance protein 3 (MDR3). Inhibition of these and other transmembrane proteins by drugs is responsible for 20-40% of DILI cases.⁷⁻¹¹ Hence, models for these diseases would not only benefit PFIC patients but also the wider public. However, current *in vitro* systems are unsuitable to adequately study transporter functionality and drug toxicity.

Current cell models used in pharmacological testing include two-dimensionally (2D) cultured cell lines or primary human hepatocytes (PHH), as well as sandwich cultured PHH and two-dimensional (3D) organoids. A 2D culture allows for high throughput workflows; however, the architecture and insufficient functionality of these systems limit their use in hepatic modeling.^{12,13} Moreover, immortal cell lines are ineffective for personalized medicine, since human polymorphisms in phase I and II enzymes and hepatic transporters are not accounted for.¹⁴⁻¹⁶ In comparison, sandwich cultured PHH and organoid systems are better suited for patient-specific transport and toxicity studies thanks to their 3D architecture and origin from primary human tissue. Yet, PHH availability is limited and *in vitro* expansion remains a challenge. Meanwhile, patient-derived ICOs are readily available and easily expandable. Previous studies have shown ICO potential in disease modeling and drug toxicity testing, albeit with limitations due to incomplete hepatic maturation.¹⁷⁻¹⁹

To improve hepatic maturation and thus the predictive power of ICOs for pharmacological research, it has been suggested to closely mimic the microenvironment of the hepatic niche.²⁰ Proposed strategies include changes in media composition and physical stimuli, such as the extracellular matrix (ECM) and shear stress.²⁰⁻²³ The ECM of the liver is mostly composed of laminins, fibronectin, and collagens which take part in guiding hepatoblasts to proliferate or differentiate into hepatocytes. Matrigel™ contains many ECM proteins and is therefore a widely used matrix to mimic ECM *in vitro*. However, its batch-to-batch variation and animal-origin make Matrigel™ a poor candidate for standardized human drug and disease models.²⁴ Hence, alternative human recombinant ECM proteins are being investigated for their applicability in cell culture and potential for steering hepatic maturation. Several studies have identified laminins (LN) to support hepatic

maturation *in vitro*. Especially, human recombinant LN111, LN211, LN332, LN411 and LN511 were reported to maintain hepatic phenotypes in PHH and promote hepatic differentiation in induced pluripotent stem cells and ICOs.²⁵⁻³¹

Another physical stimulus promoting the hepatic fate *in vivo* is shear stress caused by blood perfusion. Incorporation of shear stress into cell culture systems through microfluidics or perfusion bioreactors has been reported to improve hepatic maturation of HepG2 and rat hepatocytes.^{32,33} Besides perfusion culture, microfluidics and macro-scale bioreactors also improve reproducibility through increased automation and environmental control. Both aspects are desirable for testing drug toxicity, kinetics, and long-term exposure effects. Moreover, such systems have the potential to combine tissue-specific micro-environments and connect to other organ systems, thereby opening the door to investigate absorption, distribution, metabolism, and excretion of a drug of interest across multiple organs.³⁴⁻³⁶

Recently, hollow fiber membrane (HFM) technology has been tested to combine the ECM and shear stress strategies in one system. HFMs are being used for water purification and clinically for blood purification, including kidney and liver dialysis.³⁷ This system was also downscaled to create a portable bioartificial liver device and tested for *in vitro* modeling of liver biology.³⁸⁻⁴¹ Yet, this bioartificial liver still required large amounts of PHH which are difficult to obtain for regular pharmacological testing. Other studies have tested further downscaling of HFM systems and showed successful culture and function of different organ models, including human kidney, intestine, and bile duct.⁴²⁻⁴⁷

Here, we built on these studies to develop a human hepatic HFM culture system using patient-derived intrahepatic cholangiocyte progenitors. We tested whether ECM proteins of the hepatic niche promote cell attachment and monolayer formation of cells derived from healthy donor ICOs on HFMs. Key hepatic markers and functions, such as phase I and II enzymes and transporter proteins were investigated in HFM cultures. As a first step toward disease modeling, we assessed whether ICOs derived from a PFIC3 patient could be cultured on HFMs and preserve the disease phenotype. Our findings highlight the potential of combining HFM culture systems with patient ICOs for future disease modeling and drug testing.

Materials and Methods

ICO culture

ICOs were established and cultured as described previously.¹⁹ Use of tissue for our studies was ethically approved by different collaborating University Centers (MEC-2014-060; STEM 1-402/K; Metabolic Biobank: 19-489). Briefly, ICOs were cultured in droplets of 70% (v/v) Matrigel™ (Corning) and expansion medium containing AdDMEM/F12 (Gibco), 1% (v/v) penicillin-streptomycin (Gibco), 1% (v/v) GlutaMax (Gibco), 10 mM HEPES (Gibco), 2% (v/v) B27 without vitamin A (Gibco), 1.25 mM N-Acetylcysteine (Sigma), 10 mM nicotinamide (Sigma), 10 nM gastrin (Sigma), 10% RSP01 (v/v) conditioned media (homemade), 50 ng/mL EGF (Peprotech), 100 ng/mL FGF10 (Peprotech), 25 ng/mL HGF (Peprotech), 5 mM A83-01 (Tocris Bioscience), 10 mM forskolin (Tocris Bioscience). Every 7 days, the cultures were passaged at a split ratio of 1:3 to 1:6 by mechanical fragmentation. All cultures were kept in a humidified atmosphere of 20% O₂ and 5% CO₂ at 37°C and media were refreshed every other day.

Hollow fiber membrane preparation

MicroPES™ (polyethersulfone) hollow fiber membranes (HFMs) were extracted from SepaPlas®06 cartridges (Heinz Meise GmbH), cut into 3 cm pieces, incubated with 70% EtOH for 30 minutes on a roller bench and washed three times with sterile PBS. Meanwhile, L-DOPA (L-3,4-dihydroxyphenylalanine) was dissolved to 2 mg/mL in 10 mM Tris buffer (pH 8.5) in the dark at 37°C in a carousel overnight. Next, the solution was filter sterilized and added to the sterile HFMs. L-DOPA and HFMs were then incubated for 4 hours in the dark at 37°C in a carousel. Thereafter, the L-DOPA solution was aspirated and the HFMs washed twice with sterile PBS. L-DOPA-coated HFMs were stored at 4°C for 1 week or used immediately for ECM coating. ECM components were thawed on ice and diluted in cold PBS to the appropriate concentration (Matrigel™, 10 µg/mL; LN111, LN211, LN332, LN411 and LN511 (BioLamina) each at 10 µg/mL). Up to 15 HFMs were transferred to 5 mL ECM solution and incubated for 2 hours in the dark at 37°C in a carousel, followed by cell seeding.

ICO cell seeding and culture on HFMs

For single cell seeding, ICOs were harvested with TripLE™ Select (Gibco) and digested until single cells by repeated cycles of mechanical fragmentation and 3-minute incubations in a 37°C water bath. Single cells were then treated with prewarmed PBS containing 5 mM MgCl₂ and 0.5 mg/mL DNase I (Merck) solution for 10 minutes and thereafter centrifuged at 190 g for 5 minutes at 4°C. Next, cells were diluted in expansion medium containing 10 µM Y27632 (Sigma), counted manually and if needed further diluted to reach 0.5x10⁶ cells/mL.

For seeding ICO fragments, ICOs were harvested with cold AddMEM/F12 containing 1% (v/v) penicillin-streptomycin, 1% (v/v) GlutaMax, 10 mM HEPES and fragmented mechanically. After centrifugation at 70 g for 5 minutes at 4°C, cells were resuspended in expansion medium to obtain ICOs from one well plate per 6 mL expansion medium.

Next, two ECM-coated HFMs per 2 mL Eppendorf tube were incubated horizontally with 1 mL cell solution in a humidified atmosphere of 5% CO₂ in air at 37°C. After 30 minutes, cell solutions were gently resuspended by a 360° rotation, followed by 3.5 hours of undisturbed incubation. Thereafter, cell-laden HFMs were transferred to 6-well plates containing expansion medium with or without 10 µM Y27632, which was refreshed weekly. Left-over cell solutions were centrifuged briefly at 70 g for 5 minutes at 4°C and cultured, as described previously, in droplets of 70% (v/v) Matrigel™ and expansion medium with or without 10 µM Y27632 as ICO controls.

After 10 days of expansion, ICOs and HFM cultures were pre-treated with 25 ng/mL BMP7 (Peprotech) for 3 days, whereafter media were changed to hepatic differentiation medium composed of AddMEM/F12 medium supplemented with, 1% (v/v) penicillin-streptomycin, 1% (v/v) GlutaMax, 10 mM HEPES, 1% (v/v) B27, EGF (50 ng/mL), 1.25 mM N-Acetylcysteine, gastrin (10 nM), HGF (25 ng/mL), FGF19 (100 ng/mL, Peprotech), A83-01 (500 nM), DAPT (10 µM, Selleck Chemicals), BMP7 (25 ng/mL), and dexamethasone (30 µM, Sigma). Differentiated HFM cultures will be referred to as hepatocyte-like HFMs (HL-HFMs) from here on. After seven days of differentiation cells were used for functional- or gene expression-analyses.

Cell confluency tracing

HFM cultures were stained with calcein-AM (Santa Cruz Biotechnology) every few days through incubation with 0.5 µM calcein-AM in expansion or differentiation medium for 15 minutes at 37°C. Thereafter, medium was refreshed with expansion or differentiation medium without calcein-AM and HFMs were imaged using an inverted Olympus IX53 epifluorescence microscope at 2x magnification. Fluorescence intensities were quantified for the full length of two HFMs per donor with ImageJ software (Win64 version: <https://imagej.net/Fiji/Downloads>) and the corrected total cell fluorescence was determined.

RNA isolation and quantitative RT-qPCR

RNA was isolated from whole liver tissue, ICOs and HL-HFMs using the RNeasy Mini Kit (Qiagen) according to the manufacturer's protocol including the use of β-mercaptoethanol (Merck). For cell lysis of HL-HFMs, 3 HL-HFMs per condition were vortexed for 1 minute in 350 µL RLT buffer, followed by a 5-minute incubation at room temperature (RT). Next, samples were centrifuged shortly and stored at -80°C until further use. The remaining RNA isolation from whole liver tissue, ICOs and

HL-HFMs was performed according to the manufacturer's protocol. Next, RNA was quantified using a D-1000 spectrophotometer (NanoDrop, Thermo Fisher Scientific) and cDNA was synthesized using the iScript cDNA synthesis kit (Bio-Rad) according to the manufacturer's protocol. Relative mRNA of genes of interest was quantified by real-time PCR using the SYBR Green method (Bio-Rad) and validated primers (Table S1). Normalization was performed using reference genes *RPL19* and *HPRT*. Statistical analysis was performed using a non-parametric Kruskal-Wallis test followed by a Dunn's multiple comparison using GraphPad Prism software version 9.3.0 (<https://www.graphpad.com/>).

Immunofluorescence

ICOs were harvested with Cell Recovery Solution (Corning) and incubated on a roller bench for 30 minutes at 4°C. After a brief wash with PBS, ICOs and HL-HFMs were incubated in 4% (v/v) buffered formaldehyde (Klinipath) on a roller bench at 4°C for 45 minutes. Fixated samples were stored in PBS at 4°C until further use. For wholemount immunocytochemistry HL-HFMs were cut into 0.75-1 cm pieces and blocked in washing buffer (WB; 1x PBS + 1% (w/v) BSA + 0.1% (v/v) Tween 20) containing 10% (v/v) goat serum (Sigma) for 1 hour at RT. HL-HFMs were then incubated with primary antibodies (Table S2) in WB overnight at 4°C, followed by washing in WB three times for 20 minutes. Incubation with secondary antibodies (Table S3) and DAPI (1 µg/mL, Thermo Fisher Scientific) was done for 2 hours at RT, followed by washing three times in WB for 10 minutes at RT. Next, HL-HFMs were mounted on Lab-Tek™ II Chambered Coverglass (Nunc) with ProLong™ Diamond Antifade Mountant (Invitrogen) and imaged within 1 week. Wholemount immunocytochemistry on ICOs was performed as described previously using primary and secondary antibodies (Tables S2 and S3).⁴⁸ For paraffin-based immunocytochemistry HL-HFMs were cut into 5 mm pieces and mounted vertically in agarose droplets (2.5%, w/v). Agarose droplets were dehydrated (70% ethanol, 96% ethanol, 100% ethanol and xylene) overnight and embedded in paraffin. Paraffin blocks were cut into 5-µm slices using a microtome. The slices were rehydrated in xylene, 100% ethanol, 96% ethanol, 70% ethanol and water, followed by antigen retrieval in TRIS-EDTA (pH 9.0) for 30 minutes at 95°C. The slices were washed three times in 1x PBS for 5 minutes and blocked in WB containing 10% goat serum for 1 hour at RT. The slices were then incubated with primary antibodies (Table S2) overnight at 4°C. Next, the slices were washed three times with 1x PBS containing 0.1% Tween 20 for 10 minutes and incubated with secondary antibodies and DAPI (1 µg/mL) for 1 hour at RT. The slices were washed three times in 1x PBS with 0.1% Tween 20 for 10 minutes and mounted in FluorSave (EMD Milipore). Imaging was performed on a Leica TCS SP8 confocal microscope.

Phase I and II enzyme activity

Cytochrome P450 activity in ICOs, PHH, HepaRG and HL-HFMs was assessed using a CYP substrate cocktail as described previously.¹⁷ In short, cells were exposed

to a substrate cocktail and parent compounds and metabolites were quantified, including midazolam (metabolite hydroxymidazolam), tolbutamide (metabolite 4-hydroxytolbutamide), bupropion (hydroxybupropion), and 7-hydroxycoumarin (metabolite 7-hydroxycoumarin glucuronide). Measurements were done at timepoints of maximum metabolite formation as determined previously,¹⁷ which differed per hepatic cell model (ICOs: 24 hours; PHH: 4 hours; HepaRG: 8 hours). Culture and exposure of ICOs, PHH and HepaRG were performed in previous experiments.¹⁷ HL-HFMs were exposed to substrate cocktails in 1 mL medium at day seven of differentiation. After 24 hours, 200 μ L medium was collected in glass vials containing 200 μ L acidified MeOH (0.1% (v/v) formic acid), vortexed and stored at -20°C until LC-MS/MS analysis as described previously.¹⁷

Transporter assay

For pre-incubation with inhibitors, ICOs or HL-HFMs were treated with fresh differentiation medium containing 5 μ M valsopodar (PSC-833, Selleck Chemicals), 5 μ M KO-143 (Selleck Chemicals), and 5 μ M MK-571 (Selleck Chemicals) as inhibitors or an equivalent amount of DMSO for 30 minutes at 37°C. Thereafter, cultures were refreshed with differentiation medium containing inhibitors or DMSO and 0.5 or 1 μ M calcein-AM for 15 minutes at 37°C. Next, HL-HFMs were refreshed with differentiation medium containing inhibitors or DMSO for 30 minutes at 37°C, followed by imaging. For transport assays without pre-incubation HL-HFMs were refreshed with differentiation medium containing inhibitors or DMSO and 1 μ M calcein-AM for 15 minutes at 37°C. Prior to imaging, HL-HFMs were washed three times with differentiation medium. Finally, three fields of view of each HFM were imaged using an inverted Olympus IX53 epifluorescence microscope at 10x magnification. Mean fluorescence of HL-HFMs was determined using ImageJ software.

Meanwhile, media of technical triplicate ICO cultures were refreshed with differentiation medium containing inhibitors or DMSO and imaged immediately and every hour for 16 hours using an automated Leica THUNDER microscope and Imager Live Cell Assay. Fluorescence signal of ICO cultures was determined by analyzing particles in ImageJ software after selecting thresholds and circularity settings to isolate ICO lumen (size=0.01-Infinity, circularity=0.4-1.00) and full ICOs (size=0.01-Infinity, circularity=0.0-1.00). Lumen fluorescence was determined as the percentage of full ICO fluorescence relative to 0 hours.

Results

Establishing ICOs on HFMs

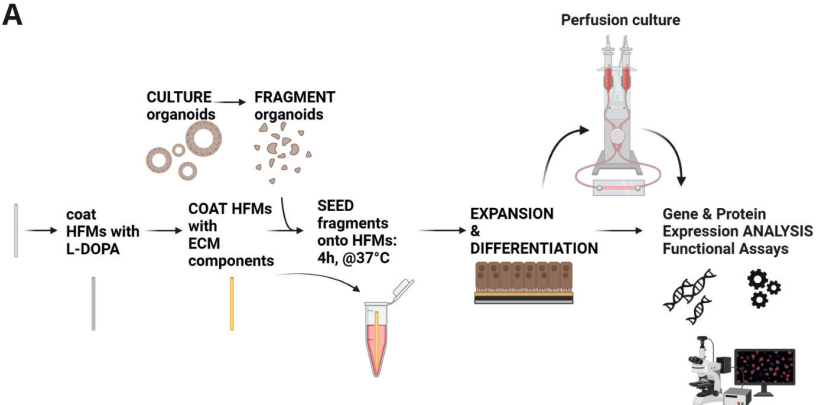
As described previously, cells can be cultured on HFMs coated with ECM components.⁴³⁻⁴⁵ Here, we explored whether ICO cells could be cultured and differentiated toward the hepatic fate on HFMs. First, HFMs were coated with L-DOPA to prime the HFM for protein attachment. Next, the HFMs were coated with Matrigel™ to offer cell attachment sites to the cells. ECM distribution across the HFMs was mostly homogeneous and did not differ between coating a single or multiple HFMs simultaneously (Figure S1A-B). HFM edges and occasional stripes across the HFMs represent reduced ECM coverage, likely indicative of ECM removal through handling the HFMs with tweezers and extraction from incubation tubes. In the future, perfusion chambers will be used for each step from ECM coating to functional assays, thus circumventing damage to ECM or cell layers. Cell seeding using single cells from ICO cultures resulted in large variations of seeding success across experiments (data not shown). Monolayer formation, if at all, was only observed after 16 days under expansion conditions (Figure 1B, i, iii, v). To overcome this, we tested the seeding of ICO fragments on HFMs. Leak-tight monolayer formation from ICO fragments was observed within 7-10 days of expansion culture (Figure 1B, ii, iv, vi; Figure S1C) with good reproducibility (data not shown). Thus, further cell seeding was performed with ICO fragments only. Monolayers were retained well during culture. Long-term culture was successful up to 21 days after the start of differentiation compared to organoid cultures, which collapsed when kept in culture longer than 10 days after the start of differentiation (Figure S3).

Immunofluorescence data indicated that cell monolayers on HFMs assumed simple columnar polarization. The cell membrane facing the HFM showed heightened localization of basolateral markers, E-cadherin and sodium-taurocholate co-transporting polypeptide (NTCP). Moreover, nuclei were located closer to the HFM. In contrast, F-actin was found highly expressed on the cell membrane facing away from the HFM, indicative of the apical cell domain (Figure 1D).

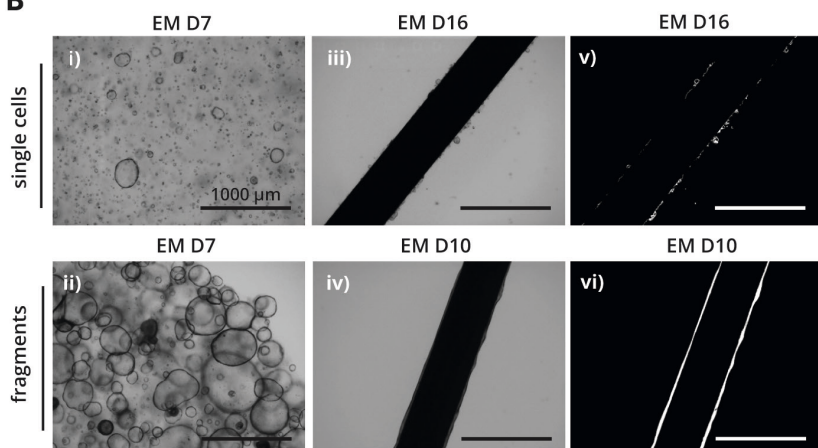
Human recombinant laminins perform similarly to Matrigel™

To comply with the 3Rs, improve hepatic maturation and increase translational confidence, we tested whether Matrigel™ could be replaced by human recombinant laminins (LN) using three ICO donors. ICO cell culture on HFMs coated with LN111, LN211, LN332, LN411 and LN511 was comparable to Matrigel™ HFM cultures (Figure S2). Monolayers formed within 7 days for most laminins, while HFMs coated with LN332 displayed monolayer formation after 10 days. For all conditions, cells were expanded for 10 days and differentiated for 7 days, followed by gene expression analysis. Donor-matched whole liver tissue and differentiated conventional Matrigel™ droplet ICO cultures aided as control conditions. No significant

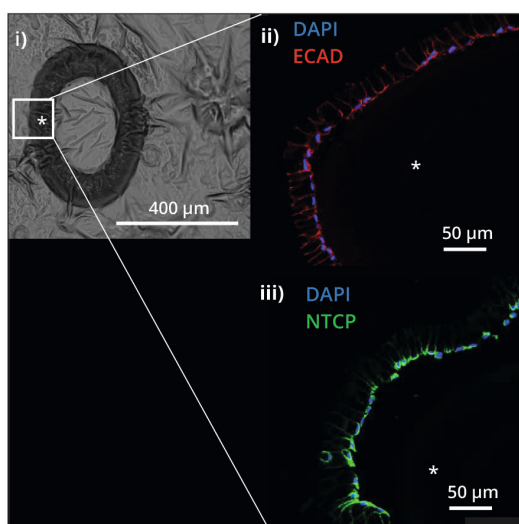
A



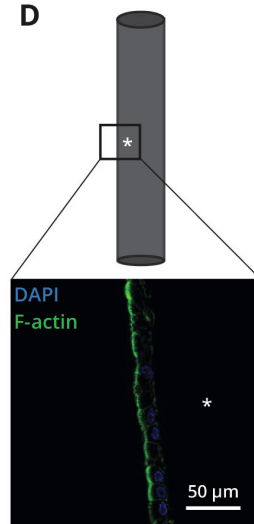
B



C



D



← **Figure 1. ICO cells can be cultured on HFMs and form polarized monolayers. A)** Workflow of ICO culture and analyses on HFMs. **B)** Cell growth in Matrigel™ droplets or on HFMs from ICO fragments or single cells. Brightfield images of conventional ICO culture in Matrigel™ (**i, ii**) and HFM cultures (**iii, iv**) at different days (D7, D10, D16) of expansion. HFMs are visible as large black fibers, covered by cells (**iii, iv**). Black and white overlay after running a threshold on images (**iii, iv**) with ImageJ to indicate cell locations (**v, vi**). **C)** Brightfield (**i**) and immunofluorescent (**ii, iii**) images of HFM rings embedded in paraffin showing the cell monolayer on the outside of the HFM. HFM material is indicated with an asterisk. Immunofluorescence images showing basolateral markers E-cadherin (ECAD, red) and sodium-taurocholate co-transporting polypeptide (NTCP, green), and nuclei (DAPI, blue) (**ii, iii**). **D)** Schematic and wholemount immunofluorescent image of HFM (asterisk) side view. F-actin is shown in green and nuclei in blue (DAPI).

differences (p-value > 0.05) between the groups were found likely due to high interdonor variance. Nonetheless, differences in gene expression trends were observed. Based on most of the selected genes, such as *ALB* and *CYP3A4*, *CYP2B6*, *CYP2C9* and *CYP2C19*, HL-HFMs outperformed ICO controls (Figure 2). In contrast, *ABCB1* and *ABCB11* encoding for apical transporters ATP binding cassette subfamily B member 1 (MDR1) and BSEP, respectively, were expressed similarly in HL-HFMs and ICO controls. Some donors showed lower expression of these genes in HL-HFMs. Notably, *ALB* and most genes involved in drug metabolism displayed donor variation in each condition. Overall, laminin conditions promoted gene expression of hepatic markers similarly as Matrigel™, albeit generally at lower levels compared to gene expression in whole liver tissue.

HL-HFMs show phase I and II enzyme activity

To test enzyme activity involved in drug metabolism, HL-HFMs, ICOs, HepaRG and PHH were exposed to cocktails of specific enzyme substrates as described previously.¹⁷ Enzyme activities of cytochrome P450 enzymes 2B6, 2C9 and 3A4, and UGT were determined by measuring metabolite formation (pmol/10⁶ cells; Figure 3A-D). Notably, for ICO controls the activity of CYP2B6 and CYP2C9 could not be determined, as metabolites were not formed (Figure 3B and C). Interestingly, activities of these two enzymes were detectable in HL-HFMs originating from the same donors as ICO cultures. CYP2C9 activity in HL-HFMs was higher than in HepaRG but lower than in PHH, except for one donor (Figure 3B). In comparison, CYP2B6 activity was comparable between HL-HFMs and HepaRG, while PHH outperformed the other models (Figure 3C). Notably, CYP3A4 activity was higher in HL-HFMs compared to any other hepatic model, although with interdonor variation. Finally, phase II enzyme UGT performed similarly in all four hepatic models, again displaying interdonor variation in HL-HFMs (Figure 3D).

HL-HFMs display ABC transporter expression and activity

Future toxicity studies and disease modeling using HL-HFMs rely on functional hepatic transporters, such as superfamilies ATP-binding cassette (ABC) transporters.

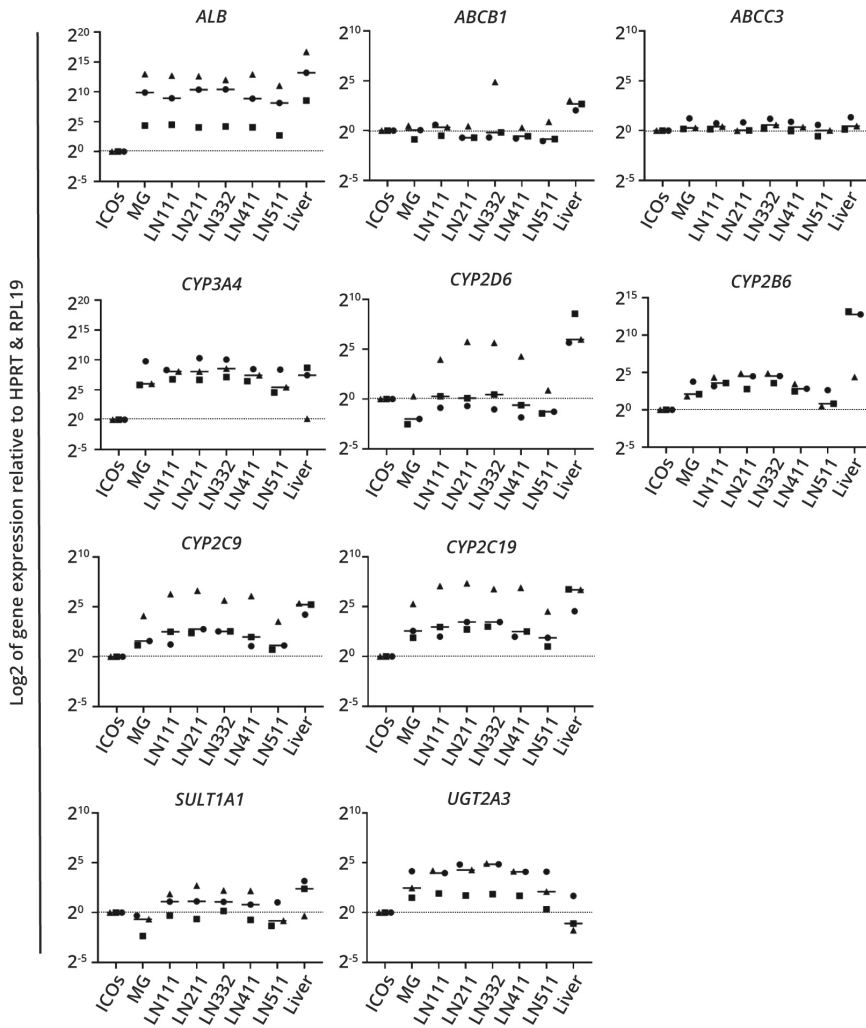


Figure 2. Gene expression of ICO cells after seven days of differentiation on HFMs.

Relative gene expression was determined using reference genes *RPL19* and *HPRT* (ΔC_T) and is displayed as log₂. Gene expressions of Matrigel™- (MG) and laminin-coated (LN) hepatocyte-like HFMs (HL-HFMs) are shown next to those of conventional differentiated ICO cultures (ICOs, dotted line) and whole liver tissue (liver). The latter two were used as controls. All conditions were donor-matched as represented by matching black symbols. Each dot represents the mean of technical triplicates of each ICO donor; 3 donors. *ALB*, Albumin; *ABCB1*, ATP binding cassette subfamily B member 1; *ABCC3*, ATP binding cassette subfamily C member 3; *CYP3A4*, cytochrome P450 3A4; *CYP2D6*, cytochrome P450 2D6; *CYP2B6*, cytochrome P450 2B6; *CYP2C9*, cytochrome P450 2C9; *CYP2C19*, cytochrome P450 2C19; *SULT1A1*, Sulfotransferase family 1A member 1; *UGT2A3*, UDP glucuronosyltransferase family 2 member A3.

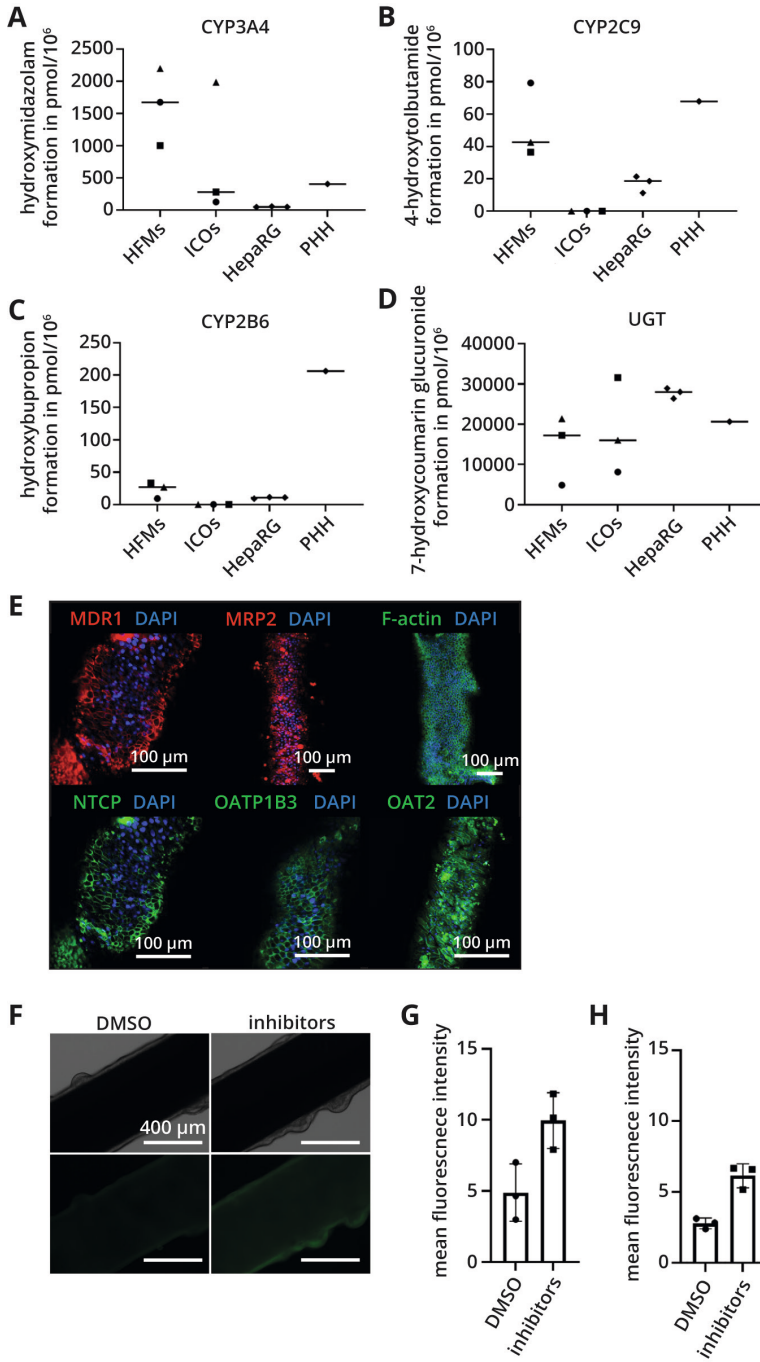
Therefore, we set out to test whether protein expression and function of such transporters could be measured in HL-HFMs. First, we confirmed protein expression of a selection of transporters on HL-HFMs through immunofluorescence (Figure 3E). The results indicate homogenous expression of the target proteins MDR1, MRP2 (ATP binding cassette subfamily C member 2), F-actin (actin filaments), NTCP (sodium-taurocholate co-transporting polypeptide), OATP1B3 (Solute carrier organic anion transporter family member 1B3), OAT2 (Organic anion transporter 2) in cell membranes. Next, we investigated the export of the fluorescent substrate calcein from HL-HFM cells. The parent compound calcein-AM can be transported by the ABC transporter MDR1, while the fluorescent product calcein, which is formed through esterase cleavage of calcein-AM in the cell, can be secreted by ABC transporters, such as MRP2 and MRP3.^{49,50} Upon inhibition of these transporters using PSC-833, KO-143 and MK-571, intracellular calcein accumulation was observed (Figure 3F-H). Interestingly, short exposures to inhibitors did not differ in effect from continuous supply of inhibitors (Figure 3G-H). Meanwhile, uninhibited transporters were able to secrete calcein as indicated by the lower mean fluorescence intensity.

PFIC3 patient model on HL-HFMs

As a proof of concept for disease modeling, we chose PFIC3, a disease caused by mutations in the gene *ABCB4*, resulting in diminished or absent function of the encoded ABC transporter MDR3. We generated organoids from a patient with a homozygous *ABCB4* mutation (glu1012*), which results in absence of the carboxyl-terminal cytoplasmic ATP-binding site and thereby putatively in absence of protein function.⁵¹⁻⁵³ Culturing patient-derived cells in a controlled perfused environment may allow to study transport dysfunction and identify potential treatments. In addition, this reflects the possibility to study DILI caused by MDR3 interference. To this end, we first investigated whether PFIC3 patient ICO cells would grow on Matrigel™-coated HFMs and compared this to an age- and sex-matched healthy control (Figure 4A-B). Within 7 days, monolayers had formed on HFMs with PFIC3 patient and healthy control ICO cells. The PFIC3 patient HL-HFMs retained monolayer integrity after differentiation. Monolayer integrity was less in healthy control HL-HFMs, which may be a coincidental or donor-specific finding, as cell detachment from HFMs is observed occasionally with some donors (data not shown). Differentiated PFIC3 patient ICOs and HL-HFMs showed deficient expression of the affected *ABCB4* compared to the healthy control (Figure 4C). Other ABC transporters were similarly expressed in healthy control and PFIC3 patient HL-HFMs and ICOs. Generally, ABC transporter expression was higher in ICOs than in HL-HFMs for both donors as observed previously for other donors.

Functional assay to study PFIC3 in ICOs

To establish an appropriate *in vitro* assay for functional assessment of PFIC3, we investigated whether calcein transport in ICOs could distinguish between the PFIC3

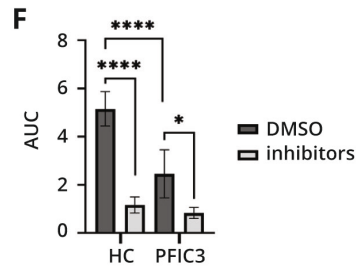
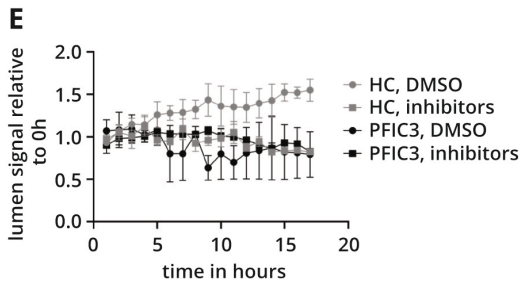
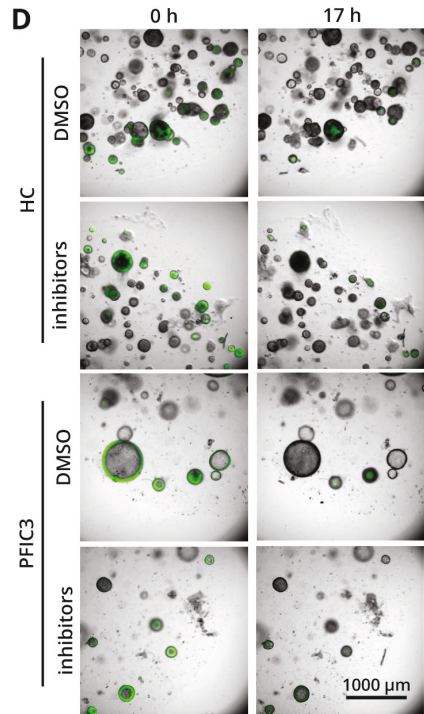
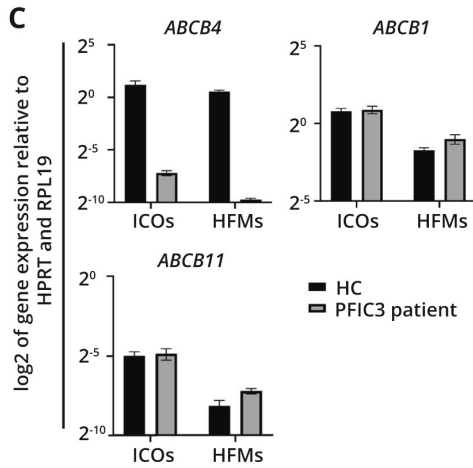
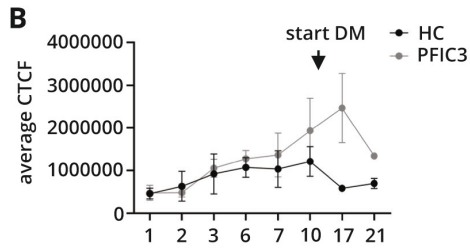
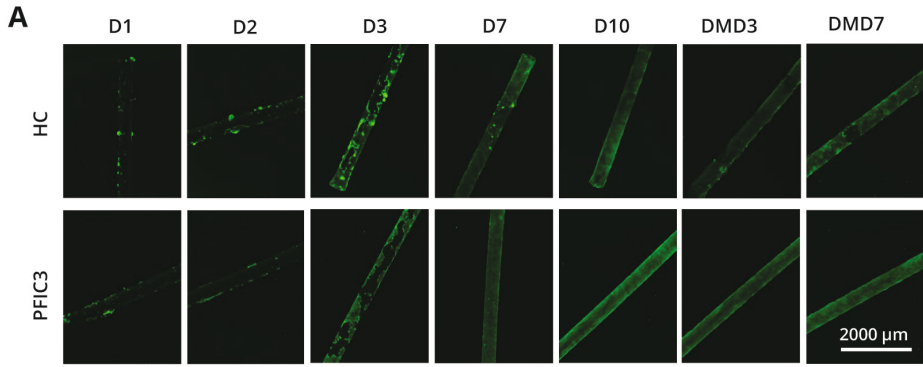


← **Figure 3. Hepatocyte-like HFMs express hepatic proteins and functionality. A-D)** Activity of phase I and II enzymes after seven days of differentiation was measured through metabolite formation per 10^6 cells after 24 hours. **A)** CYP3A4 activity displayed as formation of hydroxymidazolam from parent compound midazolam. **B)** CYP2C9 activity displayed as formation of 4-hydroxytolbutamide from parent compound tolbutamide. **C)** CYP2B6 activity displayed as formation of hydroxybupropion from parent compound bupropion. **D)** UGT activity displayed as formation of 7-hydroxycoumarin glucuronide from parent compound 7-hydroxycoumarin. Conventional differentiated ICO Matrigel™ droplet cultures (24 hours), HepaRG cells (8 hours) and primary human hepatocytes (PHH; 4 hours) were used as controls. ICO controls and hepatocyte-like HFMs (HL-HFMs) were donor-matched, as indicated by the matching black symbols. Black symbols of HepaRG conditions represent three separate experiments at different passages. PHH data represents the mean of technical triplicates of 10 mixed donors. **E)** Protein expression in HL-HFMs displayed by immunofluorescence: MDR1, ATP binding cassette subfamily B member 1; MRP2, ATP binding cassette subfamily C member 2; F-actin, actin filaments; NTCP, sodium-taurocholate co-transporting polypeptide; OATP1B3, Solute carrier organic anion transporter family member 1B3; OAT2, Organic anion transporter 2. Images are representative for Matrigel™-coated HL-HFMs after seven days of differentiation and show HFM top views. Nuclear staining is shown with DAPI (blue). **F-H)** Function of superfamilies ATP-binding cassette (ABC) transporters was assessed by exposing HL-HFMs at day seven of differentiation to calcein-AM with or without (DMSO) transporter inhibitors (PSC-833, KO-143 and MK-571, each 5 μ M). **F)** Representative images of monolayer morphologies (brightfield) and fluorescent intracellular calcein (GFP channel). HFMs can be seen as large black fibers on brightfield images. **G-H)** Quantification of mean fluorescence intensities after continuous (**G**) or brief (**H**) exposure to inhibitors. Each dot represents one field of view of an HFM.

patient and a healthy control. To this end, we supplied ICOs of both donors with calcein-AM and observed hydrolyzed calcein transport into the ICO lumen over time (Figure 4D-E). Transport was inhibited by continuous supply of ABC transporter inhibitors to stall MDR3 function.^{54,55} After 9 hours, differences between inhibition and control conditions could be observed in healthy control ICOs which progressed to 17 hours (Figure 4E-F). In comparison, PFIC3 patient ICOs showed little to no calcein accumulation in ICO lumens independent of inhibitor presence, indicating lack of MDR3 function.

Discussion

To improve translational confidence of *in vitro* pharmacological models for studies concerning DILI, research has focused on improving hepatic maturation. ICOs are of particular interest due to their expandability, patient-origin, and functional drug metabolism.^{19,56-58} Yet, hepatic maturity of ICOs remains limited.^{17,18,59} The present study demonstrates that hepatic maturation of ICOs is improved when cultured on HFMs coated with human recombinant laminins or Matrigel™. Moreover, we demonstrate that the HL-HFM system has the potential for drug testing and disease modeling as showcased using a PFIC3 casus.



← **Figure 4. PFIC3 patient donor ICOs can be grown on HFMs and maintain the disease phenotype.** **A)** Monolayer confluency was assessed on several days (D) of cell expansion and differentiation (DM) on Matrigel™-coated HFMs using live cell staining calcein-AM. Healthy donor ICO cells grown on HFMs (HC) served as controls. **B)** Quantification of live cell staining in **A**, represented by average corrected total cell fluorescence (CTCF) of two independent fibers per donor as determined by ImageJ. **C)** Gene expression of healthy and patient donor ICO cells after seven days of differentiation on Matrigel™-coated HFMs. Conventional ICO cultures in Matrigel™ droplets served as controls. Relative gene expression was determined using reference genes *RPL19* and *HPRT* (Δ CT) and is shown as log₂. *ABCB4*, ATP binding cassette subfamily B member 4; *ABCB1*, ATP binding cassette subfamily B member 1; *ABCB11*, ATP binding cassette subfamily B member 11. **D-E)** PFIC3 patient donor ICOs display impaired functionality in standard Matrigel™ droplet culture. **D)** Representative images of healthy control (HC) and PFIC3 patient (PFIC3) ICOs treated with calcein-AM and inhibitor cocktails (PSC-833, KO-143 and MK-571, each 5 μ M) or DMSO after 0 and 17 hours (h). Overlays of brightfield and GFP-channel images are shown. **E)** Quantification of fluorescence signal in ICO lumens of healthy control donor (HC) and PFIC3 patient donor (PFIC3) ICOs treated with calcein-AM and inhibitor cocktails (PSC-833, KO-143 and MK-571, each 5 μ M) or DMSO relative to 0 hours. Each dot represents the mean of three technical replicates. **F)** Area under the curve (AUC) of fluorescence intensities shown in E. **** = $p < 0.0001$; * = $p = 0.0353$.

HFM culture improves hepatic maturation of ICO cells

Here, we show that culture of ICO-derived cells on Matrigel™-coated HFMs improves hepatic maturation compared to conventional ICO culture in Matrigel™ droplets. This can likely be attributed to the architecture of the HFM culture system, which allows for closer proximity to nutrients and oxygen as well as free diffusion of waste products into the surrounding media. In contrast, conventionally cultured ICOs are fully embedded within the Matrigel™ matrix and contain an enclosed lumen causing cellular waste products such as bile salts to accumulate.^{28,60} Indeed, previous studies suggested that increased proximity to oxygen and nutrient supply can improve hepatic maturation in primary hepatocytes and ICOs.^{61,62} Interestingly, these changes could in turn be responsible for the occasionally observed reduction of ABC transporter expression, since expression of these transporters is responsive to changes in metabolism and bile salt concentrations.^{63,64} We anticipate that closer control on the balance between bile acid concentrations and exposure to nutrients and oxygen in a perfusion bioreactor will lead to further improvement of hepatic maturation.

Human recombinant ECM proteins can replace Matrigel™

Matrigel™ is an animal-derived product with high batch-to-batch variations.²⁴ To improve consistency of hepatic maturation of ICOs and thus translational confidence toward humans, we aimed to replace Matrigel™ with human recombinant laminins. Laminins are composed of α , β and γ -chains which provide anchor points for other proteins and, α -chains in particular, for cells.^{27,65} LN111, containing isoform $\alpha 1$, is the major laminin component in Matrigel™.^{66,67} It has previously been shown to support ICO growth and differentiation when combined with a synthetic hydrogel

based on polyisocyanopeptides.²⁸ Matrigel™ also contains laminins with alpha chain isoforms such as $\alpha 3$, $\alpha 4$ and $\alpha 5$.²⁴ Our results indicate that coatings with pure forms of these laminin isoforms on HFMs promote cell proliferation and hepatic maturation similarly to Matrigel™-coated HFMs. Hence, human recombinant laminins are suitable replacements for Matrigel™ and make the HL-HFM system more compliant with the 3Rs.

Still, compared to liver samples hepatic maturation on HFMs remains incomplete. *In vivo*, laminins surround the progenitor cells during regeneration and are responsible for hepatoblast proliferation and biliary differentiation.^{68,69} This might in part explain the partial hepatic maturation on HFMs. Meanwhile, other proteins, especially fibronectin, are known to steer hepatocyte differentiation and halt proliferation *in vivo*.^{68,70} In line with this, we observed poor cell attachment and proliferation on HFMs coated with human-derived fibronectin making downstream analyses impossible (data not shown). Using combination coatings of laminins and fibronectin might promote both proliferation and improved hepatic differentiation. Alternatively, addition of fibrinogen to the culture could enhance formation of cell-secreted fibronectin into the active fibronectin fibrils and thus facilitate cell interactions.⁷¹

Drug metabolism in HL-HFMs

Gene expression of phase I and II enzymes in ICO cells were improved when cultured on HFMs compared to conventional Matrigel™ droplet culture. These expression trends were also reflected by enzyme activity. Moreover, HL-HFMs perform well compared to PHH for most enzyme expressions and activities tested.

To predict DILI, it is important that *in vitro* models represent human polymorphisms of target enzymes.¹⁴⁻¹⁶ Variation in gene expression and enzyme activity of CYP3A4, CYP2B6, and UGT among ICO donors cultured on HFMs suggests that the system accounts for such polymorphisms. Interestingly, we observed previously reported polymorphisms in CYP2C9 in enzyme activity of HL-HFM cultures, but not gene expression.¹⁴ This could be a result of the overall low genetic variation in our group of donors tested as well as the low enzyme activity of CYP2C9 compared to PHH. Inclusion of more independent experiments, more ICO donors, and further improvement of maturation might give a better representation of human polymorphisms, as well as sex-related differences.^{72,73} In the future, genotyping of ICO donors to allow for targeted inclusion of polymorphisms might represent another useful approach.

While gene expression and enzyme activity correlate for each culture model, this is not always the case for intradonor variations in the HL-HFM conditions. For example, the highest expression of CYP2C9 on HL-HFMs showed only intermediate metabolite formation. This may be caused by the non-linear relationship between

gene- and protein-expression and function due to temporal or spatial disconnects, proliferation status or silent nuclei.⁷⁴⁻⁷⁶

Working with HFMs comes with technical challenges. The use of certain culture components, such as polystyrene culture plates, are known to bind hydrophobic chemicals, as was observed for bupropion.^{17,77} Various environmental chemicals have also been reported to adsorb to polyethersulfone, however underlying adsorption mechanisms remain unclear.⁷⁸ For future drug metabolism studies of HL-HFM cultures potential depletion of parent compounds or metabolites on polyethersulfone needs to be investigated.

Disease modeling

The HL-HFM model presented here not only allows for DILI assessment, but also to study genetic diseases affecting ABC transporters, such as PFIC3, showcased in this study. Current approaches to study PFIC3 are based on genetically engineered mouse models or cell lines such as HEK-293T and HepG2.^{51,79-85} Here, we demonstrate that ICOs derived from a PFIC3 patient reflect the patient phenotype. We show that the three-dimensional architecture of ICOs allows for transporter assays to assess MDR3 function, which is affected in PFIC3 patients. While ICOs may be used for high-throughput applications, these cultures are not suitable for long-term drug exposure studies. Cultures typically collapse within 10 days of differentiation in conventional Matrigel™ droplet cultures, characterized by collapse of cystic ICO structures and the formation of two-dimensional growth, likely due to Matrigel™ degradation (Figure S3B). Here, we have shown that HFMs are more suitable to support long-term culture, putatively thanks to the simpler architecture and non-biodegradable support material.

Importantly, the option for long-term culture and the use of patient-derived cells make this HL-HFM system a valuable tool for personalized PFIC3 therapeutic research. The patient-derived cells reflect the full genetic background of the donor, which is crucial in personalized approaches considering the large genetic and phenotypic heterogeneity of this disease.^{5,82} Currently, ursodeoxycholic acid (UDCA), used to counteract the detergent effect of bile salts in the liver, is the sole available treatment for PFIC3 patients.^{5,86} Yet, liver transplantation is often inevitable.⁵ Meanwhile, AAV and mRNA-based gene editing strategies are being developed and tested in the aforementioned models.⁸³⁻⁸⁵ More recently, ivacaftor, a known potentiator for the cystic fibrosis transmembrane conductance regulator, has been described to rescue MDR3 function in HEK-293T and HepG2 genetically edited with patient mutations.⁸¹ With our new *in vitro* model, gene therapy strategies and other therapeutics can be tested for functional correction and for long-term effects in a patient-specific manner.

To assess MDR3 functionality we used calcein-AM, which is not a specific MDR3 substrate but can be transported by several ABC transporters.^{49,50,87} Of note, despite the use of broad ABC transporter inhibitors, we observed occasional fluorescence signal in lumens of single ICOs under inhibition conditions in healthy controls. Similar observations were made in PFIC3 patient ICOs. Incomplete inhibition or passive diffusion might explain these findings. The use of MDR3 specific inhibitors, genetic knockouts, and MDR3-specific substrates, such as radioactively labeled phosphatidylcholine, would be valuable additions to investigate MDR3 function and pathology.^{51,82}

Future perspectives and conclusion

Separate analysis of apical and basolateral domains is valuable for pharmacokinetic studies and disease modeling. Most existing hepatic HFM systems mimic *in vivo* hepatocyte cord architecture, without access to the apical domain.^{38,40,41} The HL-HFM system offers separate access to both compartments and can be interfaced with a custom bioreactor which is currently being optimized (TNO Leiden, design confidential). It allows for automated perfusion of the inner and outer HFM compartment to mimic counter current blood and bile flow. This will introduce not only light shear stress on the cells, but is also expected to mimic oxygen, hormone, and nutrient gradients across the HFM, all of which are anticipated to support further hepatic maturation.^{32,33,88,89} Through incorporation of environmental controls, such as oxygen and pH meters, more standardization and control can be achieved. Separate sampling from both compartments facilitates separate analysis of drug and metabolite conversion and trafficking across the HL-HFM. Repeated dosing as well as long-term exposures to candidate compounds will allow for in-depth toxicity and pharmacokinetic studies.

With the European laws on reducing animal use, *in vitro* models are increasingly demanded to assess body-wide effects of a candidate drug. To address this need, our HL-HFM is developed within a consortium to establish a body-on-a-tube system. Intestinal, kidney and, bile duct HFM systems have previously been developed.⁴³⁻⁴⁷ Once the HL-HFM system has been optimized and characterized further, all organ mimics will be combined and used for multi-organ pharmacology studies.

In conclusion, we have developed a novel culture system, wherein patient-derived ICO cells are cultured on laminin-coated HFMs. Improved hepatic maturation showcases the system's potential for pharmacokinetic and toxicology studies to predict DILI. In the future, more ICO donors (both healthy and patients) and therapeutics will elucidate the systems full potential for pharmacological research.

Authorship statement

I designed and proposed most of the methodology and the experimental design with input from AM (postdoctoral researcher). We performed experiments together or in parallel and analyzed the data. LC-MS/MS was performed by TS. I wrote the first draft of the manuscript and implemented the contributions of the co-authors and external reviewers up to the current manuscript. During the whole process I asked for and implemented input and feedback from the other contributors to this study.

References

1. Cook D, Brown D, Alexander R, et al. Lessons learned from the fate of AstraZeneca's drug pipeline: a five-dimensional framework. *Nat Rev Drug Discov.* 2014;13(6):419-431. doi:10.1038/NRD4309
2. Watkins PB. Drug Safety Sciences and the Bottleneck in Drug Development. *Clin Pharmacol Ther.* 2011;89(6):788-790. doi:10.1038/CLPT.2011.63
3. Babai S, Auclert L, Le-Louët H. Safety data and withdrawal of hepatotoxic drugs. *Therapies.* 2021;76(6):715-723. doi:10.1016/j.therap.2018.02.004
4. Almomen SM, Almaghrabi MA, Alhabardi SM, et al. Exploring Indicators of Hepatotoxicity-Related Post-Marketing Regulatory Actions: A Retrospective Analysis of Drug Approval Data. *Saudi Journal of Health Systems Research.* 2022;2(1):27-31. doi:10.1159/000521296
5. Schatz SB, Jüngst C, Keitel-Anselmo V, et al. Phenotypic spectrum and diagnostic pitfalls of ABCB4 deficiency depending on age of onset. *Hepatol Commun.* 2018;2(5):504-514. doi:10.1002/hep4.1149
6. Pedersen J, Matsson P, Bergström C, et al. Early identification of clinically relevant drug interactions with the human bile salt export pump (BSEP/ABCB11). *Toxicol Sci.* 2013;136(2):328-343. doi:10.1093/toxsci/kft197
7. Liu H, Sahi J. Role of Hepatic Drug Transporters in Drug Development. *J Clin Pharmacol.* 2016;56(S7):S11-S22. doi:10.1002/jcph.703
8. Sundaram V, Björnsson ES. Drug-induced cholestasis. *Hepatol Commun.* 2017;1(8):726-735. doi:10.1002/HEP4.1088
9. Sgro C, Clinard F, Ouazir K, et al. Incidence of drug-induced hepatic injuries: A French population-based study. *Hepatology.* 2002;36(2):451-455. doi:10.1053/jhep.2002.34857
10. Weaver RJ, Blomme EA, Chadwick AE, et al. Managing the challenge of drug-induced liver injury: a roadmap for the development and deployment of preclinical predictive models. *Nat Rev Drug Discov.* 2020;19(2):131-148. doi:10.1038/s41573-019-0048-x
11. Björnsson E, Olsson R. Outcome and prognostic markers in severe drug-induced liver disease. *Hepatology.* 2005;42(2):481-489. doi:10.1002/HEP.20800
12. Fernandez-Checa JC, Bagnaninchi P, Ye H, et al. Advanced preclinical models for evaluation of drug-induced liver injury – consensus statement by the European Drug-Induced Liver Injury Network [PRO-EURO-DILI-NET]. *J Hepatol.* 2021;75(4):935-959. doi:10.1016/j.jhep.2021.06.021

13. Kuna L, Božić I, Kizivat T, et al. Models of Drug Induced Liver Injury (DILI) – Current Issues and Future Perspectives. *Curr Drug Metab.* 2018;19(10):830. doi:10.2174/1389200219666180523095355
14. Zhou SF, Liu JP, Chowbay B. Polymorphism of human cytochrome P450 enzymes and its clinical impact. *Drug Metab Rev.* 2009;41(2):89-295. doi:10.1080/03602530902843483
15. Mangó K, Kiss ÁF, Fekete F, Erdős R, Monostory K. CYP2B6 allelic variants and non-genetic factors influence CYP2B6 enzyme function. *Sci Rep.* 2022;12(1):1-14. doi:10.1038/S41598-022-07022-9
16. Cao X, Durairaj P, Yang F, Bureik M. A comprehensive overview of common polymorphic variants that cause missense mutations in human CYPs and UGTs. *Biomedicine & Pharmacotherapy.* 2019;111:983-992. doi:10.1016/J.BIOPHA.2019.01.024
17. Bouwmeester MC, Tao Y, Proença S, et al. Drug Metabolism of Hepatocyte-like Organoids and Their Applicability in In Vitro Toxicity Testing. *Molecules.* 2023;28(2):621. doi:10.3390/MOLECULES28020621
18. Lehmann V, Schene IF, Ardisasmita AI, et al. The potential and limitations of intrahepatic cholangiocyte organoids to study inborn errors of metabolism. *J Inherit Metab Dis.* 2022;45(2):353-365. doi:10.1002/JIMD.12450
19. Huch M, Gehart H, Van Boxtel R, et al. Long-term culture of genome-stable bipotent stem cells from adult human liver. *Cell.* 2015;160(1-2):299-312. doi:10.1016/j.cell.2014.11.050
20. Chen C, Soto-Gutierrez A, Baptista PM, Spee B. Biotechnology Challenges to In Vitro Maturation of Hepatic Stem Cells. *Gastroenterology.* 2018;154(5):1258-1272. doi:10.1053/j.gastro.2018.01.066
21. Sawitza I, Kordes C, Götze S, Herebian D, Haussinger D. Bile acids induce hepatic differentiation of mesenchymal stem cells. *Sci Rep.* 2015;5:13320. doi:10.1038/SREP13320
22. Ren M, Yan L, Shang CZ, et al. Effects of sodium butyrate on the differentiation of pancreatic and hepatic progenitor cells from mouse embryonic stem cells. *J Cell Biochem.* 2010;109(1):236-244. doi:10.1002/JCB.22401
23. Varghese DS, Alawathugoda TT, Ansari SA. Fine tuning of hepatocyte differentiation from human embryonic stem cells: Growth factor vs. Small molecule-based approaches. *Stem Cells Int.* 2019;2019:5968236. doi:10.1155/2019/5968236
24. Aisenbrey EA, Murphy WL. Synthetic alternatives to Matrigel. *Nat Rev Mater.* 2020;5(7):539-551. doi:10.1038/S41578-020-0199-8
25. Kallis YN, Robson AJ, Fallowfield JA, et al. Remodelling of extracellular matrix is a requirement for the hepatic progenitor cell response. *Gut.* 2011;60(4):525-533. doi:10.1136/GUT.2010.224436
26. Cameron K, Tan R, Schmidt-Heck W, et al. Recombinant Laminins Drive the Differentiation and Self-Organization of hESC-Derived Hepatocytes. *Stem Cell Reports.* 2015;5(6):1250-1262. doi:10.1016/J.STEMCR.2015.10.016
27. Suzuki N, Yokoyama F, Nomizu M. Functional Sites in the Laminin Alpha Chains. *Connect Tissue Res.* 2005;46(3):142-152. doi:10.1080/03008200591008527
28. Ye S, Boeter JWB, Mihajlovic M, et al. A Chemically Defined Hydrogel for Human Liver Organoid Culture. *Adv Funct Mater.* 2020;30(48):2000893. doi:10.1002/adfm.202000893
29. Kanninen LK, Harjumäki R, Peltoniemi P, et al. Laminin-511 and laminin-521-based matrices for efficient hepatic specification of human pluripotent stem cells. *Biomaterials.* 2016;103:86-100. doi:10.1016/J.BIOMATERIALS.2016.06.054

30. Watanabe M, Zemack H, Johansson H, et al. Maintenance of Hepatic Functions in Primary Human Hepatocytes Cultured on Xeno-Free and Chemical Defined Human Recombinant Laminins. *PLoS One*. 2016;11(9):e0161383. doi:10.1371/journal.pone.0161383
31. Ong J, Serra MP, Segal J, et al. Imaging-Based Screen Identifies Laminin 411 as a Physiologically Relevant Niche Factor with Importance for i-Hep Applications. *Stem Cell Reports*. 2018;10(3):693-702. doi:10.1016/j.stemcr.2018.01.025
32. Dash A, Simmers MB, Deering TG, et al. Hemodynamic flow improves rat hepatocyte morphology, function, and metabolic activity in vitro. *Am J Physiol Cell Physiol*. 2013;304(11):C1053-1063. doi:10.1152/AJPCELL.00331.2012
33. Li W, Li P, Li N, et al. Matrix stiffness and shear stresses modulate hepatocyte functions in a fibrotic liver sinusoidal model. *Am J Physiol Gastrointest Liver Physiol*. 2021;320(3):G272-G282. doi:10.1152/ajpgi.00379.2019
34. Leung CM, de Haan P, Ronaldson-Bouchard K, et al. A guide to the organ-on-a-chip. *Nature Reviews Methods Primers*. 2022;2:33. doi:10.1038/S43586-022-00118-6
35. Shen JX, Youhanna S, Shafagh RZ, Kele J, Lauschke VM. Organotypic and Microphysiological Models of Liver, Gut, and Kidney for Studies of Drug Metabolism, Pharmacokinetics, and Toxicity. *Chem Res Toxicol*. 2020;33(1):38-60. doi:10.1021/acs.chemrestox.9b00245
36. Bale SS, Moore L, Yarmush M, Jindal R. Emerging in Vitro Liver Technologies for Drug Metabolism and Inter-Organ Interactions. *Tissue Eng Part B Rev*. 2016;22(5):383-394. doi:10.1089/ten.TEB.2016.0031
37. Morelli S, Piscioneri A, Salerno S, de Bartolo L. Hollow Fiber and Nanofiber Membranes in Bioartificial Liver and Neuronal Tissue Engineering. *Cells Tissues Organs*. 2022;211(4):447-476. doi:10.1159/000511680
38. Hoffmann SA, Müller-Vieira U, Biemel K, et al. Analysis of drug metabolism activities in a miniaturized liver cell bioreactor for use in pharmacological studies. *Biotechnol Bioeng*. 2012;109(12):3172-3181. doi:10.1002/bit.24573
39. Mueller D, Tascher G, Müller-Vieira U, et al. In-depth physiological characterization of primary human hepatocytes in a 3D hollow-fiber bioreactor. *J Tissue Eng Regen Med*. 2011;5(8):207-218. doi:10.1002/term.418
40. Zeilinger K, Schreiter T, Darnell M, et al. Scaling Down of a Clinical Three-Dimensional Perfusion Multicompartment Hollow Fiber Liver Bioreactor Developed for Extracorporeal Liver Support to an Analytical Scale Device Useful for Hepatic Pharmacological In Vitro Studies. *Tissue Eng Part C Methods*. 2011;17(5):549-556. doi:10.1089/ten.tec.2010.0580
41. Lübberstedt M, Müller-Vieira U, Biemel KM, et al. Serum-free culture of primary human hepatocytes in a miniaturized hollow-fibre membrane bioreactor for pharmacological in vitro studies. *J Tissue Eng Regen Med*. 2015;9(9):1017-1026. doi:10.1002/term.1652
42. Unger RE, Huang Q, Peters K, Protzer D, Paul D, Kirkpatrick CJ. Growth of human cells on polyethersulfone (PES) hollow fiber membranes. *Biomaterials*. 2005;26(14):1877-1884. doi:10.1016/j.biomaterials.2004.05.032
43. Wang Z, Faria J, van der Laan LJW, Penning LC, Masereeuw R, Spee B. Human Cholangiocytes Form a Polarized and Functional Bile Duct on Hollow Fiber Membranes. *Front Bioeng Biotechnol*. 2022;10:868857. doi:10.3389/fbioe.2022.868857
44. Jansen J, de Napoli IE, Fedecostante M, et al. Human proximal tubule epithelial cells cultured on hollow fibers: Living membranes that actively transport organic cations. *Sci Rep*. 2015;5:16702. doi:10.1038/srep16702

45. Chen C, Jochems PGM, Salz L, et al. Bioengineered bile ducts recapitulate key cholangiocyte functions. *Biofabrication*. 2018;10(3):034103. doi:10.1088/1758-5090/aac8fd
46. Jochems PGM, van Bergenhenegouwen J, van Genderen AM, et al. Development and validation of bioengineered intestinal tubules for translational research aimed at safety and efficacy testing of drugs and nutrients. *Toxicology in Vitro*. 2019;60:1-11. doi:10.1016/j.tiv.2019.04.019
47. Sendino Garví E, Masereeuw R, Janssen MJ. Bioengineered Cystinotic Kidney Tubules Recapitulate a Nephropathic Phenotype. *Cells*. 2022;11(1). doi:10.3390/CELLS11010177
48. Dekkers JF, Alieva M, Wellens LM, et al. High-resolution 3D imaging of fixed and cleared organoids. *Nat Protoc*. 2019;14(6):1756-1771. doi:10.1038/s41596-019-0160-8
49. Sarkadi B, Homolya L, Szakács G, Váradi A. Human multidrug resistance ABCB and ABCG transporters: Participation in a chemoimmunity defense system. *Physiol Rev*. 2006;86(4):1179-1236. doi:10.1152/physrev.00037.2005
50. Caetano-Pinto P, Janssen MJ, Gijzen L, Verscheijden L, Wilmer MJG, Masereeuw R. Fluorescence-Based Transport Assays Revisited in a Human Renal Proximal Tubule Cell Line. *Mol Pharm*. 2016;13(3):933-944. doi:10.1021/acs.molpharmaceut.5b00821
51. Gordo-Gilart R, Andueza S, Hierro L, et al. Functional analysis of ABCB4 mutations relates clinical outcomes of progressive familial intrahepatic cholestasis type 3 to the degree of MDR3 floppase activity. *Gut*. 2015;64(1):147-155. doi:10.1136/GUTJNL-2014-306896
52. Ishigami M, Tominaga Y, Nagao K, et al. ATPase activity of nucleotide binding domains of human MDR3 in the context of MDR1. *Biochim Biophys Acta Mol Cell Biol Lipids*. 2013;1831(4):683-690. doi:10.1016/j.bbalip.2012.12.016
53. Behrendt A, Golchin P, König F, et al. VASOR: Accurate prediction of variant effects for amino acid substitutions in multidrug resistance protein 3. *Hepatol Commun*. 2022;6(11):3098-3111. doi:10.1002/hep4.2088
54. SOLVO introducing PSC 833 the specific P-gp inhibitor and new drug transporter services (mouse Bcrp1, OAT3, OCT2-metformin) - News - Solvo Biotechnology. Accessed January 23, 2023. <https://www.solvobiotech.com/news/solvo-introducing-psc-833-the-specific-p-gp-inhibitor-and-new-drug-transporter>
55. Smith AJ, van Helvoort A, van Meer G, et al. MDR3 P-glycoprotein, a phosphatidylcholine translocase, transports several cytotoxic drugs and directly interacts with drugs as judged by interference with nucleotide trapping. *Journal of Biological Chemistry*. 2000;275(31):23530-23539. doi:10.1074/jbc.M909002199
56. Prior N, Inacio P, Huch M. Liver organoids: From basic research to therapeutic applications. *Gut*. 2019;68(12):2228-2237. doi:10.1136/gutjnl-2019-319256
57. Gómez-Mariano G, Matamala N, Martínez S, et al. Liver organoids reproduce alpha-1 antitrypsin deficiency-related liver disease. *Hepatol Int*. 2020;14(1):127-137. doi:10.1007/s12072-019-10007-y
58. Nuciforo S, Heim MH. Organoids to model liver disease. *JHEP Reports*. 2020;3(1):100198. doi:10.1016/j.jhepr.2020.100198
59. Ardisasmita AI, Schene IF, Joore IP, et al. A comprehensive transcriptomic comparison of hepatocyte model systems improves selection of models for experimental use. *Commun Biol*. 2022;5(1):1094. doi:10.1038/s42003-022-04046-9

60. Schneeberger K, Sánchez-Romero N, Ye S, et al. Large-Scale Production of LGR5-Positive Bipotential Human Liver Stem Cells. *Hepatology*. 2020;72(1):257-270. doi:10.1002/hep.31037
61. Bouwmeester MC, Bernal PN, Oosterhoff LA, et al. Bioprinting of Human Liver-Derived Epithelial Organoids for Toxicity Studies. *Macromol Biosci*. 2021;21(12):2100327. doi:10.1002/MABI.202100327
62. Nahmias Y, Kramvis Y, Barbe L, et al. A novel formulation of oxygen-carrying matrix enhances liver-specific function of cultured hepatocytes. *The FASEB Journal*. 2006;20(14):2531-2533. doi:10.1096/fj.06-6192fje
63. Chan J, Vandeberg JL. Hepatobiliary transport in health and disease. *Clin Lipidol*. 2012;7(2):189-192. doi:10.2217/clp.12.12
64. Belkahlia S, Khan AUH, Gitenay D, et al. Changes in metabolism affect expression of ABC transporters through ERK5 and depending on p53 status. *Oncotarget*. 2017;9(1):1114-1129. doi:10.18632/ONCOTARGET.23305
65. Timpl R, Brown JC. The laminins. *Matrix Biology*. 1994;14(4):275-281. doi:10.1016/0945-053X(94)90192-9
66. Hughes CS, Postovit LM, Lajoie GA. Matrigel: A complex protein mixture required for optimal growth of cell culture. *Proteomics*. 2010;10(9):1886-1890. doi:10.1002/PMIC.200900758
67. Timpl R, Rohde H, Robey PG, Rennard SI, Foidart JM, Martin GR. Laminin—a glycoprotein from basement membranes. *Journal of Biological Chemistry*. 1979;254(19):9933-9937. doi:10.1016/S0021-9258(19)83607-4
68. Lorenzini S, Bird TG, Boulter L, et al. Characterisation of a stereotypical cellular and extracellular adult liver progenitor cell niche in rodents and diseased human liver. *Gut*. 2010;59(5):645-654. doi:10.1136/gut.2009.182345
69. Takayama K, Nagamoto Y, Mimura N, et al. Long-Term Self-Renewal of Human ES/iPS-Derived Hepatoblast-like Cells on Human Laminin 111-Coated Dishes. *Stem Cell Reports*. 2013;1(4):322-335. doi:10.1016/j.STEMCR.2013.08.006
70. Sánchez A, Álvarez AM, Pagan R, et al. Fibronectin regulates morphology, cell organization and gene expression of rat fetal hepatocytes in primary culture. *J Hepatol*. 2000;32(2):242-250. doi:10.1016/S0168-8278(00)80069-0
71. Li R, Liu J, Ma J, et al. Fibrinogen improves liver function via promoting cell aggregation and fibronectin assembly in hepatic spheroids. *Biomaterials*. 2022;280:121266. doi:10.1016/j.biomaterials.2021.121266
72. Meibohm B, Beierle I, Derendorf H. How important are gender differences in pharmacokinetics? *Clin Pharmacokinet*. 2002;41(5):329-342. doi:10.2165/00003088-200241050-00002
73. Zucker I, Prendergast BJ. Sex differences in pharmacokinetics predict adverse drug reactions in women. *Biol Sex Differ*. 2020;11:32. doi:10.1186/S13293-020-00308-5/TABLES/3
74. Mirauta BA, Seaton DD, Bensaddek D, et al. Population-scale proteome variation in human induced pluripotent stem cells. *Elife*. 2020;9:e57390. doi:10.7554/ELIFE.57390
75. Brion C, Lutz SM, Albert FW. Simultaneous quantification of mrna and protein in single cells reveals post-transcriptional effects of genetic variation. *Elife*. 2020;9:e60645. doi:10.7554/ELIFE.60645

76. Buccitelli C, Selbach M. mRNAs, proteins and the emerging principles of gene expression control. *Nature Reviews Genetics*. 2020;21(10):630-644. doi:10.1038/S41576-020-0258-4
77. Palmgrén JJ, Mönkkönen J, Korjamo T, Hassinen A, Auriola S. Drug adsorption to plastic containers and retention of drugs in cultured cells under in vitro conditions. *European Journal of Pharmaceutics and Biopharmaceutics*. 2006;64(3):369-378. doi:10.1016/j.ejpb.2006.06.005
78. MacKeown H, Benedetti B, Scapuzzi C, Di Carro M, Magi E. A Review on Polyethersulfone Membranes in Polar Organic Chemical Integrative Samplers: Preparation, Characterization and Innovation. *Crit Rev Anal Chem*. Published online 2022. doi:10.1080/10408347.2022.2131374
79. Andress EJ, Nicolaou M, Romero MR, et al. Molecular mechanistic explanation for the spectrum of cholestatic disease caused by the S320F variant of ABCB4. *Hepatology*. 2014;59(5):1921-1931. doi:10.1002/HEP.26970
80. Park HJ, Kim TH, Kim SW, et al. Functional characterization of ABCB4 mutations found in progressive familial intrahepatic cholestasis type 3. *Sci Rep*. 2016;6:26872. doi:10.1038/srep26872
81. Delaunay JL, Elbahsi A, Bruneau A, et al. Ivacaftor-Mediated Potentiation of ABCB4 Missense Mutations Affecting Critical Motifs of the NBDs: Repositioning Perspectives for Hepatobiliary Diseases. *Int J Mol Sci*. 2023;24(2):1236. doi:10.3390/IJMS24021236
82. Gordo-Gilart R, Hierro L, Andueza S, et al. Heterozygous ABCB4 mutations in children with cholestatic liver disease. *Liver International*. 2016;36(2):258-267. doi:10.1111/liv.12910
83. Wei G, Cao J, Huang P, et al. Synthetic human ABCB4 mRNA therapy rescues severe liver disease phenotype in a BALB/c.Abc4^{-/-} mouse model of PFIC3. *J Hepatol*. 2021;74(6):1416-1428. doi:10.1016/j.jhep.2020.12.010
84. Siew SM, Cunningham SC, Zhu E, et al. Prevention of Cholestatic Liver Disease and Reduced Tumorigenicity in a Murine Model of PFIC Type 3 Using Hybrid AAV-piggyBac Gene Therapy. *Hepatology*. 2019;70(6):2047-2061. doi:10.1002/HEP.30773
85. Weber ND, Odriozola L, Martínez-García J, et al. Gene therapy for progressive familial intrahepatic cholestasis type 3 in a clinically relevant mouse model. *Nat Commun*. 2019;10(1):5694. doi:10.1038/s41467-019-13614-3
86. Frider B, Castillo A, Gordo-Gilart R, et al. Reversal of advanced fibrosis after long-term ursodeoxycholic acid therapy in a patient with residual expression of MDR3. *Ann Hepatol*. 2015;14(5):745-751. doi:10.1016/S1665-2681(19)30771-9
87. Evseenko DA, Paxton JW, Keelan JA. ABC drug transporter expression and functional activity in trophoblast-like cell lines and differentiating primary trophoblast. *Am J Physiol Regul Integr Comp Physiol*. 2006;290(5):1357-1365. doi:10.1152/ajpregu.00630.2005
88. Ehrlich A, Duche D, Ouedraogo G, Nahmias Y. Challenges and Opportunities in the Design of Liver-on-Chip Microdevices. *Annu Rev Biomed Eng*. 2019;21:219-239. doi:10.1146/ANNUREV-BIOENG-060418-052305
89. Esch MB, Prot JM, Wang YI, et al. Multi-cellular 3D human primary liver cell culture elevates metabolic activity under fluidic flow. *Lab Chip*. 2015;15(10):2269-2277. doi:10.1039/c5lc00237k

Supplemental Data

Supplemental Materials and Methods

Permeability assay

HFM's were prepared as described using L-DOPA and LN332 and placed in a 3D-printed Eppendorf-tube insert made of a cell-compatible resin (TNO Leiden, design confidential). Organoid fragments were seeded on the HFM-insert construct in a 2-mL Eppendorf tube for 4 hours under constant rotation at 0.5 RPM. Cell-laden HFMs were cultured in expansion medium for 7 days. Then, cell-laden HFMs were primed and differentiated as described. A leakage assay was performed using 0.1 mg/ml FITC-inulin in HBSS with 10 mM HEPES (pH 7.4). The HL-HFM lumen was perfused at a speed of 50 μ L/minute (500 μ L effluent in total) for 10 minutes using a custom 3D-printed perfusion bioreactor made of a cell-compatible resin (TNO Leiden, design confidential) and a peristaltic pump (Ismatec). Before the assay, tubing was assembled and rinsed with 70% ethanol for 10 minutes, with MQ water for 10 minutes, with HBSS/10 mM HEPES (pH 7.4) for 10 minutes and with the FITC-inulin solution for 5 minutes at a speed of 100 μ L/minute. The perfusion bioreactor was saturated with HBSS/HEPES 10 mM (pH 7.4). The cell-laden HFM-insert was washed with HBSS/HEPES 10 mM (pH 7.4). Then, the perfusion bioreactor and HFM-insert were assembled (design confidential), 710 μ L of HBSS/HEPES 10 mM (pH 7.4) was added to the outer, apical compartment, and the bioreactor chamber was closed. The system was checked for leakage before connecting the tubing and running the assay. A nail polish-covered fiber was used as a negative control. A positive control (no cells, coated with L-DOPA and LN332) was lost due to technical issues. Basal effluent was collected to an Eppendorf tube and measured in triplicates (100 μ l each) on a 96-well plate for fluorescence measurements. 500-550 nm emission wavelengths were measured using a standard fluorescence plate reader. Fluorescence intensities were corrected for background (HBSS/HEPES 10 mM, pH 7.4). Statistical difference was determined using a non-parametric unpaired t-test.

Supplemental Figures

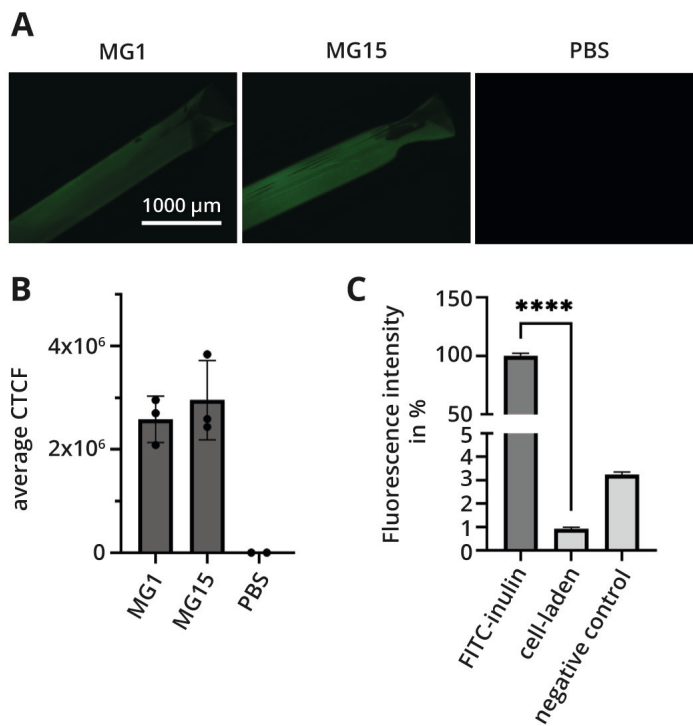


Figure S1. ECM and cell confluency on HFMs. **A)** Immunofluorescence of LN111 detected on HFMs coated with Matrigel™ (MG) or PBS. A single (MG1) or 15 (MG15) HFMs were incubated at once in an Eppendorf tube. **B)** Quantification of **A** represented as the average corrected total cell fluorescence (CTCF) of three parts of one HFM determined by ImageJ. **C)** Quantification of FITC-inulin leakage from the HFM lumen into the outer apical compartment. HFM was cell-laden or covered in nail polish (negative control). The fluorescence of the FITC-inulin solution perfused through the fibers during preparation was set to 100%. n = 3, **** < 0.0001.

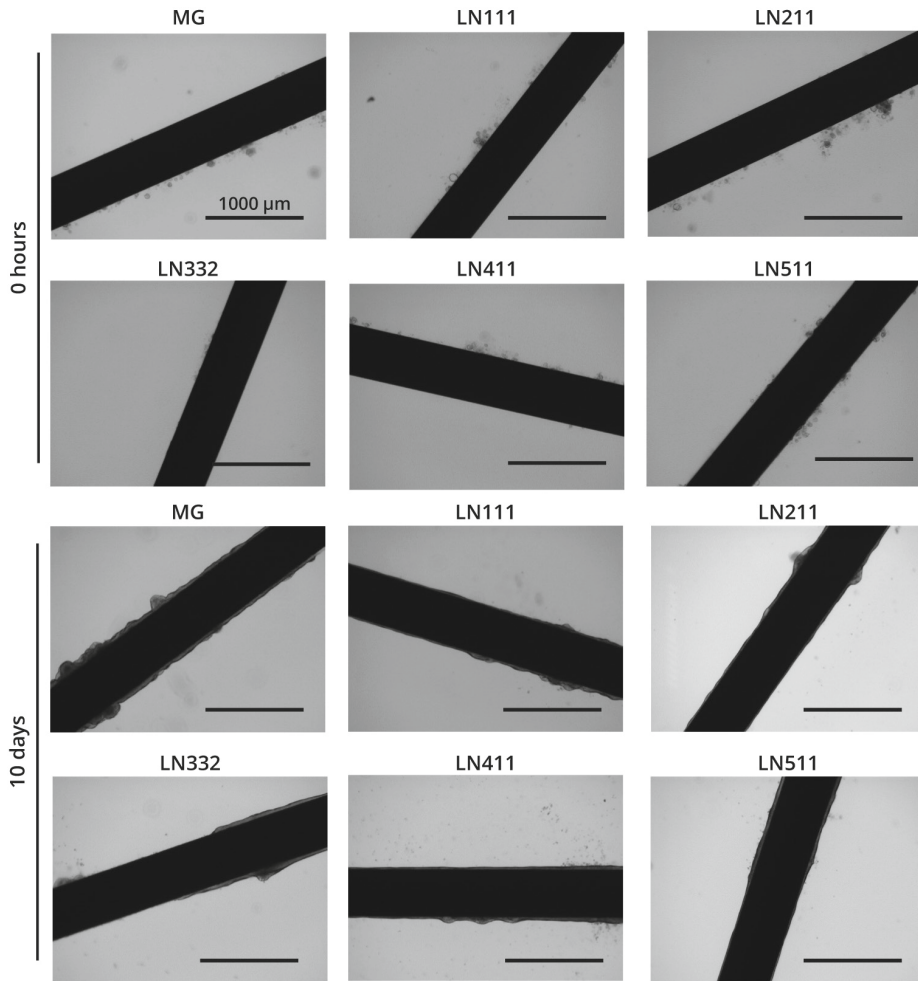


Figure S2. Human recombinant laminins (LN) promote monolayer formation of ICO-derived cells on HFMs as well as Matrigel™ (MG). Brightfield images at 0 hours and after 10 days of expansion are shown. HFMs can be seen as large black bars. Scale bars represent 1000 μm.

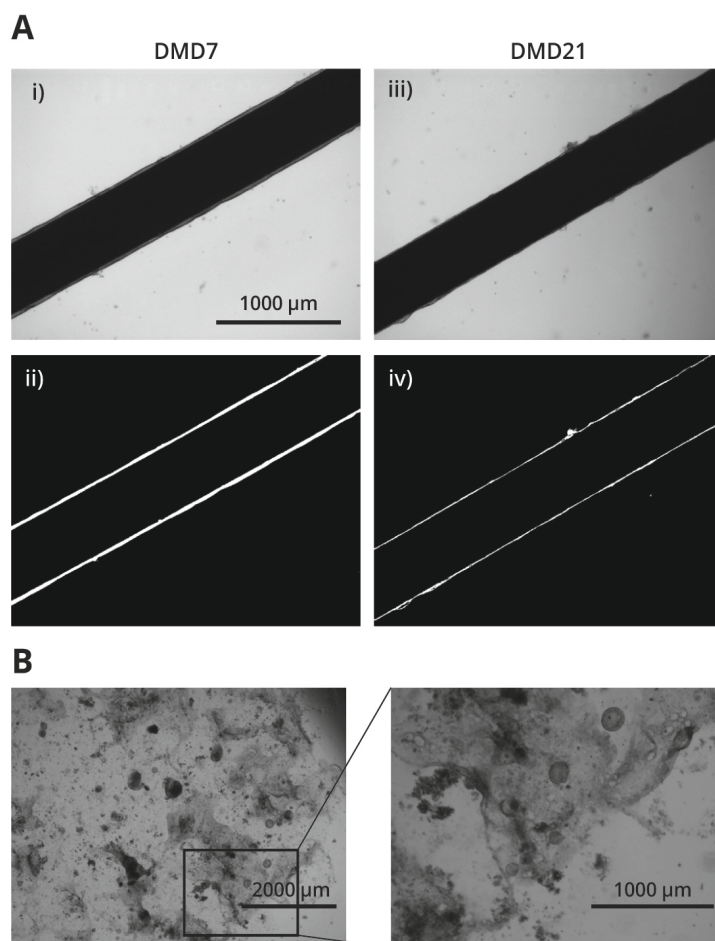


Figure S3. Long-term culture of ICO-derived cells on HFMs and in standard Matrigel™ droplet culture. A) Representative brightfield (i, iii) and black and white (ii, iv) image of ICO-derived cells on HFMs after 7 (i, ii) and 21 (iii, iv) days of differentiation tested for three ICO donors. **B)** Representative brightfield images of Matrigel™ droplet culture of ICOs on day 11 of differentiation.

Supplemental Tables

Table S1. Validated primers for RT-qPCR

Primer name	Sequence (5'-3')	T _m in °C
<i>ALB</i> -Fw	GTTTCGTTACACCAAGAAAGTACC	64
<i>ALB</i> -Rv	GACCACGGATAGATAGTCTTCTG	64
<i>CYP2B6</i> -Fw	CTACCAAGATCAAGAGTTCCTG	63
<i>CYP2B6</i> -Rv	ATTTCAAGAAGCCAGAGAAGAG	63
<i>CYP2C9</i> -Fw	GACAGAGACGACAAGCAC	62
<i>CYP2C9</i> -Rv	AATCACACGTTCAATCTCTTCC	62
<i>CYP2C19</i> -Fw	GGGACAGAGACAACAAGCA	60
<i>CYP2C19</i> -Rv	CCTGGACTTAGCTGTGACC	60
<i>CYP2D6</i> -Fw	GAGGTGCTGAATGCTGTC	61
<i>CYP2D6</i> -Rv	AGGTCATCCTGTGCTCAG	61
<i>CYP3A4</i> -Fw	TGATGGTCAACAGCCTGTGCTGG	60
<i>CYP3A4</i> -Rv	CCACTGGACCAAAAGGCCTCCG	60
<i>HPRT</i> -Fw	TATTGTAATGACCAGTCAACAG	60
<i>HPRT</i> -Rv	GGTCCTTTTCACCAGCAAG	60
<i>ABC1</i> -Fw	CAGTGGCTCACACCCGTAATC	61
<i>ABC1</i> -Rv	GCCAGGCTGGTCTTGAATC	61
<i>ABCC3</i> -Fw	GTCCGCAGAATGGACTTGAT	60
<i>ABCC3</i> -Rv	TCACCACTTGGGGATCATT	60
<i>RPL13A</i> -Fw	GTGAAGGCATCAACATTCTG	60
<i>RPL13A</i> -Rv	GATAGGCAAACCTTTCTGTAGG	60
<i>SULT1A1</i> -Fw	TTCCTTGAGTTCAAAGCCC	65
<i>SULT1A1</i> -Rv	TGTCTTCAGGAGTCGTGG	65
<i>UGT2A3</i> -Fw	AATACTCGGCTGTATGATTGG	58
<i>UGT2A3</i> -Rv	CATAGATCCCATTTCACC	58

Abbreviations: Fw, forward; T_m, melting temperature; Rv, reverse

Table S2. Primary antibodies for immunofluorescence

Antigen	Supplier	Cat. number	Raised in	Dilution	Incubation
BCRP	Santa Cruz	sc-377176	mouse	1:50	o/n at 4°C
BSEP	Santa Cruz	sc-74500	mouse	1:50	o/n at 4°C
ECAD	BD Biosciences	610181	mouse	1:50	o/n at 4°C
HNF4α	Novus Biologicals	NBP1-89679	rabbit	1:50	o/n at 4°C
Integrin α6	Novus Biologicals	NBP1-85747	rabbit	1:50	o/n at 4°C
LN111	Abcam	ab11575	rabbit	1:300	o/n at 4°C
MATE1	Novus Biologicals	NBP1-87909	rabbit	1:50	o/n at 4°C
MDR1	Santa Cruz	sc-55510	mouse	1:50	o/n at 4°C
MDR3	Santa Cruz	sc-58221	mouse	1:50	o/n at 4°C
MRP2	Abcam	ab187644	rabbit	1:50	o/n at 4°C
MRP3	Novus Biologicals	NBP2-37923	rabbit	1:50	o/n at 4°C
NTCP	Novus Biologicals	NBP1-60109	rabbit	1:50	o/n at 4°C
OAT2	Novus Biologicals	NBP1-62660	rabbit	1:50	o/n at 4°C
OATP1B3	Novus Biologicals	NBP1-80980	rabbit	1:50	o/n at 4°C
OCT1	Novus Biologicals	NBP1-59464	rabbit	1:50	o/n at 4°C
Phalloidin-Alexa 488	Thermo Fisher Scientific	A12379	-	1:400	o/n at 4°C
ZO1	Thermo Fisher Scientific	40-2300	rabbit	1:50	o/n at 4°C

Table S3. Secondary antibodies for immunofluorescence

Antigen	Supplier	Cat. number	Raised in	Dilution	Incubation
Anti-mouse-Alexa 488	Thermo Fisher Scientific	A11029	goat	1:100	2h at RT
Anti-rabbit-Alexa 488	Thermo Fisher Scientific	A11008	goat	1:100	2h at RT
Anti-mouse-Alexa 647	Thermo Fisher Scientific	A21236	goat	1:100	2h at RT
Anti-rabbit-Alexa 647	Thermo Fisher Scientific	A21245	goat	1:100	2h at RT



5

Summarizing Discussion

Rare pediatric liver disorders can be very destructive to the lives of patients and their families. Often, therapeutic options are limited to symptomatic care and precise disease mechanisms remain elusive. The relatively low incidence of each individual disease and the often widespread geographic distribution of patients complicate research and treatment development. In this thesis, we have investigated the potential of patient-derived liver organoids to study such rare pediatric liver diseases. We characterized organoids from several monogenic liver disorders and showed that organoids express functional biomarkers of these diseases (**Chapter 2**). We uncovered that liver organoids possess a hybrid phenotype, combining hepatocyte and cholangiocyte characteristics. This led us to investigate whether patient-derived liver organoids would be interesting to study the rare perinatal disease biliary atresia (BA), in which the hepatobiliary tree is occluded and becomes fibrotic (**Chapter 3**). We found that organoids from different hepatobiliary regions of BA patients can be cultured and biobanked. Further characterization showed that BA patient organoids display BA specific growth behavior and increased sensitivity to viral infections. While we showed that various hepatocyte and cholangiocyte functions can be studied in liver organoids in **Chapter 2**, our data also indicated that several hepatocyte functions are currently limited in this *in vitro* system. Therefore, we devised a novel culture strategy to increase hepatic maturation in liver organoids (**Chapter 4**). We found that hepatic functions, such as drug metabolism, improve when liver organoid cells are cultured on hollow fiber membranes (HFM) coated with extracellular matrix (ECM) proteins of the hepatic niche. Moreover, we demonstrated that hepatic transepithelial transporter defects such as progressive familial intrahepatic cholestasis type 3 (PFIC3) can be studied in patient-derived liver organoids. Collectively, these findings suggest that liver organoids may be suitable for drug testing for (specific) rare pediatric liver disorders. In the following chapter, I will summarize our findings and discuss their implications for the future use of liver organoids to study rare pediatric liver disorders.

Patient-derived liver organoids for modeling rare pediatric liver disorders

In this thesis we investigated the usefulness of patient-derived liver organoids to study rare pediatric liver diseases. The rarity and often heterogeneity of these diseases complicates the investigation of underlying disease mechanisms and the development of treatments. In recent years, increasing investment in this field has resulted in breakthroughs for several patient groups.¹⁻³ Currently, a variety of approaches is used to research these diseases, including individual case studies, clinical trials, such as n-of-1 trials, animal models, patient-specific fibroblasts, patient-derived iPSCs, organoids and precision-cut liver slices.³⁻⁸ Various approaches have successfully provided insight in disease mechanisms or helped in clinical

decision-making.^{1-3,8} However, for many rare pediatric liver diseases no appropriate *in vitro* model or therapy exists.⁹⁻¹⁴ Our aim was to elucidate whether patient-derived liver organoids are a useful tool to model and study rare pediatric liver disorders.

In **Chapter 2**, we evaluated which rare monogenic diseases can be studied with liver-derived intrahepatic cholangiocyte organoids (ICOs) based on gene-expression and function. In our experience, the protocol to establish ICOs allows for relatively easy sharing of biopsies around the globe, thereby reducing the limitation of global distribution of patient material. We demonstrated that patient organoids express key phenotypic features of different monogenic liver disorders. Various functions affected by monogenic mutations are expressed in liver organoids and allow us to distinguish between healthy control and patient organoid phenotypes. We showcased that basic metabolic functions, but also hepatocyte-specific functions, such as copper metabolism, can be studied in ICOs. Moreover, we demonstrated that ICOs are particularly useful to study transepithelial transport functions. The next step would be to characterize each monogenic liver disorder modeled in organoids in more detail, by increasing the sample size, generating isogenic controls, and unraveling disease mechanisms for relevant monogenic liver disorders. Moreover, comparison of *in vivo* patient and *in vitro* organoid phenotypes will be necessary to ensure that the model accurately reflects disease phenotypes. For example, it would be interesting to investigate how the clinical biomarker of methylmalonic acidemia (MMA) in organoids correlates with the *in vivo* biomarker expression.

In the case of cystic fibrosis (CF) we were able to demonstrate that ICOs, similarly to airway and intestinal organoids, reflect phenotypic consequences of mutations in the cystic fibrosis transmembrane conductance regulator (CFTR) and can be used to study drug efficacy.⁹⁻¹⁴ CF affects multiple organs, with progressive lung disease being the major cause of clinical complications and mortality.² Hence, respiratory defects have been the focus of clinical and laboratory studies. Meanwhile, CF-associated liver disease (CFLD) occurs in 10-15% of CF patients and remains poorly understood.^{1,15} Prolonged survival of patients due to early diagnosis and improved disease management has led to CFLD being a significant clinical complication of CF.¹⁵⁻¹⁷ Various hypotheses on the underlying mechanisms of CFLD have been proposed, including cholestasis-induced fibrosis and dysregulated cholangiocyte immunomodulation as a consequence of CFTR mutations.^{1,15,18-20} However, none has been definitively linked to CFLD in patients, thus hampering prediction and prevention of CFLD.^{15,21} Although intestinal organoids are now routinely used to identify effective treatments for CF patients, CFLD cannot be predicted in this gut model. Moreover, the effect of novel therapeutics such as ivacaftor and tezacaftor on CFLD is currently unclear.^{15,22-24} ICOs could be a valuable tool to complement existing CF organoid models to study CF-related liver disorders in a personalized manner. Expression of CFTR and organoid architecture make ICOs suitable to

study cholestatic diseases. Moreover, indications from our studies in **Chapter 3** showing retained immunobiology in patient ICOs open the doors to study putative immunomodulatory mechanisms related to CFLD in ICOs.

Aside from CFLD, current models are also limited in predicting whether novel CF medication causes drug induced liver injury (DILI). As a result, several compounds such as ivacaftor and tezacaftor have recently been reported to induce DILI in some individuals.^{25,26} DILI is caused by adverse reactions to the foreign compound or formation of unintended metabolites which cause tissue damage and eventually lead to acute liver failure.²⁷ Despite extensive drug testing prior to acceptance by the FDA or EMA, DILI is frequently observed for various drugs.²⁸⁻³⁰ Recent studies have provided increasing evidence that mechanisms underlying DILI are multifactorial.^{29,31} Moreover, susceptibility factors seem to differ between patients which explains why current drug testing strategies do not adequately predict DILI.²⁹ In recent years, emphasis has shifted toward defining and identifying adverse outcome pathways (AOPs) to predict DILI.³²⁻³⁴ AOPs are theoretical frameworks used in toxicology to define and link key events leading to drug toxicity.³²⁻³⁴ As such AOPs aid in unraveling and understanding mechanisms underlying DILI. To that end, liver *in vitro* models to study DILI are being developed for high content analysis allowing careful inspection of key events involved in underlying mechanisms.³⁵ Adequate expression of relevant enzymes and transporters is essential for an *in vitro* model to display drug toxicity sensitivities akin to *in vivo* hepatocytes. For example, if drug metabolizing enzymes are not properly expressed potentially toxic intermediate metabolites are not formed, and thus no toxicity will be detected.^{36,37} Similarly, poor expression of a transepithelial transporter responsible for timely export of otherwise toxic compounds can lead to false positive detection of drug toxicity. Recent work has established that ICOs express key drug metabolism genes well, compared to other patient-derived models such as iPSC-derived hepatocyte-like cells (iPSC-HLCs).³⁸ Previous work by our group showed that this transcriptomic profile of ICOs is reflected in function as ICOs can predict drug toxicity.³⁹ Moreover, we show that liver organoids display interdonor heterogeneity in gene expression and function, suggesting ICO suitability for personalized drug testing. However, it remains to be determined whether this heterogeneity reflects true differences between patients. ICOs from more patients ought to be tested and outcomes correlated with *in vivo* data in order to elucidate whether this liver model can indeed predict patient-specific drug metabolizing capacities. In addition, specific evaluation of metabolism of CF medication and involved AOPs leading to drug toxicity should be performed in ICOs to clarify their potential in predicting DILI for patients with CF and other rare diseases, and thus safeguard patient well-being.

Gene editing in ICOs

For many monogenic liver disorders, new developments in gene therapy present promising alternatives to conventional therapies. In the case of Wilson disease, the first in-human trial using an adeno-associated vector-based monogenic augmentation therapy is currently under way.⁴⁰⁻⁴³ While this is a great leap forward, a gene correction approach would be more desirable than gene augmentation. CRISPR-Cas9 systems as well as CRISPR-derived prime- and base-editing have been proposed as accurate and efficient approaches to correct patient-specific mutations. We envision that ICOs will be a useful tool to test and tailor patient-specific gene editing strategies. Our group and others have previously shown that gene editing of organoids using CRISPR-derived systems is efficient and does not result in off-target effects.⁴⁴⁻⁴⁷ In the context of disease modeling, the ease of gene editing in ICOs and subsequent clonal expansion are useful for the generation of isogenic controls. These are established by introducing or correcting patient-specific mutations in healthy control or patient organoids. This is especially useful for monogenic diseases with poor geno- and phenotype correlation, such as DNA polymerase gamma (POLG)-related disease. Mutations affecting POLG lead to mitochondrial DNA depletion resulting in neurological malfunction such as epilepsy, muscle weakness, and liver dysfunction or failure.^{48,49} Heterogeneity in onset, mutation and severity have resulted in the definition of various diseases caused by POLG mutations, such as Alpers–Huttenlocher syndrome and myocerebrohepatopathy.⁴⁸ We envision that the use of isogenic control ICOs will aid in unraveling relationships between geno- and phenotypes of POLG-related disorders. In addition, gene editing of potential downstream targets affected by a given mutation can aid in unraveling disease mechanisms. To this end, our group is currently devising gene-editing strategies and expanding the development of functional assays for various monogenic liver disorders in ICOs.

Other patient-derived hepatocyte *in vitro* models

Skin fibroblasts are widely used to study rare monogenic disorders *in vitro* in a personalized manner. Fibroblasts are readily available and easy to handle. Yet, their origin suggests that their potential to study hepatocyte-specific disorders is limited. Indeed, literature reports on modeling liver disease with fibroblasts is scarce.³ Our comparison of ICOs and fibroblasts to liver tissue further underscores that fibroblasts lack expression of various hepatocyte-specific genes (**Chapter 2**). Rather, fibroblasts are useful to study generic biochemical defects which affect various cell types. Hence, for hepatocyte-specific functions, such as drug metabolism, hepatocyte-specific cell models are preferred. Due to their origin and bipotent nature ICOs were considered an ideal patient-derived hepatocyte *in vitro* model. However, we uncovered that ICOs do not express all relevant hepatocyte-specific genes (**Chapter 2**). Rather, ICOs express a mixture of some cholangiocyte- and hepatocyte-specific genes and functions. Hence, with current culture conditions,

ICOs are suitable to study a selection of hepatocyte functions affected in rare liver disorders, such as copper metabolism or transepithelial transport.

Since our studies with ICOs commenced, various other novel patient-derived *in vitro* models have been developed to study hepatocyte biology and disease. Primary human hepatocytes (PHH) are considered the gold standard to study hepatocyte functions. Previously, the use of PHH in disease modeling was hampered due to the need of significant amounts of starting material, expansion difficulties, and rapid loss of hepatic functions *in vitro*. In recent years, a myriad of promising culture methods has been developed to improve long-term expansion and hepatic function of PHH. Hu *et al.* 2018 reported improved long-term culture of PHH and maintenance of hepatic functions when cultured as organoids.⁵⁰ However, in our experience and according to others, this protocol is successful for fetal tissue only, with very low success rates of establishing stable hepatocyte organoid lines from pediatric or adult liver tissue.^{38,51,52} Work is ongoing to improve the culture conditions and we anticipate that this model will be very useful in the future. Others have established a protocol wherein PHH are allowed to revert to a fetal-like hepatic state for propagation and are re-differentiated when needed.⁵³ While, this proved to be a robust method, final hepatic maturity did not reach original PHH levels. Yet another approach to model hepatocytes *in vitro* using patient-derived cells involves direct transdifferentiation of skin fibroblasts or urine-derived stem cells through lentiviral expression of transcription factors essential for liver development.^{54,55} These are very promising in terms of the ease of sampling skin or urine compared to liver tissue for PHH or ICOs. However, hepatic maturation and reports on disease modeling remain limited. Unfortunately, this is the case for various other novel hepatocyte models.^{53,56} Moreover, characterization of many new models often lacks comparison to PHH or liver tissue.³⁸ Similarly, only few key hepatocyte markers and functions, such as albumin and drug metabolizing enzyme CYP3A4, are examined by most studies. These limitations in study design make it difficult to conclude how well these models mimic hepatic functions and whether they can be used to study specific rare liver diseases.

One exception are iPSC-based hepatocyte models. iPSCs are well-established and widely used patient-derived *in vitro* models for rare monogenic disorders.³ To generate iPSCs from patients suffering from rare monogenic disorders, cell sources which allow low invasive sampling methods, such as dermal fibroblasts or peripheral blood cells, are commonly used. Successful modeling of various rare liver diseases using iPSC-HLCs has been showcased, such as the urea cycle disorder citrullinemia type 1, mitochondrial DNA depletion syndrome 3 and hypercholesterolemia.^{3,57-59} Nonetheless, not all monogenic liver disorders can be studied in iPSC-HLCs to date due to limited hepatic maturation, as also seen in ICOs.^{38,60} It has been suggested that the genetic reprogramming methods to generate iPSC-HLCs can affect the cells'

maturation capacities.^{61,62} Indeed, it was shown that reprogramming can activate normally silenced genes by affecting DNA methylation.⁶³⁻⁶⁶ In one example, human endogenous retroviral genes were activated as a byproduct of iPSC generation.⁶⁵ These genes have been suggested to maintain cell pluripotency and can thus inhibit differentiation.^{67,68} Therefore, the field of iPSC-HLCs faces specific hurdles concerning robust reprogramming methods, expansion, and differentiation to the hepatic fate. This suggests that iPSC-derived models are currently less suitable to study diseases with unclear geno- and phenotype correlations.^{3,69,70} In such cases, ICOs might present a better choice.

Recently, an unbiased transcriptomic wide comparison pipeline for hepatocyte-like cells derived from various sources, including hepatocytes, intrahepatic cholangiocytes, iPSCs, and fibroblasts was developed by our group.³⁸ Overall, the study confirmed the previous notion that no hepatocyte model fully mimics the PHH transcriptome. Some hepatic markers were well expressed in multiple models and yet again others could not be detected in any model. Interestingly, each model displayed their individual strengths. For example, ICOs performed better in drug metabolism, while iPSC-HLCs performed better in urea metabolism. Since the focus of this study was not the direct comparison between these two model systems, no further in-depth proteomics or functional assays were performed. Such functional comparisons would be very useful to uncover whether existing models can synergize in research on monogenic liver disorders. Importantly, continuous improvements of differentiation protocols for any hepatic *in vitro* model will likely yield a larger array of functions that can be studied in the future.

While functional performance of a model is one of the most important aspects, financial investment, time to first assay, expansion potential, and protocol complexity can also affect the successful adoption of a novel *in vitro* model. In the case of ICOs and iPSC-HLCs, protocols and investment requirements differ significantly. The generation of iPSC-HLCs is known to be difficult and time-consuming due to low reprogramming efficiency, continuous need for characterization and manual colony picking.^{69,71-75} Eventually, iPSC-HLCs can be generated within a minimum of 40 days.^{75,76} In comparison, ICOs are generated and maintained using a relatively simple protocol and are ready to use within a minimum of one to two weeks of sampling a patient biopsy. Depending on the function of interest, an additional week of differentiation is required before functional assays can commence. Naturally, for both models additional time is required if larger cell numbers are desired.

In the end the model choice must be made based on the expression of the function of interest, availability and flexibility of laboratory infrastructure, and the invasiveness of sampling patient material. In some cases, functions affected by monogenic liver disorders are well expressed in fibroblasts making invasive needle

biopsies or extensive reprogramming protocols unnecessary. In other instances, more mature hepatic models such as ICOs or iPSC-based models are desirable. Thanks to the ease of culturing, ICOs are preferred if the function of interest is expressed sufficiently to distinguish between healthy and patient organoids. In addition, the genomic stability of ICOs is advantageous for studying diseases with unclear geno- and phenotype relations. However, needle biopsies are more invasive than skin biopsies and come with risks of internal bleeding, which may lead to choosing iPSC-HLCs over ICOs.

Liver organoids to study biliary atresia

Since **Chapter 2** revealed that ICOs retain various cholangiocyte characteristics, we were interested to see whether BA could be studied using patient-derived ICOs. In BA, the biliary tree is obstructed and fibrotic, thus prohibiting bile flow from the liver into the intestine. While the pathogenesis remains unclear, the phenotype strongly suggests that cholangiocytes lining the biliary tree play a central role in BA.⁷⁷ Importantly, timing and severity differences between extra- and intrahepatic symptoms suggest differential underlying mechanisms or susceptibilities of cholangiocytes of different hepatobiliary regions during specific developmental periods. Extra- and intrahepatic bile ducts develop from different progenitors, which could be an important factor underlying these spatiotemporal differences.⁷⁷ Following the establishment of organoid cultures from intrahepatic cholangiocyte progenitors (ICOs), protocols have been developed to generate organoid cultures from extrahepatic bile duct (ECOs) and gallbladder cholangiocyte progenitors (GCOs).^{78,79} Since these organoids retain regional differences *in vitro* we hypothesized that they would be useful to study regional heterogeneity of BA.^{78,79} Therefore, we tested whether organoids could be cultured from these three hepatobiliary regions from BA patient tissue. We demonstrated successful culture and cryopreservation of BA patient organoids, but also showed that growth behavior of BA ICOs differed from control organoids. Despite normal organoid morphologies, transcriptome analyses suggested that BA organoids differed from control organoids, especially in genes involved in ECM remodeling and proliferation, both of which are functions putatively involved in BA pathogenesis.^{78,80-84} Various hypotheses on BA pathogenesis exist, including exposure to an environmental or metabolic toxin, viral infections, and a dysregulated immune response.^{78,85} Since liver organoids are a minimalistic model of the biliary epithelium, the exact mechanism of action of a virus or toxin can be studied in isolation from other cell types. To gain insight into whether liver organoids are indeed suitable to test existing hypotheses, we treated BA and control organoids with a synthetic viral analog (poly I:C) and a previously identified plant toxin (biliatresone) known to cause BA in animals.^{86,87} We found that biliatresone provoked upregulation of cellular stress responses such as glutathione metabolism

in BA, healthy and non-BA disease control ECOs. Poly I:C exposure elicited BA-specific responses on a transcriptomic level, including ECM remodeling and pro-fibrotic signals. Overall, our data suggests that liver organoids represent an interesting human *in vitro* model to study BA.

While we only discussed the most conspicuous findings in the transcriptomics analyses in **Chapter 3**, we anticipate that our large dataset contains many more valuable insights to unravel the pathogenesis of BA. This large dataset deserves an in-depth discourse separate from this initial characterization of BA patient liver organoids. It would be useful to increase the sample size to ensure sufficient statistical power to eliminate current uncertainties. Similarly, it would be interesting to include datasets from previous studies of BA organoids. Importantly, taking along BA patient liver tissue or blood samples in the transcriptomics analysis as reference as well as cross-checking clinical records of the patients might aid in connecting *in vitro* and *in vivo* findings.

One of the most supported hypotheses for BA pathogenesis assumes involvement of a viral infection combined with a dysregulated immune reaction. Indeed, besides forming the tight epithelial barrier of the bile ducts, cholangiocytes are known to be immunocompetent. Cholangiocytes are antigen presenting cells (APCs) and can recognize pathogens through pattern-recognition receptors, such as toll-like receptors (TLRs), and elicit downstream inflammatory reactions.^{88,89} However, the specific mechanisms involved remain poorly understood, partly because interspecies differences in immunobiology such as antigen presentation and TLR reactivity complicate the study of underlying mechanisms.^{88,90} Thus, human cholangiocyte models such as liver organoids are valuable tools to study human cholangiocyte immunobiology. Our transcriptomics data support this notion and suggest that cholangiocytes might be actively involved in altering the immune response in BA. Alternatively, the organoids may react abnormally due to their origin from the fibroinflammatory environment of BA patient tissue. In the future, cholangiocyte immunomodulatory functions and putative dysregulation thereof should be studied in more detail. Initially, it will be necessary to confirm our findings that BA patient organoids modulate the ECM and secrete immunomodulatory compounds. By repeating immunological insults, we may discriminate between immunological dysregulation as the cause or consequence of BA.

To identify whether upregulated pro-fibrotic signals in BA organoids have functional implications, the effects of specific cytokines, conditioned media or organoid co-cultures on hepatic stellate cells might be a useful approach. Potentially, one could mimic intrahepatic fibrosis in BA *in vitro* by combining BA patient ICOs with hepatic stellate cells. Such study designs have previously been shown to successfully mimic liver fibrosis.⁹¹⁻⁹³ Using hepatic stellate cells from a healthy donor would

help in identifying whether BA patient cholangiocytes provoke fibrosis through dysregulated ECM remodeling. Other immune cells likely involved in BA pathogenesis include macrophages, natural killer cells, and T-cells.⁸⁸ Previously, interactions between human cholangiocytes and T-cells have been studied *in vitro* through two-dimensional transwell culture and cytokine stimulation.^{89,94–97} Similar approaches using liver organoids could be useful to gain insight into the immunomodulatory capacity of BA patient and healthy cholangiocytes from different hepatobiliary regions and the effects thereof on relevant immune cells. Such *in vitro* studies will aid in understanding underlying cellular and molecular mechanisms specific for cholangiocyte immunobiology.

Importantly, *in vitro* models lack many aspects of the complex network of biological interactions and chemical signaling constituting immunobiology. Despite interspecies differences, rodent models such as mice remain a useful model to study the full picture of immune dysregulation involved in BA, provided that interpretations of *in vivo* findings are done cautiously and under consideration of interspecies differences.^{90,98} Together mouse *in vivo* and human *in vitro* studies will likely synergize to unravel immunobiology underlying BA.

To gain insight into how viral infections are involved in BA pathogenesis, a broad array of viruses and specific viral proteins ought to be tested. To date, most studies focus on rotaviruses, while it is well known that viral strains encountered in BA patient tissues are highly heterogeneous.^{88,99} The use of poly I:C in our study not only limits our results to information on RNA viruses, but also does not allow the study of cholangiocyte-virus interactions. The latter has been proposed to be a key mechanism behind cholangiocyte specificity of BA.^{88,100,101} Particularly, viral capsid proteins, such as rotavirus proteins VP4 and VP7, have been proposed to have high affinity for cholangiocyte receptors, thus increasing viral entry in this cell type.^{100,101} Certain amino acid sequences have been identified to bind to cell surface receptors.^{101,102} Specifically, the amino acid sequence SRL present on capsid or attachment proteins of various viruses associated with BA has been identified as a key player.^{101,103–105} This peptide specifically binds to the cell surface domain of the cholangiocyte heat shock cognate 70 (Hsc70).¹⁰¹ The involvement of SRL-Hsc70 interaction in the pathogenesis of human BA remains poorly understood.⁸⁸ Therefore, studying the effect of the SRL peptide on human liver organoids will be useful to gain understanding in the involvement of viral infections in BA.

Aside from environmental insults, genetic and epigenetic susceptibility factors have also been proposed to be involved in BA pathogenesis.⁷ Single nucleotide polymorphisms (SNPs) in promoter or non-coding regions of several genes involved in the regulation of immune responses and cell polarity have previously been associated with BA.^{106–109} Such SNPs may contribute to the large heterogeneity of

clinical presentation of BA. Since organoids reflect a patient's genome, this model lends itself to investigate the effects of polymorphisms on BA pathogenesis.^{69,110} Aside from genomic aberrancies, DNA methylation has been proposed as a factor involved in BA pathogenesis.^{111,112} These studies suggested that hypomethylation leads to expression of inflammatory genes such as INF-gamma. Whether liver organoids are suitable to study such BA patient-specific epigenetic aberrancies is unclear since epigenetic stability in liver organoids remains elusive.^{69,110} Meanwhile, epigenetic drifts have recently been identified in long-term cultures of intestinal organoids.^{113,114} Potentially, the epigenome of liver organoids is similarly affected by long-term culture which would limit their applicability in studying disease mechanisms dependent on epigenetics. Future studies will be necessary to unravel whether epigenetic drifts occur in liver organoids, and whether these divert the *in vitro* model from the patient and affected disease mechanisms. Putative epigenetic instability could be alleviated by adjustments to culture protocols, such as incorporation of hypoxia during expansion, which has previously helped to increase epigenetic stability in iPSC cultures.^{115,116} Interestingly, despite potential epigenetic drifts, we have identified clear differences between BA and control patient transcriptomes. BA organoids display higher inflammatory signatures than healthy controls under the same conditions. This might suggest that DNA hypomethylation is retained in BA organoids *in vitro*. While it remains important to investigate epigenetic drifts *in vitro*, our data indicate that sufficient differences remain between healthy and diseased organoids to study disease mechanisms and treatments.

Recently two other groups have reported their experiences with BA patient-derived organoids.¹¹⁷⁻¹¹⁹ Interestingly, differences in organoid morphology and polarity were observed between our and these studies. While this might be due to slight differences in study design, well known variations in BA occurrence, pathology and severity around the globe might also be reflected by these differences.¹²⁰⁻¹²⁵ If this were true, liver organoids would represent a more powerful tool to study BA than assumed so far. Naturally, differences due to varying study designs need to be excluded first by investigating the effects of matrix stiffness as discussed in **Chapter 3**. However, if differences in morphology and polarity remain after streamlining culture conditions, a harmonized multi-laboratory study could clarify whether global variation in BA is represented by patient-derived liver organoids. As part of such a study, laboratories and hospitals world-wide involved in BA patient care and research could collectively evaluate relationships between patients' clinical presentations, genomics and epigenetics, infection history, ethnicity, disease progression, and histology with *in vitro* performance of patient-matched organoids at baseline as well as in response to environmental factors. In that way, more pieces of the puzzle that is BA pathogenesis may be connected.

Hollow fiber membrane technology to improve hepatic maturation of ICO-derived cells

In **Chapter 2**, we demonstrated that ICOs express a mixture of hepatobiliary functions and not purely those of a mature hepatocyte. To improve hepatic maturity of ICOs, we devised a novel culture strategy (**Chapter 4**). We showed that ICO-derived cells can be cultured on hollow fibers made of porous polyethersulfone membranes coated with ECM proteins of the hepatic niche. Cells formed confluent monolayers and showed improved expression of key hepatic markers, such as albumin and phase I and II drug metabolizing enzymes, compared to conventional organoid culture. As a first step toward disease modeling using this novel hepatocyte-like hollow fiber membrane (HL-HFM) system, we demonstrated that PFIC3 patient ICO-derived cells can be cultured on HFMs. Moreover, we demonstrated that the functions of transmembrane transporters such as MDR3 affected in PFIC3 can be studied in ICOs in both conventional cultures and HL-HFMs. We believe that the HL-HFM system is a powerful tool to study liver disease including DILI, steatosis, and cholestasis as well as long-term effects of therapeutic strategies for rare pediatric liver diseases, such as PFIC3, in a personalized manner.

While we showed that expression of some hepatocyte-specific genes and functions are improved when culturing ICO-derived cells on HFMs, broader characterization is needed to determine exactly which functions and thus which diseases can be studied using the HL-HFM system. To that end, we are currently expanding functional characterization of drug metabolism in HL-HFMs. Moreover, molecular pathways affected in mentioned diseases of interest, such as lipid metabolism and bile acid metabolism and transport, should be characterized in-depth.

Thorough characterization of hepatic functions in the HL-HFM is also crucial for DILI prediction.²⁸⁻³⁰ The recent shift toward the use of AOPs to define and predict DILI has put emphasis on the development of *in vitro* models suitable for high content analysis.³²⁻³⁵ Since no single *in vitro* model is capable of recapitulating all aspects underlying DILI, the field focuses on developing specialized *in vitro* models to inform about specific DILI aspects.³⁵ As a whole these models are anticipated to aid in the development of safer therapies. We believe that the architecture of the HL-HFM, the option for perfusion culture, the potential for long-term culturing, and use of patient-derived cells makes the system especially useful to study mechanisms leading to cholestatic DILI. To that end, relevant molecular events and pathways putatively involved in cholestatic DILI need to be thoroughly characterized in the HL-HFM. For example, cholestasis modeling in HL-HFMs could be validated by using troglitazone, verapamil or cyclosporin, drugs well known to induce cholestasis through inhibition of the bile salt export pump (BSEP) and MDR3.¹²⁶⁻¹³⁰ Importantly, this would also serve for functional validation of PFIC2 and PFIC3 modeling as BSEP

and MDR3 are affected in these monogenic disorders. Furthermore, as suggested earlier, it would be very valuable to assess the risk of DILI of CFTR potentiators and correctors, such as ivacaftor and tezacaftor, in HL-HFMs. Finally, we anticipate that repeated and long-term drug-exposure can be studied using HL-HFMs. To this end, maintenance of relevant cellular functions needs to be evaluated in long-term culture of the HL-HFM system.

The architecture of the HL-HFM system lends itself well for transepithelial transport studies. In various monogenic liver disorders, such as CF, PFIC2 and PFIC3, transmembrane transporters required for ion homeostasis or the transport of bile acids are affected. Although we have shown that ICOs in conventional culture are suitable to study these functions in a patient specific manner, ICOs cannot be cultured continuously for more than 10 days. Overgrowth in expansion condition, organoid collapse and two-dimensional growth in differentiation conditions makes the conventional culture system unsuitable for long-term studies. Moreover, ICO architecture prevents sampling of products secreted by cells to the apical domain. This complicates mechanistic and pharmacokinetic studies for which the exact contents of the apical cell domain are of interest. The HL-HFM system satisfies these needs since it offers easy access to both cell domains and long-term culture. Currently, a bioreactor is being tested for culturing the HL-HFM system. The design of this bioreactor allows perfusion and separate access to each cell domain.

Other designs aiming to incorporate aspects of the microanatomy of the hepatic niche include other larger scale HFM bioreactors and microfluidic liver-on-a-chip systems. Like our HL-HFM bioreactor, these systems are designed to include media perfusion, which has been suggested to provide oxygen levels and gradients similar to what hepatocytes encounter *in vivo*.¹³¹⁻¹³³ Hepatocytes have a high demand for oxygen to maintain their metabolic functions and different oxygen concentrations *in vitro* have been shown to promote or inhibit hepatocyte maturation.¹³¹⁻¹³³ However, microfluidic liver-on-a-chip systems offer limited oxygen availability and control compared to conventional culture vessels, due to low ratios of surface-to-volume and thus cells-to-medium.^{134,135} Our larger scale HL-HFM system is unlikely to encounter this limitation.

Aside from oxygen provision, separate access to the apical and basolateral cell domain is crucial for mechanistic disease and pharmacokinetic studies. While previous HFM bioreactor systems offer media perfusion and access to the basolateral compartment, the apical domain is inaccessible.¹³⁶⁻¹³⁹ Likewise, apical cell domains of cells cultured in microfluidic liver-on-a-chip systems regularly connect to bile canaliculi, but the design does not allow separate access.^{140,141} To our knowledge, only one system design incorporated the separation of the apical and basolateral domains.¹⁴² Similar to a transwell system, HepaRG were cultured

on a flat porous membrane which divided the culture chamber into an upper and lower channel. These were fed by medium reservoirs at either end through gravity-induced flow using a rocker. Interestingly, this study reported that inclusion of the apical compartment and introduction of perfusion on both sides of the hepatocytes promoted hepatic maturation. This finding further underlines the importance of incorporating both sinusoidal (basolateral) and bile (apical) compartments when mimicking hepatic microarchitecture. Currently, we are optimizing said bi-directional perfusion in our HL-HFM system. Compared to the transwell-like HepaRG system, the HL-HFM system not only allows for more control in terms of perfusion speed, but can also be multiplexed with other organ mimics to study multi-organ effects of a disease or drug of interest.

Modeling BA with the HFM system

The architecture of the HFM system could be suitable to study BA. Early mechanisms of BA pathogenesis are thought to involve breach of the epithelial layer that constitutes the bile duct. Therefore, permeability studies using the HFM perfusion bioreactor could be useful to study putatively involved toxins or viruses and underlying mechanisms. Importantly, access to both the apical and basolateral cell domains in the HL-HFM system allows to study domain specific virus or toxin interactions. Currently, it remains unclear whether viral entry in BA occurs at the apical or basolateral domain of cholangiocytes. The previously suggested Hsc70 involved in viral entry is expressed on the apical domain of cholangiocytes, while other surface proteins thought to be involved in viral entry are expressed on the basolateral domain.^{101,143,144} The apico-basal separation in the HL-HFM system could aid in determining viral entry points. Similarly, first insights on biliatresone domain specificity have recently been provided by a study utilizing a bile duct-on-a-chip device with similar apico-basal separation.¹⁴⁵ The study indicated that biliatresone causes more severe barrier breach in mouse cholangiocytes when administered from the basolateral domain. Similarly, to conventional organoid culture this system made use of a collagen hydrogel, which is molded to leave an empty channel for cell culture. As such, the cellular apical domain faces inward as is the case *in vivo*. This might be advantageous since bile concentration, curvature and ECM stiffness might mimic the *in vivo* situation more closely than is the case in the HL-HFM. However, the architecture of this bile duct-on-a-chip system also complicates harvesting of basolaterally secreted components, such as bile acids and glucose.^{146,147} Here, the HL-HFM system is more suited since the basolateral compartment can be easily accessed by collecting effluent from this compartment of the bioreactor.

Strategies to further improve hepatic maturation of ICOs

Extracellular matrix

We have demonstrated that human recombinant laminins are a suitable replacement for Matrigel™ in the HL-HFM system. Looking at the liver microenvironment it becomes apparent that the use of single laminin isoforms does not recapitulate the complete liver ECM. Potentially, combinations of different laminin isoforms could further improve hepatic maturation of ICOs. Importantly, several laminins are responsible for guiding hepatoblast development rather than hepatic maturation.^{148,149} Thus, other ECM components, such as perlecan, vitronectin, collagens, and fibronectin will be important to explore. However, as we already found with fibronectin, ECMs promoting differentiation also halt proliferation. Thus, to promote initial proliferation and yield confluent monolayers, combinations of fibronectin with proliferation promoting ECMs, such as LN111, might be a good avenue to explore. Indeed, previous work has shown that combinations of ECM components such as different isoforms of laminins, fibronectin, and different collagens affect hepatic maturation of iPSCs and bipotential mouse embryonic liver progenitor cells.^{150,151} Potentially, replacing Matrigel™ with human recombinant ECM components in conventional organoid culture could also improve hepatic maturation of ICOs and make the system more compliant with the 3R's principle. Previously, the combination of a synthetic hydrogel based on polyisocyanopeptides and human recombinant LN111 was shown to be an excellent substitute for Matrigel™.¹⁵² While LN111 promoted hepatic maturity to similar degrees as Matrigel™, combinations of different ECM components which are known to promote hepatic maturation could potentially improve hepatic maturation of ICOs further. Alternatively, key integrin-binding motifs of relevant ECMs could be chemically linked to the synthetic hydrogel as has previously been done with generic cell adhesion motifs.^{153,154} As such a hydrogel specific for hepatic differentiation could be synthesized.

Media composition

Aside from the microarchitecture and ECM composition, soluble factors play a crucial role in steering hepatic maturation *in vivo*. Hence, delicate orchestration of media composition is a vital aspect in improving hepatic maturation *in vitro*. Being derived from bipotent cholangiocyte progenitors, ICOs should be able to mature into functional hepatocytes. Yet, our data reveal that current culture conditions do not suffice to push the cells toward fully mature hepatocytes. Interestingly, it has recently been demonstrated that the differentiation medium supposedly promoting hepatocyte differentiation in ICOs also elicits cholangiocyte differentiation in human embryonic stem cells and iPSCs.^{38,155} This underlines the need to optimize the 'hepatocyte' differentiation medium used in ICO culture. A recent comparison of current hepatocyte models provides an excellent overview of the different differentiation media in combination with an overview of how well each model

mimics the transcriptional profile of hepatocytes.³⁸ This overview is a useful tool to guide improvements of media formulations. Importantly, cell origin was found to strongly affect differentiation potential and may dictate what cues a cell requires for hepatic maturation. For example, while iPSCs may require mimicry of organogenesis, ICOs may require signals appearing after liver damage. These aspects ought to be taken along when designing new differentiation media.

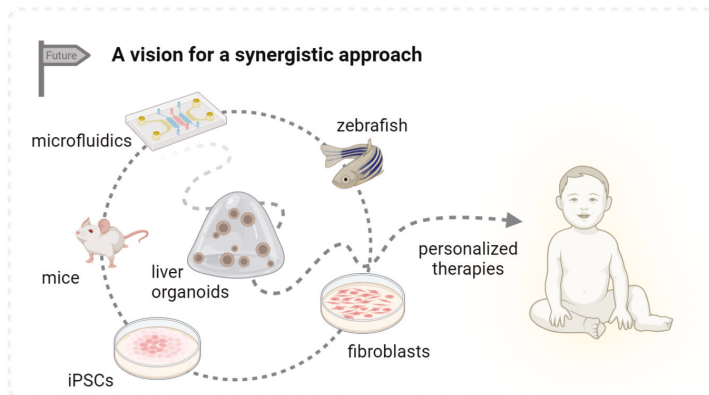
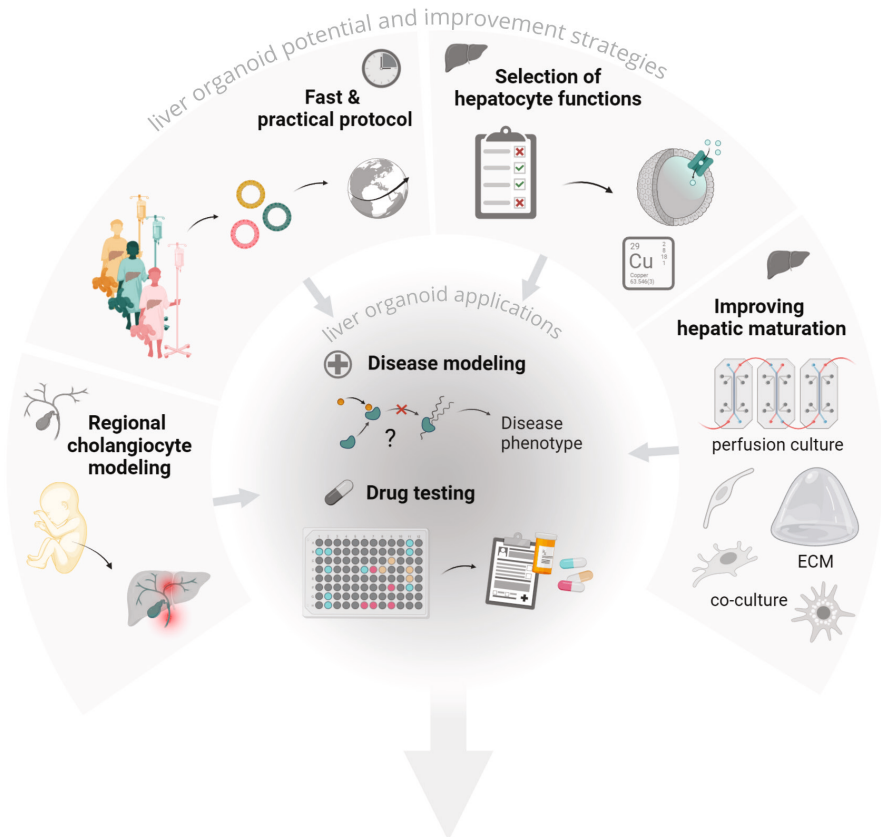
Co-cultures

To fully reconstruct the hepatic niche in health and disease, a variety of other cell types, including Kupffer cells, hepatic stellate cells, sinusoidal endothelial cells, cholangiocytes, and natural killer cells ought to be included in the model. *In vivo*, these cells help to regulate ECM composition, secrete growth factors, and partake in inflammation and tissue repair. Therefore, inclusion of the various cell types of the hepatic niche will likely improve hepatic differentiation of ICOs. Indeed, previous studies have made use of micropatterned co-cultures where islands of hepatocytes are surrounded by non-parenchymal cells.¹⁵⁶⁻¹⁵⁸ Long-term viability and function made these systems useful to study hepatic function for up to six weeks.¹⁵⁸ Liver-on-a-chip approaches have also utilized co-cultures with various cell types including endothelial and Kupffer cells.^{159,160} The studies reported improved hepatic maturation, by demonstrating increases in key hepatic functions such as drug metabolism, bile transport and albumin and urea secretion. Others have demonstrated improvement of hepatic maturity of iPSC-HLCs when co-cultured with endothelial and mesenchymal cells.^{161,162} Similar approaches using ICOs are currently being assessed in our laboratory. We expect that hepatic maturity of the model will be suitable to study a broader array of hepatic functions and diseases. On the other hand, co-cultures complicate the culturing systems through adaptations to the culture media and matrices to sustain different cell types. Moreover, while better modeling the physiologic organ, co-cultures lose the simplicity of studying a cell-specific reaction in isolation.

Figure 1. The potential and limitations of liver organoids and outlook for their use in modeling rare pediatric liver disorders. Liver organoids can be easily established and shared with researchers around the world. Furthermore, liver organoids are suitable to model a selection of hepatocyte functions, including copper metabolism and transepithelial transport functions. The availability of liver organoids of varying hepatobiliary origin allows for the regional modeling of cholangiocytes and associated cholangiopathies, such as biliary atresia. Through the use of perfusion technologies, co-cultures, and matrix (ECM) engineering the hepatic niche can be mimicked more closely *in vitro* resulting in improved hepatic maturity of liver organoids. Our findings and suggestions for future research suggest that liver organoids are a strong tool to study disease mechanisms and test drugs in a personalized manner. We envision that patient-derived liver organoids will synergize with other models, such as microfluidics platforms, animal models, patient-derived induced pluripotent stem cells (iPSCs) and fibroblasts, to one day relieve patient suffering through the development of personalized therapies. →

Hepatic zonation

Another interesting aspect to be mimicked *in vitro* is hepatic zonation. Depending on their location within the liver lobule, hepatocytes specialize in certain functions. This is steered by gradients of the various cues which hepatocytes encounter. For example, oxygen concentration is highest close to the portal vein and decreases



toward the central vein. ECM components also change throughout the zones, with laminins mostly present periportally, while fibronectin is found mostly pericentrally.¹⁶³ Likewise growth factors steering hepatic fate differ across the zones. Currently, most efforts in generating mature hepatocytes *in vitro* do not introduce a zonation pattern or aim to develop a specific zonal hepatocyte phenotype. Instead, most research focusses on the generic hepatocyte markers albumin, phase I drug metabolism and urea secretion, which represent a mixture of functions from various hepatic zones. More directed mimicry of hepatic zonation could yield improvement of specific functions of interest. In isolation, varying oxygen concentrations have been used to provoke expression of hepatic functions specific to the respective hepatic zone.^{132,164} Similarly, ECM gradients were shown to promote zonation-specific phenotypes.¹⁶⁵ If the full array of hepatic functions is to be studied, all zones could be mimicked *in vitro* by including the full gradients of ECM, oxygen, and growth factors in one system. As has been shown before, perfusion cultures are especially suitable to generate oxygen gradients.^{132,164} Similarly, hormone, nutrient and growth factor gradients are expected to arise under gentle perfusion. Hence, the HL-HFM system would be suitable to test the mimicry of these gradients since the bioreactor allows to control media perfusion. While ECM gradients have previously only been achieved on flat surfaces using chemical and irradiation strategies, the perfused HFM system might offer a simpler solution.¹⁶⁶⁻¹⁶⁸ ECM components used to mimic the hepatic niche *in vitro* are sensitive to washing steps. Therefore, ECM gradients could be generated on HFMs by sequential coating and washing steps of varying ECM components in the perfusion bioreactor.

Conclusion

In this thesis we have demonstrated that patient-derived liver organoids are a useful tool to study various rare liver and metabolic disorders affecting the hepatobiliary tract. Several diseases such as BA, CF, PFIC3, Wilson disease and MMA can currently be studied with ICOs. Although liver organoids were previously praised as a new break-through hepatocyte model, we have shown that organoids from all hepatobiliary regions are at least equally useful for researching cholangiopathies.

I believe that liver organoids can be a truly powerful tool to aid in unravelling the disease mechanisms underlying BA. The development of new technologies, such as organ chips and co-culture strategies, are exciting not only to study the disease mechanisms of rare diseases but also to improve the hepatic maturity of ICOs. Applying the myriad of culture improvement strategies to ICOs will likely produce a fantastic patient-derived hepatocyte model. We have taken the first steps toward improving hepatic maturation of ICOs and in doing so have demonstrated that the ICO application range can be broadened to facilitate the study of (cholestatic) disease

mechanisms. Similarly, we anticipate that these improvements in hepatic maturation of ICOs will aid in the development of safe therapeutics for (rare) liver diseases in a personalized manner in the future. With the exciting new avenues ahead of us, I hope that patient-derived liver organoids will one day aid in relieving patient suffering as Heracles came to rescue Prometheus from the nightly mutilation of his liver.

"Heracles [raised] his bow and [shot] down Zeus's avenging eagle as it soared out of the sun towards them. (...) 'Thank you, Heracles,' said the Titan. (...) 'You are ridding the world of its foulest beasts, its dragons, serpents and many-headed monsters (...) for the world to be made safe for humankind to flourish.'"

From Heroes - The myths of the Ancient Greek heroes retold, by Stephen Fry¹⁶⁹

Authorship statement

I conceptualized and set-up the general discussion; I conducted the literature search and wrote the general discussion. I revised the text once, after comments of my supervisors. The general discussion represents my opinion and view which may differ from that of my supervisors.

References

1. Paranjape SM, Mogayzel PJ. Cystic fibrosis in the era of precision medicine. *Paediatr Respir Rev.* 2018;25:64-72. doi:10.1016/J.PRRV.2017.03.001
2. Elborn JS. Cystic fibrosis. *The Lancet.* 2016;388(10059):2519-2531. doi:10.1016/S0140-6736(16)00576-6
3. Escribá R, Ferrer-Lorente R, Raya Á. Inborn errors of metabolism: Lessons from iPSC models. *Rev Endocr Metab Disord.* 2021;22(4):1189-1200. doi:10.1007/S11154-021-09671-Z
4. Forny P, Hochuli M, Rahman Y, et al. Liver neoplasms in methylmalonic aciduria: An emerging complication. *J Inherit Metab Dis.* 2019;42(5):793-802. doi:10.1002/JIMD.12143
5. Palma E, Doornebal EJ, Chokshi S. Precision-cut liver slices: a versatile tool to advance liver research. *Hepatol Int.* 2019;13(1):51-57. doi:10.1007/S12072-018-9913-7/FIGURES/5
6. Stockler-Ipsiroglu S, Potter BK, Yuskiv N, Tingley K, Patterson M, van Karnebeek C. Developments in evidence creation for treatments of inborn errors of metabolism. *J Inherit Metab Dis.* 2021;44(1):88. doi:10.1002/JIMD.12315
7. Asai A, Miethke A, Bezerra JA. Pathogenesis of biliary atresia: Defining biology to understand clinical phenotypes. *Nat Rev Gastroenterol Hepatol.* 2015;12(6):342-352. doi:10.1038/nrgastro.2015.74
8. Kok G, Tseng L, Schene IF, et al. Treatment of ARS-deficiencies with specific amino acids. *Genetics in Medicine.* 2021;23(11):2202-2207. doi:10.1038/s41436-021-01249-z
9. Sachs N, Papaspyropoulos A, Ommen DDZ, et al. Long-term expanding human airway organoids for disease modeling. *EMBO J.* 2019;38(4):e100300. doi:10.15252/EMBJ.2018100300
10. Ramalho AS, Förstová E, Vonk AM, et al. Correction of CFTR function in intestinal organoids to guide treatment of cystic fibrosis. *Eur Respir J.* 2021;57(1):1902426. doi:10.1183/13993003.02426-2019
11. de Poel E, Lefferts JW, Beekman JM. Intestinal organoids for Cystic Fibrosis research. *Journal of Cystic Fibrosis.* 2020;19:S60-S64. doi:10.1016/J.JCF.2019.11.002
12. Dekkers JF, Berkers G, Kruisselbrink E, et al. Characterizing responses to CFTR-modulating drugs using rectal organoids derived from subjects with cystic fibrosis. *Sci Transl Med.* 2016;8(344):344ra84. doi:10.1126/scitranslmed.aad8278
13. Amatngalim GD, Rodenburg LW, Aalbers BL, et al. Measuring cystic fibrosis drug responses in organoids derived from 2D differentiated nasal epithelia. *Life Sci Alliance.* 2022;5(12):e202101320. doi:10.26508/lsa.202101320
14. Dekkers JF, Wiegerinck CL, De Jonge HR, et al. A functional CFTR assay using primary cystic fibrosis intestinal organoids. *Nat Med.* 2013;19(7):939-945. doi:10.1038/nm.3201

15. Betapudi B, Aleem A, Kothadia JP. *Cystic Fibrosis And Liver Disease*. StatPearls Publishing; 2023. Accessed May 30, 2023. <https://www.ncbi.nlm.nih.gov/books/NBK556086/>
16. Keogh RH, Szczesniak R, Taylor-Robinson D, Bilton D. Up-to-date and projected estimates of survival for people with cystic fibrosis using baseline characteristics: A longitudinal study using UK patient registry data. *J Cyst Fibros*. 2018;17(2):218-227. doi:10.1016/J.JCF.2017.11.019
17. Athanazio RA, da Silva Filho LVRF, Vergara AA, et al. Brazilian guidelines for the diagnosis and treatment of cystic fibrosis. *J Bras Pneumol*. 2017;43(3):219-245. doi:10.1590/S1806-37562017000000065
18. Fiorotto R, Strazzabosco M. Pathophysiology of Cystic Fibrosis Liver Disease: A Channelopathy Leading to Alterations in Innate Immunity and in Microbiota. *Cell Mol Gastroenterol Hepatol*. 2019;8(2):197-207. doi:10.1016/J.JCMGH.2019.04.013
19. Witters P, Libbrecht L, Roskams T, et al. Liver disease in cystic fibrosis presents as non-cirrhotic portal hypertension. *J Cyst Fibros*. 2017;16(5):e11-e13. doi:10.1016/J.JCF.2017.03.006
20. Leeuwen L, Fitzgerald DA, Gaskin KJ. Liver Disease in Cystic Fibrosis. *Paediatr Respir Rev*. 2014;15(1):69-74. doi:10.1016/J.PRRV.2013.05.001
21. Lewindon PJ, Shepherd RW, Walsh MJ, et al. Importance of hepatic fibrosis in cystic fibrosis and the predictive value of liver biopsy. *Hepatology*. 2011;53(1):193-201. doi:10.1002/HEP.24014
22. Barry PJ, Plant BJ, Nair A, et al. Effects of ivacaftor in patients with cystic fibrosis who carry the G551D mutation and have severe lung disease. *Chest*. 2014;146(1):152-158. doi:10.1378/CHEST.13-2397
23. Wark PAB, Cookson K, Thiruchelvam T, Brannan J, Dorahy DJ. Lumacaftor/ Ivacaftor improves exercise tolerance in patients with Cystic Fibrosis and severe airflow obstruction. *BMC Pulm Med*. 2019;19(1):106. doi:10.1186/S12890-019-0866-Y
24. Haq I, Almulhem M, Soars S, Poulton D, Brodrie M. Precision Medicine Based on CFTR Genotype for People with Cystic Fibrosis. *Pharmgenomics Pers Med*. 2022;15:91-104. doi:10.2147/PGPM.S245603
25. Van Der Meer R, Touw DJ, Heijerman HGM. Prevention of drug-related complications in cystic fibrosis. *Curr Opin Pulm Med*. 2019;25(6):666-673. doi:10.1097/MCP.0000000000000625
26. Lowry S, Mogayzel PJ, Oshima K, Karnsakul W. Drug-induced liver injury from elexacaftor/ ivacaftor/tezacaftor. *Journal of Cystic Fibrosis*. 2022;21(2):e99-e101. doi:10.1016/j.jcf.2021.07.001
27. Francis P, Navarro VJ. Drug Induced Hepatotoxicity. *StatPearls*. Published online November 11, 2022. Accessed March 3, 2023. <https://www.ncbi.nlm.nih.gov/books/NBK557535/>
28. Ostapowicz G, Fontana RJ, Schioødt FV., et al. Results of a prospective study of acute liver failure at 17 tertiary care centers in the United States. *Ann Intern Med*. 2002;137(12):947-954. doi:10.7326/0003-4819-137-12-200212170-00007
29. Mosedale M, Watkins PB. Drug-Induced Liver Injury: Advances in Mechanistic Understanding that will Inform Risk Management. *Clin Pharmacol Ther*. 2017;101(4):469. doi:10.1002/CPT.564
30. Fu S, Wu D, Jiang W, et al. Molecular biomarkers in drug-induced liver injury: Challenges and future perspectives. *Front Pharmacol*. 2020;10:1667. doi:10.3389/fphar.2019.01667

31. Dragovic S, Vermeulen NPE, Gerets HH, et al. Evidence-based selection of training compounds for use in the mechanism-based integrated prediction of drug-induced liver injury in man. *Arch Toxicol*. 2016;90(12):2979. doi:10.1007/S00204-016-1845-1
32. Vinken M. Adverse outcome pathways and drug-induced liver injury testing. *Chem Res Toxicol*. 2015;28(7):1391. doi:10.1021/ACS.CHEMRESTOX.5B00208
33. Vinken M. Adverse outcome pathways as tools to assess drug-induced toxicity. *Methods Mol Biol*. 2016;1425:325-337. doi:10.1007/978-1-4939-3609-0_14
34. Leist M, Ghallab A, Graepel R, et al. Adverse outcome pathways: opportunities, limitations and open questions. *Arch Toxicol*. 2017;91(11):3477-3505. doi:10.1007/s00204-017-2045-3
35. Weaver RJ, Blomme EA, Chadwick AE, et al. Managing the challenge of drug-induced liver injury: a roadmap for the development and deployment of preclinical predictive models. *Nat Rev Drug Discov*. 2020;19(2):131-148. doi:10.1038/s41573-019-0048-x
36. Ye H, Nelson LJ, Del Moral MG, Martínez-Naves E, Cubero FJ. Dissecting the molecular pathophysiology of drug-induced liver injury. *World J Gastroenterol*. 2018;24(13):1373. doi:10.3748/WJG.V24.I13.1373
37. Fernandez-Checa JC, Bagnaninchi P, Ye H, et al. Advanced preclinical models for evaluation of drug-induced liver injury – consensus statement by the European Drug-Induced Liver Injury Network [PRO-EURO-DILI-NET]. *J Hepatol*. 2021;75(4):935-959. doi:10.1016/j.jhep.2021.06.021
38. Ardisasmita AI, Schene IF, Joore IP, et al. A comprehensive transcriptomic comparison of hepatocyte model systems improves selection of models for experimental use. *Commun Biol*. 2022;5(1):1094. doi:10.1038/s42003-022-04046-9
39. Bouwmeester MC, Tao Y, Proença S, et al. Drug Metabolism of Hepatocyte-like Organoids and Their Applicability in In Vitro Toxicity Testing. *Molecules*. 2023;28(2):621. doi:10.3390/MOLECULES28020621
40. Vivet therapeutics. VTX-801 - Wilson disease therapeutics. Accessed May 29, 2023. <https://www.vivet-therapeutics.com/pipeline/wilsons-disease-at-a-glance/>
41. Murillo O, Collantes M, Gazquez C, et al. High value of 64Cu as a tool to evaluate the restoration of physiological copper excretion after gene therapy in Wilson's disease. *Mol Ther Methods Clin Dev*. 2022;26:98-106. doi:10.1016/j.omtm.2022.06.001
42. Murillo O, Luqui DM, Gazquez C, et al. Long-term metabolic correction of Wilson's disease in a murine model by gene therapy. *J Hepatol*. 2016;64(2):419-426. doi:10.1016/j.jhep.2015.09.014
43. A Phase I/II Study of VTX-801 in Adult Patients With Wilson's Disease - Full Text View - ClinicalTrials.gov. Accessed April 27, 2023. <https://clinicaltrials.gov/ct2/show/NCT04537377?cond=wilson+disease&draw=2>
44. Schene IF, Joore IP, Oka R, et al. Prime editing for functional repair in patient-derived disease models. *Nat Commun*. 2020;11(1):1-8. doi:10.1038/s41467-020-19136-7
45. Artegiani B, Hendriks D, Beumer J, et al. Fast and efficient generation of knock-in human organoids using homology-independent CRISPR-Cas9 precision genome editing. *Nat Cell Biol*. 2020;22(3):321-331. doi:10.1038/s41556-020-0472-5
46. Artegiani B, van Voorthuijsen L, Lindeboom RGH, et al. Probing the Tumor Suppressor Function of BAP1 in CRISPR-Engineered Human Liver Organoids. *Cell Stem Cell*. 2019;24(6):927-943.e6. doi:10.1016/j.stem.2019.04.017

47. Hendriks D, Brouwers JF, Hamer K, et al. Engineered human hepatocyte organoids enable CRISPR-based target discovery and drug screening for steatosis. *Nature Biotechnology* 2023. Published online February 23, 2023;1-15. doi:10.1038/s41587-023-01680-4
48. Hikmat O, Naess K, Engvall M, et al. Simplifying the clinical classification of polymerase gamma (POLG) disease based on age of onset; studies using a cohort of 155 cases. *J Inherit Metab Dis*. 2020;43(4):726-736. doi:10.1002/JIMD.12211
49. Rahman S, Copeland WC. POLG-related disorders and their neurological manifestations. *Nat Rev Neurol*. 2019;15(1):40. doi:10.1038/S41582-018-0101-0
50. Hu H, Gehart H, Artegiani B, et al. Long-Term Expansion of Functional Mouse and Human Hepatocytes as 3D Organoids. *Cell*. 2018;175(6):1591-1606.e19. doi:10.1016/j.cell.2018.11.013
51. Hendriks D, Artegiani B, Hu H, Chuva de Sousa Lopes S, Clevers H. Establishment of human fetal hepatocyte organoids and CRISPR-Cas9-based gene knockin and knockout in organoid cultures from human liver. *Nat Protoc*. 2021;16(1):182-217. doi:10.1038/S41596-020-00411-2
52. Peng WC, Kraaier LJ, Kluiver TA. Hepatocyte organoids and cell transplantation: What the future holds. *Exp Mol Med*. 2021;53(10):1512-1528. doi:10.1038/S12276-021-00579-X
53. Fu GB, Huang WJ, Zeng M, et al. Expansion and differentiation of human hepatocyte-derived liver progenitor-like cells and their use for the study of hepatotropic pathogens. *Cell Res*. 2018;29(1):8-22. doi:10.1038/S41422-018-0103-X
54. Tang W, Guo R, Shen S jun, et al. Chemical cocktails enable hepatic reprogramming of human urine-derived cells with a single transcription factor. *Acta Pharmacol Sin*. 2018;40(5):620-629. doi:10.1038/S41401-018-0170-Z
55. Ballester M, Bolonio M, Santamaria R, Castell J V., Ribes-Koninckx C, Bort R. Direct conversion of human fibroblast to hepatocytes using a single inducible polycistronic vector. *Stem Cell Res Ther*. 2019;10(1):1-10. doi:10.1186/s13287-019-1416-5
56. Xie B, Sun D, Du Y, et al. A two-step lineage reprogramming strategy to generate functionally competent human hepatocytes from fibroblasts. *Cell Res*. 2019;29(9):696-710. doi:10.1038/S41422-019-0196-X
57. Akbari S, Sevinç GG, Ersoy N, et al. Robust, Long-Term Culture of Endoderm-Derived Hepatic Organoids for Disease Modeling. *Stem Cell Reports*. 2019;13(4):627-641. doi:10.1016/J.STEMCR.2019.08.007
58. Jing R, Corbett JL, Cai J, et al. A Screen Using iPSC-Derived Hepatocytes Reveals NAD+ as a Potential Treatment for mtDNA Depletion Syndrome. *Cell Rep*. 2018;25(6):1469-1484. e5. doi:10.1016/j.celrep.2018.10.036
59. Cayo MA, Mallanna SK, Di Furio F, et al. A Drug Screen using Human iPSC-Derived Hepatocyte-like Cells Reveals Cardiac Glycosides as a Potential Treatment for Hypercholesterolemia. *Cell Stem Cell*. 2017;20(4):478-489.e5. doi:10.1016/j.stem.2017.01.011
60. Chen C, Soto-Gutierrez A, Baptista PM, Spee B. Biotechnology Challenges to In Vitro Maturation of Hepatic Stem Cells. *Gastroenterology*. 2018;154(5):1258-1272. doi:10.1053/j.gastro.2018.01.066
61. Doss MX, Sachinidis A. Current Challenges of iPSC-Based Disease Modeling and Therapeutic Implications. *Cells*. 2019;8(5):403. doi:10.3390/CELLS8050403

62. Mandai M, Watanabe A, Kurimoto Y, et al. Autologous Induced Stem-Cell-Derived Retinal Cells for Macular Degeneration. *New England Journal of Medicine*. 2017;376(11):1038-1046. doi:10.1056/NEJMc1706274
63. Choi J, Lee S, Mallard W, et al. A comparison of genetically matched cell lines reveals the equivalence of human iPSCs and ESCs. *Nat Biotechnol*. 2015;33(11):1173-1181. doi:10.1038/NBT.3388
64. Yamanaka S. Pluripotent Stem Cell-Based Cell Therapy—Promise and Challenges. *Cell Stem Cell*. 2020;27(4):523-531. doi:10.1016/j.stem.2020.09.014
65. Koyanagi-Aoi M, Ohnuki M, Takahashi K, et al. Differentiation-defective phenotypes revealed by large-scale analyses of human pluripotent stem cells. *Proc Natl Acad Sci U S A*. 2013;110(51):20569-20574. doi:10.1073/pnas.1319061110
66. Nishizawa M, Chonabayashi K, Nomura M, et al. Epigenetic Variation between Human Induced Pluripotent Stem Cell Lines Is an Indicator of Differentiation Capacity. *Cell Stem Cell*. 2016;19(3):341-354. doi:10.1016/j.stem.2016.06.019
67. Santoni FA, Guerra J, Luban J. HERV-H RNA is abundant in human embryonic stem cells and a precise marker for pluripotency. *Retrovirology*. 2012;9(1):1-15. doi:10.1186/1742-4690-9-111
68. Macfarlan TS, Gifford WD, Driscoll S, et al. Embryonic stem cell potency fluctuates with endogenous retrovirus activity. *Nature*. 2012;487(7405):57-63. doi:10.1038/NATURE11244
69. Prior N, Inacio P, Huch M. Liver organoids: From basic research to therapeutic applications. *Gut*. 2019;68(12):2228-2237. doi:10.1136/gutjnl-2019-319256
70. Lee J, Mun SJ, Shin Y, Lee S, Son MJ. Advances in liver organoids: model systems for liver disease. *Arch Pharm Res*. 2022;45(6):390-400. doi:10.1007/s12272-022-01390-6
71. Gu W, Gaeta X, Sahakyan A, et al. Glycolytic Metabolism Plays a Functional Role in Regulating Human Pluripotent Stem Cell State. *Cell Stem Cell*. 2016;19(4):476-490. doi:10.1016/j.stem.2016.08.008
72. Haridhasapavalan KK, Raina K, Dey C, Adhikari P, Thummer RP. An Insight into Reprogramming Barriers to iPSC Generation. *Stem Cell Rev Rep*. 2020;16(1):56-81. doi:10.1007/s12015-019-09931-1
73. Zhang J, Wilson GF, Soerens AG, et al. Functional Cardiomyocytes Derived From Human Induced Pluripotent Stem Cells. *Circ Res*. 2009;104(4):e30-e41. doi:10.1161/CIRCRESAHA.108.192237
74. Rashidi H, Luu NT, Alwahsh SM, et al. 3D human liver tissue from pluripotent stem cells displays stable phenotype in vitro and supports compromised liver function in vivo. *Arch Toxicol*. 2018;92(10):3117. doi:10.1007/S00204-018-2280-2
75. Castro-Viñuelas R, Sanjurjo-Rodríguez C, Piñeiro-Ramil M, et al. Tips and tricks for successfully culturing and adapting human induced pluripotent stem cells. *Mol Ther Methods Clin Dev*. 2021;23:569-581. doi:10.1016/j.omtm.2021.10.013
76. Chen YF, Tseng CY, Wang HW, Kuo HC, Yang VW, Lee OK. Rapid Generation of Mature Hepatocyte-Like Cells from Human Induced Pluripotent Stem Cells by an Efficient Three-Step Protocol. *Hepatology*. 2012;55(4):1193. doi:10.1002/HEP.24790
77. Lendahl U, Lui VCH, Chung PHY, Tam PKH. Biliary Atresia – emerging diagnostic and therapy opportunities. *EBioMedicine*. 2021;74:103689. doi:10.1016/J.EBIOM.2021.103689

78. Roos FJM, Verstegen MMA, Muñoz Albarinos L, et al. Human Bile Contains Cholangiocyte Organoid-Initiating Cells Which Expand as Functional Cholangiocytes in Non-canonical Wnt Stimulating Conditions. *Front Cell Dev Biol.* 2021;8:630492. doi:10.3389/fcell.2020.630492
79. Rimland CA, Tilson SG, Morell CM, et al. Regional Differences in Human Biliary Tissues and Corresponding In Vitro-Derived Organoids. *Hepatology.* 2021;73(1):247-267. doi:10.1002/HEP.31252
80. Smith M, Zuckerman M, Kandaneeratchi A, Thompson R, Davenport M. Using next-generation sequencing of microRNAs to identify host and/or pathogen nucleic acid signatures in samples from children with biliary atresia – a pilot study. *Access Microbiol.* 2020;2(7):acmi000127. doi:10.1099/ACMI.0.000127
81. Mikami T, Saegusa M, Mitomi H, Yanagisawa N, Ichinoe M, Okayasu I. Significant correlations of E-cadherin, catenin, and CD44 variant form expression with carcinoma cell differentiation and prognosis of extrahepatic bile duct carcinomas. *Am J Clin Pathol.* 2001;116(3):369-376. doi:10.1309/VV6D-3GAH-VEJM-DUJT
82. Cruickshank SM, Southgate J, Wyatt JJ, Selby PJ, Trejdosiewicz LK. Expression of CD44 on bile ducts in primary sclerosing cholangitis and primary biliary cirrhosis. *J Clin Pathol.* 1999;52(10):730-734. doi:10.1136/JCP.52.10.730
83. Min J, Ningappa M, So J, Shin D, Sindhi R, Subramaniam S. Systems Analysis of Biliary Atresia Through Integration of High-Throughput Biological Data. *Front Physiol.* 2020;11:966. doi:10.3389/fphys.2020.00966
84. Whitby T, Schroeder D, Kim HS, et al. Modifications in Integrin Expression and Extracellular Matrix Composition in Children with Biliary Atresia. *Klin Padiatr.* 2015;227(1):15-22. doi:10.1055/s-0034-1389906
85. Hartley JL, Davenport M, Kelly DA. Biliary atresia. *The Lancet.* 2009;374(9702):1704-1713. doi:10.1016/S0140-6736(09)60946-6
86. Lorent K, Gong W, Koo KA, et al. Identification of a plant isoflavonoid that causes biliary atresia. *Sci Transl Med.* 2015;7(286). doi:10.1126/SCITRANSLMED.AAA1652
87. Harper P, Plant JW, Unger DB. Congenital biliary atresia and jaundice in lambs and calves. *Aust Vet J.* 1990;67(1):18-22. doi:10.1111/J.1751-0813.1990.TB07385.X
88. Ortiz-Perez A, Donnelly B, Temple H, Tiao G, Bansal R, Mohanty SK. Innate Immunity and Pathogenesis of Biliary Atresia. *Front Immunol.* 2020;11:329. doi:10.3389/FIMMU.2020.00329/BIBTEX
89. Syal G, Fausther M, Dranoff JA. Advances in cholangiocyte immunobiology. *Am J Physiol Gastrointest Liver Physiol.* 2012;303(10):G1077. doi:10.1152/AJPGI.00227.2012
90. Mestas J, Hughes CCW. Of Mice and Not Men: Differences between Mouse and Human Immunology. *The Journal of Immunology.* 2004;172(5):2731-2738. doi:10.4049/JIMMUNOL.172.5.2731
91. Akil A, Endsley M, Shanmugam S, et al. Fibrogenic Gene Expression in Hepatic Stellate Cells Induced by HCV and HIV Replication in a Three Cell Co-Culture Model System. *Sci Rep.* 2019;9(1):1-12. doi:10.1038/S41598-018-37071-Y
92. Han B, Mo H, Svarovskaia E, Mateo R. A primary human hepatocyte/hepatic stellate cell co-culture system for improved in vitro HBV replication. *Virology.* 2021;559:40-45. doi:10.1016/J.VIROL.2021.03.012

93. Lee HJ, Mun SJ, Jung CR, et al. In vitro modeling of liver fibrosis with 3D co-culture system using a novel human hepatic stellate cell line. *Biotechnol Bioeng*. 2023;120(5):1241-1253. doi:10.1002/BIT.28333
94. Jiang GX, Zhong XY, Cui YF, et al. IL-6/STAT3/TFF3 signaling regulates human biliary epithelial cell migration and wound healing in vitro. *Mol Biol Rep*. 2010;37(8):3813-3818. doi:10.1007/s11033-010-0036-z
95. Kamihira T, Shimoda S, Nakamura M, et al. Biliary epithelial cells regulate autoreactive T cells: Implications for biliary-specific diseases. *Hepatology*. 2005;41(1):151-159. doi:10.1002/HEP.20494
96. Cruickshank SM, Southgate J, Selby PJ, Trejdosiewicz LK. Expression and cytokine regulation of immune recognition elements by normal human biliary epithelial and established liver cell lines in vitro. *J Hepatol*. 1998;29(4):550-558. doi:10.1016/S0168-8278(98)80149-9
97. Leon MP, Bassendine MF, Gibbs P, Thick M, Kirby JA. Immunogenicity of biliary epithelium: Study of the adhesive interaction with lymphocytes. *Gastroenterology*. 1997;112(3):968-977. doi:10.1053/GAST.1997.V112.PM9041260
98. Boraschi D, Li D, Li Y, Italiani P. In Vitro and In Vivo Models to Assess the Immune-Related Effects of Nanomaterials. *Int J Environ Res Public Health*. 2021;18(22):11769. doi:10.3390/IJERPH182211769
99. Mack CL. The Pathogenesis of Biliary Atresia: Evidence for a Virus-Induced Autoimmune Disease. *Semin Liver Dis*. 2007;27(3):233. doi:10.1055/S-2007-985068
100. Wang W, Donnelly B, Bondoc A, et al. The Rhesus Rotavirus Gene Encoding VP4 Is a Major Determinant in the Pathogenesis of Biliary Atresia in Newborn Mice. *J Virol*. 2011;85(17):9069. doi:10.1128/JVI.02436-10
101. Mohanty SK, Donnelly B, Lobeck I, et al. The SRL peptide of rhesus rotavirus VP4 protein governs cholangiocyte infection and the murine model of biliary atresia. *Hepatology*. 2017;65(4):1278-1292. doi:10.1002/hep.28947
102. Mohanty SK, Donnelly B, Temple H, et al. Rhesus rotavirus receptor-binding site affects high mobility group box 1 release, altering the pathogenesis of experimental biliary atresia. *Hepatol Commun*. 2022;6(10):2702-2714. doi:10.1002/HEP4.2024
103. Drut R, Drut RM, Gómez MA, Rúa EC, Lojo MM. Presence of human papillomavirus in extrahepatic biliary atresia. *J Pediatr Gastroenterol Nutr*. 1998;27(5):530-535. doi:10.1097/00005176-199811000-00007
104. Domiati-Saad R, Brian Dawson D, Margraf LR, Finegold MJ, Weinberg AG, Rogers BB. Cytomegalovirus and human herpesvirus 6, but not human papillomavirus, are present in neonatal giant cell hepatitis and extrahepatic biliary atresia. *Pediatr Dev Pathol*. 2000;3(4):367-373. doi:10.1007/S100240010045
105. Fjær RB, Bruu AL, Nordbø SA. Extrahepatic bile duct atresia and viral involvement. *Pediatr Transplant*. 2005;9(1):68-73. doi:10.1111/J.1399-3046.2005.00257.X
106. Arikan C, Berdeli A, Kilic M, Tumgor G, Yagci R V., Aydogdu S. Polymorphisms of the ICAM-1 gene are associated with biliary atresia. *Dig Dis Sci*. 2008;53(7):2000-2004. doi:10.1007/s10620-007-9914-1
107. Udomsinprasert W, Tencomnao T, Honsawek S, et al. +276 G/T single nucleotide polymorphism of the adiponectin gene is associated with the susceptibility to biliary atresia. *World J Pediatr*. 2012;8(4):328-334. doi:10.1007/S12519-012-0377-X

108. Zhao R, Song Z, Dong R, Li H, Shen C, Zheng S. Polymorphism of ITGB2 gene 3'-UTR+145C/A is associated with biliary atresia. *Digestion*. 2013;88(2):65-71. doi:10.1159/000352025
109. Shih HH, Lin TM, Chuang JH, et al. Promoter polymorphism of the CD14 endotoxin receptor gene is associated with biliary atresia and idiopathic neonatal cholestasis. *Pediatrics*. 2005;116(2):437-441. doi:10.1542/PEDS.2004-1900
110. Huch M, Gehart H, Van Boxtel R, et al. Long-term culture of genome-stable bipotent stem cells from adult human liver. *Cell*. 2015;160(1-2):299-312. doi:10.1016/j.cell.2014.11.050
111. Cofer ZC, Cui S, Eauclore SF, et al. Methylation Microarray Studies Highlight PDGFA Expression as a Factor in Biliary Atresia. *PLoS One*. 2016;11(3):e0151521. doi:10.1371/JOURNAL.PONE.0151521
112. Matthews RP, Eauclore SF, Mugnier M, et al. DNA hypomethylation causes bile duct defects in zebrafish and is a distinguishing feature of infantile biliary atresia. *Hepatology*. 2011;53(3):905-914. doi:10.1002/HEP.24106
113. Thalheim T, Siebert S, Quaas M, et al. Epigenetic drifts during long-term intestinal organoid culture. *Cells*. 2021;10(7):1718. doi:10.3390/cells10071718
114. Edgar RD, Perrone F, Foster AR, et al. Culture-Associated DNA Methylation Changes Impact on Cellular Function of Human Intestinal Organoids. *CMGH*. 2022;14(6):1295-1310. doi:10.1016/j.jcmgh.2022.08.008
115. Nakamura N, Shi X, Darabi R, Li Y. Hypoxia in Cell Reprogramming and the Epigenetic Regulations. *Front Cell Dev Biol*. 2021;9:609984. doi:10.3389/FCELL.2021.609984
116. Yoshida Y, Takahashi K, Okita K, Ichisaka T, Yamanaka S. Hypoxia enhances the generation of induced pluripotent stem cells. *Cell Stem Cell*. 2009;5(3):237-241. doi:10.1016/J.STEM.2009.08.001
117. Chung PHY, Babu RO, Wu Z, Wong KKY, Tam PKH, Lui VCH. Developing Biliary Atresia-like Model by Treating Human Liver Organoids with Polyinosinic:Polycytidylic Acid (Poly (I:C)). *Curr Issues Mol Biol*. 2022;44(2):644-653. doi:10.3390/CIMB44020045
118. Yue H, Sivasankaran Menon S, Ottakandathil Babu R, et al. Environmental toxin biliaratresone can induce biliary atresia: evidence from human liver organoids. Published online November 3, 2022. doi:10.21203/RS.3.RS-2185022/V1
119. Amarachintha SP, Mourya R, Ayabe H, et al. Biliary organoids uncover delayed epithelial development and barrier function in biliary atresia. *Hepatology*. 2022;75(1):89-103. doi:10.1002/HEP.32107
120. Chardot C, Carton M, Spire-Bendelac N, Pommelet C Le, Golmard JL, Auvert B. Epidemiology of biliary atresia in France: A national study 1986-96. *J Hepatol*. 1999;31(6):1006-1013. doi:10.1016/S0168-8278(99)80312-2
121. Chung PHY, Zheng S, Tam PKH. Biliary atresia: East versus west. *Semin Pediatr Surg*. 2020;29(4):150950. doi:10.1016/J.SEMPEDSURG.2020.150950
122. Jimenez-Rivera C, Jolin-Dahel KS, Fortinsky KJ, Gozdyra P, Benchimol EI. International incidence and outcomes of biliary atresia. *J Pediatr Gastroenterol Nutr*. 2013;56(4):344-354. doi:10.1097/MPG.0B013E318282A913
123. McKiernan PJ, Baker AJ, Kelly DA. The frequency and outcome of biliary atresia in the UK and Ireland. *Lancet*. 2000;355(9197):25-29. doi:10.1016/S0140-6736(99)03492-3
124. Davenport M, De Ville De Goyet J, Stringer MD, et al. Seamless management of biliary atresia in England and Wales (1999-2002). *The Lancet*. 2004;363(9418):1354-1357. doi:10.1016/S0140-6736(04)16045-5

125. Hsiao CH, Chang MH, Chen HL, et al. Universal screening for biliary atresia using an infant stool color card in Taiwan. *Hepatology*. 2008;47(4):1233-1240. doi:10.1002/HEP.22182
126. Chatterjee S, Richert L, Augustijns P, Annaert P. Hepatocyte-based in vitro model for assessment of drug-induced cholestasis. *Toxicol Appl Pharmacol*. 2014;274(1):124-136. doi:10.1016/j.taap.2013.10.032
127. He K, Cai L, Shi Q, Liu H, Woolf TF. Inhibition of MDR3 Activity in Human Hepatocytes by Drugs Associated with Liver Injury. *Chem Res Toxicol*. 2015;28(10):1987-1990. doi:10.1021/ACS.CHEMRESTOX.5B00201
128. Hendriks DFG, Puigvert LF, Messner S, Mortiz W, Ingelman-Sundberg M. Hepatic 3D spheroid models for the detection and study of compounds with cholestatic liability. *Sci Rep*. 2016;6:35434. doi:10.1038/srep35434
129. Funk C, Pantze M, Jehle L, et al. Troglitazone-induced intrahepatic cholestasis by an interference with the hepatobiliary export of bile acids in male and female rats. Correlation with the gender difference in troglitazone sulfate formation and the inhibition of the canalicular bile salt export pump (Bsep) by troglitazone and troglitazone sulfate. *Toxicology*. 2001;167(1):83-98. doi:10.1016/S0300-483X(01)00460-7
130. Smith AJ, Van Helvoort A, Van Meer G, et al. MDR3 P-glycoprotein, a phosphatidylcholine translocase, transports several cytotoxic drugs and directly interacts with drugs as judged by interference with nucleotide trapping. *J Biol Chem*. 2000;275(31):23530-23539. doi:10.1074/JBC.M909002199
131. Busche M, Rabl D, Fischer J, et al. Continuous, non-invasive monitoring of oxygen consumption in a parallelized microfluidic in vitro system provides novel insight into the response to nutrients and drugs of primary human hepatocytes. *EXCLI J*. 2022;21:144-161. doi:10.17179/excli2021-4351
132. van Wenum M, Adam AAA, van der Mark VA, et al. Oxygen drives hepatocyte differentiation and phenotype stability in liver cell lines. *J Cell Commun Signal*. 2018;12(3):575. doi:10.1007/S12079-018-0456-4
133. Scheidecker B, Shinohara M, Sugimoto M, Danoy M, Nishikawa M, Sakai Y. Induction of in vitro Metabolic Zonation in Primary Hepatocytes Requires Both Near-Physiological Oxygen Concentration and Flux. *Front Bioeng Biotechnol*. 2020;8:524. doi:10.3389/fbioe.2020.00524
134. Halldorsson S, Lucumi E, Gómez-Sjöberg R, Fleming RMT. Advantages and challenges of microfluidic cell culture in polydimethylsiloxane devices. *Biosens Bioelectron*. 2015;63:218-231. doi:10.1016/j.bios.2014.07.029
135. Dalsbecker P, Adiels CB, Goksör M. Liver-on-a-chip devices: the pros and cons of complexity. *Am J Physiol Gastrointest Liver Physiol*. 2022;323(3):G188-G204. doi:10.1152/ajpgi.00346.2021
136. Hoffmann SA, Müller-Vieira U, Biemel K, et al. Analysis of drug metabolism activities in a miniaturized liver cell bioreactor for use in pharmacological studies. *Biotechnol Bioeng*. 2012;109(12):3172-3181. doi:10.1002/bit.24573
137. Mueller D, Tascher G, Müller-Vieira U, et al. In-depth physiological characterization of primary human hepatocytes in a 3D hollow-fiber bioreactor. *J Tissue Eng Regen Med*. 2011;5(8):207-218. doi:10.1002/term.418
138. Zeilinger K, Schreiter T, Darnell M, et al. Scaling Down of a Clinical Three-Dimensional Perfusion Multicompartment Hollow Fiber Liver Bioreactor Developed for Extracorporeal Liver Support to an Analytical Scale Device Useful for Hepatic Pharmacological In Vitro Studies. *Tissue Eng Part C Methods*. 2011;17(5):549-556. doi:10.1089/ten.tec.2010.0580

139. Lübberstedt M, Müller-Vieira U, Biemel KM, et al. Serum-free culture of primary human hepatocytes in a miniaturized hollow-fibre membrane bioreactor for pharmacological in vitro studies. *J Tissue Eng Regen Med*. 2015;9(9):1017-1026. doi:10.1002/term.1652
140. Banaeiyan AA, Theobald J, Paukštyte J, Wöfl S, Adiels CB, Goksör M. Design and fabrication of a scalable liver-lobule-on-a-chip microphysiological platform. *Biofabrication*. 2017;9(1):015014. doi:10.1088/1758-5090/9/1/015014
141. Prodanov L, Jindal R, Bale SS, et al. Long-term maintenance of a microfluidic 3D human liver sinusoid. *Biotechnol Bioeng*. 2016;113(1):241-246. doi:10.1002/BIT.25700
142. Lee H, Chae S, Kim JY, et al. Cell-printed 3D liver-on-a-chip possessing a liver microenvironment and biliary system. *Biofabrication*. 2019;11(2):025001. doi:10.1088/1758-5090/aaf9fa
143. Mills DR, Haskell MD, Callanan HM, et al. Monoclonal antibody to novel cell surface epitope on Hsc70 promotes morphogenesis of bile ducts in newborn rat liver. *Cell Stress Chaperones*. 2010;15(1):39. doi:10.1007/S12192-009-0120-2
144. Lee JL, Streuli CH. Integrins and epithelial cell polarity. *J Cell Sci*. 2014;127(15):3217-3225. doi:10.1242/jcs.146142
145. Du Y, Khandekar G, Llewellyn J, Polacheck W, Chen CS, Wells RG. A Bile Duct-on-a-Chip With Organ-Level Functions. *Hepatology*. 2020;71(4):1350-1363. doi:10.1002/HEP.30918
146. Tabibian JH, Masyuk AI, Masyuk TV, O'Hara SP, LaRusso NF. Physiology of Cholangiocytes. *Compr Physiol*. 2013;3(1):541-565. doi:10.1002/CPHY.C120019
147. Banales JM, Huebert RC, Karlsen T, Strazzabosco M, LaRusso NF, Gores GJ. Cholangiocyte pathobiology. *Nat Rev Gastroenterol Hepatol*. 2019;16(5):269. doi:10.1038/S41575-019-0125-Y
148. Lorenzini S, Bird TG, Boulter L, et al. Characterisation of a stereotypical cellular and extracellular adult liver progenitor cell niche in rodents and diseased human liver. *Gut*. 2010;59(5):645-654. doi:10.1136/gut.2009.182345
149. Sánchez A, Álvarez AM, Pagan R, et al. Fibronectin regulates morphology, cell organization and gene expression of rat fetal hepatocytes in primary culture. *J Hepatol*. 2000;32(2):242-250. doi:10.1016/S0168-8278(00)80069-0
150. Kourouklis AP, Kaylan KB, Underhill GH. Substrate stiffness and matrix composition coordinately control the differentiation of liver progenitor cells. *Biomaterials*. 2016;99:82-94. doi:10.1016/j.biomaterials.2016.05.016
151. Kanninen LK, Harjumäki R, Peltoniemi P, et al. Laminin-511 and laminin-521-based matrices for efficient hepatic specification of human pluripotent stem cells. *Biomaterials*. 2016;103:86-100. doi:10.1016/J.BIOMATERIALS.2016.06.054
152. Ye S, Boeter JWB, Mihajlovic M, et al. A Chemically Defined Hydrogel for Human Liver Organoid Culture. *Adv Funct Mater*. 2020;30(48):2000893. doi:10.1002/adfm.202000893
153. Kumari J, Wagener FADTG, Kouwer PHJ. Novel Synthetic Polymer-Based 3D Contraction Assay: A Versatile Preclinical Research Platform for Fibrosis. *ACS Appl Mater Interfaces*. 2022;14(17):19212-19225. doi:10.1021/acsami.2c02549
154. Zhang Y, Tang C, Span PN, et al. Polyisocyanide Hydrogels as a Tunable Platform for Mammary Gland Organoid Formation. *Advanced Science*. 2020;7(18):2001797. doi:10.1002/ADVS.202001797
155. Mun SJ, Ryu JS, Lee MO, et al. Generation of expandable human pluripotent stem cell-derived hepatocyte-like liver organoids. *J Hepatol*. 2019;71(5):970-985. doi:10.1016/J.JHEP.2019.06.030

156. Bhatia SN, Balis UJ, Yarmush ML, Toner M. Microfabrication of hepatocyte/fibroblast co-cultures: role of homotypic cell interactions. *Biotechnol Prog*. 1998;14(3):378-387. doi:10.1021/BP980036j
157. Bhatia SN, Baus UJ, Yarmush ML, Toner M. Probing heterotypic cell interactions: hepatocyte function in microfabricated co-cultures. *J Biomater Sci Polym Ed*. 1998;9(11):1137-1160. doi:10.1163/156856298X00695
158. Khetani SR, Bhatia SN. Microscale culture of human liver cells for drug development. *Nature Biotech*. 2008;26(1):120-126. doi:10.1038/nbt1361
159. Prodanov L, Jindal R, Bale SS, et al. Long-term maintenance of a microfluidic 3D human liver sinusoid. *Biotechnol Bioeng*. 2016;113(1):241-246. doi:10.1002/BIT.25700
160. Verneti LA, Senutovitch N, Boltz R, et al. A human liver microphysiology platform for investigating physiology, drug safety, and disease models. *Exp Biol Med*. 2016;241(1):101-114. doi:10.1177/1535370215592121
161. Takebe T, Sekine K, Kimura M, et al. Massive and Reproducible Production of Liver Buds Entirely from Human Pluripotent Stem Cells. *Cell Rep*. 2017;21(10):2661-2670. doi:10.1016/J.CELREP.2017.11.005
162. Takebe T, Zhang RR, Koike H, et al. Generation of a vascularized and functional human liver from an iPSC-derived organ bud transplant. *Nat Protoc*. 2014;9(2):396-409. doi:10.1038/NPROT.2014.020
163. McClelland R, Wauthier E, Uronis J, Reid L. Gradients in the liver's extracellular matrix chemistry from periportal to pericentral zones: Influence on human hepatic progenitors. *Tissue Eng Part A*. 2008;14(1):59-70. doi:10.1089/ten.a.2007.0058
164. Ghafoory S, Stengl C, Kopany S, et al. Oxygen Gradient Induced in Microfluidic Chips Can Be Used as a Model for Liver Zonation. *Cells*. 2022;11(23):3734. doi:10.3390/CELLS11233734/S1
165. Janani G, Mandal BB. Mimicking Physiologically Relevant Hepatocyte Zonation Using Immunomodulatory Silk Liver Extracellular Matrix Scaffolds toward a Bioartificial Liver Platform. *ACS Appl Mater Interfaces*. 2021;13(21):24401-24421. doi:10.1021/acsmi.1c00719
166. Ender AM, Kaygisiz K, Räder HJ, Mayer FJ, Synatschke C V., Weil T. Cell-Instructive Surface Gradients of Photoresponsive Amyloid-like Fibrils. *ACS Biomater Sci Eng*. 2021;7(10):4798-4808. doi:10.1021/acsbmaterials.1c00889
167. Chelli B, Barbalinardo M, Valle F, et al. Neural cell alignment by patterning gradients of the extracellular matrix protein laminin. *Interface Focus*. 2014;4(1). doi:10.1098/RFSFS.2013.0041
168. Yao S, Cui J, Chen S, et al. Extracellular Matrix Coatings on Cardiovascular Materials—A Review. *Coatings 2022, Vol 12, Page 1039*. 2022;12(8):1039. doi:10.3390/COATINGS12081039
169. Fry S. *Heroes*. Penguin Random House; 2019. Accessed May 1, 2023. <https://www.penguin.co.uk/books/308231/heroes-by-fry-stephen/9781405940368>





Addendum

Nederlandse samenvatting

De hedendaagse Herakles – patiënt-eigen lever organoïden voor het modelleren van zeldzame leverziekten bij kinderen

“Twee prachtige adelaars vlogen uit de lucht en zweefden dicht bij Prometheus, waardoor het zonlicht werd geblokkeerd. Zeus riep hem toe. ‘Je zult voor altijd aan deze rots vastgeketend liggen. (...) Elke dag zullen deze adelaars je lever komen uitrukken, net zoals je mijn hart hebt uitgetrokken. Ze zullen het voor je ogen opeten. Omdat je onsterfelijk bent, groeit het elke nacht weer aan. Deze marteling zal nooit eindigen.”

*Uit Mythos – De Griekse mythen herverteld, van Stephen Fry
Vertaald vanuit de Engelse versie.*

Hoewel mensen geen onsterfelijke titanen zijn, schuilt er een kern van waarheid in de mythe van Prometheus: het fascinerende regeneratieve vermogen van de lever. Omdat het functioneren van de meeste organen afhankelijk is van de lever, is leverregeneratie een essentieel proces. Bij alle gewervelde dieren is de lever geëvolueerd om zijn massa en functie aan te vullen na letsel. Als er bijvoorbeeld 70% van de lever van een gezond mens verwijderd wordt voor orgaandonatie, dan regenereert 50% van het oorspronkelijke levervolume binnen een week. Binnen een jaar is het orgaanvolume en functioneren weer compleet hersteld.

Dit ongelooflijke regeneratieve vermogen is het resultaat van een complexe orkestratie van signalen, waaronder groeifactoren en een herstelde samenstelling van de omgevingseiwitten waarin de cellen zitten. Deze signalen bevorderen de zelfvernieuwing van elk leverceltype na acuut letsel. Er zijn echter situaties, zoals virale infecties, waarin de zelfvernieuwing van één van de twee meest voorkomende leverceltypen, hepatocyten en cholangiocyten, wordt geremd. Om de leverfunctie te redden hebben gewervelde dieren een tweede mechanisme voor leverregeneratie ontwikkeld. In gewervelden kunnen hepatocyten en cholangiocyten veranderen naar het andere celtype. Op deze manier fungeren ze als een soort stamcellen om het andere celtype aan te vullen en de leverfunctie veilig te stellen.

Toch zijn er, in tegenstelling tot Zeus' bewering van oneindige hergroei van de lever in de mythe van Prometheus, grenzen aan leverregeneratie. Chronische leverbeschadiging zal leverregeneratie uiteindelijk belemmeren. De samenstelling van eiwitten waarin de cellen zitten verandert, er ontstaat een ontstekingsomgeving en genetische fouten stapelen zich steeds meer op naarmate hepatocyten hectisch proberen het verlies van hepatocyten aan te vullen. Naarmate de omgeving van de cellen drastisch verandert, gaan regeneratiesignalen verloren en leidt leverschade tot orgaanfalen. Als gevolg hiervan sterven in de VS jaarlijks 17 van de 100.000 volwassenen aan leverfalen. In Europa bedraagt het aantal sterfgevallen als gevolg van leverfalen gemiddeld een vergelijkbaar aantal en kan in sommige landen zelfs oplopen tot 25 van de 100.000.

Het is duidelijk dat er dringend behoefte is aan oplossingen voor patiënten met een leverziekte. Er is dan ook veel onderzoek gedaan naar de veelvoorkomende leveraandoeningen, zoals niet-alcoholische leververvetting en hepatocellulair carcinoom. Individuele zeldzame leverziekten krijgen minder aandacht, ook al is het totaal aantal gevallen aanzienlijk. Ongeveer 25% van de zeldzame leverziekten treft patiënten jonger dan 5 jaar, terwijl nog eens 37% de levensverwachting van de patiënt aanzienlijk beïnvloedt. Het is een uitdaging om deze ziekten te bestuderen, omdat er veel verschillende ziektebeelden zijn binnen individuele leverziekten en het aantal patiënten binnen één ziekte beperkt is. Ook is het moeilijk om leverfuncties en functionele defecten in het laboratorium te modelleren. In dit proefschrift onderzoeken we de mogelijkheden om zulke zeldzame kinderleverziekten te onderzoeken door het gebruik van patiënt-eigen lever organoïden, met als uiteindelijk doel de zorg- en behandelingsopties voor getroffen kinderen te verbeteren.

Leveraandoeningen in kinderen en onderzoeksmodellen

De lever is een vitaal orgaan van het lichaam en verantwoordelijk voor veel essentiële functies. Het fungeert als een grote zeef waardoor het bloed wordt gefilterd. Schadelijke stoffen worden geneutraliseerd en vervangen door nuttige moleculen, waaronder hormonen en eiwitten. Hepatocyten zijn verantwoordelijk voor de meeste leverfuncties. De driedimensionale positionering van hepatocyten maximaliseert het contact met het bloed en de galkanalen om het transport van substraten en afvalproducten door het celmembraan te vergemakkelijken. Cholangiocyten zijn het op een na meest voorkomende celtype van de lever. Ze bekleden de galwegen binnen (intrahepatisch) en buiten (extrahepatisch) de lever en vergemakkelijken de galstroom uit de lever naar de galblaas en het duodenum.

Een defect of verstoring van het ingewikkelde metabolische netwerk van de lever kan tot ziekte leiden. Vooral leverziekten bij kinderen laten de vitale functie van de lever zien en de problemen die ontstaan wanneer een enkele leverfunctie tekortschiet.

Omdat de lever zo'n belangrijk en complex orgaan is, is levertransplantatie uiteindelijk de enige behandeling voor veel leverziekten bij kinderen.

Tot de belangrijkste oorzaken van levertransplantaties bij kinderen behoren cholestatische leverziekten, zoals galgangatresie en stofwisselingsstoornissen. Galgangatresie is een ziekte die voorkomt bij pasgeboren kinderen en zich manifesteert met verstopte of afwezige extrahepatische galwegen en galblaas, waardoor de galafvoer uit de lever wordt geremd. Wanneer galgangatresie onbehandeld blijft ontwikkelen de kinderen leverschade die binnen korte tijd tot orgaanfalen leidt. Het ziektemechanisme van galgangatresie is waarschijnlijk multifactorieel, maar de details en connecties blijven onduidelijk. De behandelingsopties voor patiënten zijn hierdoor beperkt tot chirurgische correctie en levertransplantatie. Ter vergelijking worden verschillende andere (monogenetische) leverziekten bij kinderen veroorzaakt door mutaties in één enkel gen dat codeert voor een enzym of een transporter. Dit resulteert vaak in een veranderde metabolische route. Belangrijke metabolieten ontbreken of stapelen tot giftige hoeveelheden op, zoals het geval is bij citrullinemie type I, een stoornis van de ureumcyclus waarbij ammoniak niet wordt verwerkt en zich ophoopt in het lichaam. Primaire familiale intrahepatische cholestase (PFIC) is een voorbeeld van een genetische ziekte, waarbij defecten in het uitscheidingsstelsel van gal leidt tot galstapeling in de lever. Dit heeft als gevolg dat de zeepachtige gal schade aan hepatocyten veroorzaken.

Uiteindelijk leiden deze functionele defecten tot falen van de lever of andere organen voordat patiënten de volwassenheid bereiken. Individuele monogenetische leverziekten zijn zeldzame ziekten, maar hun totaal voorkomen is hoog, met 1 op de 2.000 geboorten per jaar. Toch belemmeren de diversiteit, geografische spreiding van patiënten en zeldzaamheid van monogenetische leverziekten ons begrip van de onderliggende ziektemechanismen. Tragisch genoeg heeft dit ook de ontwikkeling van farmaceutische oplossingen geremd.

De afgelopen jaren hebben de toenemende investeringen op dit onderzoeksgebied geresulteerd in doorbraken voor verschillende patiëntengroepen. Momenteel worden er verschillende modellen gebruikt om deze ziekten te onderzoeken, waaronder klinische onderzoeken gebaseerd op individuele patiënten, diermodellen, patiënt-eigen fibroblasten, patiënt-eigen geïnduceerde pluripotente stamcellen en organoïden. Deze verscheidene modellen hebben met succes inzicht gegeven in ziektemechanismen en sommige hebben zelfs bijgedragen aan klinische besluitvorming. Voor veel kinderleverziekten bestaat echter nog geen geschikt model en blijven ziektemechanismen en mogelijke behandelingsopties onbekend. Hierdoor blijft de medische zorg beperkt tot symptomatische behandeling, terwijl voor andere leveraandoeningen behandelingsopties geheel afwezig zijn.

Een aantal jaar geleden werden leverorganoïden ontwikkeld en aanprezen als hét nieuwe levermodel voor zeldzame ziekten. Leverorganoïden zijn gemaakt van levercellen afkomstig van leverbiopten van patiënten of gezonde donoren. In het laboratorium worden de biopten mechanisch en met enzymen kleingemaakt om zo galepitheelcellen uit het weefsel te bevrijden. Om organoïden te vormen worden de cellen in een 3D gel geplaatst en met specifieke groeifactoren gevoed. De cellen vormen dan binnen enkele dagen holle bollen die leverorganoïden worden genoemd. Leverorganoïden zijn in staat zich zowel als hepatocyte als als cholangiocyte te specialiseren, waardoor de weg wordt geopend om zowel de lever als ook de galgang te bestuderen op basis van één biopsie van een enkele patiënt. Bovendien is gerapporteerd dat leverorganoïden gedurende meerdere maanden stabiel kunnen worden ingevroren en gekweekt, wat niet mogelijk is voor andere primaire menselijke cellen. Na de ontwikkeling van organoïden uit cholangiocyten afkomstig van de lever (intrahepatisch), zijn protocollen ontwikkeld om organoïden te genereren uit galwegen die buiten de lever zitten (extrahepatisch) en de galblaas. Sindsdien zijn er nieuwe naamgevingen ontwikkeld om onderscheid te maken tussen leverorganoïden van verschillende oorsprong. De leverorganoïden die voor het eerst werden ontwikkeld door Huch *et al.* in 2015 heten nu intrahepatische cholangiocytorvanoïden (ICO's). Andere leverorganoïden worden als volgt genoemd: leverorganoïden gemaakt van hepatocyten worden hepatocyt-organoïden genoemd; organoïden gemaakt van biopten van de extrahepatische galgang worden extrahepatische cholangiocytorvanoïden (ECO's) genoemd, terwijl organoïden gemaakt van biopten van de galblaas galblaascholangiocytorvanoïden (GCO's) worden genoemd.

Binnen de context van zeldzame leverziekten bij kinderen presenteerde het eerste rapport over leverorganoïden veelbelovende resultaten over het bestuderen van ziektemechanismen van het Alagille-syndroom en α 1-antitrypsinedeficiëntie. Het vooruitzicht van vrijwel oneindig beschikbaar patiëntenmateriaal waarmee zeldzame ziekten kunnen worden bestudeerd was aantrekkelijk. Daarom investeerde onze groep in het UMC Utrecht in de infrastructuur en (inter)nationale samenwerkingen om een Metabole Biobank op te zetten. Zo zijn leverorganoïden afkomstig uit leverweefsel van honderden patiënten en gezonde donoren opgeslagen. Deze grote biobank van leverorganoïden van verschillende zeldzame leverziekten bij kinderen biedt een waardevolle kans om het nut van leverorganoïden te ontrafelen als hulpmiddel bij onderzoek naar ziektemechanismen en klinische besluitvorming.

Evaluatie en verdere ontwikkeling van leverorganoïden als hulpmiddel bij onderzoek naar leverziekten bij kinderen

Tijdens de oprichting van onze biobank was de wereldwijde kennis over de toepasbaarheid van leverorganoïden voor het bestuderen van ziektemechanismen beperkt. Sinds het eerste rapport over leverorganoïden is er geen verdere informatie gepubliceerd over het scala aan leverfuncties dat tot uiting komt in leverorganoïden.

Hoewel Huch *et al.*, 2015 hebben aangetoond dat meerdere hepatocytfuncties kunnen worden bestudeerd in leverorganoïden, zijn er slechts beperkte functionele vergelijkingen gemaakt met humane volwassen hepatocyten of leverweefsel. Hierdoor blijft het onduidelijk of deze leverfuncties sterk genoeg tot uiting komen om ziektepatronen op te kunnen sporen. Bovendien komen verschillende levereigenschappen, zoals de uitscheiding van albumine, aanzienlijk minder tot uiting in leverorganoïden dan in leverweefsel. Samen suggereerden deze data dat leverorganoïden mogelijk niet het volledige scala van hepatocytfuncties weerspiegelen. Daarom bleef het onduidelijk welke leverfuncties en -ziekten met leverorganoïden kunnen worden bestudeerd. In dit proefschrift onderzochten we daarom het potentieel van leverorganoïden om de ziektemechanismen van monogenetische leveraandoeningen en andere zeldzame leverziekten bij kinderen te bestuderen.

Om te beginnen introduceerd **hoofdstuk 1** de wetenschappelijke en maatschappelijke belangen achter het onderzoek. In **hoofdstuk 2** hebben we op basis van genen en functionele studies bekeken welke zeldzame monogenetische ziekten kunnen worden bestudeerd met ICO's. Onze ervaring is dat het protocol om ICO's te maken het mogelijk maakt om patiëntweefsel met laboratoria in de hele wereld te delen. Dit vermindert de beperkingen die de wereldwijde distributie van patiëntmateriaal met zich meebrengt. Verder hebben we aangetoond dat organoïden van patiënten belangrijke kenmerken van verschillende monogenetische leverziekten uiten. Hierdoor zijn we in staat onderscheid te maken tussen gezonde controle- en patiëntorganoïden. We hebben laten zien dat fundamentele metabolische functies, maar ook hepatocyt-specifieke functies, zoals het kopermetabolisme, in ICO's kunnen worden bestudeerd. Bovendien hebben we aangetoond dat ICO's bijzonder nuttig zijn om galtransportfuncties te bestuderen.

Huidfibroblasten worden veel gebruikt om zeldzame monogenetische aandoeningen op gepersonaliseerde wijze in het laboratorium te bestuderen. Fibroblasten zijn gemakkelijk verkrijgbaar en eenvoudig te hanteren. Toch suggereert hun oorsprong dat hun potentieel om hepatocyt-specifieke aandoeningen te bestuderen beperkt is. De zeldzaamheid van literatuurrapporten over het modelleren van leverziekten met fibroblasten ondersteund deze speculatie. Onze vergelijking van ICO's en fibroblasten met leverweefsel onderstreept verder dat fibroblasten verschillende hepatocyt-specifieke genen niet uiten (**hoofdstuk 2**). In plaats daarvan zijn fibroblasten nuttig voor het bestuderen van generieke biochemische defecten die verschillende celtypen beïnvloeden. Voor hepatocyt-specifieke functies, zoals het metabolisme van geneesmiddelen, wordt daarom de voorkeur gegeven aan meer hepatocyt-specifieke celmodellen. Vanwege hun oorsprong en bipotente aard werden ICO's beschouwd als een ideaal model voor hepatocyten. We ontdekten echter dat ICO's niet alle relevante hepatocyt-specifieke genen uiten (**hoofdstuk 2**). In plaats daarvan uiten ICO's een mengsel van enkele cholangiocyt- en hepatocyt-

specifieke genen en functies. Daarom zijn ICO's onder de huidige omstandigheden geschikt om een selectie van hepatocytfuncties te bestuderen die zijn aangetast bij zeldzame leveraandoeningen.

De pogingen om het nut van leverorganoïden te ontrafelen zijn in **hoofdstuk 3** uitgebreid door te onderzoeken of leverorganoïden kunnen worden gebruikt om leverziekten bij kinderen met onopgeloste ziektemechanisme te bestuderen. Omdat uit **hoofdstuk 2** bleek dat ICO's verschillende cholangiocytenkenmerken behouden, waren we geïnteresseerd om te zien of galgangatresie bestudeerd kon worden met behulp van patiënt-eigen ICO's. Bij galgangatresie is de galboom doordrongen met littekenweefsel en vernauwd, waardoor de galstroom van de lever naar de darm wordt verhinderd. Hoewel het ziektemechanisme onduidelijk blijft, suggereert het ziektebeeld sterk dat cholangiocyten in de galwegen een centrale rol spelen in galgangatresie. Verder suggereren de verschillen in timing en ernst tussen symptomen in de galwegen binnen (intrahepatisch) en buiten (extrahepatisch) de lever verschillen in onderliggende mechanismen of gevoeligheden van cholangiocyten van diverse regio's en ontwikkelings-stadia. De galwegen binnen en buiten de lever ontwikkelen zich uit verschillende oorsprongscellen, wat een belangrijke factor zou kunnen zijn die ten grondslag ligt aan deze locatie- en tijdsverschillen. Na de publicatie van ICO's, zijn protocollen ontwikkeld om organoïden te genereren uit extrahepatische galwegen (ECO's) en galblaascholangiocyten (GCO's). Omdat deze organoïden in het lab regionale verschillen van de lever en de galboom behouden, vermoedden we dat ze nuttig zouden zijn om de regionale variëteit van galgangatresie te bestuderen. Daarom hebben we getest of organoïden konden worden gekweekt uit deze drie regio's van galgangatresie patiëntenweefsel. Zo hebben we aangetoond dat galgangatresie patiëntenorganoïden kunnen worden gekweekt en ingevroren. Ook hebben we aangetoond dat het groeiedrag van galgangatresie ICO's verschilde van controleorganoïden. Ondanks normaal uiterlijk van galgangatresieorganoïden suggereerde de uiting van bepaalde genen dat galgangatresie organoïden verschilden van controleorganoïden. De verschillen lagen vooral in genen die betrokken zijn bij verandering van omgevingseiwitten en groei; twee functies die vermoedelijk betrokken zijn bij het mechanisme dat leidt tot galgangatresie.

In de afgelopen decennia zijn verschillende hypothesen over het ziektemechanisme voorgesteld, waaronder virale infecties, toxines, auto-immunreacties en genetische predispositie. Van deze hypothesen wordt de betrokkenheid van virale infecties en/of een gif uit de omgeving of een giftige metaboliet het meest ondersteund door klinisch en experimenteel bewijs. Omdat leverorganoïden een minimalistisch model zijn van het galepitheel, kan het exacte werkingsmechanisme van een virus of gif afzonderlijk van andere cellen worden bestudeerd. Om inzicht te krijgen in de vraag of leverorganoïden inderdaad geschikt zijn om bestaande hypothesen te testen,

hebben we galgangatresie en controleorganoïden behandeld met een synthetisch viraal analoog (poly I:C) en een plantengif (biliatresone) waarvan bekend is dat het galgangatresie bij dieren veroorzaakt. We ontdekten dat biliatresone een verhoging van cellulaire stressreacties, zoals het glutathionmetabolisme, in galgangatresie en controle ECO's veroorzaakte. Poly I:C blootstelling veroorzaakte galgangatresie-specifieke veranderingen in de uiting van bepaalde genen, waaronder verandering van omgevingseiwitten en het vormen van littekenweefsel. Over het geheel genomen suggereren onze bevindingen dat humane leverorganoïden een geschikt model zijn om galgangatresie te bestuderen.

Hoewel we in **hoofdstuk 2** hebben laten zien dat verschillende functies van hepatocyten en cholangiocyten kunnen worden bestudeerd in leverorganoïden, gaven onze gegevens ook aan dat verschillende functies van hepatocyten momenteel beperkt zijn in dit model. Daarom onderzochten we of de levermaturing van ICO's kan worden verbeterd. Met dit doel voor ogen ontwikkelden en karakteriseerden we in **hoofdstuk 4** een nieuwe kweekmethode voor ICO's door gebruik te maken van verschillende strategieën om de omgeving van hepatocyten in de lever na te bootsen. We fragmenteerden de 3D organoïden en kweekten de losse stukjes op het oppervlak van holle poreuze vezels (HFMs). Bovendien gebruikten we omgevingseiwitten om celhechting op HFMs te faciliteren en hepatocyt-specifieke signalen na te bootsen. We zagen dat cellen strakke lagen vormden en ontdekten dat leverfuncties, zoals het metabolisme van geneesmiddelen, verbeterden in dit nieuwe kweekstelsel. Ook maken HFMs interne en externe perfusie mogelijk wanneer ze zijn aangesloten op een bioreactor en perfusiepomp, waardoor de bloed- en galstroom in het laboratorium kan worden nagebootst. Als een eerste stap in de richting van ziektemodellering onderzochten we of patiënt-eigen ICO's in het nieuwe systeem kunnen worden gekweekt. Hier lag de focus op ziekten die galtransporters aantasten, aangezien de HFM-architectuur de scheiding van celcompartimenten, die gal of bloedonderdelen produceren, mogelijk maakt. Daardoor worden functionele studies mogelijk om dergelijke ziekten te bestuderen. Zo hebben we aangetoond dat hepatische galtransporterdefecten zoals PFIC type 3 (PFIC3) bestudeerd kunnen worden in patiënt-eigen leverorganoïden. Gezamenlijk suggereren deze bevindingen dat het HFM-systeem een krachtig hulpmiddel is om leverziekten evenals de langetermijneffecten van therapeutische strategieën voor zeldzame leverziekten bij kinderen zoals PFIC3, op een gepersonaliseerde manier te bestuderen.

Ten slotte vat **hoofdstuk 5** de bevindingen van het proefschrift samen en gaat dieper in op de implicaties voor het toekomstige gebruik van leverorganoïden. Door raakvlakken tussen de uitgevoerde onderzoeken en recente literatuur te identificeren, worden toekomstige onderzoeksmogelijkheden voorgesteld om het toepassingsbereik van leverorganoïden te verbreden en ons begrip van ziektemechanismen te verbeteren.

Conclusie

In dit proefschrift hebben we aangetoond dat patiënt-eigen leverorganoïden een nuttig hulpmiddel zijn bij het bestuderen van verschillende zeldzame lever- en metabolische ziekten die de lever en de galboom aantasten. Verschillende ziekten zoals taaislijmziekte, PFIC3, de ziekte van Wilson en methylmalon acidurie kunnen momenteel met ICO's worden bestudeerd. Hoewel leverorganoïden eerder werden geprezen als hét nieuwe hepatocytenmodel, hebben we aangetoond dat organoïden uit alle regio's van de galboom minstens even nuttig zijn voor het onderzoeken van galgangaandoeningen.

Ik ben ervan overtuigd dat hepatobiliaire organoïden een werkelijk krachtig hulpmiddel kunnen zijn om te helpen bij het ontrafelen van de mechanismen die tot galgangatresie leiden. De ontwikkeling van nieuwe technologieën zoals orgaanchips en co-cultuurstrategieën zijn veelbelovend, niet alleen om de ziektemechanismen van zeldzame ziekten te bestuderen, maar ook om de levermaturing van ICO's te verbeteren. Het toepassen van de talloze verbeteringsstrategieën voor ICO-kweek zal waarschijnlijk een fantastisch, patiënt-eigen hepatocytenmodel opleveren. We hebben de eerste stappen gezet in de richting van het verbeteren van de levermaturing van ICO's en hebben daarmee aangetoond dat de toepassingen van ICO's kunnen worden uitgebreid om de studie van ziektemechanismen mogelijk te maken. We geloven dat de combinatie van leverorganoïden en andere hepatocytenmodellen een krachtig werktuig is om ziektemechanismen te ontrafelen en te helpen bij het identificeren van veilige therapeutische strategieën voor zeldzame leverziekten bij kinderen op een gepersonaliseerde manier. Met de veelbelovende nieuwe wegen die voor ons liggen, hoop ik dat patiënten-eigen hepatobiliaire organoïden op een dag zullen helpen bij het verlichten van patiëntenleed net als Heracles Prometheus kwam redden van de nachtelijke mutilatie van zijn lever.

“Heracles [hief] zijn boog en [schoot] Zeus' wrekende adelaar neer (...) 'Dank je, Heracles,' zei de Titaan. (...) 'Je bevrijdt de wereld van haar smerigste beesten, haar draken, slangen en veelkoppige monsters (...) zodat de wereld veilig wordt gemaakt zodat de mensheid kan gedijen.'”

*Uit Helden – De grote avonturen uit de Griekse mythologie, van Stephen Fry
Vertaald vanuit de Engelse versie.*

Deutsche Zusammenfassung

Der moderne Herakles – patienteneigene Organoiden zum Modellieren von seltenen Leberkrankheiten bei Kindern

„Zwei prächtige Adler flogen vom Himmel, schwebten nahe an Prometheus heran und blockierten das Sonnenlicht. Zeus rief ihm zu: ‚Du wirst für immer an diesen Felsen gekettet sein. (...) Jeden Tag werden diese Adler kommen und dir die Leber herausreißen, so wie du mir das Herz herausgerissen hast. Sie werden deine Leber vor deinen Augen essen. Weil du unsterblich bist, wächst sie jede Nacht nach. Diese Folter wird niemals enden.“

*Aus Mythos – Was uns die Götter heute sagen, von Stephen Fry
Aus der englischen Version frei übersetzt.*

Obwohl Menschen keine unsterblichen Titanen sind, steckt etwas Wahres im Mythos von Prometheus: die faszinierenden Regenerationskräfte der Leber. Da die Funktionen der meisten Organe von der Leber abhängen, ist die Leberregeneration ein wichtiger Prozess. Bei allen Wirbeltieren hat sich die Leber so entwickelt, dass sie nach einer Verletzung ihre Masse und Funktion wieder anreichert. Wenn beispielsweise 70% der Leber eines gesunden Menschen für eine Organspende entnommen werden, regeneriert innerhalb einer Woche 50% des ursprünglichen Lebervolumens. Innerhalb eines Jahres sind Organvolumen und Funktion vollständig wiederhergestellt.

Diese unglaubliche Regenerationsfähigkeit ist das Ergebnis einer komplexen Koordination von Signalen, einschließlich Wachstumsfaktoren und einer neuen Zusammensetzung der Proteine, in der sich die Zellen befinden. Diese Signale fördern die Selbsterneuerung jedes Leberzelltyps nach einer akuten Verletzung. Es gibt jedoch Situationen, beispielsweise bei Virusinfektionen, in denen die Selbsterneuerung einer der beiden zahlreichsten Leberzelltypen, Hepatozyten und Cholangiozyten, gehemmt ist. Um die Leberfunktion wiederherzustellen, haben Wirbeltiere einen zweiten Mechanismus zur Leberregeneration entwickelt. Bei Wirbeltieren können sich Hepatozyten und Cholangiozyten jeweils in den anderen Zelltyp verändern. Auf diese Weise fungieren sie als eine Art Stammzelle, um den anderen Zelltyp zu ergänzen und die Leberfunktion zu sichern.

Doch im Gegensatz zu Zeus' Behauptung eines unendlichen Nachwachsens der Leber im Mythos von Prometheus gibt es Grenzen für die Leberregeneration. Chronischer Leberschaden wird die Leberregeneration letztendlich verhindern. Die Proteinzusammensetzung verändert sich, es entsteht eine entzündliche Umgebung und genetische Fehler häufen sich zunehmend, da Hepatozyten hektisch versuchen, den Hepatozytenverlust auszugleichen. Da sich die Umgebung der Zellen dramatisch verändert, gehen Regenerationssignale verloren und Leberschäden führen zu Organversagen. Infolgedessen sterben in den USA jedes Jahr 17 von 100.000 Erwachsenen an Leberversagen. In Europa ist die Zahl der Todesfälle durch Leberversagen im Durchschnitt ähnlich hoch und kann in einigen Ländern sogar bis zu 25 von 100.000 betragen.

Es ist eindeutig, dass ein dringender Bedarf an Behandlungen für Patienten mit Lebererkrankungen besteht. An viel verbreiteten Lebererkrankungen, wie der nichtalkoholischen Fettleber und dem hepatozellulären Karzinom, wurde viel geforscht. Einzelne seltene Lebererkrankungen erhalten jedoch weniger Beachtung, obwohl die Gesamtzahl aller Fälle hoch ist. Etwa 25% von seltenen Lebererkrankungen betreffen Patienten unter 5 Jahren, während weitere 37% die Lebenserwartung der Patienten erheblich beeinträchtigen. Die Forschung an diesen Krankheiten ist eine Herausforderung, da es bei diesen einzelnen Lebererkrankungen viele verschiedene Krankheitsbilder gibt und die Anzahl der Patienten innerhalb einer Krankheit begrenzt ist. Außerdem ist es schwierig, Leberfunktionen und Funktionsdefekte im Labor zu modellieren. In dieser Doktorarbeit untersuchen wir die Möglichkeiten, solch seltene Leberkrankheiten bei Kindern mit Hilfe von patienteneigenen Leberorganoiden zu erforschen, mit dem ultimativen Ziel, die Therapiemöglichkeiten für betroffene Kinder zu verbessern.

Lebererkrankungen bei Kindern und derzeitige Forschungsmodelle

Die Leber ist ein lebenswichtiges Organ des Körpers und für viele unerlässliche Funktionen verantwortlich. Es fungiert als großes Sieb, durch das das Blut gefiltert wird. Schädliche Substanzen werden neutralisiert und durch nützliche Moleküle, darunter Hormone und Proteine, ersetzt. Hepatozyten sind für die meisten Leberfunktionen verantwortlich. Die dreidimensionale Positionierung der Hepatozyten maximiert den Kontakt mit dem Blut und den Gallengängen, um den Transport von Substraten und Abfallprodukten durch die Zellmembran zu erleichtern. Cholangiozyten sind der zweithäufigste Zelltyp der Leber. Sie kleiden die Gallengänge innerhalb (intrahepatisch) und außerhalb (extrahepatisch) der Leber aus und erleichtern den Gallenfluss von der Leber zur Gallenblase und zum Zwölffingerdarm.

Ein Defekt oder eine Störung des komplexen Stoffwechselnetzwerks der Leber kann zu Krankheiten führen. Insbesondere Lebererkrankungen bei Kindern offenbaren

die lebenswichtige Funktion der Leber und die Probleme, die entstehen, wenn eine einzelne Leberfunktion ausfällt. Da es sich bei der Leber um ein so wichtiges und komplexes Organ handelt, ist eine Lebertransplantation letztlich die einzige Behandlungsmethode für viele Lebererkrankungen bei Kindern.

Zu den Hauptursachen für Lebertransplantationen bei Kindern zählen cholestatische Lebererkrankungen wie Gallengangatresie und Stoffwechselstörungen. Gallengangatresie ist eine Erkrankung bei Neugeborenen, die sich durch verstopfte oder fehlende extrahepatische Gallenwege und Gallenblase äußert und den Gallenabfluss aus der Leber behindert. Bleibt eine Gallengangatresie unbehandelt, kommt es bei Kindern zu Leberschäden, die innerhalb kurzer Zeit zu Organversagen führen. Der Krankheitsmechanismus der Gallengangatresie ist wahrscheinlich multifaktoriell, die Zusammenhänge bleiben jedoch unklar. Die Behandlungsmöglichkeiten für Patienten beschränken sich daher auf einen chirurgischen Eingriff und Lebertransplantation. Im Vergleich dazu werden mehrere andere (monogenetische) Lebererkrankungen bei Kindern durch Mutationen in einem einzelnen Gen verursacht, das für die Kodierung eines Enzyms oder eines Transporters verantwortlich ist. Dies führt häufig zu einem veränderten Stoffwechselweg: Schlüsselmetaboliten fehlen oder reichern sich in giftigen Mengen an, wie es bei Citrullinämie Typ I der Fall ist, einer Störung des Harnstoffzyklus, bei der Ammoniak nicht verarbeitet wird und sich im Körper ansammelt. Die primäre familiäre intrahepatische Cholestase (PFIC) ist ein Beispiel für eine erbliche Erkrankung, bei der Defekte im Gallenausscheidungssystem zu einer Ansammlung von Gallenflüssigkeit in der Leber führen. Die seifenähnliche Gallenflüssigkeit schädigt die Hepatozyten.

Letztendlich führen diese Funktionsstörungen dazu, dass die Leber oder andere Organe versagen, bevor die Patienten das Erwachsenenalter erreichen. Einzelne monogenetische Leberkrankheiten sind seltene Erkrankungen, ihre Gesamtinzidenz fällt jedoch mit weltweit 1 von 2.000 Geburten pro Jahr hoch aus. Dennoch erschweren die Vielfalt, weltweite Verteilung aller Patienten und Seltenheit monogenetischer Leberkrankheiten unser Verständnis der zugrunde liegenden Krankheitsmechanismen. Tragischerweise hat dies auch die Entwicklung pharmazeutischer Lösungen behindert.

In den letzten Jahren haben zunehmende Investitionen in diesem Forschungsbereich zu Durchbrüchen für verschiedene Patientengruppen geführt. Derzeit werden mehrere Modelle zur Untersuchung dieser Krankheiten verwendet, darunter klinische Studien von einzelnen Patienten, Tiermodelle, patienteneigene Fibroblasten, patienteneigene induzierte pluripotente Stammzellen und Organoiden. Diese verschiedenen Modelle haben erfolgreich Einblicke in Krankheitsmechanismen geliefert und einige haben sogar zu Entscheidungen über Behandlungsmöglichkeiten beigetragen. Für viele Leberkrankheiten bei Kindern

gibt es jedoch noch kein geeignetes Modell und Krankheitsmechanismen und mögliche Behandlungsmöglichkeiten sind noch unbekannt. Dadurch beschränkt sich die medizinische Versorgung auf die symptomatische Behandlung, während Behandlungsmöglichkeiten für einige Lebererkrankungen gänzlich fehlen.

Vor einigen Jahren wurden Leberorganoiden als neues Lebermodell für seltene Krankheiten entwickelt und bekannt gemacht. Leberorganoiden werden aus Leberzellen hergestellt, die aus Leberbiopsien von Patienten oder gesunden Spendern entnommen werden. Im Labor werden die Biopsien mechanisch und mit Enzymen zerkleinert, um Gallenepithelzellen aus dem Gewebe freizusetzen. Zur Bildung von Organoiden werden die Zellen in ein 3D-Gel gegeben und mit spezifischen Wachstumsfaktoren gefüttert. Die Zellen bilden dann innerhalb weniger Tage hohle Bällchen, sogenannte Leberorganoiden. Leberorganoiden sind in der Lage, sich sowohl als Hepatozyten als auch als Cholangiozyten zu spezialisieren, was die Möglichkeit eröffnet, sowohl die Leber wie auch die Gallengänge anhand einer einzigen Biopsie eines einzelnen Patienten zu modellieren. Darüber hinaus wurde berichtet, dass Leberorganoiden mehrere Monate lang stabil eingefroren und kultiviert werden können, was für andere primäre menschliche Zellen nicht möglich ist. Nach der Entwicklung von Organoiden aus Cholangiozyten, die aus der Leber stammen (intrahepatisch) wurden Protokolle entwickelt, um Organoiden aus Gallengängen außerhalb der Leber (extrahepatische) und der Gallenblase zu erzeugen. Seitdem wurde eine neue Nomenklatur entwickelt, um zwischen Leberorganoiden unterschiedlicher Herkunft zu unterscheiden. Die in 2015 erstmals von Huch *et al.* entwickelten Leberorganoiden werden heute intrahepatische Cholangiozytenorganoiden (ICOs) genannt. Andere Leberorganoiden werden wie folgt benannt: Leberorganoiden, die aus Hepatozyten hergestellt werden, werden Hepatozytenorganoiden genannt; Organoiden, die aus Biopsien des extrahepatischen Gallengangs hergestellt werden, werden als extrahepatische Cholangiozytenorganoiden (ECOs) bezeichnet, während Organoiden, die aus Biopsien der Gallenblase hergestellt werden, als Gallenblasencholangiozytenorganoiden bezeichnet werden (GCOs).

Im Bereich der seltenen Leberkrankheiten bei Kindern präsentierte der erste Bericht über Leberorganoiden vielversprechende Ergebnisse, vor allem zur Untersuchung der Krankheitsmechanismen des Alagille-Syndroms und des α 1-Antitrypsin-Mangels. Die Aussicht auf nahezu unbegrenzt verfügbares Patientenmaterial zur Erforschung seltener Krankheiten war verlockend. Aus diesem Grund hat unsere Gruppe am UMC Utrecht in die Infrastruktur und (inter)nationale Zusammenarbeit investiert, um eine Metabolische Biobank einzurichten. Hierzu wurden Leberorganoiden aus Lebergewebe von Hunderten von Patienten und gesunden Spendern eingelagert. Diese große Biobank von Leberorganoiden von mehreren seltenen Leberkrankheiten bei Kindern bietet eine wertvolle Gelegenheit, den Nutzen von Leberorganoiden als

Instrument für die Erforschung von Krankheitsmechanismen und Entscheidungen über Behandlungen aufzudecken.

Begutachtung und Weiterentwicklung von Leberorganoiden als Instrument zur Erforschung von Leberkrankheiten bei Kindern

Während der Errichtung unserer Biobank war das weltweite Wissen über das Nutzen von Leberorganoiden zur Untersuchung von Krankheitsmechanismen begrenzt. Seit dem ersten Bericht über Leberorganoiden wurden keine weiteren Informationen über die Bandbreite der Leberfunktionen von Leberorganoiden veröffentlicht. Obwohl Huch *et al.*, 2015, gezeigt haben, dass mehrere Hepatozytenfunktionen in Leberorganoiden untersucht werden können, wurden nur wenige Funktionen in Leberorganoiden mit menschlichen erwachsenen Hepatozyten oder Lebergewebe verglichen. Dadurch bleibt unklar ob diese Leberfunktionen stark genug zum Ausdruck kommen um Krankheitsbilder messen zu können. Hinzu kommt, dass mehrere Lebereigenschaften, wie beispielsweise Albuminausscheidung, deutlich geringer in Leberorganoiden zum Ausdruck gebracht werden als im Lebergewebe. Zusammengefasst deuten diese Daten darauf hin, dass Leberorganoiden möglicherweise nicht das gesamte Spektrum der Hepatozytenfunktionen widerspiegeln. Daher blieb unklar, welche Leberfunktionen und -krankheiten mit Leberorganoiden untersucht werden können. Ziel dieser Arbeit war es also, das Potenzial von Leberorganoiden um Krankheitsmechanismen monogenetischer Lebererkrankungen und anderer seltener Lebererkrankungen bei Kindern zu erforschen.

Dazu wird in **Kapitel 1** das Forschungsthema eingeleitet, gefolgt von **Kapitel 2**, worin wir an Hand von Genen und Funktionsstudien untersucht haben, welche seltenen monogenetischen Erkrankungen mit ICOs erforscht werden können. Unserer Erfahrung nach ermöglicht das Protokoll zur Produktion von ICOs den Austausch von Patientengewebe mit Laboren auf der ganzen Welt. Dies verringert die Beschränkungen, welche die globale Verteilung von Patientenmaterial darstellt. Darüber hinaus haben wir gezeigt, dass Organoiden von Patienten wichtige Merkmale mehrerer monogenetischer Lebererkrankungen aufweisen. Dies ermöglicht uns zwischen gesunden Kontroll- und Patienten-Organoiden zu unterscheiden. Wir haben gezeigt, dass sowohl grundlegende Stoffwechselfunktionen als auch Hepatozyten-spezifische Funktionen, wie z. B. der Kupferstoffwechsel, in ICOs erforscht werden können. Darüber hinaus haben wir gezeigt, dass ICOs besonders nützlich sind, um Gallentransportfunktionen zu untersuchen.

Hautfibroblasten werden häufig verwendet, um seltene monogenetische Erkrankungen auf personalisierte Weise im Labor zu untersuchen. Fibroblasten sind leicht verfügbar und einfach zu handhaben. Ihr Ursprung deutet jedoch darauf hin, dass ihr Potenzial zur Erforschung Hepatocysten-spezifischer Erkrankungen

begrenzt ist. Die geringe Anzahl an Literaturberichten zur Modellierung von Lebererkrankungen mit Fibroblasten unterstützt diese Mutmaßung. Unser Vergleich von ICOs und Fibroblasten mit Lebergewebe zeigt außerdem, dass Fibroblasten mehrere Hepatozyten-spezifische Gene nicht zum Ausdruck bringen (**Kapitel 2**). Stattdessen eignen sich Fibroblasten zur Erforschung allgemeiner biochemischer Defekte, die verschiedene Zelltypen betreffen. Für Hepatozyten-spezifische Funktionen, wie etwa den Arzneimittelstoffwechsel, werden daher Hepatozyten-spezifische Zellmodelle bevorzugt. Aufgrund ihres Ursprungs und ihrer bipotenten Natur galten ICOs als ideales Modell für Hepatozyten. Wir fanden jedoch heraus, dass ICOs nicht alle relevanten Hepatozyten-spezifischen Gene zum Ausdruck bringen (**Kapitel 2**). Stattdessen bringen ICOs eine Mischung aus einigen Cholangiozyten- und Hepatozyten-spezifischen Genen und Funktionen zum Ausdruck. Daher sind ICOs unter aktuellen Bedingungen geeignet um eine Auswahl von Hepatozytenfunktionen zu untersuchen, die bei seltenen Lebererkrankungen betroffen sind.

Die Bemühungen zur Aufklärung des Nutzens von Leberorganoiden wurden in **Kapitel 3** erweitert, indem untersucht wurde, ob Leberorganoiden zur Behandlung von Kinderleberkrankheiten mit ungeklärten Krankheitsmechanismen eingesetzt werden könnten. Da in **Kapitel 2** gezeigt wurde, dass ICOs mehrere Cholangiozyteneigenschaften bewahren, waren wir daran interessiert zu sehen, ob Gallengangatresie mithilfe patienteneigener ICOs erforscht werden kann. Bei einer Gallengangatresie ist das Gallengangsystem von Narbengewebe durchwachsen und verengt, wodurch der Gallenfluss von der Leber in den Darm verhindert wird. Obwohl der Krankheitsmechanismus unklar bleibt, zeigt das Krankheitsbild eindeutig, dass Gallengangcholangiozyten eine zentrale Rolle bei der Gallengangatresie spielen. Darüber hinaus weisen die Unterschiede in Zeitpunkt und Intensität zwischen Symptomen in Gallengängen innerhalb und außerhalb der Leber deutlich auf Unterschiede in den zugrunde liegenden Mechanismen oder Anfälligkeiten von Cholangiozyten verschiedener Gallengangregionen und Entwicklungsstadien hin. Gallengängen innerhalb und außerhalb der Leber entwickeln sich aus unterschiedlichen Ursprungszellen, was ein wichtiger Faktor für diese Intensitäts- und Zeitunterschiede sein könnte. Nach der Veröffentlichung von ICOs wurden Protokolle entwickelt, um Organoiden aus extrahepatischen Gallengängen (ECOs) und Gallenblasencholangiozyten (GCOs) zu erzeugen. Da diese Organoiden im Labor regionale Unterschiede des Gallengangsystems bewahren, vermuteten wir, dass die regionale Vielfalt der Gallengangatresie mit ICOs, ECOs und GCOs modelliert werden könnte. Daher haben wir getestet, ob Organoiden aus diesen drei Gallengangregionen von Gallengangatresiepatientengewebe erzeugt werden können. Tatsächlich haben wir nachweisen können, dass Organoiden von Gallengangatresiepatienten kultiviert und eingefroren werden können. Wir haben darüberhinaus nachgewiesen, dass sich das Wachstumsverhalten

von Gallengangatresie-ICOs von Kontrollorganoiden unterscheidet. Trotz des normalen Äußerlichen der Gallengangatresieorganoiden deutete der Ausdruck einiger Gene darauf hin, dass sich die Gallengangatresieorganoiden von den Kontrollorganoiden unterscheiden. Die Unterschiede lagen hauptsächlich in Genen, die an der Veränderung von Umgebungsproteinen und Wachstum beteiligt sind; zwei Funktionen, von denen angenommen wird, dass sie am Krankheitsmechanismus der Gallengangatresie beteiligt sind.

In den letzten Jahrzehnten wurden mehrere Hypothesen zum Krankheitsauslöser von Gallengangatresie aufgestellt, darunter Virusinfektionen, Gifte, Autoimmunreaktionen und genetische Veranlagung. Von diesen Hypothesen wird die Beteiligung viraler Infektionen und/oder eines Umweltgifts oder eines giftigen Metaboliten am meisten durch klinische und experimentelle Beweise gestützt. Da Leberorganoiden ein minimalistisches Modell des Gallenepithels sind, kann der genaue Wirkmechanismus eines Virus oder Giftes unabhängig von anderen Zellen erforscht werden. Um zu ergründen, ob hepatobiliäre Organoiden tatsächlich zum Testen bestehender Hypothesen geeignet sind, haben wir Gallengangatresieorganoiden und Kontrollorganoiden mit einem viralen Imitator (Poly I:C) und einem Pflanzengift (Bilatreson), von dem bekannt ist, dass es Gallengangatresie in Tieren verursacht, behandelt. Wir stellten fest, dass Bilatreson zelluläre Stressreaktionen, wie z. B. des Glutathionstoffwechsels, bei Gallengangatresie und Kontroll-ECOs erhöht. Poly I:C verursachte Gallengangatresie-spezifische Veränderungen im Ausdruck von bestimmten Genen, einschließlich der Veränderung von Umgebungsproteinen und der Bildung von Narbengewebe. Insgesamt deuten unsere Ergebnisse daraufhin, dass menschliche hepatobiliäre Organoiden ein geeignetes Modell für Gallengangatresie sind.

Obwohl wir in **Kapitel 2** gezeigt haben, dass mehrere Funktionen von Hepatozyten und Cholangiozyten in Leberorganoiden untersucht werden können, deuten unsere Daten auch darauf hin, dass mehrere Funktionen von Hepatozyten in diesem Modell derzeit eingeschränkt sind. Deshalb haben wir untersucht, ob die Leberreife von ICOs verbessert werden kann. Zu diesem Zweck haben wir in **Kapitel 4** eine neue Kulturmethode, basierend auf verschiedenen Strategien zur Nachahmung der Umgebung von Hepatozyten in der Leber, für ICOs entwickelt und charakterisiert. Wir haben die dreidimensionalen Organoiden fragmentiert und die losen Stücke auf der Oberfläche von porösen Hohlfasern (HFMs) wachsen lassen. Darüber hinaus verwendeten wir Umgebungsproteine, um den Zellen zu erleichtern sich an die HFMs zu binden und um Hepatocytenspezifische Signale nachzuahmen. Wir sahen, wie Zellen dichte Lagen bildeten, und stellten fest, dass sich Leberfunktionen, wie beispielsweise der Arzneimittelstoffwechsel, in diesem neuen Kultursystem verbesserten. HFMs ermöglichen auch interne und externe Durchströmung, wenn sie an einen Bioreaktor und eine Perfusionspumpe angeschlossen sind,

wodurch der Blut- und Gallenfluss im Labor simuliert werden kann. Als ersten Schritt zur Krankheitsmodellierung haben wir untersucht, ob patienteneigene ICOs im neuen System wachsen können. Dabei lag der Fokus auf Erkrankungen, die Gallentransporter betreffen, da die HFM-Architektur die Trennung von Zellkompartimenten, welche Galle oder Blutbestandteile produzieren, ermöglicht. Dies begünstigt funktionelle Studien zur Erforschung solcher Erkrankungen. Somit haben wir den Nachweis erbracht, dass hepatische Gallentransporterdefekte wie PFIC Typ 3 (PFIC3) in patienteneigenen Leberorganoiden untersucht werden können. Zusammengenommen legen diese Ergebnisse nahe, dass das HFM-System ein leistungsstarkes Instrument zur personalisierten Forschung von Lebererkrankungen, sowie der langfristigen Wirkungen von Medikamenten für seltene Leberkrankheiten bei Kindern, wie z.B. PFIC3, ist.

Abschließend fasst **Kapitel 5** die Ergebnisse der Doktorarbeit zusammen und geht auf die Konsequenzen für die zukünftige Verwendung von Leberorganoiden ein. Durch die Identifizierung von Schnittstellen zwischen den durchgeführten Studien und der aktuellen Literatur werden zukünftige Forschungsmöglichkeiten vorgeschlagen, um den Anwendungsbereich von Leberorganoiden zu erweitern und unser Verständnis der Krankheitsmechanismen zu verbessern.

Schlussfolgerung

In dieser Doktorarbeit haben wir gezeigt, dass patienteneigene Leberorganoiden ein nützliches Hilfsmittel bei der Erforschung mehrerer seltener Leber- und Stoffwechselerkrankungen sind, die die Leber und das Gallengangsystem betreffen. Mehrere Krankheiten wie zystische Fibrose, PFIC3, Wilson-Krankheit und Methylmalonazidurie können derzeit mit ICOs erforscht werden. Obwohl Leberorganoiden zuvor als neues Hepatozytenmodell gefeiert wurden, haben wir nachgewiesen, dass Organoiden aus allen Gallengangregionen mindestens genauso nützlich für die Erforschung von Gallengangerkrankungen sind.

Ich bin davon überzeugt, dass Leberorganoiden ein fantastisches Instrument sein können, um die Mechanismen aufzuklären, die zu einer Gallengangatresie führen. Die Entwicklung neuer Technologien wie Organchips und Co-Kulturstrategien versprechen nicht nur die effektivere Erforschung der Krankheitsmechanismen seltener Krankheiten, sondern auch die Verbesserung der Leberreife von ICOs. Die Anwendung der zahlreichen Verbesserungsstrategien für die ICO-Kultur wird wahrscheinlich zu einem fantastischen patienteneigenen Hepatozytenmodell führen. Wir haben die ersten Schritte zur Verbesserung der Leberreife von ICOs unternommen und demonstriert, dass die Anwendungen von ICOs erweitert werden können, mit dem Ziel die Erforschung von mehr Krankheitsmechanismen zu ermöglichen. Wir sind davon überzeugt, dass die Kombination von Leberorganoiden und anderen Hepatozytenmodellen ein wirksames Instrument zur Aufklärung von

Krankheitsmechanismen sein wird und dabei helfen kann, sichere Therapiestrategien für seltene Leberkrankheiten bei Kindern auf personalisierte Weise zu identifizieren. Angesichts der vielversprechenden neuen Wege hoffe ich, dass patienteneigene Leberorganoiden eines Tages dazu beitragen werden, das Leiden der Patienten zu lindern, so wie Herakles kam, um Prometheus vor der nächtlichen Verstümmelung seiner Leber zu retten.

„Herakles [erhob] seinen Bogen und [schoss] auf den Racheadler von Zeus (...) ‚Danke, Herakles‘, sagte der Titan. (...) ‚Du befreist die Welt von ihren schlimmsten Tieren, ihren Drachen, Schlangen und vielköpfigen Monstern (...), damit die Welt sicher ist und die Menschheit gedeihen kann.“

*Aus Helden - Die klassischen Sagen der Antike neu erzählt, von Stephen Fry
Aus der englischen Version frei übersetzt.*

Acknowledgements

Für Opa Helmut, und meine starke Oma Ingrid, und die gesamte Familie (Leh) Meier. Meine Motivation, um in der Biomedizin zu arbeiten, kam von Opas Multipler Sklerose. Die vielen verschiedenen bunten Pillen, die Opa jeden Morgen, Mittag und Abend zu sich nehmen musste, um halbwegs zu funktionieren, erschraaken mich. Was jedoch schlimmer war, war wie sehr die ganze Familie untter der Krankheit zu leiden hatte. Obwohl die Pillen ja eigentlich helfen sollten, verursachten sie weitere Komplikationen. Letzendlich starb Opa nicht an Multipler Sklerose, sondern an den Nebenwirkungen der Medikamente, welche er im Kampf gegen diese Krankheit tagein tagaus schlucken musste. Obwohl ich nicht an Multipler Sklerose geforscht habe, hat mir meine Zeit in der Wissenschaft Mut gemacht. Mut, dass so viele Wissenschaftler und Ärzte ihr Herzblut investieren, um mehr über die seltsamsten Krankheiten in Erfahrung zu bringen. Mut, dass die Entwicklung neuer Therapien immer besser wird. Mut, dass Präzisionsmedizin und persönliche Medizin ihren Auftakt machen. Mut, dass Therapien der Zukunft keine Menschenleben nehmen, sondern retten werden.

When we read these dissertations and celebrate the newly declared Ph.D., we often forget that the road that led them there was not lonely. Rather, it is lined with coaches, team members, and cheer leaders. It is lined with people offering energy bars, water bottles, and massage booths to get them to the finish line of this marathon. That is why I would like to thank everyone who helped me throughout this journey.

Geachte dr. Spee, beste **Bart**. Mijn verhaal in deze hoek van de wetenschap begint bij jou. In 2015 reageerde ik op een interessant stage project bij Diergenesskunde en het RMCU: het 3D printen van een lever. Na een leuk gesprek was ik helemaal enthousiast. Zo begon ik aan een 9 maanden stage, die zo leuk was dat ik er maar 11 van maakte. Steeds fietste ik van de Yalelaan met een bakkie cellen onder mijn arm naar de overkant van de campus om daar een aantal meningsverschillen te hebben met de 3D printer. Toch bleef ik mijn stage ontzettend leuk vinden, mede omdat jouw onderzoeksgroep zo'n leuke werkomgeving bood. Zo leuk zelfs dat ik na een korte detour weer bij jou terecht kwam. Deze keer voor mijn promotieonderzoek. Ontzettend veel dank dat je in mij geloofde en me hielp de ontbrekende financiering te vinden om mijn droom mogelijk te maken. Door mijn promotietraject heen was jij mijn rots in de branding. Jouw rustige aard maar ook je grote visies voor onze projecten waren een goede voedingsbodem voor mijn ontwikkeling. Ook enorm veel dank voor alle extra mogelijkheden buiten het lab, zoals het coachingstraject, de venture challenge met Orgonex en de RM helpdesk. Ik ben ontzettend blij dat jij uiteindelijk ook officieel mijn tweede promotor bent geworden.

Geachte dr. Fuchs, beste **Sabine**. Zonder jou had mijn promotietraject nooit plaats kunnen vinden. Niet alleen omdat jij de ontbrekende financiering hebt aangereikt, maar vooral vanwege jouw groot enthousiasme en passie dat jij naar ieder project brengt. Jouw drive om voor zieke kindjes innovatieve oplossingen te vinden is zo inspirerend. Jij sleepte me al gauw mee in je enthousiasme en hoewel jouw ideeën soms overweldigend talrijk waren, hebben we een mooi pad gevonden en samen belangrijk onderzoek gedaan. Ondanks, of waarschijnlijk juist doordat, wij zeer verschillend zijn, heb ik ontzettend veel geleerd van jou. Sabine, ik ben je erg dankbaar dat je mij hebt begeleid in mijn projecten en ontwikkeling.

Geachte prof. dr. Tryfonidou, lieve **Marianna**. Ik ben jou zo dankbaar voor alle steun die jij me hebt gegeven. Hoewel je pas halverwege mijn promotietraject mijn promotor werd, voelt het alsof je er al de hele tijd was en je een beschermende hand over me hield. Officieel krijgen promovendi geen coach, zoals atleten dat vaak hebben. En toch had ik jou als coach. Van projectplannen kritisch bekijken tot mij op MS Teams laten schreeuwen "I am the f***ing Queen of organoids!" heb jij altijd geweten hoe je mijn ogen op de bal kon houden. Van harte bedankt Marianna voor alle wijsheid en steun.

Sehr geehrte dr. Schneeberger, liebe **Kerstin**. Auch ohne dich hätte mein PhD nicht statt finden können. Danke, dass du so erfolgreich warst, deinen Veni erhalten hast und somit die Finanzierung für meinen PhD frei kam. Aber vor allem ein riesiges Dankeschön für deine Unterstützung bei meiner Entscheidung diesen PhD anzugehen. Die vielen Mittage im Sommer bei Louis im Haus, an denen wir über die Zukunft und Wissenschaft redeten, haben mich letztendlich zu dieser Entscheidung gebracht. Auch während meines PhDs, zu Zeiten an denen es nicht so einfach war, warst du immer da mit einem offenen Ohr und einem guten Rat. Vielen Dank Kerstin!

Lieve **Manon**. Mijn lab bestie, mijn buddy op deze harde weg. Wij waren elkaars fietspompen als de lucht er even uit was. Je was mijn lievelingsmens op werk en ik ben zo ontzettend blij dat we dit traject tot het laatste moment mogen delen. Er bestond voor mij geen enige twijfel dat jij mijn paranimef zou worden. Ik weet eigenlijk niet zo goed hoe ik dit verder in woorden moet vatten. Mijn dank voor jou is groter dan woorden. Ik hoop dat we in de toekomst verder als elkaars coaches met thee en taart door het leven mogen wandelen. De grootste dank, Manon, voor je steun, tijd, wijsheid en vriendschap.

Dear **Alessia**. No matter where either of us is, we always have each other's back. Thank you for being one of those friends with whom it doesn't matter how long it has been since we last saw each other. Thank you for all your kind and supportive words throughout my PhD, your tips, and tricks. And thank you for returning to

the Netherlands! I missed you and I am so very happy to have you here as my paranymp.

Beste **Imre**. Dankzij jou heb ik snel mijn weg gevonden op het lab. Geduldig heb je mij alles geleerd en ervoor gezorgd dat de eerste projecten soepel liepen. Je was altijd spontaan beschikbaar als ik hulp nodig had. Ook ben ik je zeer dankbaar voor het voorwerk dat je had gedaan en waar ik een aantal projecten op mocht baseren. Oneindig veel dank voor al je hulp.

Dear dr. Myszczyzyn, dear **Adam**. Thank you immensely for your hard work and your company on all those long lab days. We made it work. Our HFM baby is alive! When Bart mentioned that a new PostDoc would come to work with me on the HFM project, I was very doubtful and not sure how the dynamic would work. But it was perfect. I think we made a great team, and I am so grateful to you for all the effort you put in to help me finalize my part of the project. I will miss our long discussions about results, future plans and problems that needed solving. Thank you so much Adam!

Dear **Ibrahim**. Thank you so much for all your help with the RNAseq work! I could not have done this without you. It was always a pleasure working with you and I am very thankful for your patient explanations and hard work. Thank you so much.

Dear **Alasdair**. It was such a pleasure working with you. I immensely enjoyed our discussions about drug innovation, cats, dogs and sofa colors. It was refreshing to work on a non-lab project. Although our project did not make it into my dissertation, I learned just as much from it as those that did. I am very grateful to you for sharing your expertise and company with me.

Ook zou ik graag mijn begeleidingscommissie, dr. **Jasper** Mullenders en prof. dr. **Madelon** Maurice, en ook mijn oud promotor prof. dr. **Niels** Geijsen willen danken. Het was erg verfrissend om jullie mening te horen tijdens onze jaarlijkse voortgangsgesprekken. Jullie hebben ervoor gezorgd dat het enthousiasme ook focus kreeg en de projecten haalbaar waren. Hierin wil ik Jasper speciaal danken voor zijn steun en tips. Dankzij jou heb ik vanaf het begin al snel mijn ritme kunnen vinden in een 'high pace' werkomgeving. Van harte bedankt!

I would also like to thank the members of my assessment committee prof. dr. C.R. Berkers, prof. dr. A. de Bruin, prof. dr. J.M. Beekman, prof. dr. L. van Grunsven and prof. dr. J.M. Wells for assessing my dissertation.

Of course, these last years would not have been the same without my two groups; the STEAM lab and Fuchs lab/PedGastro group. Thanks to all of you who made lunch

and coffee breaks so enjoyable, laughed with me at lab outings and conferences, and made work discussions so interesting.

Special thanks to dr. Penning, beste **Louis**. Bedankt voor de aanmoedigen om wetenschapscommunicatie niet uit ogen te verliezen, je luisterend oor en natuurlijk je vertrouwen om voor Bikkel en je huis te mogen zorgen. Ook wil ik **Monique, Lisa, Roos-Anne, Loes** en **Jesse** speciaal danken voor jullie hulp met qPCRs, kleuringen, FIS assays en voor jullie gezelligheid. Many thanks also to **Anke, Sawsan, Emilia, Irena, Gautam, Indi, Martijn**, and all other members of the Fuchs group and PedGastro for the help and gezelligheid. Special thanks also to prof. dr. **Edward Nieuwenhuis** for the great feedback during meetings. Also, many thanks to dr. **Nalan Liv, Tineke Veenendaal** and dr. **Judith J. M. Jans** for your help with electron microscopy and metabolic analyses.

Thank you also to my students **Emil, Cristiana** and **Anne**. All three of you were such different people and students and you taught me a lot during your stay with us. Thank you for all your many questions and hard work.

Ook wil ik het RM helpdesk team, en met name **Stephan** en **Ria** van harte danken voor jullie vertrouwen en de kansen die ik kreeg bij het RM helpdesk. Ik heb ontzettend genoten van onze tijd samen.

Ondanks dat ik de meeste tijd in Utrecht op het lab heb besteed, was mijn sociale kring bijna net zo belangrijk voor het succesvol afronden van mijn PhD. Vooral veel dank aan **Menno, Lian, Marijn, Jorin, Nicole, Ruud, Ava** en **Erik** voor alle aanmoedigende en uitdagende gesprekken. Jullie steun heeft enorm geholpen om door te bikkelen en wat liever voor mezelf te zijn. Also, many thanks to all other friends who patiently waited for me to finalize this dissertation.

Liebste Familie, liebste **Oma Ingrid, Oma Vicky, Claudia, Stefan, Oma Rose, Heidrun** und **Ralph**. Vielen Dank für eure Geduld und auch euer Interesse an meiner Forschung während der letzten Jahre. Danke auch für die entspannenden und geselligen Wochenenden, die mir immer wieder neue Energie gaben.

Liebste **Mama**, liebster **Papa**. Vielen Dank, dass ihr mir immer die Freiheit gegeben habt um meinen Träumen zu folgen. Mit eurem Vertrauen und eurer Unterstützung, als ich nach Neuseeland wollte, habt ihr mir gezeigt, dass ich Dinge wagen kann. Dass meine Träume es Wert sind. Vielen Dank auch dafür, dass ihr mir eure Abenteuerlust mitgegeben habt. Ich werde euch immer dankbar sein, dass ihr mir das Studium ermöglicht habt, um diese Doktorarbeit machen zu können. Danke auch für euren Enthusiasmus wenn ich wieder was neues aus dem Labor erzählt habe und auf Servietten Diagramme zeichnete, um euch Gentechnik und Stammzellen

zu erklären. Mit euch an meiner Seite habe ich immer das Gefühl, dass ich alles schaffen kann. Danke, dass ihr meine größten Fans seid. Von Herzen, vielen Dank für eure Unterstützung in den letzten Jahren.

En zoals altijd, het beste als laatst. **Koen**, van harte, heel veel dank voor jouw geduld, jouw wijsheid en steun. Jij bent mijn thuis, mijn veilige plek. Jouw warmte gaf mij vertrouwen. Jouw nuchtere blik heeft mij de weg gewezen. Zonder jou was ik er nooit gekomen. Bedankt dat je altijd in mij geloofde, me altijd hebt aangemoedigd en met mij alle kleine en grote successen hebt gevierd. Bedankt met heel mijn hart.

Curriculum Vitae

Vivian Lehmann was born on the 26th of March 1994 in Duisburg, Germany. She grew up with her parents and grandparents in Krefeld, Germany. Living in the same house as her granddad who suffered from Multiple Sclerosis was confronting. The many colorful pills that should have helped him only added new symptoms to his suffering. During these years, Vivian's interest in personalized medicine started and her motivation to pursue a scientific career in biomedicine developed. In 2010, Vivian moved to Wanaka, New Zealand to experience a different culture. Here, she fell in love with biotechnology and the possibilities it brings to cure diseases and feed the world. After finishing high school in New Zealand,



Vivian moved back to Europe where she started her Bachelor of Biotechnology at Wageningen University and Research in 2012. As part of this study, she joined the laboratory of dr. ir. Arjen Schots to perform a three-month long research internship focusing on the production of nematode proteins in plants for future vaccine use. After graduating successfully, she commenced her Master of Regenerative Medicine and Technology at Utrecht University in 2015. During this time, Vivian joined the laboratory of dr. Bart Spee and dr. Louis C. Penning for 11 months to perform a research internship on the three-dimensional bioprinting of liver tissue from human liver organoids in combination with the design and fabrication of a perfusion culture chamber for future drug testing. Subsequently, Vivian performed a writing assignment with prof. dr. Patricia Y. W. Dankers on smart biomaterials for regenerative medicine. After some time in the Netherlands, it was time to explore international waters again. In 2017, Vivian moved to Sherbrooke, Quebec, Canada to pursue an eight-month long research internship at the laboratory of dr. ing. Patrick Vermette on the vascularization of murine islets. Together they published their work titled 'Method for isolation of pancreatic blood vessels, their culture and coculture with islets of Langerhans' in the journal *Biotechnology Progress* in 2018.

Besides hands-on science, Vivian had enjoyed spreading her knowledge and enthusiasm about science to the non-scientific audience since her Bachelor studies. In 2017, she returned to Utrecht University for a minor in Science Education and Communication. As part of this semester, she joined U-Talent and the communications department of the Hubrecht institute for an internship. During this time, Vivian represented the Hubrecht Institute at the yearly conference of EuroStemCell and organized a Masterclass on organoids for high school students.

The Hubrecht Institute and U-Talent have continued to use Vivian's script every year since.

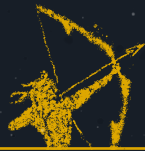
Following her graduation from the Master of Regenerative Medicine and Technology in early 2018, it was time to take some time off studying. Vivian spent some time backpacking through Mexico and worked at a boulder gym in Utrecht. Although Vivian enjoyed her time perfecting latte art and meeting different people with the same love for the outdoors and climbing, science was calling her ever louder. Eventually, Vivian returned to the laboratory of dr. Bart Spee, dr. Louis Penning and dr. Kerstin Schneeberger to pursue her PhD on liver organoids. With the wish to focus on medical applications, a sandwich PhD position was arranged with dr. Sabine Fuchs. Part of their work was published in the Journal of Inherited Metabolic Disease in 2022 titled 'The potential and limitations of intrahepatic cholangiocyte organoids to study inborn errors of metabolism'. Moreover, Vivian presented their work at different (inter)national conferences as well as on the podcast of the Journal of Inherited Metabolic Disease. In the four years of her PhD, Vivian enjoyed the diversity of working in two different groups and aided in strengthening their collaborations.

Vivian's love for science communication continued to grow throughout her PhD and she ensured to incorporate it into her work. She was involved in several outreach programs where she visited primary schools, was present at open days of museums and universities as an expert, and joined the communications team of the Regenerative Medicine Centre Utrecht to establish and write for the RM helpdesk website. Similarly, Vivian created and wrote for a science news website together with friends. Vivian continues to be involved with the Regenerative Medicine Centre Utrecht for science communication.

Working in a product-oriented field, Vivian was also involved in a venture challenge to aid establish a company around an invention by dr. Bart Spee and dr. Kerstin Schneeberger. Although Vivian learned that the business world is not her cup of tea, she is proud to have been involved in the process to make the company Orgonex become established.

After many years exploring different options within science, Vivian sees a clear path in front of her and is currently exploring the options to combine the role of science program coordinator with her skills in science communication.

Several figures in this dissertation were created with BioRender.com



Rare pediatric liver disorders can be very destructive to the lives of patients and their families. Often, therapeutic options are limited to symptomatic care and precise disease mechanisms remain elusive. The relatively low incidence of each individual disease and the often widespread geographic distribution of patients complicate research and treatment development. In this dissertation, we have investigated the potential of patient-derived liver organoids to study such rare pediatric liver diseases.

